To the Graduate Council:

I am submitting herewith a thesis written by Michael J. Taylor entitled "Second Law Optimization of a Sensible Heat Thermal Energy Storage System with a Distributed Storage Element." I have examined the final copy of this thesis for form and content and recommend that it be accepted in partial fulfillment of the requirements for the degree of Master of Science, with a major in Mechanical Engineering.

R. J. Crane, Major Professor

J. R. Parsons, Major Professor

We have read this thesis
and recommend its acceptance:

Accepted for the Council:

Vice Provost
and Dean of The Graduate School

STATEMENT OF PERMISSION TO USE

In presenting this thesis in partial fulfillment of the requirements for a Master of Science degree at The University of Tennessee, Knoxville, I agree that the Library shall make it available to borrowers under rules of the Library. Brief quotations from this thesis are allowable without special permission, provided that accurate acknowledgment of the source is made.

Permission for extensive quotation from or reproduction of this thesis may be granted by my major professors, or in their absence, by the Head of Interlibrary Services when, in the opinion of either, the proposed use of the material is for scholarly purposes. Any copying or use of the material in this thesis for financial gain shall not be allowed without my written permission.

Signature Michael J. Taylor

Date May 16, 1986

SECOND LAW OPTIMIZATION OF A SENSIBLE HEAT THERMAL ENERGY STORAGE SYSTEM WITH A DISTRIBUTED STORAGE ELEMENT

A Thesis

Presented for the

Master of Science

Degree

The University of Tennessee, Knoxville

Michael J. Taylor

June 1986

DEDICATION

This thesis is affectionately dedicated to my daughters, Betsy Marie and Laurie Michelle. They have, in their own way, taught me more than any formal education.

ACKNOWLEDGMENTS

I have arrived at this point in my career through the faith and encouragement of many people; too many to thank each one of them individually. I must, however, single out a few for special recognition.

First and foremost is my family and especially my wife Barbara. Her emotional support has been (within acceptable engineering tolerances) constant, unfailing, and much appreciated.

A sincere thank you also goes to my committee, especially Professors Krane and Parsons, whose enthusiasm and support went beyond anything in their job description.

I would also like to acknowledge the use of the University of Tennessee Computing Center, and particularly the assistance of Mrs. Sue Smith, for their help in arriving at the results presented in this study.

Last, and certainly not least, I would like to thank the Oak Ridge National Laboratory, Engineering Technology Division Word Processing Center for typing the manuscript and the Engineering Technology Division Reports Office for preparing some of the figures used in this report.

ABSTRACT

This numerical study defined the behavior of a sensible heat thermal energy storage system whose physical design and operation had been optimized to minimize the production of thermodynamic irreversibilities. Unlike previous studies, it included the effects of transient conduction within the storage material.

A dimensionless set of governing equations was defined for a complete storage-removal cycle that included the effects of entropy generation due to convection and viscous effects in the flowing fluid, two-dimensional transient conduction within the storage material, and to convection due to the discharged hot fluid coming to equilibrium with the environment during the storage period. A computer program was written to solve this equation set and this program was in turn controlled by a sophisticated optimization routine to determine a dimensionless storage time, flow channel half-height, and heat transfer coefficient that resulted in a minimum amount of availability destruction.

The results of this analysis showed that entropy generation within the storage material due to transient conduction was a major contributor to the total thermal irreversibilities associated with the operation of a sensible heat thermal energy storage system. For the counterflow configuration and over the range of design variables examined, material entropy generation accounted for between 26.% and 60.% of the total thermal availability destruction that occurred during a complete storage-removal cycle. It was also shown that the storage material aspect ratio (the ratio of a section's half-thickness to its length) had a

significant impact on the optimum design of a storage system. Its influence was second only to the fluid mass velocity.

Other significant results of this study were:

a. The thermodynamic efficiencies for the storage systems were extremely poor in that it destroyed from 20.% to 82.% of the entering thermal and pressure availability.

b. A counterflow configuration without a dwell period was shown to operate more efficiently than a parallel flow configuration with or without a dwell period. Depending on the value of the dimensionless mass velocity, the parallel flow configurations increased the total thermal entropy generated, over the corresponding counterflow design, from 12.% to 67.%.

c. Dwell periods were shown to be impractical because of their extreme length; dimensionless times on the order of 6500.0 were required. These are much greater than the optimum storage period times defined for the counterflow configurations without dwell periods, which ranged from 0.5 to 6.0.

PREFACE

To study, and when the occasion arises to put what one has learned into practice — is that not deeply satisfying?

Confucius

The purpose of computing is insight, not numbers.

R. W. Hamming

Everything should be made as simple as possible, but no simpler.

Albert Einstein

TABLE OF CONTENTS

SECTION		PAGE
1.	INTRODUCTION	1
	Background and General Statement of the Problem	1
	Previous Related Studies: Second Law Aspects of Thermal Analysis	4
	Related Studies of Sensible Heat Thermal Energy Storage Systems	10
	Detailed Problem Statement	15
2.	DEVELOPMENT OF THE ANALYTICAL MODEL	23
	Selection of the Physical System to be Modeled	23
	Definition of a Second Law Figure of Merit	23
	Definition of Governing Equations	31
	Non-Dimensionalization of the Governing Equations	41
	Closure of the Model and Description of the Optimization Study	58
3.	DEVELOPMENT OF THE NUMERICAL MODEL	68
	Discussion of the Optimization Routine Used in the Study	68
	Description of the Program to Calculate the Figure of Merit	70
	Verification of the Numerical Model	82
4.	PRESENTATION AND ANALYSIS OF RESULTS	86
	Description of the Study and Summary of Results	86
	Analysis of the Results	88
	Unconstrained Counterflow Cases Without a Dwell Period	107
	Unconstrained Parallel Flow Cases	136
	Constrained Counterflow Cases Without a Dwell Period	139
	Critique of the Mathematical Model	143
5.	CONCLUSIONS AND RECOMMENDATIONS	152
	Recommendations for Future Study	154
	LIST OF REFERENCES	157

TABLE OF CONTENTS (continued)

SECTION		PAGE
APPENDIXES		163
APPENDIX A.	ENTROP SUBROUTINE GLOSSARY, PROGRAM LISTING, AND SAMPLE OUTPUT	164
APPENDIX B.	DEVELOPMENT OF DISCRETIZED TRANSIENT CONDUCTION EQUATIONS FOR THE STORAGE ELEMENT	215
APPENDIX C.	DESCRIPTION OF MODIFICATIONS TO PERMIT INTEGRATION OF DISCRETE VALUES	225
APPENDIX D.	VERIFICATION OF TWO CRITICAL CALCULATIONS PERFORMED BY THE ENTROP COMPUTER PROGRAM	234
VITA		241

LIST OF TABLES

TABLE		PAGE
1.1	Summary of Availability and Energy Analyses of a 300 MW(e) Coal-Fired Generating Plant	7
4.1	Optimization Results for Unconstrained, Counterflow Design Cases for Inlet Fluid Temperature Excess of 2.0, Material Aspect Ratio of 0.01, and Initial Material Temperature Excess of 1.1	89
4.2	Optimization Results for Unconstrained, Counterflow Design Cases for Inlet Fluid Temperature Excess of 2.0, Material Aspect Ratio of 0.01, and Initial Material Temperature Excess of 1.3	90
4.3	Optimization Results for Unconstrained, Counterflow Design Cases for Inlet Fluid Temperature Excess of 2.0, Material Aspect Ratio of 0.05, and Initial Material Temperature Excess of 1.1	91
4.4	Optimization Results for Unconstrained, Counterflow Design Cases for Inlet Fluid Temperature Excess of 2.0, Material Aspect Ratio of 0.05, and Initial Material Temperature Excess of 1.3	92
4.5	Optimization Results for Unconstrained, Counterflow Design Cases for Inlet Fluid Temperature Excess of 3.0, Material Aspect Ratio of 0.01, and Initial Material Temperature Excess of 1.1	93
4.6	Optimization Results for Unconstrained, Counterflow Design Cases for Inlet Fluid Temperature Excess of 3.0, Material Aspect Ratio of 0.01, and Initial Material Temperature Excess of 1.3	94
4.7	Optimization Results for Unconstrained, Counterflow Design Cases for Inlet Fluid Temperature Excess of 3.0, Material Aspect Ratio of 0.05, and Initial Material Temperature Excess of 1.1	95
4.8	Optimization Results for Unconstrained, Counterflow Design Cases for Inlet Fluid Temperature Excess of 3.0, Material Aspect Ratio of 0.05, and Initial Material Temperature Excess of 1.3	96

LIST OF TABLES (continued)

TABLE		PAGE
4.9	Optimization Results for Unconstrained, Parallel Flow Design Cases Without a Dwell Period	97
4.10	Optimization Results for Unconstrained, Parallel Flow Design Cases with a Dwell Period	98
4.11	Optimization Results for Cases Where the Storage System NTU was Constrained to a Value of 10.0 or Less	99
4.12	Optimization Results for Cases Where Storage Period First Law Efficiency was Constrained to a Value of 0.90 or Greater	100
4.13	Physical Interpretation of the Major Dimensionless Variables Used to Describe the Entropy Generation Characteristics of a Sensible Heat Thermal Energy Storage System	102
4.14	The Storage Material Temperature Distribution at the End of the Storage Period for a Nominal, Optimized, Counterflow Storage System	113
4.15	The Storage Material Temperature Distribution at the End of the Removal Period for a Nominal, Optimized, Counterflow Storage System	114
4.16	Summary of Terms in the Figure of Merit for an Optimum, Medium Temperature Design Case Showing the Influence of λ on the Behavior of the Figure of Merit	125
4.17	Summary of Unconstrained, Counterflow Design Cases Used to Verify the Accuracy of the Optimization Results	146
B.1	Partial Summary of the Operation of the Original Instruction String to Read the Banded Matrix	221
B.2	Summary of Coefficients and Associated Constants for Discretized, Non-Dimensionalized Material Conduction Equations	224

LIST OF TABLES (continued)

TABLE		PAGE
D.1	Comparison of Storage Material Temperatures Calculated by ENTROP with those Calculated by Equation D.1	239

LIST OF FIGURES

FIGURE		PAGE
1.1	Schematic Representation of a Flat Slab Sensible Heat Thermal Energy Storage System	17
1.2	Illustration of a Flat Slab Thermal Energy Storage Unit	18
1.3	Typical Storage Material Average Temperature and Fluid Outlet Temperature History for a Complete Storage-Removal Cycle	20
2.1	Illustration of Adiabatic Lines of Symmetry for a Typical Flat Slab Storage Unit	24
2.2	Cross Section of Symmetrical Slice of Storage Material and Flow Channel	25
3.1	Schematic Representation of the Most General ENTROP Execution Sequence	72
3.2	Schematic Representation of the Fluid-Material Transient Temperature Response Calculations	79
4.1	Optimum Values of Fo_s for the Unconstrained, Counterflow Design Cases with $T_{m,o,s}/T_\infty = 1.1$ . . .	108
4.2	Optimum Values of G_s^+ for the Unconstrained, Counterflow Design Cases with $T_{m,o,s}/T_\infty = 1.1$ . . .	109
4.3	Optimum Values of Bi_s for the Unconstrained, Counterflow Design Cases with $T_{m,o,s}/T_\infty = 1.1$ . . .	110
4.4	Average Material and Fluid Outlet Temperature History for an Optimum, Unconstrained, Counterflow Medium Temperature Design Case	112
4.5	Temperature Distribution in the Storage Material at the End of the Storage Period for an Optimum, Unconstrained, Counterflow, Medium Temperature Design Case	115
4.6	Temperature Distribution in the Storage Material at the End of the Removal Period for an Optimum, Unconstrained, Counterflow, Medium Temperature Design Case	116

LIST OF FIGURES (continued)

FIGURE		PAGE
4.7	Optimum Values for the Figure of Merit for the Unconstrained, Counterflow Design Cases with $T_{m,o,s}/T_\infty = 1.1$	118
4.8	Optimum Values for the Number of Thermal Entropy Units for the Unconstrained, Counterflow Design Cases with $T_{m,o,s}/T_\infty = 1.1$	120
4.9	Optimum Values for the Availability Distribution Ratio for the Unconstrained, Counterflow Design Cases with $T_{m,o,s}/T_\infty = 1.1$	121
4.10	Optimum Amounts of Entering Pressure Availability for the Unconstrained, Counterflow Design Cases with $T_{m,o,s}/T_\infty = 1.1$	123
4.11	Optimum Amounts of Entering Thermal Availability for the Unconstrained, Counterflow Design Cases with $T_{m,o,s}/T_\infty = 1.1$	124
4.12	Optimum Values for the Storage System Size for the Unconstrained, Counterflow Design Cases with $T_{m,o,s}/T_\infty = 1.1$	128
4.13	First Law Efficiencies for the Optimized, Unconstrained, Counterflow Design Cases with $T_{m,o,s}/T_\infty = 1.1$	130
4.14	Optimum Distribution of Thermal Availability Destruction During the Storage Period for the Unconstrained, Counterflow, Design Cases with $T_{m,o,s}/T_\infty = 1.1$ and $T_{f,i,s}/T_\infty = 2.0$	132
4.15	Optimum Values for the Figure of Merit for the Unconstrained, Counterflow Design Cases with $T_{m,o,s}/T_\infty = 1.1$ and $T_{m,o,s}/T_\infty = 1.3$	135
4.16	Optimum Values for the Figure of Merit for the Unconstrained Counterflow and Unconstrained Parallel Flow Design Cases with $T_{m,o,s}/T_\infty = 1.1$ . .	137
4.17	Optimum Values for the Figure of Merit for the Unconstrained and Constrained Counterflow Design Cases	140

LIST OF FIGURES (continued)

FIGURE		PAGE
4.18	Results of the Verification Procedure for the G_s^+ Optimization Variable for the Counterflow, Unconstrained Design Cases	147
4.19	Results of the Verification Procedure for the Bi_s Optimization Variable for the Unconstrained, Counterflow Design Cases	148
4.20	Results of the Verification Procedure for the Fo_s Optimization Variable for the Unconstrained, Counterflow Design Cases	149
B.1	Illustration of the Coordinate System and Nodal Numbering Sequence Used in the Discretization of the Material Conduction Equation	217
B.2	Illustration of the Form of a Typical Coefficient Matrix for Discretized Flat Slab Conduction Equations	219
C.1	Illustration of the Physical System Used to Permit the One-Dimensional Integration of Discrete Values	228
C.2	Illustration of the Physical System Used by Simpson's One Third Rule for Two-Dimensional Integration	231
C.3	Schematic Representation of the Calculating Sequence Used to Perform Two-Dimensional Integration of Discrete Values	233

LIST OF SYMBOLS

A = Heat transfer surface area of representative section

Bi = Biot Number

Cp = Constant pressure specific heat

Dh = Hydraulic diameter of the representative section's flow channel

d = Half-height of the representative section's flow channel

Fo = Fourier number

f = Moody or Darcy friction factor

G^+ = Dimensionless mass flow term

g_c = Constant relating force, mass, and acceleration in Newton's Second Law

h = Specific enthalpy or convective heat transfer coefficient

k = Thermal conductivity

L = Length of representative section

$\dot{m}$ = Fluid mass flow rate

N = Number of entropy generation units

P = Pressure

Pr = Prandtl number

Ph = Heated perimeter of the representative section's flow channel

Q = Total heat transferred

$\dot{Q}$ = Rate of heat transfer

R = Gas constant

S = Entropy

s = Specific entropy

$Sgen$ = Total entropy generated

$\dot{S}gen$ = Rate of entropy generation

$\dot{S}'''gen$ = Volumetric rate of entropy generation in the storage material

$\dot{S}'gen$ = Rate of entropy generation in the fluid per unit length of flow channel

St = Stanton number

T = Temperature

t = Time

LIST OF SYMBOLS (continued)

U = Internal Energy

V = Fluid velocity

V^+ = Dimensionless aspect ratio

W = Entering availability of both hot and cold fluid streams

w = Half-thickness of representative section's storage material

X = Dimensionless axial coordinate

x = Axial coordinate

Y = Dimensionless transverse coordinate

y = Transverse coordinate

Z = Dimensionless coordinate

z = Coordinate

Greek Letters

α = Thermal diffusivity of storage material

β = Dimensionless pressure

Γ = Unit width of storage material-fluid channel

Δ = Change in a variable

ε = Second law efficiency

η = Thermal or first law efficiency

Θ = Dimensionless temperature

λ = Availability distribution ratio

ρ = Fluid density

τ = Dimensionless mass velocity

Ψ = Entering availability of an individual fluid stream

ψ = Entering specific availability of an individual fluid stream

Subscripts

c = complete cycle

cs = cross sectional

i = inlet condition

e = exit condition

LIST OF SYMBOLS (continued)

f = fluid stream

m = storage material

o = initial condition

r = removal period

s = storage period

ss = steady state

ΔP = due to pressure drop

ΔT = due to temperature gradient

w = wall

$\Delta\beta$ = due to dimensionless pressure drop

$\Delta\theta$ = due to dimensionless temperature gradient

∞ = ambient condition

Superscripts

n = next time increment

n+1 = most current time increment

1. INTRODUCTION

Background and General Statement of the Problem

The 1973 Middle East oil embargo forced changes in many prevailing social, political, and engineering conventions. Long standing assumptions of unlimited, easily accessible energy resources were no longer viable. In an attempt to lessen the impact of this and future shortages, national conservation goals were formally defined. These goals included but were not limited to:

a. using less of an energy resource to do a particular task,

b. doing several tasks (concurrently or sequentially) with the same portion of an energy resource, and

c. using different energy resource, ones more closely matching the desired tasks.

Perhaps most important there was a resurgence of the concept that the real value of an energy resource, the one to be conserved, was its potential to do useful work rather than its energy content. The United States Congress even directed that a study be conducted to determine the relevance of this idea to federal energy conservation programs [1].

Even though the maximum useful work concept had been in existance for more than a century, its acceptance as an analytical tool was delayed by a largely recalcitrant technical community. Defining useful work meant utilizing the Second Law of Thermodynamics as an integral part of the analysis and the majority of thermal engineers were reluctant to do this. Ideas involving the Second Law of Thermodynamics,

and its associated property entropy, had been traditionally presented to students within a strict, classical scientific framework. Consequently, many thermal engineers came to consider these concepts as "too abstract to use seriously." As a result of this intellectual inertia it was not until very recently that second law considerations began to be incorporated into the mainstream of thermal engineering analysis [2,3,4,5,6,7,8,9,10,11,12,14]. In recent years the acceptance and application of the second law has increased to the point that several special technical sessions have been held at National Heat Transfer Conferences to discuss the subject. References [3-13] were presented at at the 1984 ASME/AIChE National Heat Transfer Conference session and demonstrate that second law considerations have been found to be useful in virtually all areas of thermal engineering.

The purpose of this study is to add to this growing body of second law oriented thermal analyses. This will be accomplished by conducting a design optimization study of a particular thermal system: a sensible heat thermal energy storage system with a distributed storage element. Heat transfer processes in general, and storage systems in particular, are inherently irreversible thus destroying much of the potential of a resource. As such they are a fertile area for productive second law study. These types of systems were in service during the early 1970's and their value as a conservation tool also received renewed appreciation after the oil embargo.

Feasibility studies conducted early in the post embargo era identified them as an especially practical means of achieving conservation

goals. They were particularly useful in situations where the supply of and demand for thermal energy did not occur simultaneously. Specifically they could:

a. improve the overall efficiency of large energy producing systems through load leveling,

b. enhance the development of alternative energy resources such as solar, and

c. decrease the consumption of energy resources through the use of waste heat recovery systems.

Since these initial studies, these systems have indeed found many residential, commercial, and industrial applications [15,16,17,18,19,20].

A particular type of system, the sensible heat thermal energy storage system, has become one of the most common types of units. This is due in part to their relatively low cost and inherently simple design. Sophisticated analytical techniques have been developed to facilitate their design and operation [21,22,23,24] and they continue to be considered an appropriate field for study by the federal government [25,26]. This technology base however is grounded firmly in the First Law of Thermodynamics. A storage system is considered more efficient if, for the same energy input, it stores more thermal energy than another comparably size unit. This procedure results in high first law efficiencies, but it also produces systems that destroy most of the potential of an energy resource. While this has been, and continues to be, an acceptable design philosophy [25], it is in direct conflict with modern conservation efforts.

The specific goal of this study is to define geometry and process parameters that will permit these types of storage systems to operate with minimum thermodynamic irreversibilities. The specific storage system to be modeled is a counterflow regenerator. It consists of a storage material that is alternately exposed to hot and cold fluid streams. The material stores sensible heat energy during the storage period and discharges it during the removal period. During normal operation the two fluid streams alternately counterflow in the same channel.

Previous Related Studies: Second Law Aspects of Thermal Analysis

The recent increase in the application of the Second Law of Thermodynamics to thermal analysis resulted from the renewed interest in conservation that occurred during and after the 1973 oil embargo. This change was necessary because the emphasis of conservation programs had changed from maximizing energy transfer across a process to conserving the potential of energy resources. The following brief discussion explains the reasons for this shift in priorities and the resulting need for using the Second Law of Thermodynamics.

In a qualitative sense the purpose of most industrial thermal systems is to utilize an energy resource to cause a change. For example, burning fuel to change a fluid's temperature and pressure to generate electricity or using a hot effluent stream to change the temperature of a solid slab to store waste heat. It follows then that the most valuable property of an energy resource, the one to be conserved, is its ability to produce such changes. This maximum useful work concept had

been defined, forgotten and then rediscovered many times in the past; especially when energy supplies were cheap and plentiful. It took the oil embargo to gel the idea that total energy resources were indeed limited and that true conservation consisted of maximizing the useful work available in them.

To implement this new standard, it was necessary to be able to define the maximum useful work available in a given energy resource. Energy, or more correctly internal energy, could not by itself give an indication of useful work and was therefore inadequate as a measure of performance. Several definitions were presented in attempts to rigorously quantify useful work. Availability or available work became the most prominent and often used. It is defined as an extensive property that describes the maximum useful work that could be done by a given amount of energy. Expressed in terms of thermodynamic properties for a unit mass of homogeneous flowing fluid with negligible kinetic and potential energies [26]:

$$\psi = \Delta h - T_{\infty} (s_i - s_e) \qquad (1\text{-}1)$$

Availability is thus defined in terms of three thermodynamic properties: enthalpy, temperature, and entropy. Enthalpy changes are calculated by the First Law of Thermodynamics and are directly related to net changes in heat and work. Entropy is a property of matter that measures the degree of disorder at the microscopic level. Most important from an availability conservation perspective, entropy is not conserved

as is internal energy. The natural state is for entropy to be generated in a real (irreversible) system. Associated with this production is a loss of ability to do useful work. Because entropy is calculated using the Second Law of Thermodynamics, implementing availability analyses required the quantitative application of the Second Law of Thermodynamics to thermal analysis.

With this availability function as a tool, it was possible to address conserving the potential of energy resources. As with the traditional first law approach, an availability comparison could be easily formulated to describe any system of interest. Analytically this comparison was defined [1] as:

$$\varepsilon = \frac{\text{availability required for a task}}{\text{availability in the inputs}} \qquad (1\text{-}2)$$

This ratio and other slight variations were adopted as the thermodynamic efficiencies needed to implement meaningful conservation studies.

An excellent example of an availability analysis using equation (1-2) can be found in [28]. In this study the authors conducted both availability and energy analyses of a nominal 300 MW(e) coal-fired generating plant. The results of this study are summarized in Table 1.1. While the net efficiencies are essentially the same, the distribution between process steps is quite different. The energy (first law) results indicate that the greatest inefficiency occurs in the condenser and cooling towers. The availability (second law) analysis, however, shows that the biggest inefficiency (destruction of availability) is in the combustion and steam generator steps.

Table 1.1. Summary of availability and energy analyses of a 300 MW(e) coal-fired generating plant

Process step	% of entering availability destroyed	% of entering energy lost
Boiler	45.0	0.0
Exhaust stack	5.0	8.0
Turbine	5.0	1.0
Condenser and ultimate heat sink	5.0	50.0
Generator	7.0	7.0
Total	67.0	66.0

These results were first presented in order to identify areas where conservation efforts would be the most effective. Obviously, the direction of research and development would be profoundly effected by which set of results were chosen as the benchmark. The question that follows is, "Which is the correct set?" Quite simply, there is no single totally correct choice. First and second law results represent two different, but equally valid, realities. The particular reality, or blend of realities, to be observed at any given time is a function of economics. This realization has lead Bejan [29] to define an optimal thermal design as the least irreversible system the designer can afford.

In the past, combustion processes were not seriously considered for efficiency improvement because of low fuel costs. Currently however, one of the major objectives of the Electric Power Research Institute is to improve the heat rate (BTU/KW(e)) of fossil-fired plants [30]. This is due, in part, to rapidly escalating fuel costs.

Macroscopic availability balances of entire processes are especially useful when thermal analysis is combined with other disciplines such as economics and optimization. Two recent examples of this type of analyses are by Frangopoulos [11] and Hesselmann [13]. Frangopoulos conducted an optimization of the costs of a typical thermal power plant. The objective function contained both initial and operating costs, the optimization was constrained by second law considerations, and the entropy generation characteristics of the plant components were calculated by performing macroscopic availability balances.

Hesselmann optimized the investment costs of a heat exchanger network for the case of constant inlet fluid availability.

Some of the most interesting recent results have been produced when the focus of the analysis was shifted to the individual components of a process. These studies defined the entropy generation characteristics of system components as a function of their geometries and operating conditions. These types of analyses were facilitated by the application of the Guoy-Stadola [31] theorem which states that the rate of availability destruction is proportional to the rate of entropy generation. Expressed mathematically this gives:

$$\left(\begin{array}{c}\text{Rate of availability} \\ \text{destruction}\end{array}\right) = T_{\infty}\ \dot{S}gen \qquad (1\text{-}3)$$

This theorem permits the second law analysis of components as a function of their own operating characteristics. This capability can best be illustrated by examining the second law inequality which has been rearranged to indicate the degree of irreversibility of a thermodynamic system:

$$\dot{S}gen = \frac{dS}{dt} + \frac{\dot{Q}}{T} - \sum_{out} \dot{m}s + \sum_{in} \dot{m}s \qquad (1\text{-}4)$$

Equation (1-4) states that the rate of entropy generation is a function of the working fluids specific entropy, heat transfer rates, mass flow rates, and entering and exiting temperatures and pressures. The value of these, and therefore the rate of entropy generation, can all be

influenced by the design and operation of a component. Utilizing equations (1-3) and (1-4) thus permits the designer to incorporate second law effects directly into the design process.

A typical example of this new generation of second law oriented thermal analysis is by Perez-Blanco [5] and deals with performance enhancement of heat exchangers. Almost all methods of enhancing heat transfer performance decrease thermal entropy generation but increase pressure entropy generation. This suggests there is some optimum level of enhancement that results in a minimum amount of total entropy generation. Building on earlier work by Bejan [14], Perez-Blanco defined an analytical relationship for the total entropy generated by a smooth tube heat exchanger as a function of typical design parameters. These included Reynolds, Prandtl, Brinkman, and Nusselt numbers as well as the friction factor, aspect ratio, and inlet fluid temperature. Using this model, the author defined entropy generation characteristics of the heat exchanger for two types of enhancement; a reduced heat transfer area and a reduced temperature difference across the tube walls. It was shown that enhancements which reduced temperature differences produced the lowest rates of entropy generation. These results also reinforced the cost intensive nature of optimum second law designs.

Related Studies of Sensible Heat Thermal Energy Storage Systems

Sensible heat thermal energy storage systems that operate with separate storage-removal periods can be classified by either their operating or physical characteristics. From an operating perspective, there

are two basic categories of units: those which use a single fluid and those which employ two simultaneous heat transfer fluids. Those using a single fluid are referred to as storage units [21] and those with two simultaneous heat transfer fluids are called thermal storage exchangers [21]. Both types can be made to operate in either a single blow or periodic mode of operation. A single blow operating mode occurs when the fluid inlet temperature experiences a step change and then remains constant at the elevated valve until the end of the period. Classifications based on geometry generally fall into one of four groups:

a. continuous elements of storage material with discrete passages,

b. metallic wire mesh as the storage material, as in the matrix of a rotary regenerator,

c. packed beds with small particles of storage material, and

d. ceramic or refractory storage materials stacked in orderly arrays.

Although there are many possible combinations of geometry and operating modes, the mathematical models used to define their performance are quite similar and have been solved in varying degrees of complexity by many investigators.

Thermal energy storage systems have been the object of serious study since the mid 1920's. These early studies by Anzelius [32], Nusselt [33], Hausen [34], and Schumann [35] developed analytical solutions for the transient behavior of a simplified model; a continuous slab of material exposed on one side to a moving fluid and perfectly insulated on the other side. A major assumption for these studies was

that there was a zero thermal conductivity in the direction of flow and an infinite conductivity normal to the flow. Subsequent analyses became more sophisticated and solution techniques more elaborate. Larson [36] extended the early work by Schumann [35] to include arbitrary initial material and entering fluid temperatures.

Coppage and London [37] summarized the state of periodic regenerator theory and then developed a supplemental approximate theory for extrapolating these known solutions to other conditions (i.e., initial or boundary) of interest. London [38] later presented computer generated solutions for this same type of equipment. As with previous studies, these results were determined using the assumptions of zero material conductivity in the flow direction and infinite conductivity normal to the flow. Much later, Willmott [39] also presented computer generated solutions for this simplified model.

One of the most recent and thorough analyses of continuous material storage systems was conducted by Szego [22]. In this numerical study he accounted for the effects of axial and transverse conduction in the storage material, modeled both flat slab and hollow cylinder geometries, and considered single and two fluid operation. Szego's work formed the basis of a text by Schmidt and Willmott [21] that contains the most current summary of first law analytical techniques and operating procedures for thermal energy storage units of all kinds.

Packed bed storage systems were defined analytically by Rosen [40] and numerically by Handley [41]. These studies considered the effects on finite particle conductivity in the direction of the flowing fluid.

As with most other investigators, they both made the assumption of negligible thermal conductivity in the longitudinal direction. Subsequent efforts by Jefferson [42] and Riaz [43] included the effects of transverse conduction. These results, however, were not applicable to continuous storage materials.

As previously indicated, these results were based on the First Law of Thermodynamics; that is performance parameters were defined to maximize the amount of thermal energy stored. Bejan [44] was the first to demonstrate the importance of applying the Second Law of Thermodynamics to thermal energy storage systems. He stated that since availability was the commodity of interest, storage systems should be designed to store availability rather than thermal energy; that is they should operate with a minimum of entropy generation.

In this study, Bejan modeled the storage period of a simple system using a set of governing equations designed to emphasize rates of entropy generation rather than energy storage. His system consisted of a well stirred bath placed in an insulated vessel and initially at thermal equilibrum with the atmosphere. A hot gas entered the system, was cooled by flowing through a heat exchanger immersed in the bath, and was then discharged to the atmosphere. Bejan defined a figure of merit that was a function of entropy generation due to convection and viscous losses within the heat exchanger duct and to the discharged fluid coming to equilibrum with the atmosphere. He determined independent optimum storage times and heat exchanger sizes that minimized the total rates of entropy generation during the storage period. Bejan's results

established two very important characteristics of storage units designed to operate with a minimum of thermal irreversibility. That is:

a. when operated at optimum storage times, the first law efficiency (amount of thermal energy stored) was very poor, and

b. depending on the particular operating point, optimum heat exchanger sizes were much larger than traditional units.

Mathiprakasam and Beeson [45] extended the second law analysis of simple storage systems to include both the storage and removal periods. They conducted an analytical study of a storage system with both rectangular and circular flow passages and defined the effects of flow direction, mass flow rate, and cycle times on the second law efficiency of the system. Their major assumptions, which limit the applicability of the results, were that the pressure drop in the flow channel was zero and the thermal conductivity of the storage material was zero in the flow direction and infinite normal to the flow.

Perhaps the most rigorous and sophisticated second law analyses of systems with lumped storage elements are those of Krane. In one study [46] he substantially modified and extended Bejan's model [44] of a system with a lumped storage element that was both heated and cooled by flowing gas streams. Krane's analysis, which included both viscous and thermal sources of entropy generation, was the first to show that an entire storage-removal cycle (as opposed to the storage period alone) must be analyzed in order to optimize the design and operation of a sensible heat system. This study also showed that from 70.% to 90.% of the entering availability was destroyed by irreversibilities. Another

significant result was that the first law efficiency of an optimum system is quite low. In a second study Krane [47] performed the first second law study of a sensible heat system with joulean heating of the storage element. This analysis showed that irreversibilities in electrically-heated sensible heat systems destroyed from 60.% to 80.% of the availability that entered the system during a complete storage-removal cycle.

Detailed Problem Statement

The preceding discussion demonstrates the need for a second law oriented thermal analysis of a sensible heat storage system with practical composition and operating parameters. All of the second law oriented studies conducted to date have modeled the storage material as a lumped element; that is with an infinite thermal conductivity. Because of this assumption, entropy generation due to heat transfer through finite temperature gradients has not been considered. Also at the present time, it has not been demonstrated that a sophisticated optimization study utilizing the individual temperature and pressure components of entropy generation is practical.

The goal of the present study is to extend Krane's analysis [46] of a lumped element system to include the effects of a storage material with a finite thermal conductivity. Solving this problem will relax the last major simplifying assumption of previous studies and generate useable results for second law oriented thermal analysis in general and thermal energy storage systems in particular. It will extend the rigor

of existing thermal energy storage analysis and demonstrate the practicality of designing real equipment by minimizing the rate of entropy generation.

To fix ideas, consider the sensible heat thermal energy storage system shown schematically in Figure 1.1. It consists of a storage material unit with associated piping and valving to permit a counterflow arrangement of fluid. In an actual system, two such units are operated in parallel to provide a continuous stream of heated fluid to the load. The storage material has a geometric configuration with discrete fluid passages that allow the fluid to contact the storage material. This study is focused on a specific geometry: the flat slab. This configuration consists of a number of small aspect ratio channels of rectangular cross-section for the flowing fluid, connected in parallel and separated by slabs of the heat storage material as shown in Figure 1.2.

The storage system operates in a thermodynamic cycle with a single cycle consisting of both a storage period and removal period. During the storage period, valves A and B are open and valves C and D are closed. A constant mass flowrate, $\dot{m}_s$, of hot fluid at a constant inlet temperature, $T_{f,i,s}$, and pressure, $P_{f,i,s}$, enters through valve A, passes through the flow channel, and is then discharged to the atmosphere through valve B. This exiting fluid has a temperature greater than ambient but its pressure is equal to ambient pressure. During this time, both the average temperature of the storage material and the fluid outlet temperature gradually approach the fluid inlet temperature. After an appropriate time, the storage period is terminated by closing

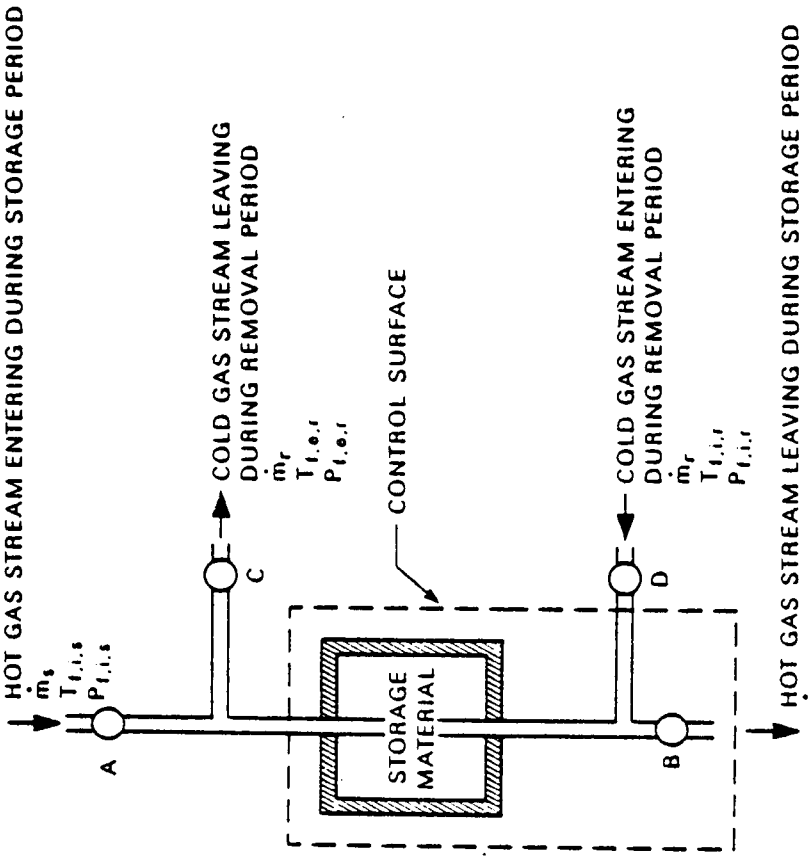


Figure 1.1. Schematic representation of a flat slab sensible heat thermal energy storage system.

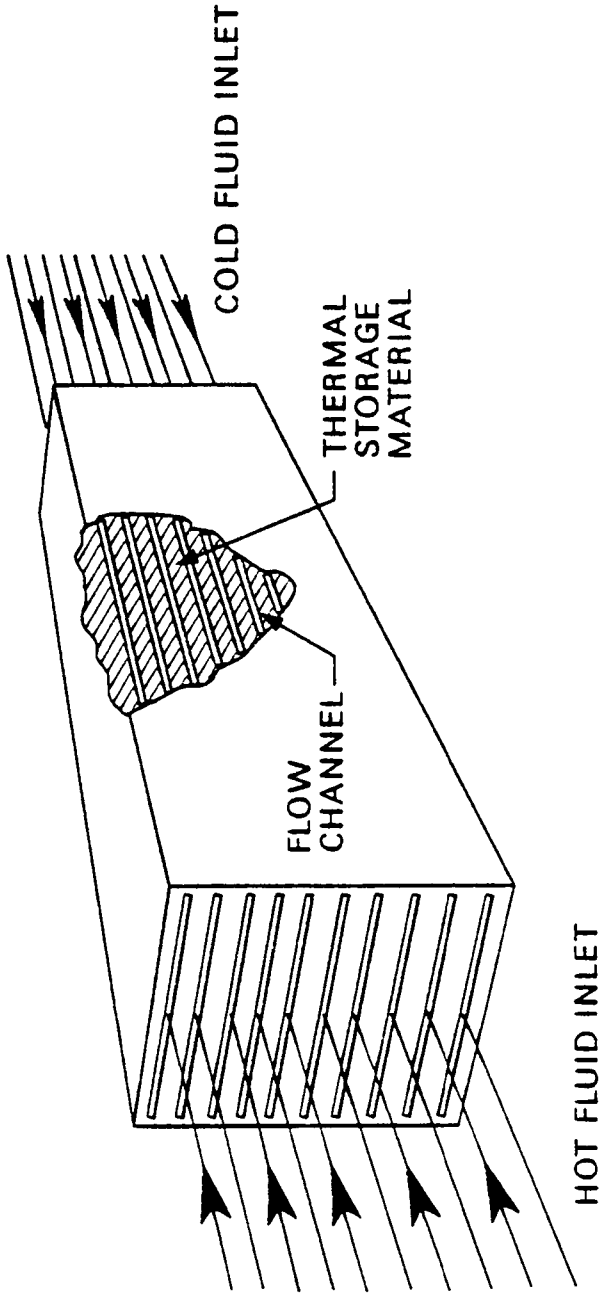


Figure 1.2. Illustration of a flat slab thermal energy storage unit.

valves A and B. At the end of the storage period there are two operating options. These are to begin the removal period immediately or go through a dwell period and then begin the removal period.

During the removal period, a constant mass flowrate, $\dot{m}_r$, of cold fluid at a constant inlet temperature, $T_{f,i,r}$, and pressure, $P_{f,i,r}$, enters the system through valve C, passes through the flow channel, and then exits the system through valve D to be used elsewhere. As was the case for the storage period, this exiting fluid has a temperature greater than ambient but a pressure equal to ambient. This removal process continues until the storage material average temperature returns to its initial value, which is also greater than ambient. Time dependent average material and fluid outlet temperature histories for this typical counterflow cycle are shown in Figure 1.3.

The specific objective of this present study is to quantify the effects of finite material thermal conductivities on the second law efficiency of a flat slab, counterflow sensible heat thermal energy storage system. To meet this objective, an analytical model based on the second law of thermodynamics will be developed and then controlled by an optimization routine. This procedure will determine an optimum set of geometry and operational parameters that result in a minimum amount of generated entropy for a complete storage-removal cycle. Geometry parameters to be investigated are the storage material aspect ratio (i.e., the ratio of a section's half-thickness to its length.) Also, the effects of fluid flow direction (i.e., counterflow vs parallel flow), storage period fluid inlet temperature, and storage period

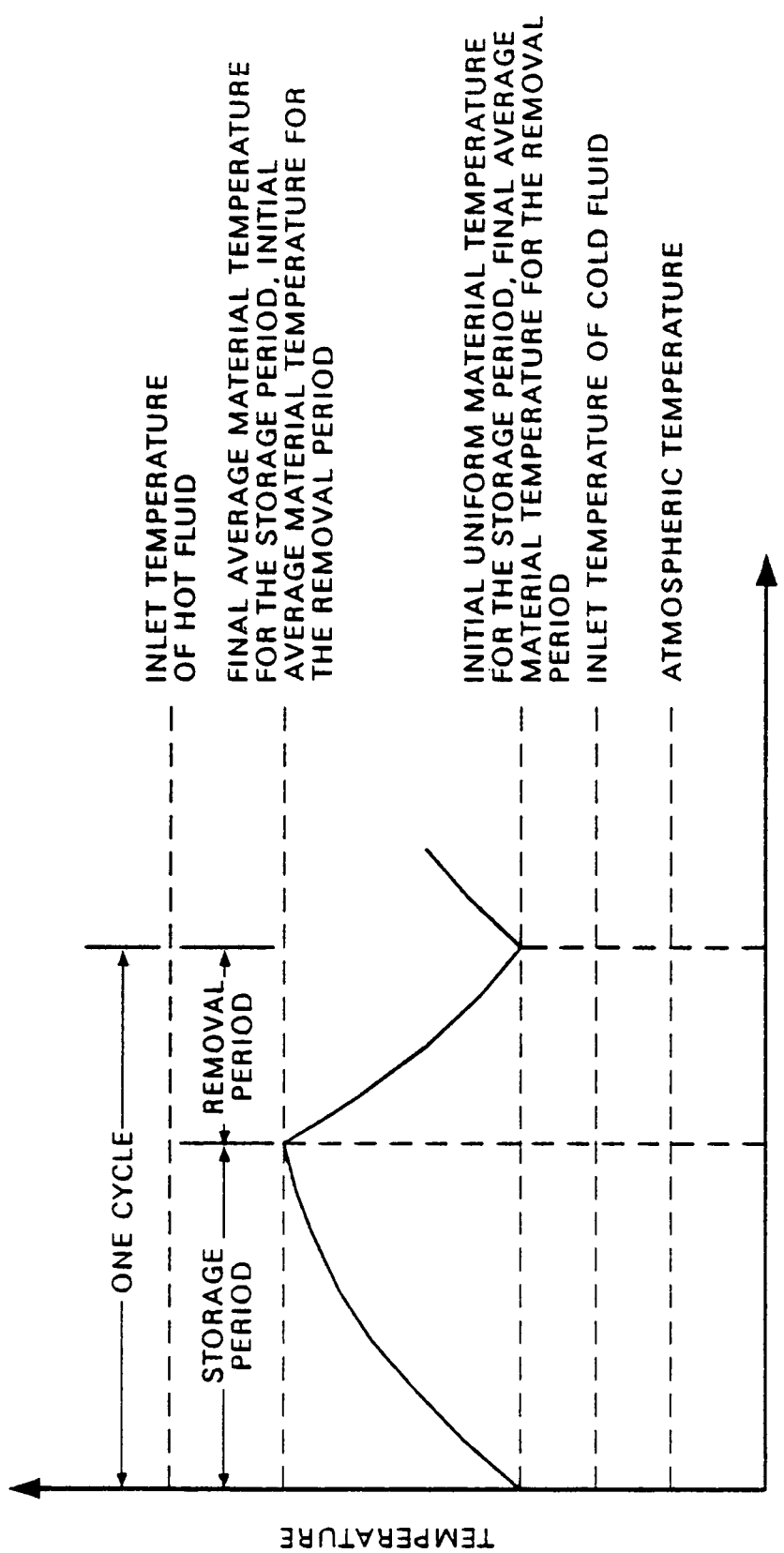


Figure 1.3. Typical storage material average temperature and fluid outlet temperature history for a complete storage-removal cycle.

initial material temperature will also be examined. The following is a summary of the major assumptions to be utilized in formulating the analytical model:

a. There are three sources of entropy generation common to both the storage and removal periods: heat transfer through the finite temperature difference between the flowing fluid and the storage material, conduction heat transfer through finite temperature gradients within the storage material, and viscous effects in the flowing fluid.

b. There is an additional source of entropy generation during the storage period due to heat transfer through the finite temperature difference between the discharged hot gas and ambient. All of the availability in the exiting hot gas is destroyed and this destruction is to be charged to the storage period when calculating values for the figure of merit.

c. The system is operated in a cycle consisting of both a storage and removal period and possibly a dwell period.

d. Both the storage and removal periods are initiated by a step change in the fluid inlet temperature which thereafter remains constant.

e. The same fluid, an ideal gas with constant specific heat, flows through the unit in both the storage and removal periods. The mass flow rate can differ between the storage and removal periods but remains constant during each period.

f. The hot and cold fluids exit the storage unit at atmospheric pressure and enter at a pressure just great enough to overcome the pressure drop due to viscous effects.

g. There is no phase change in either the storage material or flowing fluid and each have constant properties.

h. There is a constant convective heat transfer coefficient along the length of the storage element.

i. There is two-dimensional conduction within the storage material and one-dimensional (i.e., conservation of energy) for the flowing fluid in the flow direction.

j. The initial temperature distribution within the storage material is uniform and greater than the ambient temperature. This represents a "tare capacity" which permits the storage system to deliver a thermal energy to the load.

k. There are no heat losses to the surroundings from the storage material.

2. DEVELOPMENT OF THE ANALYTICAL MODEL

Selection of the Physical System to be Modeled

For this study of a flat slab configuration, it is assumed that each flow channel and storage material section is identical and the fluid mass flowrate in each channel is the same. With these stipulations, it is possible to define surfaces of symmetry as illustrated in Figure 2.1. Accordingly, it is necessary to model only one symmetrical section of the complete storage unit. This representative section has a length L, a material half-thickness w, a flow channel half-height d, and a unit width Γ into the paper and is illustrated in Figure 2.2.

Definition of a Second Law Figure of Merit

To meet the objectives of this study, it is necessary to define a figure of merit that is a function of the entropy generation characteristics of the storage unit. Using the methodology of Krane [46,47], the following second law oriented figure of merit can be defined for a generic, sensible heat thermal energy storage system operating in a complete cycle:

$$N_c = \left(\begin{array}{c}\text{entropy generation}\\ \text{number for a}\\ \text{cycle}\end{array}\right) = \frac{\left(\begin{array}{c}\text{total availability}\\ \text{destroyed during}\\ \text{a cycle}\end{array}\right)}{\left(\begin{array}{c}\text{total availability of the}\\ \text{hot and cold fluids that}\\ \text{enter the system}\\ \text{during a cycle}\end{array}\right)} . \qquad (2.1)$$

As can be seen, the behavior of N_c is directly related to the degree of irreversibility of the storage system. As it approaches a

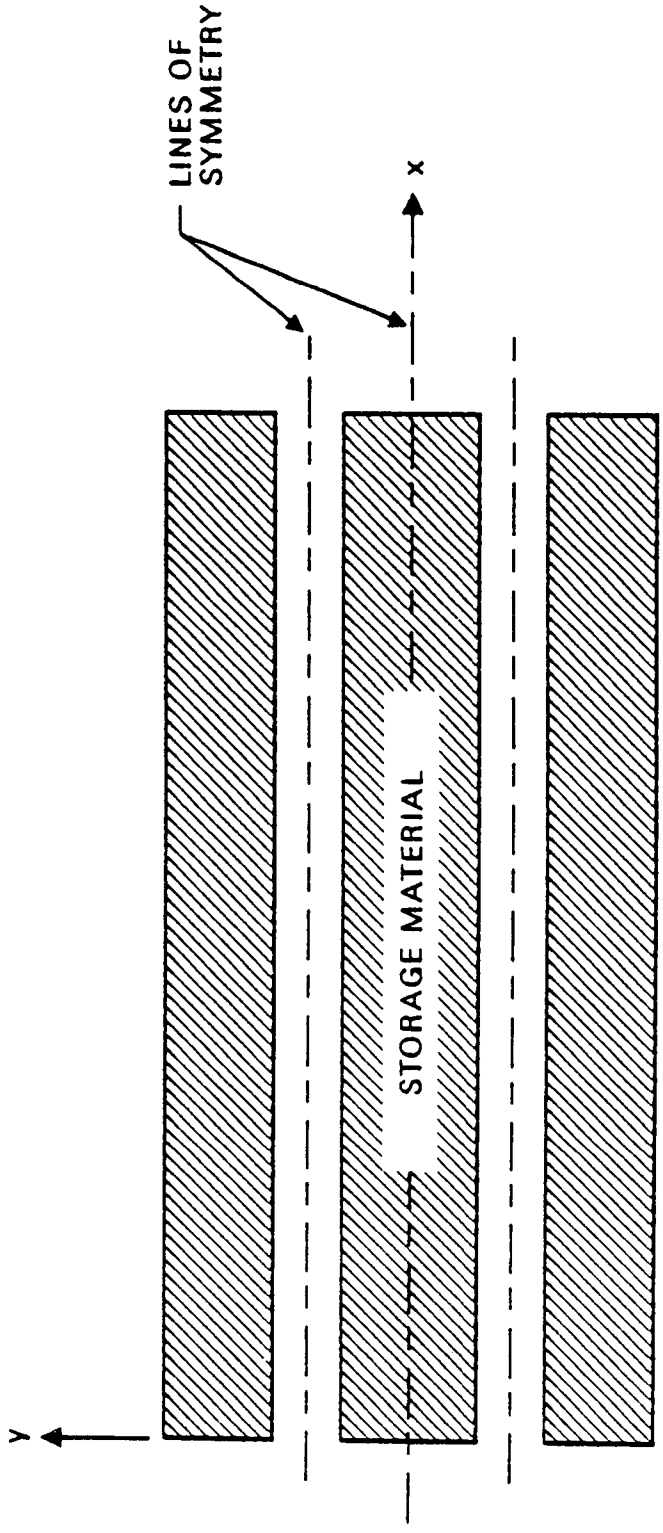


Figure 2.1. Illustration of adiabatic lines of symmetry for a typical flat slab storage unit.

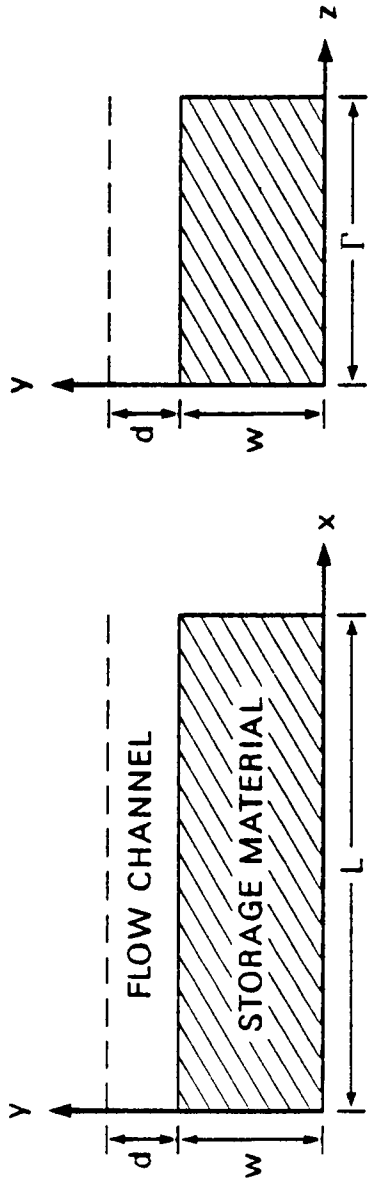


Figure 2.2. Cross section of symmetrical slice of storage material and flow channel.

limiting value of one, all of the entering availability is destroyed. A value of zero indicates a completely reversible operation with no availability destruction. Accordingly, a system storing availability should be designed and operated to minimize the value of N_c.

To begin the development of the figure of merit, we conduct an availability balance for the representative section during the storage period. This gives:

$$\left(\begin{array}{c}\text{total availability}\\ \text{of the entering}\\ \text{hot fluid}\end{array}\right)_s + \left(\begin{array}{c}\text{initial availability}\\ \text{of the storage}\\ \text{material}\end{array}\right)_s$$

$$= \left(\begin{array}{c}\text{final availability}\\ \text{of the storage}\\ \text{material}\end{array}\right)_s + \left(\begin{array}{c}\text{total availability}\\ \text{destroyed during}\\ \text{the storage period}\end{array}\right)_s . \qquad (2.2)$$

Note that equation (2.2) reflects the assumption that the fluid availability contained in the exiting hot fluid during the storage period is assumed to be completely destroyed and is considered a part of the total destruction that occurs during the storage period. A similar availability balance for the removal period results in:

$$\left(\begin{array}{c}\text{total availability}\\ \text{of the entering}\\ \text{cold fluid}\end{array}\right)_r + \left(\begin{array}{c}\text{initial availability}\\ \text{of the storage}\\ \text{material}\end{array}\right)_r$$

$$= \begin{pmatrix}\text{final availability}\\ \text{of the storage}\\ \text{material}\end{pmatrix}_r + \begin{pmatrix}\text{total availability}\\ \text{of the exiting}\\ \text{cold fluid}\end{pmatrix}_r \qquad (2.3)$$

$$+ \begin{pmatrix}\text{total availability}\\ \text{destroyed during}\\ \text{the removal period}\end{pmatrix}_r .$$

Because the system operates in a cycle, we can immediately specify that:

$$\begin{pmatrix}\text{initial availability of}\\ \text{the storage material}\end{pmatrix}_s = \begin{pmatrix}\text{final availability of}\\ \text{the storage material}\end{pmatrix}_r \qquad (2.4a)$$

and

$$\begin{pmatrix}\text{initial availability of}\\ \text{the storage material}\end{pmatrix}_r = \begin{pmatrix}\text{final availability of}\\ \text{the storage material}\end{pmatrix}_s . \qquad (2.4b)$$

Adding equations (2.2) and (2.3), and utilizing equation (2.4) we can write:

$$\begin{pmatrix}\text{total availability}\\ \text{of the entering}\\ \text{hot fluid}\end{pmatrix}_s + \begin{pmatrix}\text{total availability}\\ \text{of the entering}\\ \text{cold fluid}\end{pmatrix}_r =$$

$$\begin{pmatrix}\text{total availability}\\ \text{of the exiting}\\ \text{cold fluid}\end{pmatrix}_r + \begin{pmatrix}\text{total availability}\\ \text{destroyed during}\\ \text{the storage period}\end{pmatrix}_s \qquad (2.5)$$

$$+ \begin{pmatrix}\text{total availability}\\ \text{destoyed during}\\ \text{the removal period}\end{pmatrix}_r .$$

Expressed algebraically, equation (2.5) yields:

$$\left(\Psi_{s,i} + \Psi_{r,i}\right) = \Psi_{r,e} + \left(\Psi_{destroyed}\right)_s + \left(\Psi_{destroyed}\right)_r \cdot \qquad (2.6)$$

Now recall the Gouy-Stodola theorem [31], which states that the availability destroyed is proportional to the entropy generated. Applying this to our system results in:

$$\left(\Psi_{destroyed}\right)_s = T_\infty \, Sgen_s \qquad (2.7a)$$

and

$$\left(\Psi_{destroyed}\right)_r = T_\infty \, Sgen_r \cdot \qquad (2.7b)$$

Equations (2.6) and (2.7) can be used to define the total availability destroyed during a cycle as:

$$\begin{aligned} \left(\Psi_{destroyed}\right)_s + \left(\Psi_{destroyed}\right)_r &= \left[\Psi_{s,i} + \left(\Psi_{r,i} - \Psi_{r,e}\right)\right] \\ &= \left(T_\infty Sgen_s + T_\infty Sgen_r\right) \cdot \end{aligned} \qquad (2.8)$$

This allows the qualitative figure of merit given by equation (2.1), to be rewritten algebraically as:

$$N_c = \frac{\left(T_\infty\right)\left(Sgen_s + Sgen_r\right)}{\Psi_{s,i} + \Psi_{r,i}} \cdot \qquad (2.9)$$

Realizing that there are both thermal and viscous components of $Sgen_s$ and $Sgen_r$, equation (2.9) can be expanded to give:

$$N_c = \frac{T_\infty \left(Sgen_{s,\Delta T} + Sgen_{s,\Delta P} + Sgen_{r,\Delta T} + Sgen_{r,\Delta P}\right)}{\left(\Psi_{s,i,\Delta T} + \Psi_{s,i,\Delta P} + \Psi_{r,i,\Delta T} + \Psi_{r,i,\Delta P}\right)} \quad . \tag{2.10}$$

Now define the following quantities:

$$W_{\Delta P} \equiv \left(\begin{array}{c}\text{total availability contained} \\ \text{in the entering hot and cold} \\ \text{fluids due to pressures} \\ \text{greater than ambient}\end{array}\right) = \Psi_{s,i,\Delta P} + \Psi_{r,i,\Delta P} \tag{2.11a}$$

and

$$W_{\Delta T} \equiv \left(\begin{array}{c}\text{total availability contained} \\ \text{in the entering hot and cold} \\ \text{fluids due to temperatures} \\ \text{greater than ambient}\end{array}\right) = \Psi_{s,i,\Delta T} + \Psi_{r,i,\Delta T} \quad . \tag{2.11b}$$

Substituting equation (2.11) into equation (2.10) results in:

$$N_c = \frac{(T_\infty)\left(Sgen_{s,\Delta T} + Sgen_{s,\Delta P}\right)}{W_{\Delta P} + W_{\Delta T}} + \frac{(T_\infty)\left(Sgen_{r,\Delta T} + Sgen_{r,\Delta P}\right)}{W_{\Delta P} + W_{\Delta T}} \quad . \tag{2.12}$$

Now define a new parameter:

$$\lambda \equiv \left(\begin{array}{c}\text{availability distribution} \\ \text{ratio}\end{array}\right) \equiv \frac{W_{\Delta P}}{W_{\Delta T}} \quad . \tag{2.13}$$

The availability distribution ratio is an indication of how the total availability of the entering hot and cold fluids is distributed between that due to pressures and to temperatures being greater than ambient. Rewriting equation (2.12) in terms of λ gives:

$$N_c = \left(\frac{\lambda}{1+\lambda}\right) N_{\Delta P} + \left(\frac{1}{1+\lambda}\right) N_{\Delta T} \qquad (2.14a)$$

where:

$$N_{\Delta P} = \left(\begin{array}{c}\text{number of entropy}\\ \text{generation units}\\ \text{due to viscous}\\ \text{effects}\end{array}\right) = \frac{(T_\infty)\ (Sgen_{s,\Delta P} + Sgen_{r,\Delta P})}{W_{\Delta P}} \qquad (2.14b)$$

and

$$N_{\Delta T} = \left(\begin{array}{c}\text{number of entropy}\\ \text{generating units}\\ \text{due to heat transfer}\\ \text{through finite}\\ \text{temperature differences}\end{array}\right) = \frac{(T_\infty)\ (Sgen_{s,\Delta T} + Sgen_{r,\Delta T})}{W_{\Delta T}} . \qquad (2.14c)$$

The reason for defining λ is now apparent. It permits the entropy generation number, N_c, to be written as the sum of two separate terms: one due to viscous effects and one due to heat transfer across a finite temperature difference. Because of the assumption used in this analysis that the storage and removal period fluids enter the flow channel at a pressure just great enough to overcome viscous effects (and therefore exit at atmospheric pressure), all of the entering pressure availability is destroyed and the $N_{\Delta P}$ term always has the value one.

Definition of Governing Equations

To actually calculate a value for the figure of merit, it is necessary to define relationships for $W_{\Delta P}$, $W_{\Delta T}$, $Sgen_{s,\Delta T}$ and $Sgen_{r,\Delta T}$. The $Sgen_{\Delta P}$ terms are not required for this analysis because of the assumption that $N_{\Delta P}$ always has the value one.

The entering availability of a unit mass of fluid in a steady state, steady flow process with negligible changes in kinetic and potential energy is given by [27]:

$$\psi = (h_{f,i} - h_\infty) - T_\infty (s_{f,i} - s_\infty) \ . \qquad (2.15)$$

For an ideal gas with constant specific heats we can write [27]:

$$(h_{f,i} - h_\infty) = Cp\ (T_{f,i} - T_\infty) \qquad (2.16a)$$

and

$$(S_\infty - S_{f,i}) = -Cp\ln\left(\frac{T_{f,i}}{T_\infty}\right) + R\ln\left(\frac{P_{f,i}}{P_\infty}\right) \ . \qquad (2.16b)$$

Substituting equation (2.16) into equation (2.15) and rearranging gives:

$$\psi = CpT_\infty\left[\left(\frac{T_{f,i} - T_\infty}{T_\infty}\right) - \ln\left(\frac{T_{f,i}}{T_\infty}\right) + \frac{R}{Cp}\ln\left(\frac{P_{f,i}}{P_\infty}\right)\right] . \qquad (2.17)$$

The total entering availability over some elapsed time is therefore:

$$\Psi = \dot{m} \int_{t=0}^{t_1} \psi \, dt \quad . \tag{2.18}$$

Because neither ψ or $\dot{m}$ are functions of time, equation (2.18) reduces to:

$$\Psi = \dot{m}\psi t_1 \quad . \tag{2.19}$$

Separating equation (2.19) into temperature and pressure components yields:

$$\Psi_{\Delta T} = \dot{m}CpT_\infty t_1 \left[\left(\frac{T_{f,i} - T_\infty}{T_\infty}\right) - \ln \left(\frac{T_{f,i}}{T_\infty}\right)\right] \tag{2.20a}$$

and

$$\Psi_{\Delta P} = \dot{m}Cp \; T_\infty t_1 \left[\frac{R}{Cp} \ln \left(\frac{P_{f,i}}{P_\infty}\right)\right] \quad . \tag{2.20b}$$

Finally, evaluating equation (2.20) for both the storage and removal period and summarizing the results yields:

$$W_{\Delta T} = \dot{m}_s CpT_\infty t_s \left[\left(\frac{T_{f,i,s} - T_\infty}{T_\infty}\right) - \ln\left(\frac{T_{f,i,s}}{T_\infty}\right)\right]$$

$$+ \dot{m}_r CpT_\infty t_r \left[\left(\frac{T_{f,i,r} - T_\infty}{T_\infty}\right) - \ln\left(\frac{T_{f,i,r}}{T_\infty}\right)\right] \qquad (2.21a)$$

and

$$W_{\Delta P} = \dot{m}_s CpT_\infty t_s \left[\frac{R}{Cp} \ln\left(\frac{P_{f,i,s}}{P_\infty}\right)\right]$$

$$+ \dot{m}_r CpT_\infty t_r \left[\frac{R}{Cp} \ln\left(\frac{P_{f,i,r}}{P_\infty}\right)\right]. \qquad (2.21b)$$

To develop the $(Sgen)_{\Delta T}$ terms, it is necessary to define expressions for the rates of entropy generation due to temperature gradients within the storage material, convective heat transfer between the flowing fluid and the material, and convective heat transfer between the hot fluid discharged during the storage period and the atmosphere.

Bejan [14] has derived the following relationship for the rate of entropy generation in a unit volume of material due to conduction through finite temperature gradients:

$$\dot{S}'''_{gen} = \frac{k_m}{T_m^2} (\nabla T)^2 \ . \tag{2.22}$$

The total entropy generated in an arbitrary volume of material during some finite time period is found by integrating equation (2.22) over both volume and time. The total entropy generated in the representative section during the storage period as a result of conduction within the material can be written as:

$$Sgen_{\Delta T,m,s} = \int_{t=0}^{t_s} \int_{x=0}^{L} \int_{y=0}^{w} \int_{z=0}^{l} \frac{k_m}{T_{m,s}^2} \left[\left(\frac{\partial T_{m,s}}{\partial x} \right)^2 + \left(\frac{\partial T_{m,s}}{\partial y} \right)^2 \right] dzdydxdt \tag{2.23a}$$

and for the removal period as:

$$Sgen_{\Delta T,m,r} = \int_{t=t_s}^{t_r} \int_{x=L}^{0} \int_{y=w}^{0} \int_{z=0}^{l} \frac{k_m}{T_{m,r}^2} \left[\left(\frac{\partial T_{m,r}}{\partial x} \right)^2 + \left(\frac{\partial T_{m,r}}{\partial y} \right)^2 \right] dzdydxdt \ . \tag{2.23b}$$

Again utilizing the results of Bejan (14), the rate of entropy generation due to convective heat transfer per unit length of flowing fluid can be written as:

$$\dot{S}gen = \left(\frac{hA}{L}\right) \frac{(T_f - T_w)^2}{T_f^2} \quad . \tag{2.24}$$

Defining the (A/L) term in equation (2.24) as a unit width, Γ, and noting that the total amount of entropy generated in the representative section as a result of convective heat transfer is determined by integrating equation (2.24) over length and time; the following equation can be written for the storage period:

$$Sgen_{f,\Delta T,s} = \int_{t=0}^{t_s} \int_{x=0}^{L} \frac{h_s \Gamma (T_{f,s} - T_{w,s})^2}{T_{f,s}^2} \, dxdt \tag{2.25a}$$

and for the removal period:

$$Sgen_{f,\Delta T,r} = \int_{t=t_s}^{t_r} \int_{x=L}^{0} \frac{h_r \Gamma \, (T_{f,r} - T_{w,r})^2}{T_{f,r}^2} \, dxdt \quad . \tag{2.25b}$$

The availability destroyed as a result of the hot fluid exiting the storage system to the surroundings can also be described by equation (2.18). There is no pressure availability destroyed because the fluid exits the system at atmospheric pressure. Thus, the total availability destroyed as a result of the hot fluid exiting to the surroundings during the storage period is given by:

$$\Psi_{exit} = \int_{t=o}^{t_s} \dot{m}_s Cp T_\infty \left[\left(\frac{T_{f,e,s} - T_\infty}{T_\infty} \right) - \ln \left(\frac{T_{f,e,s}}{T_\infty} \right) \right] dt \quad . \tag{2.26}$$

Equation (2.26) follows from equation (2.18) and the time integral remains because the fluid outlet temperature is a function of time.

Substituting equations (2.21), (2.23), (2.25), and (2.26) into (2.14) and recalling that $N_{\Delta P}$ is equal to one, the following second law figure of merit can be defined for the representative section of the storage system shown in Figure 2.1:

$$N_c = \left(\frac{\lambda}{1+\lambda}\right) + \left(\frac{1}{1+\lambda}\right) N_{\Delta T} \tag{2.27a}$$

where:

$$N_{\Delta T} = \frac{T_\infty \, Sgen_{m,\Delta T,s} + T_\infty \, Sgen_{m,\Delta T,r} + T_\infty Sgen_{f,\Delta T,s} + T_\infty \, Sgen_{f,\Delta T,r} + \Psi_{exit}}{W_{\Delta T}} , \tag{2.27b}$$

$$\lambda = \frac{W_{\Delta P}}{W_{\Delta T}} , \tag{2.27c}$$

$$W_{\Delta P} = \dot{m}_s Cp T_\infty t_s \left[\frac{R}{Cp} \ln\left(\frac{P_{f,i,s}}{P_\infty}\right)\right] + \dot{m}_r Cp T_\infty t_r \left[\frac{R}{Cp} \ln\left(\frac{P_{f,i,r}}{P_\infty}\right)\right], \tag{2.27d}$$

$$W_{\Delta T} = \dot{m}_s Cp T_\infty t_s \left[\left(\frac{T_{f,i,s} - T_\infty}{T_\infty}\right) - \ln\left(\frac{T_{f,i,s}}{T_\infty}\right)\right] + \dot{m}_r Cp T_\infty t_r \left[\left(\frac{T_{f,i,r} - T_\infty}{T_\infty}\right) - \ln\left(\frac{T_{f,i,r}}{T_\infty}\right)\right], \tag{2.27e}$$

$$Sgen_{m,\Delta T,s} = k_m \int_{t=0}^{t_s} \int_{x=0}^{L} \int_{y=0}^{w} \int_{z=0}^{l} \left[\frac{\left(\frac{\partial T_{m,s}}{\partial x}\right)^2 + \left(\frac{\partial T_{m,s}}{\partial y}\right)^2}{T_{m,s}^2} \right] dzdydxdt \quad , \tag{2.27f}$$

$$Sgen_{m,\Delta T,r} = k_m \int_{t=t_s}^{t_r} \int_{x=L}^{0} \int_{y=w}^{0} \int_{z=0}^{l} \left[\frac{\left(\frac{\partial T_{m,r}}{\partial x}\right)^2 + \left(\frac{\partial T_{m,r}}{\partial y}\right)^2}{T_{m,r}^2} \right] dzdydxdt \quad , \tag{2.27g}$$

$$Sgen_{f,\Delta T,s} = \int_{t=0}^{t_s} \int_{x=0}^{L} \frac{h_s \Gamma \, (T_{f,s} - T_{w,s})^2}{T_{f,s}^2} \, dxdt \quad , \tag{2.27h}$$

$$Sgen_{f,\Delta T,r} = \int_{t=t_s}^{t_r} \int_{x=L}^{0} \frac{h_r \Gamma \, (T_{f,r} - T_{w,r})^2}{T_{f,r}^2} \, dxdt \quad , \tag{2.27i}$$

and

$$\Psi_{exit} = \int_{t=0}^{t_s} \dot{m}_s C_p T_\infty \left[\left(\frac{T_{f,e,s} - T_\infty}{T_\infty} \right) - \ln \left(\frac{T_{f,e,s}}{T_\infty} \right) \right] dt \quad . \tag{2.27j}$$

An examination of equation (2.27) shows that to calculate a value for the figure of merit, it is necessary to specify transient fluid and material temperatures as well as fluid inlet temperatures and pressures. Expressions will now be defined to generate this information.

The transient temperature response of the representative section of the storage system is governed by a coupled set of differential equations, a one-dimensional conservation of energy for the fluid, and a two-dimensional transient heat conduction equation for the storage material. We can write for the material during the storage period:

$$\frac{\partial^2 T_{m,s}}{\partial x^2} + \frac{\partial^2 T_{m,s}}{\partial y^2} = \frac{1}{\alpha} \frac{\partial T_{m,s}}{\partial t} \quad . \tag{2.28}$$

The energy balance for hot fluid during the storage period can be written as:

$$\left(\frac{\dot{m}_s Cp_f L}{h_s A} \right) \frac{\partial T_{f,s}}{\partial x} = (T_{w,s} - T_{f,s}) \quad . \tag{2.29}$$

The initial and boundary conditions for the storage period are:

$$@t < 0 \quad T_{f,s} = T_{m,o,s} \quad , \tag{2.30a}$$

where $T_{m,o,s}$ is a constant, greater than ambient.

$$@t > 0 \quad @x = 0 \quad T_{f,s} = T_{f,i,s} \quad \frac{\partial T_{m,s}}{\partial y} = 0 \quad 0 \leq y \leq w \quad , \tag{2.30b}$$

$$@x = L \quad \frac{\partial T_m}{\partial y} = 0 \quad 0 \leq y \leq w \quad , \tag{2.30c}$$

$$@y = 0 \quad \frac{\partial T_m}{\partial x} = 0 \quad 0 \leq x \leq L \ , \tag{2.30d}$$

and

$$@y = w \quad -k_m \frac{\partial T_{m,s}}{\partial y} = h_s \ (T_{w,s} - T_{f,s}) \quad 0 \leq x \leq L \ . \tag{2.30e}$$

In a similar manner, the following mathematical description can be written for the material and cold fluid during the removal period:

$$\frac{\partial^2 T_{m,r}}{\partial x^2} + \frac{\partial^2 T_{m,r}}{\partial y^2} = \frac{1}{\alpha} \frac{\partial T_{m,r}}{\partial t} \tag{2.31}$$

and

$$\left(\frac{\dot{m}_r Cp_f L}{h_r A} \right) \frac{\partial T_{f,r}}{\partial x} = (T_{w,r} - T_{f,r}) \ . \tag{2.32}$$

Where the initial and boundary conditions for the removal period are given by:

$$@t = t_s \quad T_{m,o,r} = f(x,y) \ , \tag{2.33a}$$

$$@t > t_s \quad @x = 0 \quad \frac{\partial T_{m,r}}{\partial y} = 0 \quad 0 \leq y \leq w \ , \tag{2.33b}$$

$$@x = L \quad T_{f,r} = T_{f,i,r} \quad \frac{\partial T_{m,r}}{\partial y} = 0 \quad 0 \leq y \leq w \ , \tag{2.33c}$$

$$@y = 0 \quad \frac{\partial T_{m,r}}{\partial y} = 0 \quad 0 \leq x \leq L \ , \tag{2.33d}$$

and

$$@y = w \quad -k_m \frac{\partial T_{m,r}}{\partial y} = h_r \ (T_{w,r} - T_{f,r}) \ . \tag{2.33e}$$

For the constant property fluid and constant mass flowrate assumptions, the relationship for the fluid pressure drop in the non-circular flow channel is given by:

$$(\Delta P) = (P_{f,i} - P_\infty) = \left(\frac{fL}{Dh}\right) \left(\frac{\rho V^2}{2g_c}\right) \ . \tag{2.34}$$

Equation (2.34) can be rewritten for the storage period as:

$$(\Delta P)_s = (P_{f,i,s} - P_\infty) = \left(\frac{f_s L}{Dh}\right) \left(\frac{\rho V_s^2}{2g_c}\right) \tag{2.35a}$$

and for the removal period as:

$$(\Delta P)_r = (P_{f,i,r} - P_\infty) = \left(\frac{f_r L}{Dh}\right) \left(\frac{\rho V_r^2}{2g_c}\right) \ . \tag{2.35b}$$

Together with the figure of merit, equation (2.27); equations (2.28), (2.29), (2.30), (2.31), (2.32), (2.33), and (2.35) form a

complete set of governing equation for the representative section of storage unit.

Non-Dimensionalization of the Governing Equations

To ensure the broadest applicability of the results of this study, the set of governing equations are non-dimensionalized as follows. The following dimensionless temperature and pressure groups are defined:

$$\Theta = \frac{T - T_\infty}{T_{f,i,s} - T_\infty} \tag{2.36}$$

and

$$\beta = \frac{P - P_\infty}{P_{f,i,s} - P_\infty} \, . \tag{2.37}$$

Following Szego [22], we introduce the following dimensionless groups:

$$X = \frac{x}{L} \, , \tag{2.38a}$$

$$Y = \frac{y}{w} \, , \tag{2.38b}$$

$$V^+ = \frac{w}{L} \, , \tag{2.38c}$$

$$Bi = \frac{hw}{k_m} \, , \tag{2.38d}$$

$$Fo = \frac{\alpha t}{w^2} \, , \tag{2.38e}$$

and

$$G^{+} = \frac{Phk_m}{\dot{m}Cp_f} \quad . \tag{2.38f}$$

Note also that the dimensionless heat exchanger size, NTU, can be defined in terms of the above dimensionless groups as:

$$NTU = \frac{G^{+}Bi}{V^{+}} \quad . \tag{2.38g}$$

The temperature and pressure groups are of a standard form and the choice of ambient values as non-dimensionalization parameters was dictated by the physical problem. Ambient conditions represent a "ground state" at which a substance has zero availability. The "x" distance is non-dimensionalized using the length of the storage unit, L. The "y" distance is non-dimensionalized using the storage material half-thickness, w. The Biot number, Bi, and the Fourier number, Fo, represent, respectively, the dimensionless convective heat transfer term and the dimensionless time. The V^{+} grouping is a storage material dimensionless aspect ratio, the ratio of the symmetrical section's half-thickness to its length. The G^{+} term represents a dimensionless mass flow per unit width of section into the paper.

To begin the non-dimensionalization of the figure of merit, recall equation (2.20a); an entering fluid's temperature availability:

$$\Psi_{\Delta T} = \dot{m}CpT_{\infty}t_1 \left[\left(\frac{T_{f,i} - T_{\infty}}{T_{\infty}} \right) - \ln \left(\frac{T_{f,i}}{T_{\infty}} \right) \right] . \tag{2.20a}$$

Rewriting equation (2.20a) in terms of the dimensionless variables gives:

$$W_{\Delta\theta} = \left(\frac{\dot{m}_s CpT_\infty w^2 Fo_s}{\alpha}\right) \overline{W}_{\Delta\theta,s} + \left(\frac{\dot{m}_r CpT_\infty w^2 Fo_r}{\alpha}\right) \overline{W}_{\Delta\theta,r} \qquad (2.39a)$$

where:

$$\overline{W}_{\Delta\theta,s} = \theta_{f,i,s}\left(\frac{T_{f,i,s}}{T_\infty} - 1\right) - \ln\left[\theta_{f,i,s}\left(\frac{T_{f,i,s}}{T_\infty} - 1\right) + 1\right], \qquad (2.39b)$$

$$\overline{W}_{\Delta\theta,r} = \theta_{f,i,r}\left(\frac{T_{f,i,s}}{T_\infty} - 1\right) - \ln\left[\theta_{f,i,r}\left(\frac{T_{f,i,s}}{T_\infty} - 1\right) + 1\right], \qquad (2.39c)$$

$$\theta_{f,i,s} = 1.0 \ , \qquad (2.39d)$$

and

$$\theta_{f,i,r} = \frac{\left(\frac{T_{f,i,r}}{T_\infty} - 1\right)}{\left(\frac{T_{f,i,s}}{T_\infty} - 1\right)} \ . \qquad (2.39e)$$

Non-dimensionalization of the entering pressure availability proceeds in an identical manner. We can immediately define the following for the entering pressure availability:

$$W_{\Delta\beta} = \left(\frac{\dot{m}_s CpT_\infty w^2 Fo_s}{\alpha}\right) \overline{W}_{\Delta\beta,s} + \left(\frac{\dot{m}_r CpT_\infty Fo_r}{\alpha}\right) \overline{W}_{\Delta\beta,r} \qquad (2.40a)$$

where:

$$\overline{W}_{\Delta\beta,s} = \frac{R}{Cp} \ln \left[\beta_{f,i,s} \left(\frac{P_{f,i,s}}{P_\infty} - 1 \right) + 1 \right] , \tag{2.40b}$$

$$\overline{W}_{\Delta\beta,r} = \frac{R}{Cp} \ln \left[\beta_{f,i,r} \left(\frac{P_{f,i,s}}{P_\infty} - 1 \right) + 1 \right], \tag{2.40c}$$

$$\beta_{f,i,s} = 1 , \tag{2.40d}$$

and

$$\beta_{f,i,r} = \frac{\left(\frac{P_{f,i,r}}{P_\infty} - 1 \right)}{\left(\frac{P_{f,i,s}}{P_\infty} - 1 \right)} . \tag{2.40e}$$

Equations (2.39) and (2.40) can now be used to non-dimensionalize λ, the availability distribution ratio. Making the indicated substitutions, equation (2.27c) becomes:

$$\lambda = \frac{\left(\frac{\dot{m}_s CpT_\infty Fo_s w^2}{\alpha} \right) \overline{W}_{\Delta\beta,s} + \left(\frac{\dot{m}_r CpT_\infty Fo_r w^2}{\alpha} \right) \overline{W}_{\Delta\beta,r}}{\left(\frac{\dot{m}_s CpT_\infty To_s w^2}{\alpha} \right) \overline{W}_{\Delta\theta,s} + \left(\frac{\dot{m}_r CpT_\infty Fo_r w^2}{\alpha} \right) \overline{W}_{\Delta\theta,r}} . \tag{2.41}$$

Cancelling out the common term $(T_\infty w^2/\alpha)$, dividing the numerator and denominator by $(1./Phk_m)$, and realizing that:

$$\frac{\dot{m}Cp_f}{Phk_m} = \frac{1}{G^+} \; ; \tag{2.42}$$

the completely non-dimensionalized availability distribution ratio can be written as:

$$\lambda = \frac{\left(\frac{Fo_s}{G_s^+}\right) \overline{W}_{\Delta\beta,s} + \left(\frac{Fo_r}{G_r^+}\right) \overline{W}_{\Delta\beta,r}}{\left(\frac{Fo_s}{G_s^+}\right) \overline{W}_{\Delta\theta,s} + \left(\frac{Fo_r}{G_r^+}\right) \overline{W}_{\Delta\theta,r}} \; . \tag{2.43}$$

To begin the non-dimensionalization of the $N_{\Delta T}$ term, recall equation (2.27f); the total entropy generated in the material during the storage period:

$$Sgen_{m,\Delta T,s} = \int_{t=0}^{t_s} \int_{x=0}^{L} \int_{y=0}^{w} \int_{z=0}^{l} k_m \left[\frac{\left(\frac{\partial T_{m,s}}{\partial x}\right)^2 + \left(\frac{\partial T_{m,s}}{\partial y}\right)^2}{T_{m,s}^2} \right] dzdydxdt \; . \tag{2.27f}$$

After a straightforward non-dimensionalization of the length, time and temperature gradient terms, we can write the following for the entropy generated in the material during the storage period:

$$Sgen_{m,\Delta\theta,s} = \left(\frac{k_m wL\Gamma}{\alpha}\right) \overline{S}gen_{m,\Delta\theta,s} \tag{2.44a}$$

where:

$$\bar{S}gen_{m,\Delta\theta,s} = \int_{Fo=o}^{Fo_s} \int_{X=0}^{1} \int_{Y=0}^{1} \int_{Z=0}^{1} [\delta \bar{S}gen_{m,\Delta\theta,s}]\, dZdYdXdFo \qquad (2.44b)$$

and

$$\delta \bar{S}gen_{m,\Delta\theta,s} = \left(\frac{T_{f,i,s}}{T_\infty} - 1\right)^2 \frac{\left[V^{+2}\left(\frac{\partial\theta_{m,s}}{\partial X}\right)^2 + \left(\frac{\partial\theta_{m,s}}{\partial Y}\right)^2\right]}{\left[\theta_{m,s}\left(\frac{T_{f,i,s}}{T_\infty} - 1\right) + 1\right]^2} . \qquad (2.44c)$$

Similarly for the removal period we can show that:

$$Sgen_{m,\Delta\theta,r} = \left(\frac{k_m wL\Gamma}{\alpha}\right) \bar{S}gen_{m,\Delta\theta,r} \qquad (2.45a)$$

where:

$$\bar{S}gen_{m,\Delta\theta,r} = \int_{Fo=Fo_s}^{Fo_r} \int_{X=1}^{0} \int_{Y=1}^{0} \int_{Z=1}^{0} [\delta \bar{S}gen_{m,\Delta\theta,r}]\, dZdYdXdFo \qquad (2.45b)$$

and

$$\delta \bar{S}gen_{m,\Delta\theta,r} = \left(\frac{T_{f,i,s}}{T_\infty} - 1\right)^2 \frac{\left[V^{+2}\left(\frac{\partial\theta_{m,r}}{\partial X}\right)^2 + \left(\frac{\partial\theta_{m,r}}{\partial Y}\right)^2\right]}{\left[\theta_{m,r}\left(\frac{T_{f,i,s}}{T_\infty} - 1\right) + 1\right]^2} . \qquad (2.45c)$$

The non-dimensionalization of the fluid entropy generation terms proceeds in the same manor. Beginning with equation (2.27h) which gave the total entropy generated in the fluid during the storage period:

$$Sgen_{f,\Delta T,s} = \int_{t=0}^{t_s} \int_{x=0}^{L} \frac{h_s \Gamma \, (T_{f,s} - T_{w,s})^2}{T_{f,s}^2} \, dxdt \, , \qquad (2.27h)$$

and proceeding as before with other temperature terms results in the following equivalent dimensionless quantity:

$$Sgen_{f,\Delta\theta,s} = \left(\frac{h_s \Gamma L w^2}{\alpha}\right) \left[\bar{S}gen_{f,\Delta\theta,s}\right] \qquad (2.46a)$$

where:

$$\bar{S}gen_{f,\Delta\theta,s} = \int_{Fo=o}^{Fo_s} \int_{X=0}^{1} \left[\delta Sgen_{f,\Delta\theta,s}\right] dXdFo \qquad (2.46b)$$

and

$$\delta\bar{S}gen_{f,\Delta\theta,s} = \frac{\left(\frac{T_{f,i,s}}{T_\infty} - 1\right)^2 (\theta_{f,s} - \theta_{w,s})^2}{\left[\theta_{f,s}\left(\frac{T_{f,i,s}}{T_\infty} - 1\right) + 1\right]^2} \, . \qquad (2.46c)$$

The identical operation for the removal period term, (2.27i), results in:

$$Sgen_{f,\Delta\theta,r} = \left(\frac{h_r \Gamma L w^2}{\alpha}\right) [\bar{S}gen_{f,\Delta\theta,r}] \qquad (2.47a)$$

where:

$$\bar{S}gen_{f,\Delta\theta,r} = \int_{Fo=Fo_s}^{Fo_r} \int_{X=1}^{0} [\delta\bar{S}gen_{f,\Delta\theta,r}]\, dX dFo \qquad (2.47b)$$

and

$$\delta\bar{S}gen_{f,\Delta\theta,r} = \frac{\left(\frac{T_{f,i,s}}{T_\infty} - 1\right)^2 (\theta_{f,r} - \theta_{w,r})^2}{\left[\theta_{f,r}\left(\frac{T_{f,i,s}}{T_\infty} - 1\right) + 1\right]^2} \; . \qquad (2.47c)$$

The equation for the exiting availability that is destroyed due to the discharged hot fluid coming to equilibrium with the environment is non-dimensionalized in a manner identical to the entering fluid availability term. This operation results in:

$$\Psi_{exit} = \left(\dot{m}_s C_p T_\infty w^2\right) \bar{\Psi}_{exit} \qquad (2.48a)$$

where:

$$\overline{\Psi}_{exit} = \int_{Fo=o}^{Fo_s} \delta\overline{\Psi}_{exit} \; dFo \tag{2.48b}$$

and

$$\delta\overline{\Psi}_{exit} = \theta_{f,e,s}\left(\frac{T_{f,i,s}}{T_\infty} - 1\right) - \ln\left[\theta_{f,e,s}\left(\frac{T_{f,i,s}}{T_\infty} - 1\right) + 1\right]. \tag{2.48c}$$

Equations (2.39), (2.44), (2.45), (2.46), (2.47), and (2.48) are used to non-dimensionalize the $N_{\Delta T}$ term in (2.27b). Making these substitutions gives:

$$N_{\Delta T} = \frac{\left(\frac{T_\infty k_m w L \Gamma}{\alpha}\right)\overline{S}gen_{m,\Delta\theta,s} + \left(\frac{T_\infty k_m w L \Gamma}{\alpha}\right)\overline{S}gen_{m,\Delta\theta,r} + \left(\frac{T_\infty h_s \Gamma L w^2}{\alpha}\right)\overline{S}gen_{f,\Delta\theta,s} + \left(\frac{T_\infty h_r \Gamma L w^2}{\alpha}\right)\overline{S}gen_{f,\Delta\theta,r} + \left(\dot{m}_s Cp T_\infty w^2\right)\overline{\Psi}_{exit}}{\left(\frac{\dot{m}_s Cp T_\infty Fo_s w^2}{\alpha}\right)\overline{W}_{\Delta\theta,s} + \left(\frac{\dot{m}_r Cp T_\infty Fo_r w^2}{\alpha}\right)\overline{W}_{\Delta\theta,r}}. \tag{2.49}$$

Cancelling out the common term T_∞/α and factoring out a $w^2\Gamma k_m$ term from the numerator and denominator of (2.49) results in:

$$N_{\Delta T} = \frac{\left(\frac{L}{w}\right)\overline{S}gen_{m,\Delta\theta,s} + \left(\frac{L}{w}\right)\overline{S}gen_{m,\Delta\theta,r} + \left(\frac{h_s L}{k_m}\right)\overline{S}gen_{f,\Delta\theta,s} + \left(\frac{h_r L}{k_m}\right)\overline{S}gen_{f,\Delta\theta,r} + \left(\frac{\dot{m}_s Cp}{\Gamma k_m}\right)\overline{\Psi}_{exit}}{\left(\frac{\dot{m}_s Cp Fo_s}{\Gamma k}\right)\overline{W}_{\Delta\theta,s} + \left(\frac{\dot{m}_r Cp Fo_r}{\Gamma k}\right)\overline{W}_{\Delta\theta,r}}. \tag{2.50}$$

Note that the variable Γ represents a unit width (i.e., into the paper) of the representative fluid-material section. For the flat slab configuration, the unit width is also the heated perimeter, Ph. Making this substitution into equation (2.50) and noting that

$$\frac{L}{w} = \frac{1}{V^+} ,$$

$$\frac{hL}{k_m} = \frac{Bi}{V^+} ,$$

and

$$\frac{\dot{m}Cp_f}{Phk_m} = G^+ ;$$

the completely non-dimensionalized $N_{\Delta T}$ term can be written as:

$$N_{\Delta T} = \frac{\left(\frac{1}{V^+}\right)\overline{S}gen_{m,\Delta\theta,s} + \left(\frac{1}{V^+}\right)\overline{S}gen_{m,\Delta\theta,r} + \left(\frac{Bi,s}{V^+}\right)\overline{S}gen_{f,\Delta\theta,s} + \left(\frac{Bi,r}{V^+}\right)\overline{S}gen_{f,\Delta\theta,r} + \left(\frac{1}{G_s^+}\right)\overline{\Psi}_{exit}}{\left(\frac{Fo_s}{G_s^+}\right)\overline{W}_{\Delta\theta,s} + \left(\frac{Fo_r}{G_r^+}\right)\overline{W}_{\Delta\theta,r}} . \qquad (2.51)$$

Equations (2.43) and (2.51) can now be utilized to calculate a value of the figure of merit as a function of the dimensionless system of variables.

The non-dimensionalization of the fluid-material thermal response equations is quite straightforward and will not be repeated here. The reader is invited to read references [21] and [22] for details. The dimensionless transient response equations for the storage period are then:

$$V^{+2}\frac{\partial^2\theta_{m,s}}{\partial X^2}+\frac{\partial^2\theta_{m,s}}{\partial Y^2}=\frac{\partial\theta_{m,s}}{\partial Fo} \tag{2.52}$$

and

$$\frac{\partial\theta_{f,s}}{\partial X}+\left(\frac{G_s^{+}Bi_s}{V^{+}}\right)(\theta_{f,s}-\theta_{w,s})=0\ . \tag{2.53}$$

The initial and boundary conditions are given by:

$$@\ Fo=0\quad \theta_{m,o,s}=\frac{\left(\frac{T_{m,o,s}}{T_\infty}-1\right)}{\left(\frac{T_{f,i,s}}{T_\infty}-1\right)}\ , \tag{2.54a}$$

$$@\ X=0\quad \theta_{f,s}=\theta_{f,i,s}\qquad \frac{\partial\theta_{m,s}}{\partial Y}=0\qquad 0\leq Y\leq 1\ , \tag{2.54b}$$

$$@\ X=1\qquad \frac{\partial\theta_{m,s}}{\partial Y}=0\qquad 0\leq Y\leq 1\ , \tag{2.54c}$$

$$@\ Y=0\qquad \frac{\partial\theta_{m,s}}{\partial X}=0\qquad 0\leq X\leq 1\ , \tag{2.54d}$$

and

$$@\ Y=1 \qquad \frac{\partial \theta_{m,s}}{\partial Y} = Bi_s\ [\theta_{f,s} - \theta_{w,s}] \qquad 0 \leq X \leq 1\ . \qquad (2.54e)$$

Similarily we can write for the removal period:

$$v^{+2}\ \frac{\partial^2 \theta_{m,r}}{\partial X^2} + \frac{\partial^2 \theta_{m,r}}{\partial Y^2} = \frac{\partial \theta_{m,r}}{\partial Fo} \qquad (2.55)$$

and

$$\frac{\partial \theta_{f,r}}{\partial X} + \left(\frac{G_r^+ Bi_r}{v^+}\right)\ (\theta_{f,r} - \theta_{w,r}) = 0\ . \qquad (2.56)$$

The initial and boundary conditions are given by:

$$@\ Fo=Fo_s \qquad \theta_{m,o} = F(X,Y)\ , \qquad (2.57a)$$

$$@X=0 \qquad \frac{\partial \theta_{m,r}}{\partial Y} = 0 \qquad 0 \leq Y \leq 1\ , \qquad (2.57b)$$

$$@X=1 \qquad \theta_{f,r} = \theta_{f,i,r} \qquad \frac{\partial \theta_{m,r}}{\partial Y} = 0 \qquad 0 \leq Y \leq 1\ , \qquad (2.57c)$$

$$@Y=0 \qquad \frac{\partial \theta_{m,r}}{\partial X} = 0 \qquad 0 \leq X \leq 1\ , \qquad (2.57d)$$

and

$$@Y=1 \qquad \frac{\partial \Theta_{m,r}}{\partial Y} = Bi_r \left[\Theta_{f,r} - \Theta_{w,r}\right] \quad 0 \leq X \leq 1 \; . \qquad (2.57e)$$

To begin the non-dimensionalization of the pressure drop equations, recall equation (2.34):

$$(P_{f,i} - P_\infty) = \left(\frac{fL}{Dh}\right)\left(\frac{\rho V^2}{2g_c}\right) . \qquad (2.34)$$

Define the following terms:

$$A_{cs} = Phd$$

and

$$Dh = 4d \; .$$

Substituting Dh = 4d into (2.34) results in:

$$(P_{f,i} - P_\infty) = \left(\frac{f}{8}\right)\left(\frac{LPh}{A_{cs}}\right)\left(\frac{\rho V^2}{g_c}\right) . \qquad (2.58)$$

Recognizing that:

$$\frac{G^+ Bi}{V^+} = \frac{PhLh}{\dot{m}Cp_f} , \qquad (2.59)$$

and solving this term for PhL, and substituting the result into equation (2.58) gives:

$$(P_{f,i} - P_{\infty}) = \left(\frac{f}{8}\right)\left(\frac{G^{+}Bi}{V^{+}}\right)\left(\frac{\dot{m}Cp_{f}}{A_{cs}h}\right)\left(\frac{\rho V^{2}}{g_{c}}\right) \quad . \tag{2.60}$$

Noting that:

$$\frac{\dot{m}}{A_{cs}} = \rho V \text{ and } \frac{h}{\rho VCp} = St \quad ,$$

and rewriting equation (2.60) gives:

$$(P_{f,i} - P_{\infty}) = \left(\frac{f}{8St}\right)\left(\frac{G^{+}Bi}{V^{+}}\right)\left(\frac{\rho V^{2}}{g_{c}}\right). \tag{2.61}$$

Recalling Reynolds analogy [56]:

$$StPr^{2/3} = \frac{f}{8} \quad ,$$

equation (2.61) becomes:

$$(P_{f,i} - P_{\infty}) = Pr^{2/3}\left(\frac{G^{+}Bi}{V^{+}}\right)\left(\frac{1}{\rho g_{c}}\right)\left(\frac{\dot{m}}{A_{cs}}\right)^{2} \quad . \tag{2.62}$$

The ideal gas equation of state yields:

$$\frac{1}{\rho} = \frac{RT_{f,i}}{P_{f,i}} \quad . \tag{2.63}$$

Rewriting equation (2.63) in terms of the dimensionless variables gives:

$$\frac{1}{\rho} = \frac{RT_\infty}{P_\infty}\left[\frac{\theta_{f,i}\left(\frac{T_{f,i,s}}{T_\infty} - 1\right) + 1}{\beta_{f,i}\left(\frac{P_{f,i,s}}{P_\infty} - 1\right) + 1}\right] . \qquad (2.64)$$

Substituting equation (2.64) into equation (2.62) gives:

$$\frac{P_{f,i}}{P_\infty} - 1 = Pr^{2/3}\ \frac{G^+Bi}{V^+}\left[\frac{\theta_{f,i}\left(\frac{T_{f,i,s}}{T_\infty} - 1\right) + 1}{\beta_{f,i}\left(\frac{P_{f,i,s}}{P_\infty} - 1\right) + 1}\right]\tau \qquad (2.65a)$$

where:

$$\tau \equiv \left[\frac{\dot{m}}{A_{cs}\ P_\infty}\sqrt{\frac{RT_\infty}{g_c}}\right]^2 . \qquad (2.65b)$$

τ is a dimensionless mass velocity parameter common in thermal analysis problems.

An inspection of equation (2.40b) and equation (2.40c) shows that the pressure ratio $P_{f,i}/P_\infty$ is required to calculate the inlet fluids pressure availability. Solving equation (2.65a) for the required inlet pressure excess (i.e., an amount greater than ambient) and substituting the value of $\beta_{f,i,s}$ as given by (2.40d), the following can be written for the fluid inlet pressure excess during the storage period:

$$\frac{P_{f,i,s}}{P_\infty} = 0.5 + \sqrt{0.25 + \Delta\beta_s} \qquad (2.66a)$$

where:

$$\Delta\beta_s = Pr^{2/3}\left(\frac{G_s^+ Bi_s}{V^+}\right)\left[\theta_{f,i,s}\left(\frac{T_{f,i,s}}{T_\infty} - 1\right) + 1\right]\tau_s \,. \qquad (2.66b)$$

Substituting the definition of $\beta_{f,i,r}$ given by equation (2.40e) into equation (2.65a) and solving for the inlet fluid pressure excess during the removal period gives:

$$\frac{P_{f,i,r}}{P_\infty} = 1.0 + \sqrt{\Delta\beta_r} \qquad (2.67a)$$

where:

$$\Delta\beta_r = Pr^{2/3}\left(\frac{G_r^+ Bi_r}{V^+}\right)\frac{\left[\theta_{f,i,r}\left(\frac{T_{f,i,s}}{T_\infty} - 1\right) + 1\right]\tau_r}{\left[\frac{\left(\frac{P_{f,i,s}}{P_\infty} - 1\right) + 1}{\left(\frac{P_{f,i,s}}{P_\infty} - 1\right)}\right]} \,. \qquad (2.67b)$$

To complete the set of governing equations it is necessary to make an observation concerning material temperatures and to discuss certain aspects of the execution of the numerical model. The dimensionless wall temperature variable, Θ_w, which appears in several equations is actually the temperature of the solid storage material evaluated at Y=1. Thus, we may write for the storage period:

$$\Theta_{w,s} = f\,(X,Y,\Theta_{m,s}) \qquad (2.68a)$$

and for the removal period:

$$\theta_{w,r} = f\,(X,Y,\theta_{m,r})\ . \qquad (2.68b)$$

Prior to the analysis of the removal period, three variables must be defined; G_r^+, Bi_r, and τ_r. It is assumed that their value is a simple ratio of their storage period amount. However, because of geometry considerations, whichever constant is used to ratio τ_s must also be used to ratio G_s^+ and Bi_s. The reasons for this requirement can be explained by examining equations (2.38f), (2.38d), and (2.65b). They represent, respectively, definitions for G^+, Bi, and τ_s, and we observe that each equation contains several constant terms. These are either material or fluid physical properties, ambient temperatures and pressures, or a storage material geometry parameter. The physical properties are assumed to be the same for the storage and removal periods, ambient conditions and material geometry cannot change between the storage and removal periods. Because of the presence of these constants, the ratio of τ_r to τ_s reduces to a ratio of fluid mass flowrates. Specifically, it reduces to the square of the ratio of removal period to storage period mass flowrates. We now observe that the ratio of G_r^+ to G_s^+ reduces to the ratio of mass flowrates for the storage and removal periods. We observe that this is the inverse of the square root of the ratio of τ_r to τ_s. We conclude that whichever constant is multiplied by τ_s to determine τ_r; the inverse of the square root of that constant must also be used to determine the value of G_r^+. Because it is assumed

that the heat transfer coefficient, h, in equation (2.38d) is a linear function of the fluid mass flowrate; Bi_s must also be multiplied by the square root of the same constant to define Bi_r. Incorporating this requirements into the mathematical model results in:

$$\tau_r = f\ (C_1, \tau_s)\ , \tag{2.69a}$$

$$G_r^+ = f\ (C_1, G_s^+)\ , \tag{2.69b}$$

and

$$Bi_r = f\ (C_1, Bi_s)\ . \tag{2.69c}$$

Closure of the Model and Description of the Optimization Study

The set of non-dimensionalized equations that describe the entropy generation characteristics of the representative section of storage unit are summarized below.

$$N_c = \left(\frac{\lambda}{1+\lambda}\right) + \left(\frac{1}{1+\lambda}\right) N_{\Delta T} \tag{2.27a}$$

$$\lambda = \frac{\dfrac{Fo_s}{G_s^+}\,\overline{W}_{\Delta\beta,s} + \dfrac{Fo_r}{G_r^+}\,\overline{W}_{\Delta\beta,r}}{\dfrac{Fo_s}{G_s^+}\,\overline{W}_{\Delta\theta,s} + \dfrac{Fo_r}{G_r^+}\,\overline{W}_{\Delta\theta,r}} \tag{2.43}$$

$$G_r^+ = f\ (C_1, G_s^+) \tag{2.69b}$$

$$\overline{W}_{\Delta\beta,s} = \frac{R}{Cp} \ln\left[B_{f,i,s}\left(\frac{P_{f,i,s}}{P_\infty} - 1\right) + 1\right] \tag{2.40b}$$

$$\overline{W}_{\Delta\beta,r} = \frac{R}{Cp} \ln\left[B_{f,i,r}\left(\frac{P_{f,i,s}}{P_\infty} - 1\right) + 1\right] \tag{2.40c}$$

$$\beta_{f,i,s} = 1 \tag{2.40d}$$

$$\beta_{f,i,r} = \frac{\left(\frac{P_{f,i,r}}{P_\infty} - 1\right)}{\left(\frac{P_{f,i,s}}{P_\infty} - 1\right)} \tag{2.40e}$$

$$\overline{W}_{\Delta\Theta,s} = \Theta_{f,i,s}\left(\frac{T_{f,i,s}}{T_\infty} - 1\right) - \ln\left[\Theta_{f,i,s}\left(\frac{T_{f,i,s}}{T_\infty} - 1\right) + 1\right] \tag{2.39b}$$

$$\overline{W}_{\Delta\Theta,r} = \Theta_{f,i,r}\left(\frac{T_{f,i,s}}{T_\infty} - 1\right) - \ln\left[\Theta_{f,i,r}\left(\frac{T_{f,i,s}}{T_\infty} - 1\right) + 1\right] \tag{2.39c}$$

$$\Theta_{f,i,s} = 1 \tag{2.39d}$$

$$\Theta_{f,i,r} = \frac{\left(\frac{T_{f,i,r}}{T_\infty} - 1\right)}{\left(\frac{T_{f,i,s}}{T_\infty} - 1\right)} \tag{2.39e}$$

$$N_{\Delta T} = \frac{\left(\frac{1}{V^+}\right)\overline{S}gen_{m,\Delta\theta,s} + \left(\frac{1}{V^+}\right)\overline{S}gen_{m,\Delta\theta,r} + \left(\frac{Bi_s}{V^+}\right)\overline{S}gen_{f,\Delta\theta,s} + \left(\frac{Bi_r}{V^+}\right)\overline{S}gen_{f,\Delta\theta,r} + \left(\frac{1}{G_s^+}\right)\overline{\Psi}_{exit}}{\left(\frac{Fo_s}{G_s^+}\right)\overline{W}_{\Delta\theta,s} + \left(\frac{Fo_r}{G_r^+}\right)\overline{W}_{\Delta\theta,r}} \qquad (2.51)$$

$$Bi_r = f\ (C_1, Bi_s) \qquad (2.69c)$$

$$\overline{S}gen_{m,\Delta\theta,s} = \int_{Fo=0}^{Fo_s} \int_{X=0}^{1} \int_{Y=0}^{1} \int_{Z=0}^{1} \delta\overline{S}gen_{m,\Delta\theta,s}\ dZdYdXdFo \qquad (2.44b)$$

$$\delta\overline{S}gen_{m,\Delta\theta,s} = \left(\frac{T_{f,i,s}}{T_\infty} - 1\right)^2 \frac{V^{+2}\left(\frac{\partial\theta_{m,s}}{\partial X}\right)^2 + \left(\frac{\partial\theta_{m,s}}{\partial Y}\right)^2}{\left[\theta_{m,s}\left(\frac{T_{f,i,s}}{T_\infty} - 1\right) + 1\right]^2} \qquad (2.44c)$$

$$\overline{S}gen_{m,\Delta\theta,r} = \int_{Fo=Fo_s}^{Fo_r} \int_{X=1}^{0} \int_{Y=1}^{0} \int_{Z=1}^{0} \delta\overline{S}gen_{m,\Delta\theta,r}\ dZDYdXdFo \qquad (2.45b)$$

$$\delta\overline{S}gen_{m,\Delta\theta,r} = \left(\frac{T_{f,i,s} - 1}{T_\infty}\right)^2 \frac{V^{+2}\left(\frac{\partial\theta_{m,r}}{\partial X}\right)^2 + \left(\frac{\partial\theta_{m,r}}{\partial Y}\right)^2}{\left[\theta_{m,r}\left(\frac{T_{f,i,s}}{T_\infty} - 1\right) + 1\right]^2} \qquad (2.45c)$$

$$\overline{S}gen_{f,\Delta\theta,s} = \int_{Fo=0}^{Fo_s} \int_{X=0}^{1} \delta\overline{S}gen_{f,\Delta\theta,s}\, dXdFo \tag{2.46b}$$

$$\delta\overline{S}gen_{f,\Delta\theta,s} = \frac{\left(\frac{T_{f,i,s}}{T_\infty} - 1\right)^2 (\theta_{f,s} - \theta_{w,s})^2}{\left[\theta_{f,s}\left(\frac{T_{f,i,s}}{T_\infty} - 1\right) + 1\right]^2} \tag{2.46c}$$

$$\theta_{w,s} = f\ (X,Y,\theta_{m,s}) \tag{2.68a}$$

$$\overline{S}gen_{f,\Delta\theta,r} = \int_{Fo=Fo_s}^{Fo_r} \int_{X=1}^{0} \delta\overline{S}gen_{f,\Delta\theta,r}\, dXdFo \tag{2.47b}$$

$$\delta\overline{S}gen_{f,\Delta\theta,r} = \frac{\left(\frac{T_{f,i,s}}{T_\infty} - 1\right)^2 (\theta_{f,r} - \theta_{w,r})^2}{\left[\theta_{f,r}\left(\frac{T_{f,i,s}}{T_\infty} - 1\right) + 1\right]^2} \tag{2.47c}$$

$$\theta_{w,r} = f\ (X,Y,\theta_{m,r}) \tag{2.68b}$$

$$\overline{\Psi}_{exit} = \int_{Fo=0}^{Fo_s} \delta\overline{\Psi}_{exit}\, dFo \tag{2.48b}$$

$$\delta\bar{\Psi}_{exit} = \theta_{f,e,s}\left(\frac{T_{f,i,s}}{T_\infty} - 1\right) - \ln\left[\theta_{f,e,s}\left(\frac{T_{f,i,s}}{T_\infty} - 1\right) + 1\right] \tag{2.48c}$$

$$V^{+2}\frac{\partial^2\theta_{m,s}}{\partial X^2} + \frac{\partial^2\theta_{m,s}}{\partial Y^2} = \frac{\partial\theta_{m,s}}{\partial Fo} \tag{2.52}$$

$$\frac{\partial\theta_{f,s}}{\partial X} + \left(\frac{G_s^+ Bi_s}{V^+}\right)(\theta_{f,s} - \theta_{w,s}) = 0 \tag{2.53}$$

$$\theta_{m,o,s} = \frac{\left(\frac{T_{m,o,s}}{T_\infty} - 1\right)}{\left(\frac{T_{f,i,s}}{T_\infty} - 1\right)} \tag{2.54a}$$

$$\theta_{f,s}(0) = \theta_{f,i,s} \tag{2.54b}$$

$$V^{+2}\frac{\partial^2\theta_{m,r}}{\partial X^2} + \frac{\partial^2\theta_{m,r}}{\partial Y^2} = \frac{\partial\theta_{m,r}}{\partial F_o} \tag{2.55}$$

$$\frac{\partial\theta_{f,r}}{\partial X} + \left(\frac{G_r^+ Bi_r}{V^+}\right)(\theta_{f,r} - \theta_{w,r}) \tag{2.56}$$

$$\theta_{f,r}(L) = \theta_{f,i,r} \tag{2.57c}$$

$$\frac{P_{f,i,s}}{P_\infty} = 0.5 + \sqrt{0.25 + \Delta\beta_s} \tag{2.66b}$$

$$\Delta\beta_s = Pr^{2/3}\left(\frac{G_s^+ Bi_s}{V^+}\right)\left[\theta_{f,i,s}\left(\frac{T_{f,i,s}}{T_\infty} - 1\right) + 1\right]\tau_s \tag{2.66b}$$

$$\frac{P_{f,i,r}}{P_\infty} = 1 + \sqrt{\Delta\beta_r} \tag{2.67a}$$

$$\Delta\beta_r = Pr^{2/3}\frac{\left(\frac{G_r^+ Bi_r}{V^+}\right)\left[\theta_{f,i,r}\left(\frac{T_{f,i,s}}{T_\infty} - 1\right) + 1\right]\tau_r}{\left[\frac{\left(\frac{P_{f,i,s}}{P_\infty} - 1\right) + 1}{\left(\frac{P_{f,i,s}}{P_\infty} - 1\right)}\right]} \tag{2.67b}$$

$$\tau_r = f(C_1, \tau_s) \tag{2.69a}$$

Thus, the numerical model consists of 37 equations in 48 variables. These 48 variables are:

N_c, λ, $N_{\Delta T}$, Fo_s, G_s^+, $\overline{W}_{\Delta\beta,s}$, Fo_r, G_r^+, $\overline{W}_{\Delta\beta,r}$,

$\overline{W}_{\Delta\theta,s}$, $\overline{W}_{\Delta\theta,r}$, C_1, $\frac{R}{Cp}$, $\beta_{f,i,s}$, $\frac{P_{f,i,s}}{P_\infty}$, $\beta_{f,i,r}$,

$\frac{P_{f,i,r}}{P_\infty}$, $\theta_{f,i,s}$, $\frac{T_{f,i,s}}{T_\infty}$, $\theta_{f,i,r}$, $\frac{T_{f,i,r}}{T_\infty}$, V^+, $\overline{S}gen_{m,\Delta\theta,s}$

$\overline{S}gen_{m,\Delta\theta,r}$, $\overline{S}gen_{f,\Delta\theta,s}$, $\overline{S}gen_{f,\Delta\theta,r}$, $\overline{\Psi}_{exit}$, $\delta\overline{S}gen_{m,\Delta\theta,s}$, $\delta\overline{S}gen_{m,\Delta\theta,r}$

$\delta\overline{S}gen_{f,\Delta\theta,s}$, $\delta\overline{S}gen_{f,\Delta\theta,r}$, $\delta\overline{\Psi}_{exit}$, Bi_s, Bi_r, $\theta_{m,s}$, $\theta_{m,r}$,

$\theta_{f,s}$, $\theta_{w,s}$, $\theta_{f,r}$, $\theta_{w,r}$, $\theta_{m,o,s}$, $\frac{T_{m,o,s}}{T_\infty}$, $\theta_{f,e,s}$, $\Delta\beta_s$,

Pr, τ_s, $\Delta\beta_r$, and τ_r.

Thus, there are 11 independent variables in the problem. For this study of a flat slab regenerator, the independent variables were chosen to be:

$$Fo_s,\ G_s^+,\ C_1,\ \frac{R}{Cp},\ \frac{T_{f,i,s}}{T_\infty},\ \frac{T_{f,i,r}}{T_\infty},\ V^+,\ Bi_s,\ \frac{T_{m,o,s}}{T_\infty},\ Pr,\ \text{and}\ \tau_s\ .$$

It is obvious that a large number and variety of design problems could be formulated with this model. Since the purpose of this present study is to define configurations which minimize the production of entropy, an optimization program was employed to control the execution of the model and systematically determine these configurations. To make it

a tractable problem it was necessary to limit the number of variables that the optimization routine could control. This was accomplished by organizing the 11 independent variables into either "design", or "optimization" variables. Design variables are defined as those whose values are fixed for a given case. Optimization variables, as the name implies, are those variables whose values are controlled by the optimization routine such that the figure of merit is minimized. For this study, the 11 independent variables were divided into eight design and three optimization variables and the distribution was made to give realistic design cases. The optimization variables were chosen to be:

$$Fo_s,\ G_s^+,\ \text{and}\ Bi_s.$$

Thus, the design variables were:

$$C_1,\ \frac{R}{Cp},\ \frac{T_{f,i,s}}{T_\infty},\ \frac{T_{f,i,r}}{T_\infty},\ V^+,\ \frac{T_{m,o,s}}{T_\infty},\ Pr,\ \text{and}\ \tau_s\ .$$

The choice of optimization variables was made to permit the simultaneous optimization of both geometry and operating parameters. The rationale for these choices can best be explained by briefly summarizing the steps in the procedure that could be used to translate the dimensionless results into an actual design. These steps, which assume that all the necessary constants have been defined, are as follows:

a. The dimensionless mass velocity design variable, τ_s, and the optimum value of the dimensionless mass flow term, G_s^+, are used to define the flow channel half-height, d.

b. The dimensionless mass velocity and the flow channel half-height are used to calculate the Reynolds number.

c. The Reynolds number and the Prandtl number (a design variable) are used to calculate the convective heat transfer coefficient, h.

d. The optimum storage period Biot number, Bi_s, and the convective heat transfer coefficient are used to calculate the storage material half-thickness, w.

e. The dimensionless storage material aspect ratio, V^+, and the material half-thickness are used to calculate the length, L, of the storage unit.

f. The optimum value of the dimensionless storage time, Fo_s, and the material half-thickness are used to calculate the dimensional storage time.

As these steps illustrate, the particular combination of design and optimization variables chosen for this study (while not necessarily unique) do permit physical characteristics such as width and length, and operating characteristics such as storage time, to be determined in a single exercise.

To summarize, this study will define the optimum physical design, operating parameters, and entropy generation characteristics of a number of design cases. An optimized system is one that operates with a minimum amount of generated entropy for a complete storage-removal cycle. This will be accomplished using the finite conductivity mathematical model defined above, running under control of an optimization program. A design case will consist of a set of values for the eight design

variables and the resulting (i.e., calculated by the optimization program) set of three optimization variables. A sufficient number of cases will be run to adequately define the effect of changes in the design variables on the optimium system. Most importantly, these optimization studies will be unconstrained. This means that the optimization program is free to minimize the figure of merit without first having satisfied some additional requirement such as a minimum first law efficiency, minimum flow channel diameter, or a maximum physical size.

3. DEVELOPMENT OF THE NUMERICAL MODEL

In order to execute the analytical model as a part of an optimization study, two separate computer programs must be available. These are a routine to calculate the figure of merit for a complete storage-removal cycle and an optimization routine to systematically determine values of the optimization variables that result in a minimum value for the figure of merit. The following information details the construction of the program to calculate the figure of merit and discusses the proprietary optimization routine selected for use in the analysis.

Discussion of the Optimization Routine Used in the Study

An optimization program which resides in the University of Tennessee computer library was utilized for the analysis. This program, GRG2, is a sophisticated routine for solving problems with either linear or non-linear objective functions and constraints. It is based on the generalized reduced gradient algorithm and has a modular construction to permit its use with completely independent objective function subroutines. The basic GRG algorithm has been extensively investigated [48,49] and the GRG2 program itself has been well documented and tested [48,50,51]. These comparative evaluations have established that GRG2 is one of the most capable and versatile non-linear optimization programs available.

For the end user, the GRG2 program is very easy to use. In addition to a specific data input format, it requires only one user supplied subroutine. This subroutine, which must be named GCOMP, calculates the

objective function for values of the optimization variables. For this study, the objective function is the figure of merit, Nc, defined in Section 2. A typical optimization sequence consists of a continuous exchange of information between GRG2 and GCOMP. The GRG2 program passes values of the optimization variables to GCOMP and in return receives a corresponding value for the figure of merit. Using its own algorithm, GRG2 systematically determines the one set of optimization variable values that result in a minimum figure of merit.

The GRG algorithm is a non-linear extension of the simplex method for linear programming. It was not possible to become technically proficient in all the facets of either the basic algorithm or the operation of the GRG2 program. However, in order to efficiently conduct an optimization exercise and insure that the program was generating accurate results, it was necessary to learn something about its behavior during an actual optimization cycle.

To determine if a particular set of results were acceptable, it was necessary to understand the meaning of certain status variables supplied by GRG2 at the end of a cycle. This experience was gained during the verification procedure and will be described later in this section. The one aspect of GRG2's operation that affected both the execution and interpretation of results was the method it used to calculate the partial derivatives of the objective function. Because of the complexity of the objective function, it was not possible to supply exact analytical relationships to calculate the partial derivatives. Accordingly, GRG2 was required to calculate them using a multistep procedure. It accomplished

this by determining the change in the ojective function for an incremental change in the optimization variable of interest. The incremental length used to determine this change is a constant embedded in the programming of GRG2 and it is not normally possible to change its value. If it is too small (relative to the magnitude of the partial derivative), GRG2 can mistakenly conclude the objective function is in a region of little of no change and stop the optimization. This situation affects the choice of the initial value of the optimization variables supplied to GRG2 at the beginning of an optimization exercise. If this initial value results in a value of the objective function in the "flats" of its surface, GRG2 cannot recover and will terminate. Small incremental lengths also prevent GRG2 from realizing when it is operating in an area of local "plateaus" far removed from the actual minimum point. If the incremental length is too large; there is the possibility that the discrete function evaluations will be made "across" a minimum point, thus preventing GRG2 from finding a true minimum value for the objective function. The specific effects this fixed incremental length had on the final results of the study will be discussed in Section 4.

Description of the Program to Calculate the Figure of Merit

The primary configuration to be examined in this study is the counterflow regenerator operating without a dwell period. A dwell period is the interval between the storage and removal periods during which the storage material temperature gradients are allowed to reach a uniform average temperature. There are, however, two other

configurations of interest: parallel flow with a dwell period and parallel flow without a dwell period. The effects of the dwell period are included in this study because entropy generation occurs as a result of the material reaching a uniform temperature. A computer program, ENTROP, was written to calculate the figure of merit, Nc, for these three configurations. It was written in double precision FORTRAN and in a form to permit interface with the GRG2 program. A listing of ENTROP, a glossary of the subroutines, and some typical output are contained in Appendix A. The following is a brief description of the operation of the program and the numerical techniques employed.

In the most macroscopic sense, the program performs five basic computations to generate the information needed to calculate a value for the figure of merit. They are:

a. calculate the total entering availability and entropy generated during the storage period,

b. determine an approximate dwell time,

c. calculate the total entropy generated during the dwell period,

d. determine an approximate removal time, and

e. calculate the total entering availability and entropy generated during the removal period.

These five basic steps are explained below and summarized in Figure 3.1.

The sequence begins with GRG2 passing the most current value for the storage period time, Fo_s, mass flow parameter, G_s^+, and Biot number, Bi_s. Using this information, ENTROP calculates the total entering fluid availability per unit time. It then calculates the fluid-material

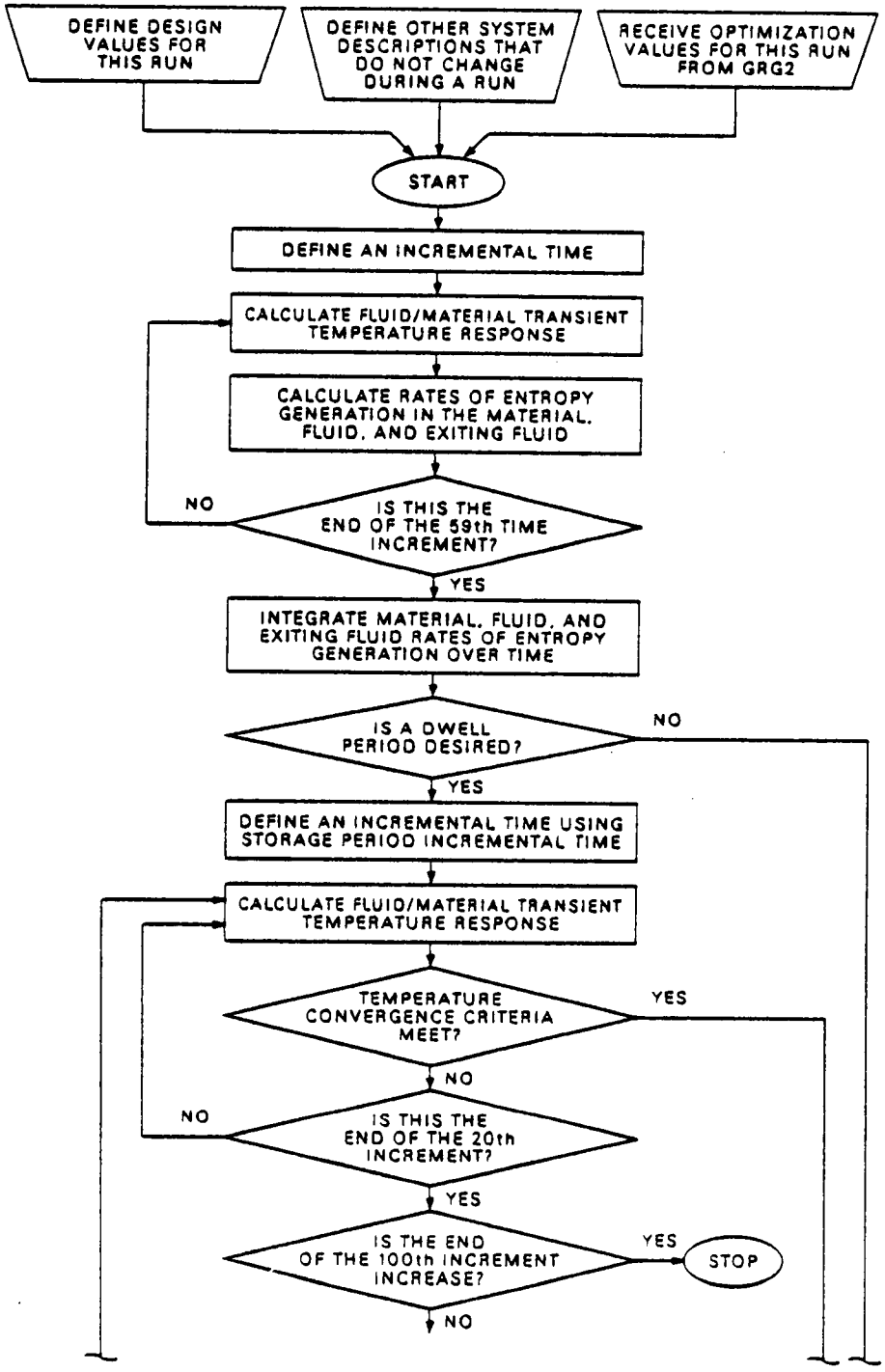


Figure 3.1. Schematic representative of the most general ENTROP execution sequence.

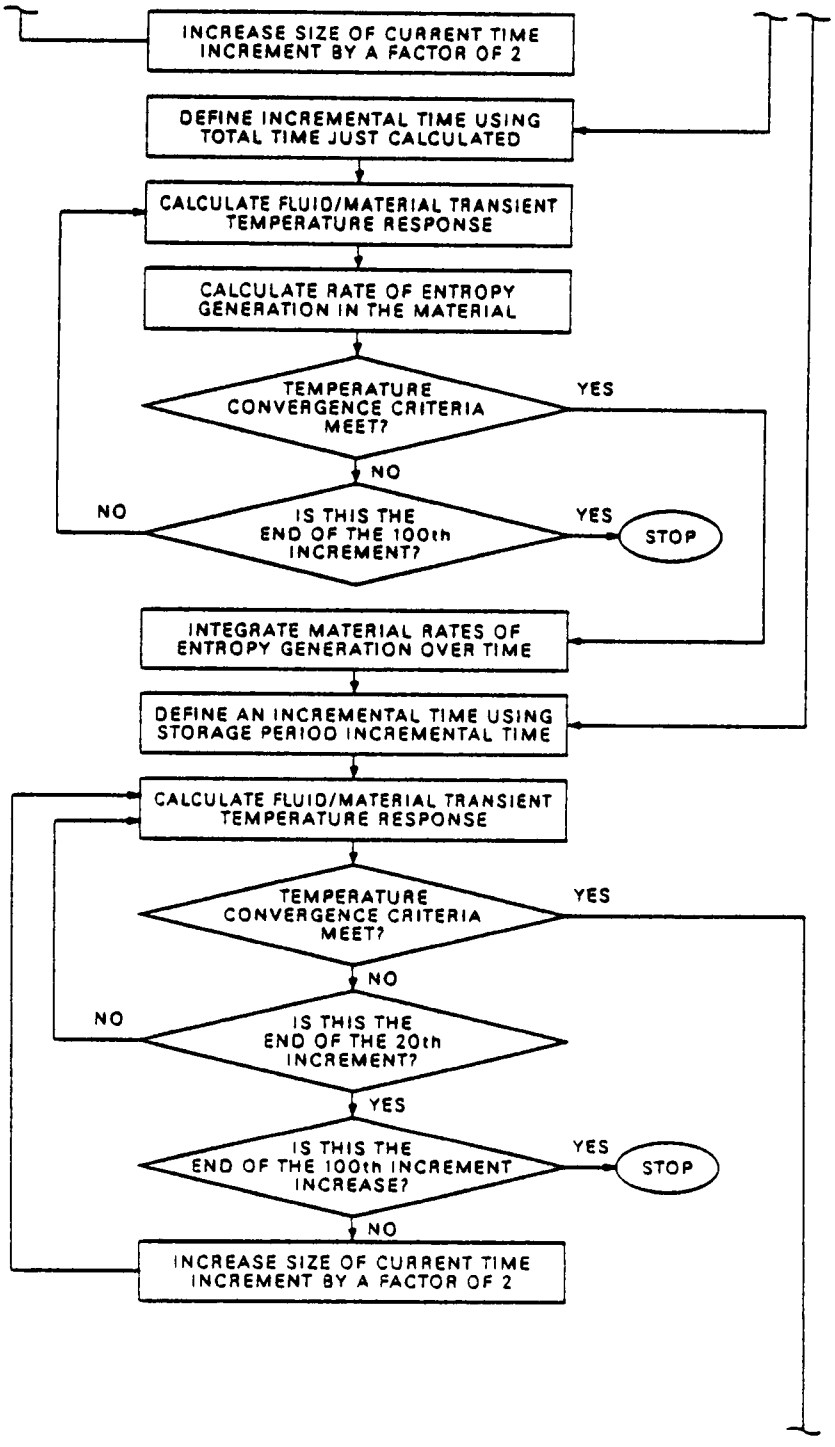


Figure 3.1. (Continued)

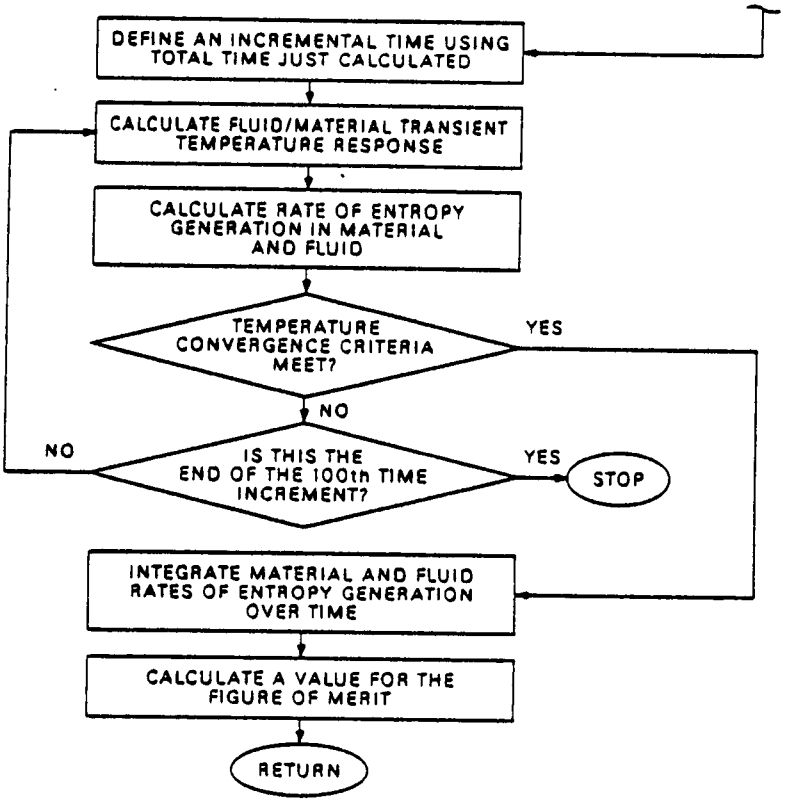


Figure 3.1. (Continued)

transient temperature response for the storage period in 59 equal time increments (i.e., $Fo_s/59$). Once the fluid and material temperature distributions have been calculated for a time increment, and before proceeding to the next increment, ENTROP:

a. Calculates the temperature gradients at each node in the material and uses them, with the temperature at each node, to calculate the rate of entropy generation at each node. These individual terms are then integrated over the material volume to determine the total entropy generation in the storage material.

b. Calculates the fluid-wall temperature difference for the nodes along the flow channel then uses them and the fluid temperature at each node to calculate the rate of entropy generation at each node. These terms are then integrated over the length of the channel to determine the rate of entropy generation in the fluid.

c. Using the fluid outlet temperature, calculates the rate of availability destroyed due to the discharged fluid coming to thermal equilibrium with the environment.

At the end of the 59 time increments, the rates of entropy generation for the material, fluid, and discharged fluid are individually integrated over time to determine the total amounts of entropy generated during the storage period.

If a dwell period is desired, ENTROP executes a two step procedure that determines an approximate time then uses it to calculate the amount of entropy generated in the material during the period. To determine an approximate dwell time, ENTROP begins an open ended calculation of the

fluid-material transient temperature response. "Open ended" in this context means for an unspecified number of time increments. The incremental time it uses is the same one used during the storage period. At the end of each time increment, the average material temperature (which does not change with time during the dwell period) is compared to the highest temperature that existed in the material at the end of the storage period. The calculations are stopped when the difference between these two has been reduced to a sufficiently small amount. This calculation/comparison sequence continues for 20 time increments at which time the incremental time is increased by a factor of two. The calculations then proceed with this larger time step. This gradually increasing incremental time permits covering a large total elapsed time in as few steps as possible while still retaining acceptable accuracy. This entire process continues until the fluid-wall temperature difference meets the convergence criteria. The approximate dwell time is then equal to the total elapsed time since the start of the calculations.

To determine the amount of entropy generated in the material during the dwell period, ENTROP takes the approximate time just defined, divides it into 59 equal increments then restarts the transient temperature response calculations. At the end of each time increment ENTROP determines the rate of entropy generation in the material exactly as it did for the storage period. Also at the end of each time period, a check is made to see if the temperature difference has met the convergence criteria. To allow for an inaccurate approximate dwell time,

this sequence can continue for up to 100 time increments. When the convergence criteria has finally been met, ENTROP stops the transient calculations and then integrates the material rates over time to determine the total amount of entropy generated in the material during the dwell period.

A similar two step procedure is also utilized for the removal period. Using an initial incremental time, ENTROP begins an open ended calculation of the fluid-material transient temperature response. These calculations proceed as they did during the dwell period with an increasing incremental time every 20 steps. The only difference is that the termination decision criterion is based on an average material temperature/initial material temperature difference. As was done during the dwell period, once an approximate time has been determined, ENTROP restarts the transient temperature calculations using 1/59 of the approximate time. At the end of each time increment, ENTROP calculates the rates of material and fluid entropy generation and checks the temperature convergence. Also as before, when the convergence criteria has finally been meet, ENTROP stops the transient calculations and then performs an integration over time to determine the total amounts of entropy generated in the material and fluid during the removal period. In addition, once the removal time has been determined, ENTROP calculates the total entering fluid availability.

At the end of these steps, ENTROP has generated all the information needed to calculate a value for the figure of merit. It then performs this calculation and returns the value to the GRG2 routine.

From this description, it is clear that calculating the fluid-material transient temperature response is one of the most critical operations of the entire sequence. To accomplish this, an iterative procedure was utilized to solve the coupled fluid-material equations. This consisted of making an initial guess of the fluid temperatures, then using them as constants in the solution of the material conduction equation. Once the material temperature distribution has been calculated, those temperatures on the convective boundary are designated as wall temperatures and used to solve the fluid temperature differential equation. The fluid temperatures thus calculated are then compared to the previous guesses. If the difference between the two is greater than a certain amount, the most recently calculated temperatures becomes the next guess. The conduction equation is then solved again using these values. This iterative sequence continues until the convergence criteria (i.e., difference between successive values) has been met at which time the resulting fluid and material temperatures are used in the entropy generation calculations. This sequence is illustrated graphically in the flow diagram shown in Figure 3.2.

As can be seen, to actually execute the above steps requires several different numerical operations. The most prominent of these are:

a. a solution of the fluid-material transient temperature response; that is the coupled material conduction equation and the fluid energy balance, and

b. the one- and two-dimensional integrations.

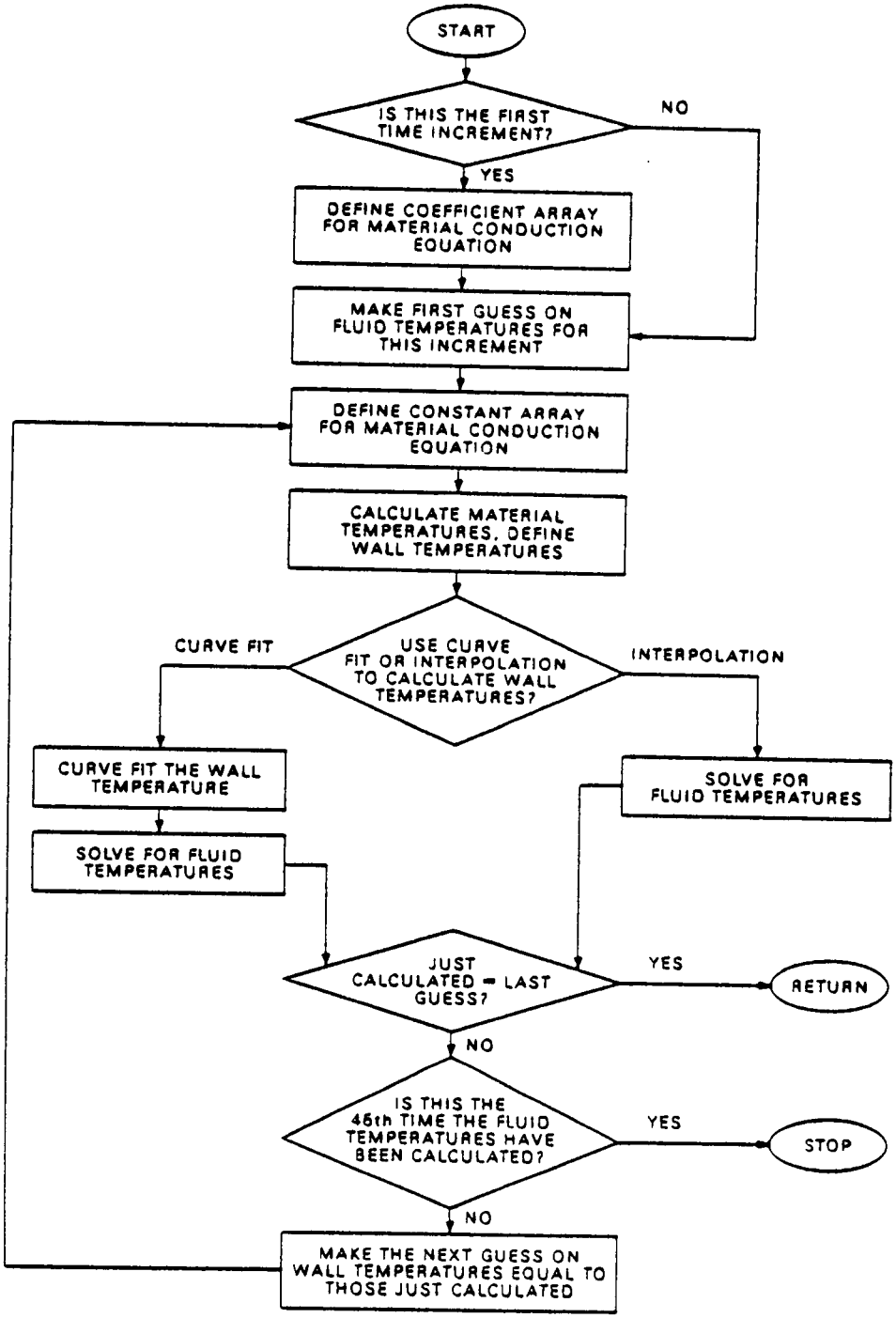


Figure 3.2. Schematic representation of the fluid-material transient temperature response calculations.

A brief discussion of the specific numerical techniques used to perform these operations follows.

The material conduction equations were discretized using standard Taylor series approximations [52]. A fully implicit scheme using central differencing for the spatial coordinates and backward differencing for the time coordinates was defined. The programming was written such that the number of nodes in each dimension was an input variable. This flexibility was necessary because it was not known ahead of time how fine a grid would be needed to give results accurate enough for the optimization algorithm. In order to solve the conduction equations under these circumstances certain procedures had to be defined. These included:

a. a means of generating the discretized equation set coefficient matrix at run time, and

b. an efficient algorithm for solving this set of equations.

The efficient algorithm was an especially critical requirement since very large equation sets often result from discretized conduction equations and they can require large amounts of computer memory and execution time. The specific one used was a banded matrix package taken from the public domain CORLIB library [53]. This package consisted of two subroutines; DGBFA and DGBSL. Working together they solve the system of linear equations, A*X=B. A is the original, sparse coefficient matrix having a banded construction. DGBFA factors this banded matrix using a gaussian elimination technique. Using these factors, DGBSL then actually solves for the unknown material temperatures. The only

additional programming required by this package was a method to read the non-zero elements of the original banded matrix, without having previously defined all of the original sparse matrix. The steps for accomplishing this as a function of a variable number of nodes are too involved to be described here but are discussed at length in Appendix B.

The fluid energy equation was treated as an initial value problem and was solved using a fourth-order Runge-Kutta technique [54]. Wall temperatures were required to solve for the fluid temperatures and two separate methods were programmed to supply them. The first was a second-order polynomial curve fit [55] of the nodal material temperatures at the convective boundary. Routines were written to define the set of simultaneous equations as a function of the number of nodes in the x direction. The routine to actually solve for the unknown fluid temperatures was taken from the CORLIB library. The second method of calculating wall temperatures, and the one eventually selected for use, was a second order interpolation [52] of the appropriate nodal temperatures.

The numerical techniques used to perform the one- and two-dimensional integrations were based on Simpson's one-third rule [54] and are quite straightforward except that they were modified to utilize finite values instead of continuous functions. The only restriction resulting from this modification was that an odd number of finite values had to be used. A detailed description of the modifications necessary to implement this procedure is contained in Appendix C.

Verification of the Numerical Model

It was known from the beginning of this study that there would be no previous results to check the accuracy of the ENTROP computer program. Consequently, it was constructed in a manner to permit verification of complete blocks of programming, individual subroutines and some critical individual instruction strings. The following is a brief description of some of the steps that were taken to verify the accuracy of the program.

Routines that performed curve fits, integrations, interpolations and solved the initial value problem were verified by using them to solve example problems with known results. Each of these example problems were written into a separate calling program, the data passed to the appropriate subroutine resident in ENTROP, and the results checked against the known answer. Other subroutines that could not be compared to known examples were verified by comparison with hand calculations. Typical of these were the routines to calculate rates of entropy generation, calculate the average material temperature, to read the banded matrix and load the DGBFA working matrix, and to calculate the discretized coefficient and constant matrix.

Certain critical individual lines of programming were verified by causing ENTROP to write out intermediate results. This included those lines used to route the program execution within GCOMP, transfer data arrays to subroutines, define initial data arrays, initialize temperature arrays between iterations, and to swap the material horizontal temperature field for the counterflow configuration.

Once key blocks of programming were constructed, they too were verified using known example problems. Typical of these, was the subroutine to perform the transient temperature response of the fluid-storage material. The operation of this iterative sequence of instructions was checked out by forcing it to duplicate a one-dimensional, lumped element storage problem from Schmidt and Willmott [21]. The exact analytical solution to this problem was programmed in a separate routine and its results compared to ENTROP's answer. A detailed summary of this comparison is contained in Appendix D.

This same, careful verification was repeated for all program elements down through the final calculation, the figure of merit. Once the entire program was constructed, its operation was compared to one particular case from Krane's well stirred bath study [46]. To model this one-dimensional, lumped element system, it was necessary to force ENTROP to operate well away from the design configuration it was ment to model. Allowing for this, the agreement with Krane's result was excellent. A more complete description of this exercise is also contained in Appendix D.

Once the entire ENTROP program had been constructed and its operation verified, a series of sensitivity runs were conducted to define optimum execution parameters such as temperature convergence criteria and number of time increments. It was known that optimization studies required more accurate models and the test for establishing some of these parameters was, therefore, their effect on the figure of merit. It was during this series of runs that the following parameters was defined:

a. The number of time increments was chosen to be 59,

b. a 9x9 nodal network was established for the storage material,

c. the temperature convergence criterion for termination of the fluid temeprature iteration was set at 5.0×10^{-4},

d. the convergence criteria for termination of material temperature iterations was set at 0.001%.

e. the second-order polynomial curve fit was more accurate than a third-order fit, and

f. first- and second-order interpolations were shown to be more accurate than a second-order curve fit.

The operation of the GRG2 program, and its somewhat involved data input format, was verified by causing it to solve a known, simple, two-dimensional, unconstrained optimization problem. The operation of the combined ENTROP, GRG2 model was examined in some detail. Although no attempt was made to learn the detailed operation of the GRG algorithm, its behavior during a typical optimization sequence was studied to build confidence that correct answers were being generated. It was during these exploratory runs that it became evident that the optimization variables had to be scaled. Scaling is often required for optimization studies and, in particular, is critical to the successful operation of the GRG2 routine. Scaling is accomplished by multiplying the objective function and the optimization variables by appropriate constants so their values within GRG2 have the same order of magnitude. The scaling is reversed within ENTROP prior to any calculations. The scaling requirement eventually became something of a hindrance during the optimization studies.

As previously explained, GRG2 requires that ranges and initial values of the optimization variables be defined prior to a run. Determining these ranges was itself an involved procedure because the behavior of the optimized surface was unknown. The scaling requirement, however, complicated the procedure because in order to accurately scale the problem, it was necessary to somewhat restrict the ranges. During the verification procedure, a set of ranges were defined for an unconstrained counterflow problem using a nominal set of medium temperature design variables. Because these ranges were necessarily small, they limited the types of design cases that could be optimized without redefining ranges and rescaling the problem. The effect of this restriction on the results of optimization study is examined later in Section 4.

4. PRESENTATION AND ANALYSIS OF RESULTS

Description of the Study and Summary of Results

A total of 36 design cases were optimized using the mathematical model and execution sequence described in the previous sections. Thirty of these cases were unconstrained optimizations dealing with both the counterflow and parallel flow configurations. Six constrained, counterflow cases were also included as a sensitivity study. The unconstrained cases were distributed as follows:

a. 24 for a counterflow configuration without a dwell period, and

b. three each for a parallel flow configuration with and without a dwell period.

Six constrained cases with two separate constraints (i.e., only one constraint active at a time) were also included. These constraints, which were imposed on the counterflow configuration without a dwell period, were:

a. the dimensionless storage unit size, NTU, was required to be ten or less, and

b. the storage period first law efficiency was required to be 0.90 or greater.

Each of the 36 design cases was defined by first specifying values for the eight design variables. Because of the original choice of design variables, it was possible to permanently fix the value of four of them without compromising the rigor of the problem. Ranges of values were defined for the remaining four design variables as a function of

the particular configuration or design being analyzed. Once a particular combination of eight design variables had been selected, GRG2 would treat them as constants and determine the value of the three optimization variables which resulted in a minimum value for the figure of merit. The four design variables that were held constant for all 36 cases and their values were:

a. the constant C_1, used to define the ratio of τ_s to τ_r, defined as 1.0,

b. the fluid property ratio R/Cp, defined as 0.2843 (air),

c. the fluid inlet temperature excess for the removal period, $T_{f,i,r}/T_\infty$, defined as 1.0, and

d. the fluid Prandtl number Pr, defined as 0.71 (air).

The counterflow configuration without a dwell period is one of the most common operating modes [21] for this type of storage system and was therefore the primary focus of this study. For the 24 unconstrained cases dealing with this design, the four design variables that were permitted to float and the values utilized for this study were:

a. the storage period fluid inlet temperature excess, $T_{f,i,s}/T_\infty$, and values of 2.0 and 3.0 were defined,

b. the dimensionless material aspect ratio, V^+, and values of 0.01 and 0.05 were defined,

c. the storage period initial material temperature excess, $T_{m,o,s}/T_\infty$, and values of 1.1 and 1.3 were defined, and

d. the storage period dimensionless mass velocity, τ_s, and values of 0.005, 0.05, and 0.5 were defined.

The results of these cases are summarized in tabular form in Tables 4.1 to 4.8.

The unconstrained analyses of the parallel flow configuration were included in the study for completeness. The intent was to investigate a small number of cases to permit a comparison to the counterflow configuration at some nominal operating point (i.e., set of eight design variables). Accordingly, only one design variable, τ_s, was varied and values of 0.005, 0.05, and 0.5 were used. The remaining three design variables that were utilized and their values were:

a. $T_{m,o,s}/T_\infty$, which was held constant at 1.1,

b. $T_{f,i,s}/T_\infty$, which was held constant at 2.0, and

c. V^+, which was held constant at 0.01.

The resulting six cases (three runs for each of two operating modes) were executed and the results are summarized in Tables 4.9 and 4.10.

The two constrained, counterflow cases were included to define the sensitivity of the figure of merit to constraints on the design and operation of a nominal system. These runs were executed with the same set of design variables as the parallel flow cases and the results are summarized in Tables 4.11 and 4.12.

Analysis of the Results

The analysis of the optimization results will begin with a series of brief explanations of the effects that changes in the optimization and design variables have on the performance of a typical storage system. Presenting this information first will facilitate understanding the detailed analyses which follow.

Table 4.1. Optimization results for unconstrained, counterflow design cases for inlet fluid temperature excess of 2.0, material aspect ratio of 0.01, and initial material temperature excess of 1.1

Variable	Storage period dimensionless mass velocity term		
	$\tau_s = 0.005$	$\tau_s = 0.05$	$\tau_s = 0.5$
N_c	0.216	0.379	0.797
NTU	52.47	36.50	23.44
G_s^+	0.106	0.084	0.064
Fo_s	4.199	4.97	5.67
Bi_s	4.951	4.33	3.68
λ	0.004	0.234	2.387
$P_{f,i,s}/P_\infty$	1.002	1.129	3.59
η_s	0.425	0.584	0.759
$\Psi_{\Delta\theta,s}$	12.16	18.09	27.30
$\Psi_{\Delta\beta,s}$	0.023	2.029	32.36
$Sgen_{m,s}$	1.036	1.37	1.77
% $Sgen_{m,s}$	55.70	47.70	30.80
$Sgen_{f,s}$	0.602	0.900	1.35
% $Sgen_{f,s}$	32.30	31.40	23.50
$Sgen_{e,s}$	0.223	0.600	2.63
% $Sgen_{e,s}$	12.00	20.90	45.70
Σ $Sgen_s$	1.861	2.868	5.76
$P_{f,i,d}/P_\infty$	1.002	1.091	2.834
$\Psi_{\Delta\theta,r}$	0.0	0.0	0.0
$\Psi_{\Delta\beta,r}$	0.029	2.199	32.80
$Sgen_{m,r}$	0.427	0.751	1.37
% $Sgen_{m,r}$	58.90	55.40	50.30
$Sgen_{f,r}$	0.298	0.605	1.35
% $Sgen_{f,r}$	41.10	44.60	49.70
Σ $Sgen_r$	0.725	1.356	2.727

Table 4.2. Optimization results for unconstrained, counterflow design cases for inlet fluid temperature excess of 2.0, material aspect ratio of 0.01, and initial material temperature excess of 1.3

Variable	Storage period dimensionless mass velocity term		
	$\tau_s = 0.005$	$\tau_s = 0.05$	$\tau_s = 0.5$
N_c	0.254	0.383	0.777
NTU	57.11	31.34	28.85
G_s^+	0.114	0.087	0.064
Fo_s	3.698	4.67	4.73
Bi_s	4.992	3.60	3.59
λ	0.004	0.161	2.15
$P_{f,i,s}/P_\infty$	1.002	1.112	3.92
η_s	0.359	0.537	0.577
$\Psi_{\Delta\theta,s}$	9.92	16.44	18.09
$\Psi_{\Delta\beta,s}$	0.021	1.619	22.91
$Sgen_{m,s}$	0.464	0.640	0.696
% $Sgen_{m,s}$	23.60	18.40	17.50
$Sgen_{f,s}$	0.277	0.523	0.571
% $Sgen_{f,s}$	14.10	15.0	14.40
$Sgen_{e,s}$	1.22	2.32	2.71
% $Sgen_{e,s}$	62.20	66.60	68.10
Σ $Sgen_s$	1.96	3.482	3.97
$P_{f,i,d}/P_\infty$	1.002	1.080	3.068
$\Psi_{\Delta\theta,r}$	0.0	0.0	0.0
$\Psi_{\Delta\beta,r}$	0.015	1.024	16.00
$Sgen_{m,r}$	0.307	0.587	0.685
% $Sgen_{m,r}$	58.40	49.90	49.60
$Sgen_{f,r}$	0.219	0.589	0.694
% $Sgen_{f,r}$	41.60	50.10	50.30
Σ $Sgen_r$	0.526	1.176	1.379

Table 4.3. Optimization results for unconstrained, counterflow design cases for inlet fluid temperature excess of 2.0, material aspect ratio of 0.05, and initial material temperature excess of 1.1

Variable	Storage period dimensionless mass velocity term		
	$\tau_s = 0.005$	$\tau_s = 0.05$	$\tau_s = 0.5$
N_c	0.389	0.470	0.823
NTU	20.34	18.65	9.14
G_s^+	0.165	0.158	0.121
Fo_s	1.648	1.90	2.51
Bi_s	6.156	5.91	3.77
λ	0.002	0.140	1.75
$P_{f,i,s}/P_\infty$	1.001	1.069	2.47
η_s	0.478	0.550	0.732
$\Psi_{\Delta\theta,s}$	3.062	3.69	6.34
$\Psi_{\Delta\beta,s}$	0.002	0.230	5.31
$Sgen_{m,s}$	0.453	0.498	0.605
% $Sgen_{m,s}$	57.30	51.80	26.80
$Sgen_{f,s}$	0.201	0.229	0.416
% $Sgen_{f,s}$	25.40	23.80	18.50
$Sgen_{e,s}$	0.137	0.234	1.23
% $Sgen_{e,s}$	17.30	24.30	54.70
Σ $Sgen_s$	0.791	0.962	2.254
$P_{f,i,d}/P_\infty$	1.002	1.049	2.04
$\Psi_{\Delta\theta,r}$	0.0	0.0	0.0
$\Psi_{\Delta\beta,r}$	0.003	0.289	5.76
$Sgen_{m,r}$	0.255	0.313	0.498
% $Sgen_{m,r}$	64.10	62.80	49.40
$Sgen_{f,r}$	0.143	0.186	0.511
% $Sgen_{f,r}$	35.90	37.20	50.60
Σ $Sgen_r$	0.398	0.499	1.009

Table 4.4. Optimization results for unconstrained, counterflow design cases for inlet fluid temperature excess of 2.0, material aspect ratio of 0.05, and initial material temperature excess of 1.3

Variable	Storage period dimensionless mass velocity term		
	$\tau_s = 0.005$	$\tau_s = 0.05$	$\tau_s = 0.5$
N_c	0.395	0.462	0.812
NTU	19.67	19.29	11.46
G_s^+	0.168	0.168	0.154
Fo_s	0.875	0.811	0.50
Bi_s	5.854	5.74	3.73
λ	0.001	0.121	1.97
$P_{f,i,s}/P_\infty$	1.002	1.072	2.69
η_s	0.271	0.253	0.167
$\Psi_{\Delta\theta,s}$	1.598	1.48	1.000
$\Psi_{\Delta\beta,s}$	0.001	0.095	0.918
$Sgen_{m,s}$	0.155	0.146	0.098
% $Sgen_{m,s}$	34.70	35.10	31.60
$Sgen_{f,s}$	0.079	0.077	0.082
% $Sgen_{f,s}$	17.70	18.30	26.20
$Sgen_{e,s}$	0.212	0.195	0.131
% $Sgen_{e,s}$	47.60	46.60	42.20
Σ $Sgen_s$	0.446	0.418	0.311
$P_{f,i,d}/P_\infty$	1.002	1.051	2.20
$\Psi_{\Delta\theta,r}$	0.0	0.0	0.0
$\Psi_{\Delta\beta,r}$	0.001	0.084	1.05
$Sgen_{m,r}$	0.110	0.101	0.061
% $Sgen_{m,r}$	60.10	59.40	46.50
$Sgen_{f,r}$	0.073	0.069	0.070
% $Sgen_{f,r}$	39.90	40.60	53.50
Σ $Sgen_r$	0.184	0.170	0.131

Table 4.5. Optimization results for unconstrained, counterflow design cases for inlet fluid temperature excess of 3.0, material aspect ratio of 0.01, and initial material temperature excess of 1.1

Variable	Storage period dimensionless mass velocity term		
	$\tau_s = 0.005$	$\tau_s = 0.05$	$\tau_s = 0.5$
N_c	0.200	0.295	0.640
NTU	50.89	39.22	28.43
G_s^+	1.104	0.087	0.072
Fo_s	4.24	4.89	5.37
Bi_s	4.89	4.50	3.95
λ	0.002	0.125	0.109
$P_{f,i,s}/P_\infty$	1.003	1.196	4.65
η_s	0.438	0.562	0.686
$\Psi_{\Delta\theta,s}$	36.77	50.50	67.25
$\Psi_{\Delta\beta,s}$	0.035	2.85	32.60
$Sgen_{m,s}$	3.17	3.89	4.66
% $Sgen_{m,s}$	61.30	54.90	42.20
$Sgen_{f,s}$	0.170	2.27	3.05
% $Sgen_{f,s}$	32.80	32.10	27.70
$Sgen_{e,s}$	0.306	0.926	3.32
% $Sgen_{e,s}$	5.90	13.10	30.10
Σ $Sgen_s$	5.167	7.094	11.03
$P_{f,i,d}/P_\infty$	1.002	1.113	3.11
$\Psi_{\Delta\theta,r}$	0.0	0.0	0.0
$\Psi_{\Delta\beta,r}$	0.467	3.47	40.95
$Sgen_{m,r}$	1.22	1.88	2.83
% $Sgen_{m,r}$	58.00	55.60	51.60
$Sgen_{f,r}$	0.886	1.50	2.66
% $Sgen_{f,r}$	42.00	44.40	48.40
Σ $Sgen_r$	2.109	3.37	5.49

Table 4.6. Optimization results for unconstrained, counterflow design cases for inlet fluid temperature excess of 3.0, material aspect ratio of 0.01, and initial material temperature excess of 1.3

Variable	Storage period dimensionless mass velocity term		
	$\tau_s = 0.005$	$\tau_s = 0.05$	$\tau_s = 0.5$
N_c	0.192	0.280	0.608
NTU	52.37	45.26	29.58
G_s^+	0.107	0.098	0.074
Fo_s	4.01	4.31	5.25
Bi_s	4.889	4.60	3.99
λ	0.002	0.117	0.917
$P_{f,i,s}/P_\infty$	1.003	1.221	4.73
η_s	0.404	0.460	0.663
$\Psi_{\Delta\theta,s}$	33.72	39.49	63.88
$\Psi_{\Delta\beta,s}$	0.033	2.49	31.31
$Sgen_{m,s}$	2.03	2.25	3.11
% $Sgen_{m,s}$	43.30	40.80	28.30
$Sgen_{f,s}$	1.14	1.34	2.09
% $Sgen_{f,s}$	24.30	24.20	19.10
$Sgen_{e,s}$	1.52	1.93	5.76
% $Sgen_{e,s}$	32.40	35.00	52.60
Σ $Sgen_s$	4.693	5.527	10.95
$P_{f,i,d}/P_\infty$	1.002	1.128	3.15
$\Psi_{\Delta\theta,r}$	0.0	0.0	0.0
$\Psi_{\Delta\beta,r}$	0.029	2.13	27.29
$Sgen_{m,r}$	1.00	1.25	2.52
% $Sgen_{m,r}$	57.90	56.30	51.40
$Sgen_{f,r}$	0.728	0.968	2.38
% $Sgen_{f,r}$	42.10	43.70	48.60
Σ $Sgen_r$	1.730	2.22	4.91

Table 4.7. Optimization results for unconstrained, counterflow design cases for inlet fluid temperature excess of 3.0, material aspect ratio of 0.05, and initial material temperature excess of 1.1

Variable	Storage period dimensionless mass velocity term		
	$\tau_s = 0.005$	$\tau_s = 0.05$	$\tau_s = 0.5$
N_c	0.350	0.407	0.695
NTU	22.41	20.40	14.70
G_s^+	0.168	0.162	0.143
Fo_s	2.24	1.95	2.28
Bi_s	6.671	6.31	5.13
λ	0.001	0.078	0.950
$P_{f,i,s}/P_\infty$	1.001	1.110	3.50
η_s	0.602	0.554	0.656
$\Psi_{\Delta\theta,s}$	12.05	10.88	14.37
$\Psi_{\Delta\beta,s}$	0.005	0.357	5.68
$Sgen_{m,s}$	1.50	1.46	1.62
% $Sgen_{m,s}$	53.90	56.80	41.90
$Sgen_{f,s}$	0.548	0.561	0.747
% $Sgen_{f,s}$	19.70	21.80	19.30
$Sgen_{e,s}$	0.732	0.552	1.50
% $Sgen_{e,s}$	26.40	21.50	38.80
Σ $Sgen_s$	2.776	2.575	3.87
$P_{f,i,d}/P_\infty$	1.002	1.064	2.44
$\Psi_{\Delta\theta,r}$	0.0	0.0	0.0
$\Psi_{\Delta\beta,r}$	0.006	0.486	7.96
$Sgen_{m,r}$	0.936	0.860	1.11
% $Sgen_{m,r}$	65.00	63.60	57.10
$Sgen_{f,r}$	0.505	0.492	0.831
% $Sgen_{f,r}$	35.00	36.40	42.90
Σ $Sgen_r$	0.144	1.35	1.938

Table 4.8. Optimization results for unconstrained, counterflow design cases for inlet fluid temperature excess of 3.0, material aspect ratio of 0.05, and initial material temperature excess of 1.3

Variable	Storage period dimensionless mass velocity term		
	$\tau_s = 0.005$	$\tau_s = 0.05$	$\tau_s = 0.5$
N_c	0.344	0.387	0.660
NTU	20.99	21.08	14.52
G_s^+	0.167	0.168	0.143
Fo_s	1.40	1.30	1.95
Bi_s	6.304	6.27	5.09
λ	0.001	0.069	0.780
$P_{f,i,s}/P_\infty$	1.001	1.111	3.49
η_s	0.416	0.388	0.590
$\Psi_{\Delta\theta,s}$	7.57	6.98	12.32
$\Psi_{\Delta\beta,s}$	0.003	0.235	4.85
$Sgen_{m,s}$	0.843	0.807	1.07
% $Sgen_{m,s}$	49.40	50.90	33.10
$Sgen_{f,s}$	0.341	0.327	0.521
% $Sgen_{f,s}$	20.00	20.70	16.10
$Sgen_{e,s}$	0.523	0.540	1.63
% $Sgen_{e,s}$	30.60	28.40	50.70
Σ $Sgen_s$	1.707	1.58	3.22
$P_{f,i,d}/P_\infty$	1.002	1.065	2.44
$\Psi_{\Delta\theta,r}$	0.0	0.0	0.0
$\Psi_{\Delta\beta,r}$	0.003	0.245	4.76
$Sgen_{m,r}$	0.563	0.517	0.917
% $Sgen_{m,r}$	63.10	63.00	56.10
$Sgen_{f,r}$	0.330	0.303	0.719
% $Sgen_{f,r}$	36.90	36.90	43.90
Σ $Sgen_r$	0.892	0.820	1.63

Table 4.9. Optimization results for unconstrained, parallel flow design cases without a dwell period

Variable	Storage period dimensionless mass velocity term		
	$\tau_s = 0.005$	$\tau_s = 0.05$	$\tau_s = 0.5$
N_c	0.313	0.4438	0.815
NTU	41.140	30.84	21.02
G_s^+	0.087	0.072	0.055
Fo_s	5.108	5.588	6.155
Bi_s	4.750	4.280	3.795
λ	0.004	0.207	2.237
$P_{f,i,s}/P_\infty$	1.001	1.111	3.435
η_s	0.586	0.706	0.843
$\psi_{\Delta\theta,s}$	18.102	23.820	34.100
$\Psi_{\Delta\beta,s}$	0.027	2.313	38.98
$Sgen_{m,s}$	1.356	1.631	1.980
% $Sgen_{m,s}$	0.490	0.380	0.220
$Sgen_{f,s}$	0.823	1.090	1.460
% $Sgen_{f,s}$	0.30	0.254	0.160
$Sgen_{e,s}$	0.585	1.550	5.580
% $Sgen_{e,s}$	0.210	0.363	0.618
Σ $Sgen_s$	2.764	4.267	9.032
$P_{f,i,d}/P_\infty$	1.001	1.078	2.720
$\Psi_{\Delta\theta,r}$	0.0	0.0	0.0
$\Psi_{\Delta\beta,r}$	0.0380	2.610	37.290
$Sgen_{m,r}$	1.580	1.870	2.280
% $Sgen_{m,r}$	0.550	0.520	0.490
$Sgen_{f,r}$	1.280	1.700	2.390
% $Sgen_{f,r}$	0.440	0.476	0.51
Σ $Sgen_r$	2.850	3.570	4.677

Table 4.10. Optimization results for unconstrained, parallel flow design cases with a dwell period

Variable	Storage period dimensionless mass velocity term		
	$\tau_s = 0.005$	$\tau_s = 0.05$	$\tau_s = 0.5$
N_c	0.301	0.427	0.810
NTU	37.130	30.950	22.150
G_s^+	0.080	0.073	0.059
Fo_s	5.320	5.530	5.930
Fo_{ss}	6833.0	6530.0	6170.0
Bi_s	4.617	4.260	3.738
λ	0.003	0.202	2.341
$P_{f,i,s}/P_\infty$	1.002	1.111	3.511
η_s	0.636	0.698	0.805
$\Psi_{\Delta\theta,s}$	20.300	23.410	30.690
$\Psi_{\Delta\beta,s}$	0.028	2.28	35.71
$Sgen_{m,s}$	1.470	1.610	1.880
% $Sgen_{m,s}$	0.360	0.339	0.250
$Sgen_{f,s}$	0.9170	1.080	1.410
% $Sgen_{f,s}$	0.220	0.226	0.188
$Sgen_{e,s}$	0.857	0.1460	3.950
% $Sgen_{e,s}$	0.210	0.305	0.524
$Sgen_{ss}$	0.843	0.619	0.280
% $Sgen_{ss}$	0.206	0.130	0.372
$P_{f,i,d}/P_\infty$	1.001	1.078	2.776
$\Psi_{\Delta\theta,r}$	0.0	0.0	0.0
$\Psi_{\Delta\beta,r}$	0.032	2.440	36.120
$Sgen_{m,r}$	1.100	1.330	1.800
% $Sgen_{m,r}$	0.550	0.53	0.49
$Sgen_{f,r}$	0.881	1.170	1.850
% $Sgen_{f,r}$	0.445	0.468	0.507
Σ $Sgen_r$	1.986	2.505	3.650

Table 4.11. Optimization results for cases where the storage system NTU was constrained to a value of 10.0 or less

Variable	Storage period dimensionless mass velocity term		
	$\tau_s = 0.005$	$\tau_s = 0.05$	$\tau_s = 0.5$
N_c	0.354	0.462	0.809
NTU	10.00	10.00	10.00
G_s^+	0.100	0.060	0.043
Fo_s	6.209	6.336	6.336
Bi_s	1.000	1.673	2.300
λ	0.001	0.064	1.521
$P_{f,i,s}/P_\infty$	1.000	1.038	2.554
η_s	0.571	0.796	0.897
$\Psi_{\Delta\theta,s}$	19.050	32.520	44.969
$\Psi_{\Delta\beta,s}$	0.007	1.133	39.070
$Sgen_{m,s}$	0.930	1.609	2.088
% $Sgen_{m,s}$	0.217	0.169	0.119
$Sgen_{f,s}$	2.320	2.501	2.400
% $Sgen_{f,s}$	0.542	0.263	0.137
$Sgen_{e,s}$	1.029	5.396	13.001
% $Sgen_{e,s}$	0.240	0.567	0.743
Σ $Sgen_s$	4.281	9.507	17.490
$P_{f,i,d}/P_\infty$	1.000	1.027	2.099
$\Psi_{\Delta\theta,r}$	0.0	0.0	0.0
$\Psi_{\Delta\beta,r}$	0.008	0.950	29.340
$Sgen_{m,r}$	0.539	1.337	2.110
% $Sgen_{m,r}$	0.220	0.303	0.364
$Sgen_{f,r}$	1.916	3.068	3.687
% $Sgen_{f,r}$	0.780	0.697	0.636
Σ $Sgen_r$	2.445	4.404	5.797

Table 4.12. Optimization results for cases where storage period first law efficiency was constrained to a value of 0.90 or greater

Variable	Storage period dimensionless mass velocity term		
	$\tau_s = 0.005$	$\tau_s = 0.05$	$\tau_s = 0.5$
N_c	0.315	0.437	0.809
NTU	51.947	31.426	18.820
G_s^+	0.813	0.08102	0.0484
Fo_s	10.00	10.00	6.525
Bi_s	6.388	3.879	3.886
λ	0.003	0.166	1.946
$P_{f,i,s}/P_\infty$	1.002	1.112	3.282
η_s	0.899	0.900	0.900
$\Psi_{\Delta\theta,s}$	37.734	37.872	41.341
$\Psi_{\Delta\beta,s}$	0.072	3.738	45.519
$Sgen_{m,s}$	1.621	1.576	2.161
% $Sgen_{m,s}$	0.176	0.159	0.158
$Sgen_{f,s}$	0.759	1.167	1.554
% $Sgen_{f,s}$	0.082	0.118	0.144
$Sgen_{e,s}$	6.845	1.167	9.960
% $Sgen_{e,s}$	0.742	0.724	0.728
Σ $Sgen_s$	9.225	9.923	13.674
$P_{f,i,d}/P_\infty$	1.001	1.079	2.614
$\Psi_{\Delta\theta,r}$	0.0	0.0	0.0
$\Psi_{\Delta\beta,r}$	0.048	2.549	34.947
$Sgen_{m,r}$	1.640	1.587	2.230
% $Sgen_{m,r}$	0.636	0.514	0.503
$Sgen_{f,r}$	0.938	1.499	2.203
% $Sgen_{f,r}$	0.364	0.486	0.497
Σ $Sgen_r$	2.579	3.056	4.433

The specific effects that change in the optimization variables have on the entropy generation characteristics of a storage system are a complicated functions of the eight design variables. Accordingly, it is neither practical nor possible to describe all of these complex interactions in detail. A greater understanding of the physics of the problem can be gained by defining individual qualitative effects (i.e., the effect of changing one variable at a time with all other variables fixed) here and then discussing combined effects in conjunction with specific results. Because the minimum value of an unconstrained optimization occurs where the partial derivatives of the objective function with respect to the optimization variables are equal to zero, it is appropriate to define cause and effect in this way. The most expeditious means of explaining these effects is to explore how they influence the terms in the figure of merit during a typical storage period. These terms are λ, $N_{\Delta P}$, and $N_{\Delta T}$, but because $N_{\Delta P}$ is by definition always one, it is only necessary to address the λ and $N_{\Delta T}$ terms. As an aid to understanding the following explanations, mathematical and verbal descriptions of the major dimensionless variables used in this study are summarized in Table 4.13.

The most straightforward influence to explain is the effect that an increase in storage time, Fo_s, has on the availability distribution ratio, λ. Qualitatively, the longer the storage period the more total pressure availability and thermal availability enters the control volume. However, the magnitude and time dependent behavior of these two quantities, and therefore the value and behavior of their ratio λ, is a

Table 4.13. Physical interpretation of the major dimensionless variables used to describe the entropy generation characteristics of a sensible heat thermal energy storage system

Variable	Definition	Verbal description
V^+	$\frac{w}{L}$	Ratio of storage material half-thickness to its length.
Bi	$\frac{hw}{K_m}$	Ratio of fluid heat transfer coefficient to the unit conductance of the storage material over the characteristic dimension w.
Fo	$\frac{\alpha t}{w^2}$	Dimensionless time. A ratio of the rate of heat conduction across w to the rate of heat storage within w^3.
G^+	$\frac{PhK_m}{\dot{m}Cp_f}$	Dimensionless mass flow per unit width into the paper. When used in conjunction with τ, it represents the half-height of the flow channel.
NTU	$\frac{G^+Bi}{V^+}$	Dimensionless size of the storage unit.
	$\frac{PhhL}{\dot{m}Cp_f}$	
N_c	Equation (2.27a)	Ratio of the total availability destroyed during some elapsed time to the total availability that entered the storage system during that time.
λ	Equation (2.43)	Ratio of the pressure availability to thermal availability that enters the storage system during some elapsed time.
$N_{\Delta P}$		Ratio of pressure availability destroyed during some elapsed time to the total pressure availability that entered the storage system during that time. For this study, always has the value one (1).
$N_{\Delta T}$	Equation (2.51)	Ratio of thermal availability destroyed during some elapsed time to the total thermal availability that entered the storage system during that time.

strong function of the other optimization variables and the eight design variables. For example, the inlet pressure availability increases for increasing τ_s and $T_{f,i,s}/T_\infty$ but gets smaller for decreases in G_s^+ and increases in V^+. If all other variables are held constant, a larger value of τ_s translates into a greater fluid velocity and therefore a larger pressure drop. To overcome these increased viscous effects the fluid inlet pressure must be increased and this results in a greater amount of pressure availability entering the control volume. An increase in $T_{f,i,s}/T_\infty$ for a fixed value of τ_s, causes a decrease in the fluid density and therefore (by 2.70) requires an increased inlet pressure. A decreased value of G_s^+ (all other variables constant) physically corresponds to a larger flow channel diameter and therefore reduced viscous effects. This permits a lower fluid inlet pressure and therefore less entering availability. An increase in V^+ results in a shorter flow channel length and therefore less pressure drop; again allowing a lower fluid inlet pressure. Changes in the optimization variable Bi_s can also effect the amount of entering pressure availability during the storage period. This term was introduced during the non-dimensionalization of the friction factor in the pressure drop equation. Accordingly, reductions in its value, all other variables the same, corresponds to reduced viscous effects and a lower inlet pressure requirement. The entering thermal availability is also influenced by changes in the design variables. An increased $T_{f,i,s}/T_\infty$ results in a greater amount of entering thermal availability. For a fixed τ_s a decreased value of G_s^+ (i.e., a larger flow channel diameter) results in

more total fluid entering the control volume and therefore more entering thermal availability.

The reader will recall that the $N_{\Delta T}$ term is a ratio of the thermal availability destroyed to the total thermal availability that entered the system during some time interval. For a given set of optimization and design variables, the total availability that enters the system increases linearly with time. However, the value and time dependent behavior of the ratio, and therefore the value of the figure of merit, N_c, depends on how much thermal availability is destroyed. Quite understandably, this destruction and its time dependent behavior are dependent on the value of the optimization and design variables. To begin the explanation of these interactions we will examine the effect of an increasing storage time on $N_{\Delta T}$.

The distribution of the destruction of availability among the various sources of irreversibility shifts with increasing time during the storage period. In the beginning of the storage period the fluid outlet temperature is low and, therefore, most of the entropy generation takes place in the storage material and the fluid. As time progresses and the fluid outlet temperature begins to rise, a greater percentage of availability destruction is due to the heat transfer between the discharged hot fluid and the environment. All three mechanisms are still generating entropy, but the destruction of availability due to the exiting fluid coming into equilibrium with the environment begins to dominate. The following is a brief summary of some of the individual influences that effect the relative magnitude of the three entropy generation mechanisms during the storage period.

a. As the dimensionless material aspect ratio, V^+, gets larger the length of the flow channel gets shorter. All other variables the same, this results in a shorter fluid-material contact time, less total heat transferred, and higher fluid outlet temperatures. Qualitatively this results in less entropy generation in the storage material and flowing fluid and more in the exiting fluid. An additional effect of increased values of V^+ is that it increases the amount of longitudinal conduction within the storage material. This results in slightly more entropy generation within the material.

b. Changes in the storage period Biot Number, Bi_s, affect the rate of heat transfer between the flowing fluid and the storage material as well as the temperature and temperature gradients within the storage material. A decrease in the value of Bi_s results in less heat transfer from the flowing fluid and, therefore, higher fluid temperatures along the entire length of the flow channel. Accordingly, the fluid outlet temperature is also greater. A decreased value of Bi_s also results in smaller temperature gradients and lower absolute temperatures within the storage material. The smaller gradients result in less entropy generation in the material, but the lower material temperatures and higher fluid temperatures result in more entropy generation in the fluid. In turn, the increased fluid outlet temperature results in more entropy generation due to the exiting fluid reaching equilibrium with the environment. An additional complication, as equation (2.44c) shows, is that the entropy generation in the storage material depends on the gradient as well as the absolute value of the temperature at a point.

Thus, it is conceivable that there are combinations of variables that can result in reduced rates of heat transfer to the material without significantly changing the total amount of entropy generated.

c. Decreases in the dimensionless mass flow term, G_s^+, result in more fluid entering the system during a given time period. All other variables the same, this has the effect of decreasing the temperature drop in the flowing fluid, which results in higher exiting temperatures. This increases the amount of entropy generated as a result of the exiting hot fluid coming to equilibrium with the environment.

d. Increases in the fluid inlet temperature excess, $T_{f,i,s}/T_\infty$ result in increased rates of entropy generation by all three mechanisms. An increase in the initial storage material temperature, with all other variables remaining constant, causes a decreased temperature difference between the flowing fluid and storage material. This results in less heat transfer between the fluid and material and higher fluid temperatures along the entire length of the flow channel. This produces less entropy generation in the material and more in the flowing and exiting fluids.

The complexity of the optimization procedure is now apparent. A change in a given variable can affect the destruction of pressure and thermal availability in opposite directions. Decreases in G_s^+ and Bi_s result in lower pressure drops but cause increased amounts of thermal availability destruction. Increases in V^+ also result in decreased pressure drops, but increased destruction of thermal availability. In addition, the relative magnitude of these effects depend a great deal on the

value of the other design variables. The analysis is further complicated because the figure of merit is a function of ratios rather than individual generation terms and these ratios are functions of both the storage and discharge periods. Quite obviously, the complex interactions among system variables make it impossible to anticipate the values or behavior of the optimization variables which result in a minimum amount of entropy generation for a given design case. Rather than generalize any further, the final values for the three optimization variables will be summarized and the discussion will shift to specific results. Figures 4.1, 4.2, and 4.3 show, respectively, the optimum value of Fo_s, G_s^+, and Bi_s for the unconstrained, counterflow cases that are to be discussed. The behavior of these variables will be discussed in conjunction with the results.

Unconstrained Counterflow Cases Without a Dwell Period

The presentation of the counterflow results begins with an overall summary of the optimum performance for a storage system then proceeds to a detailed examination of its entropy generation characteristics. To simplify the discussion, we will limit the analysis to the design cases where $T_{m,o,s}/T_\infty$ was 1.1. Similar results were reached for the cases where $T_{m,o,s}/T_\infty$ was 1.3 and it would be redundant to discuss them in the same detail.

The first of these summaries concerns the temperature response of a nominal, optimized storage unit. The particular configuration to be examined is representative of many medium temperature storage systems and is defined by:

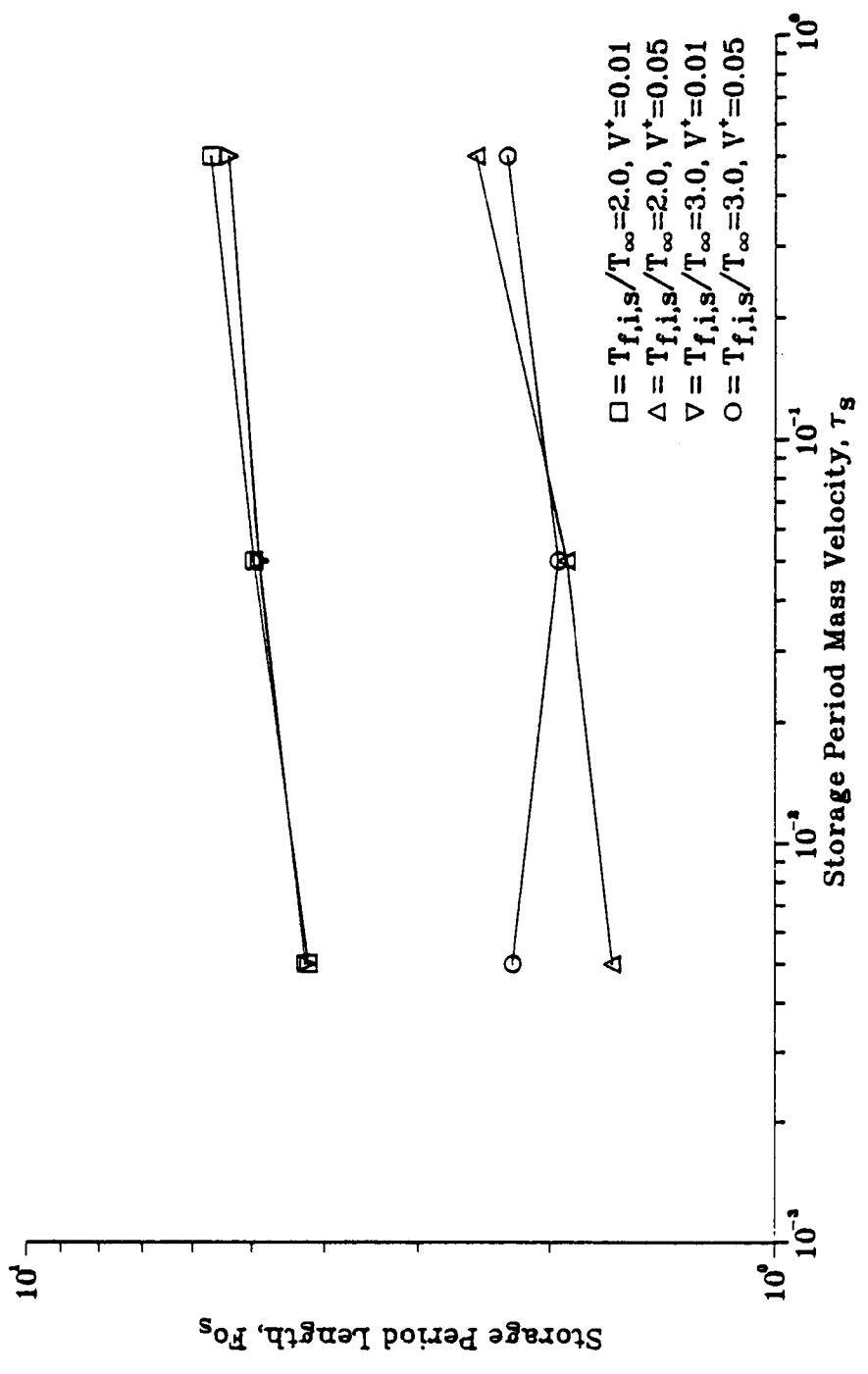


Figure 4.1. Optimum values of Fo_s for the unconstrained, counterflow design cases with $T_{m,o,s}/T_\infty$ = 1.1.

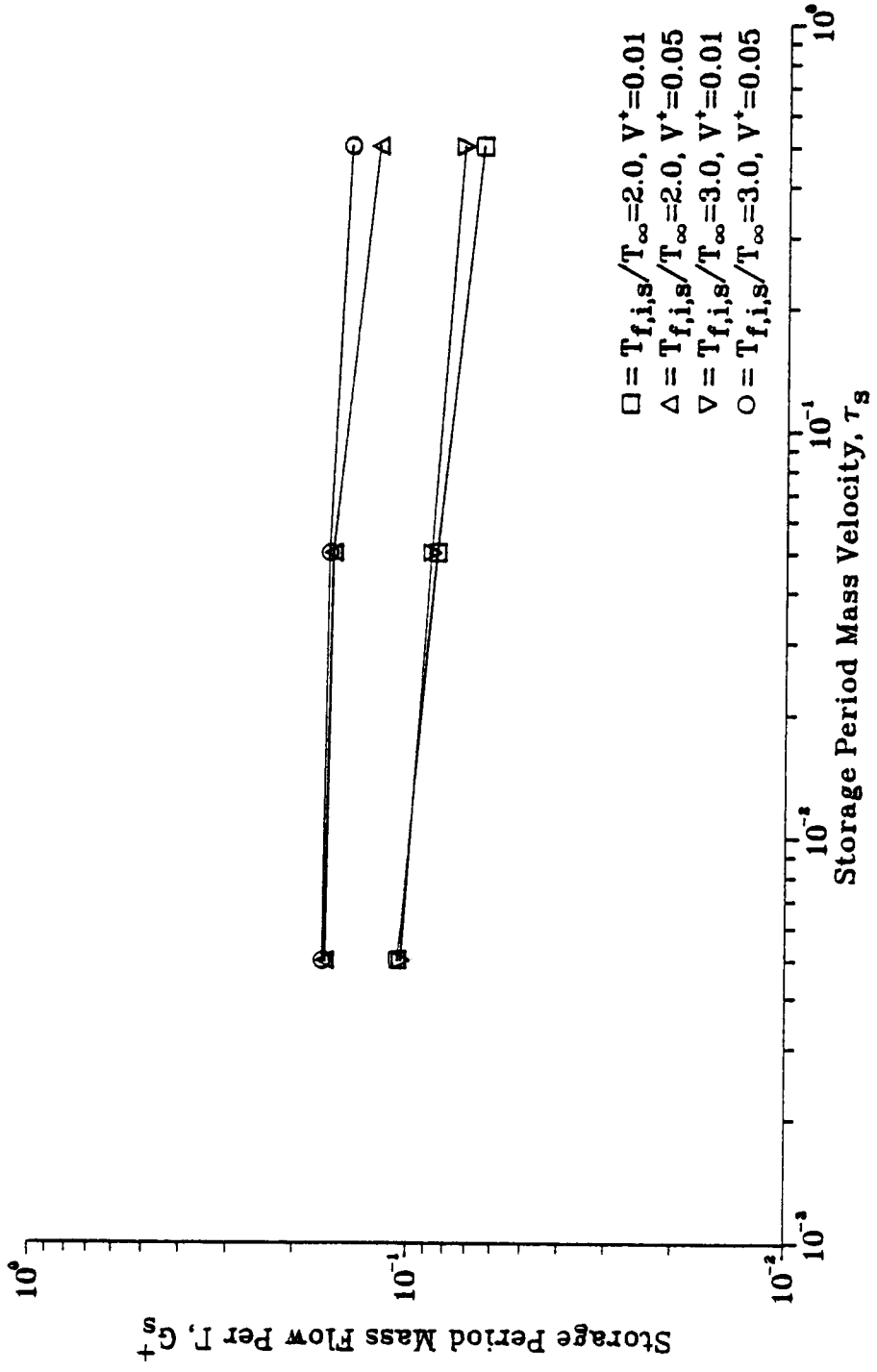


Figure 4.2. Optimum values of G_s^+ for the unconstrained, counterflow design cases with $T_{m,o,s}/T_\infty$ = 1.1.

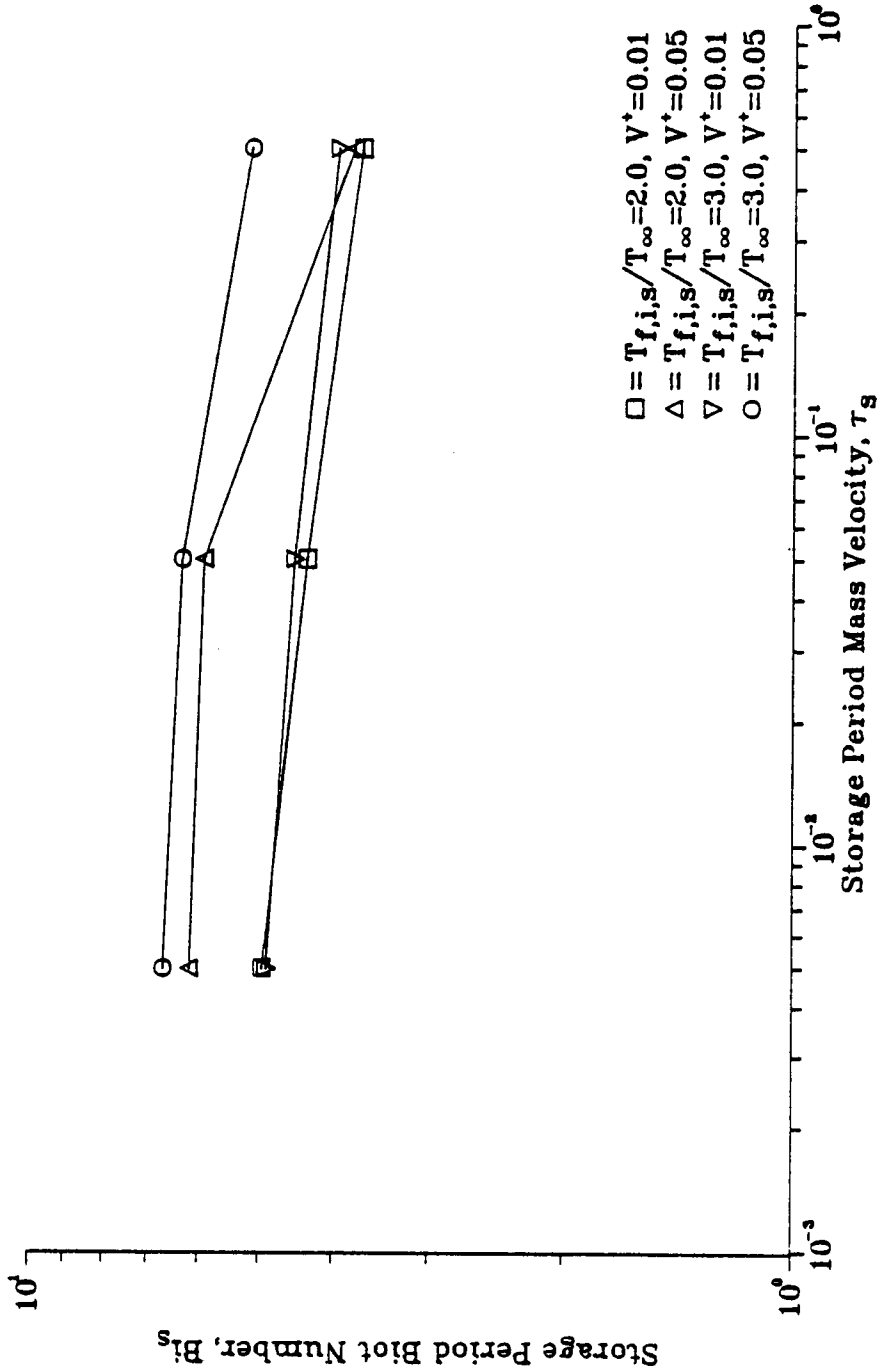


Figure 4.3. Optimum values of Bi_s for the unconstrained, counterflow design cases with $T_{m,o,s}/T_\infty$ = 1.1.

a. a $T_{f,i,s}/T_{\infty}$ of 2.0,

b. a τ_s of 0.05, and

c. a V^+ of 0.01.

The dimensionless, average storage material and fluid outlet temperatures for this nominal operating point are shown for a complete storage-removal cycle in Figure 4.4. The dimensionless temperature distributions for the material at the end of the storage and removal periods are summarized in tabular form in Tables 4.14 and 4.15 and shown graphically in Figures 4.5 and 4.6.

The temperature histories shown in Figure 4.4 are representative of sensible heat storage units in general and exhibit the expected physical behavior. The average material temperature increases with time during the storage period and decreases during the removal period. The fluid outlet temperature gradually increases during the storage period reflecting the constant fluid inlet temperature and gradually decreasing fluid-storage material temperature difference. The fluid outlet temperature during the removal period gradually decreases as a result of the decreasing average material temperature. The storage material temperature distributions shown in Figures 4.5 and 4.6 show the expected result for the small aspect ratios (i.e., very long compared to the width) utilized for this study. Specifically, the gradients in the direction normal to the flow are very steep but are more gradual in the direction parallel to the flow. In addition, the temperature distribution at the end of the removal period demonstrates one of the working assumptions of the study. The removal period is terminated when the average storage material temperature has returned to its initial value. Because of the

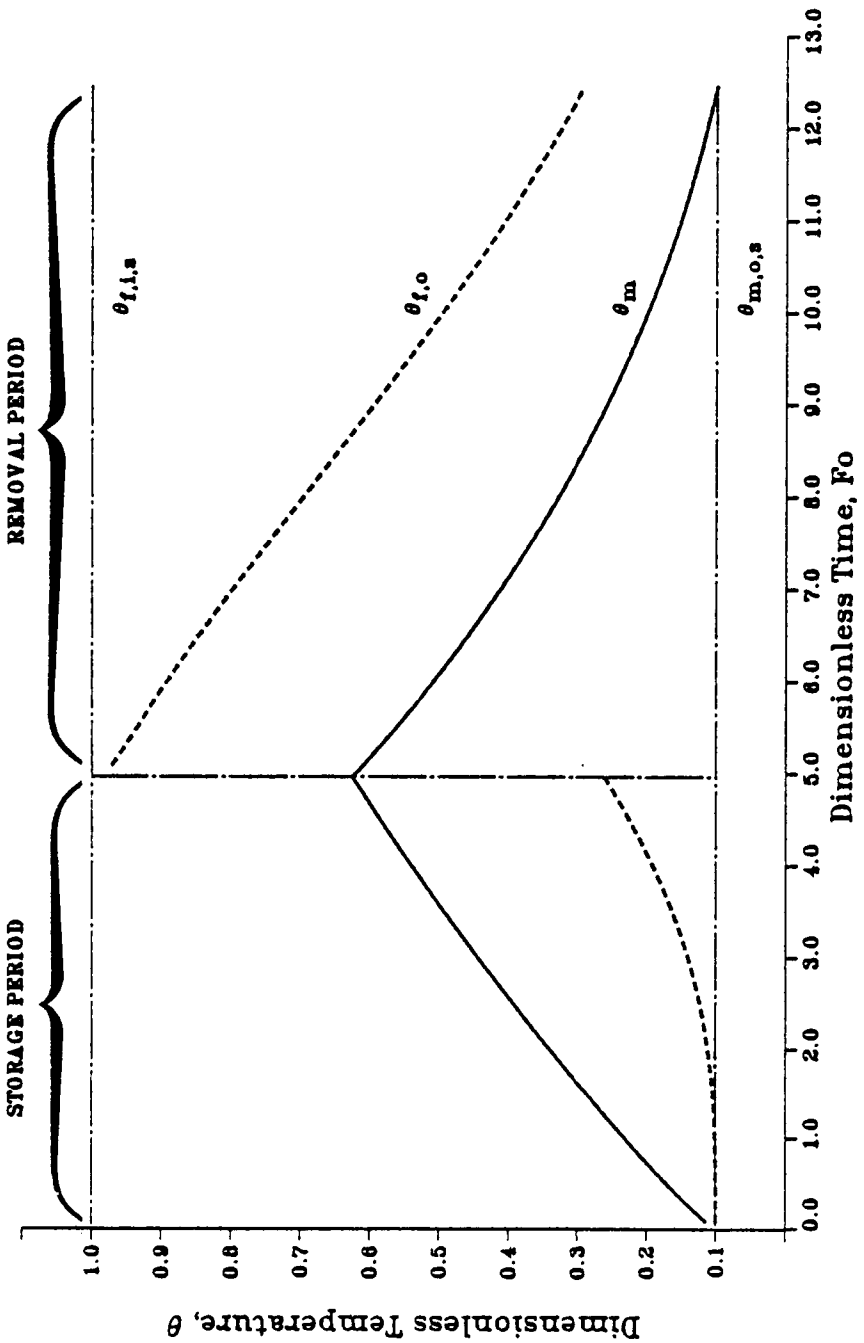


Figure 4.4. Average material and fluid outlet temperature history for an optimum, unconstrained, counterflow medium temperature design case.

Table 4.14. The storage material temperature distribution at the end of the storage period for a nominal, optimized, counterflow storage system

Dimensionless transverse coordinate	Dimensionless longitudinal coordinate								
	X = 0.0[3]	X = 0.125	X = 0.250	X = 0.375	X = 0.500	X = 0.625	X = 0.750	X = 0.875	X = 1.0[4]
Y = 1.0[1]	0.9997	0.9713	0.9020	0.7952	0.6668	0.5357	0.4172	0.3197	0.2458
Y = 0.875	0.9995	0.9682	0.8943	0.7834	0.6526	0.5213	0.4042	0.3090	0.2378
Y = 0.750	0.9993	0.9653	0.8875	0.7730	0.6403	0.5089	0.3930	0.2999	0.2309
Y = 0.625	0.9992	0.9630	0.8817	0.7642	0.6300	0.4983	0.3836	0.2922	0.2251
Y = 0.500	0.9991	0.9609	0.8769	0.7569	0.6211	0.4896	0.3759	0.2860	0.2204
Y = 0.375	0.9990	0.9593	0.8731	0.7512	0.6144	0.4828	0.3699	0.2811	0.2168
Y = 0.250	0.9989	0.9582	0.8703	0.7471	0.6096	0.4780	0.3656	0.2776	0.2142
Y = 0.125	0.9989	0.9575	0.8687	0.7446	0.6067	0.4751	0.3630	0.2755	0.2127
Y = 0.0[2]	0.9989	0.9573	0.8681	0.7438	0.6057	0.4742	0.3622	0.2749	0.2122

[1]Convective boundary

[2]Insulated boundary

[3]Fluid inlet

[4]Fluid exit

Table. 4.15. The storage material temperature distribution at the end of the removal period for a nominal, optimized, counterflow storage system

Dimensionless transverse coordinate	Dimensionless longitudinal coordinate								
	X = 0.0[3]	X = 0.125	X = 0.250	X = 0.375	X = 0.500	X = 0.625	X = 0.750	X = 0.875	X = 1.0[4]
Y = 1.0[1]	0.3104	0.2267	0.1537	0.0953	0.0525	0.0243	0.0086	0.0018	0.0000
Y = 0.875	0.3193	0.2344	0.1600	0.0999	0.0555	0.0260	0.0093	0.0020	0.0000
Y = 0.750	0.3271	0.2412	0.1654	0.1040	0.0582	0.0275	0.0100	0.0022	0.0000
Y = 0.625	0.3336	0.2470	0.1700	0.1074	0.0604	0.0288	0.0106	0.0024	0.0000
Y = 0.500	0.3390	0.2517	0.1739	0.1102	0.0623	0.0299	0.0110	0.0025	0.0000
Y = 0.375	0.3432	0.2554	0.1769	0.1125	0.0638	0.0307	0.0114	0.0026	0.0000
Y = 0.250	0.3463	0.2581	0.1790	0.1145	0.0649	0.0313	0.0117	0.0026	0.0000
Y = 0.125	0.3481	0.2597	0.1803	0.1150	0.0655	0.0317	0.0118	0.0027	0.0000
Y = 0.0[2]	0.3487	0.2602	0.1807	0.1153	0.0657	0.0318	0.0119	0.0027	0.0000

[1]Convective boundary

[2]Insulated boundary

[3]Fluid exit

[4]Fluid inlet

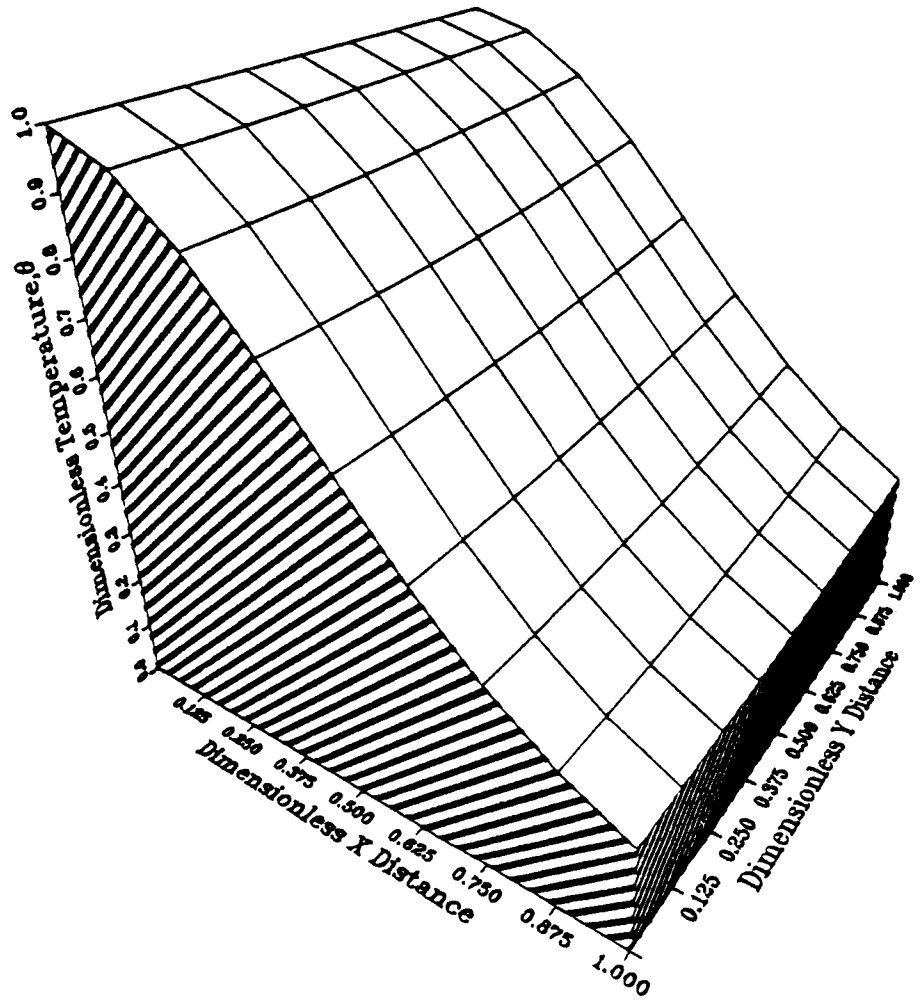


Figure 4.5. Temperature distribution in the storage material at the end of the storage period for an optimum, unconstrained, counterflow, medium temperature design case.

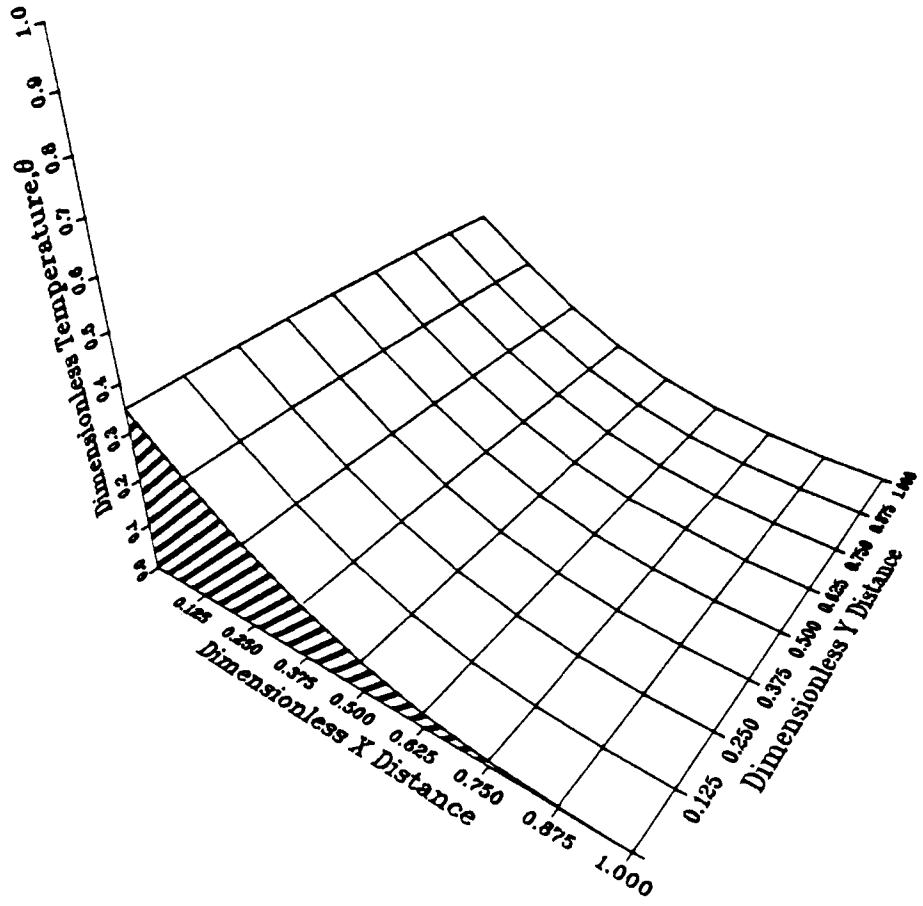


Figure 4.6. Temperature distribution in the storage material at the end of the removal period for an optimum, unconstrained, counterflow, medium temperature design case.

low fluid inlet temperature and the minimal amount of longitudinal conduction, the material temperatures in the inlet half of the unit are always much lower than the outlet half. It is these very low temperatures in the inlet half of the unit that force the average material temperature down. This has the effect of terminating the removal period before the entire unit has started to approach the initial material temperature. Thus we may conclude that the assumption of an initial uniform material temperature is not a good approximation.

Next, those parameters indicative of the overall performance of the optimized storage system are summarized. The first of these will be the figure of merit, N_c, and its components; lambda, λ, and the individual pressure and temperature entropy generation terms, $N_{\Delta P}$ and $N_{\Delta T}$. Figure 4.7 shows the figure of merit, N_c, as a function of the three design variables that were permitted to float; τ_s, $T_{f,i,s}/T_\infty$, and V^+. The most prominent result shown is that N_c increases for increasing τ_s and that τ_s has the greatest impact on N_c of all the design variables. Other characteristics of optimum performance shown are:

a. For a given τ_s and V^+; an increase in $T_{f,i,s}/T_\infty$ produces a lower value for N_c, that is a more efficient storage unit.

b. For a given τ_s and $T_{f,i,s}/T_\infty$; an increase in V^+ results in a larger value for N_c, that is a less efficient storage unit.

c. For low values of τ_s, V^+ is the second most influential variable; but as τ_s increases to its maximum value $T_{f,i,s}/T_\infty$ becomes the second most influential.

Except for the absolute values of the variables, the strong influence of τ_s and the behavior of N_c with respect to changes in $T_{f,i,s}/T_\infty$ are

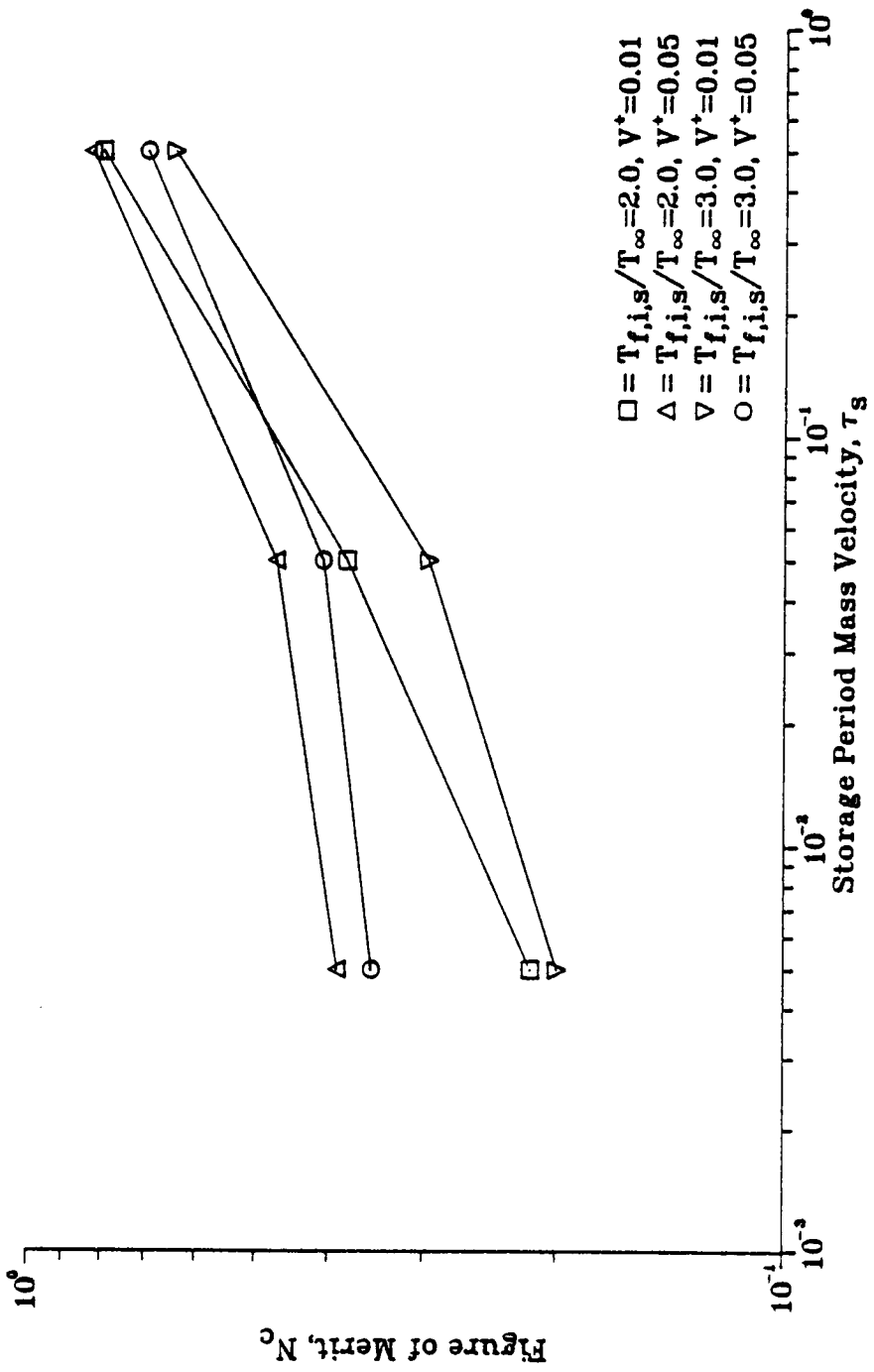


Figure 4.7. Optimum values for the figure of merit for the unconstrained, counterflow design cases with $T_{m,o,s}/T_\infty$ = 1.1.

identical to the results obtained by Krane [46] for the lumped element storage system.

Figure 4.8 shows the optimum values of the individual pressure and temperature entropy generation terms; $N_{\Delta P}$ and $N_{\Delta T}$. As this data show, the $N_{\Delta P}$ term is always unity. This reflects the requirement that the fluid must enter the storage unit at a pressure just great enough to overcome the effects of friction. It also shows that for all combinations of the three floating design variables, the fraction of entering temperature availability destroyed during a cycle increases as τ_s increases. Other characteristics of thermal availability destruction for an optimum, unconstrained, counterflow design are that:

a. for the same value of V^+, a higher $T_{f,i,s}/T_\infty$ results in a smaller fraction of the entering thermal availability being destroyed, and

b. for the same value of $T_{f,i,s}/T_\infty$ a higher value of V^+ results in more of the entering thermal availability being destroyed.

To understand the behavior of the $N_{\Delta T}$ term, recall the trends of the optimization variables shown in Figures 4.1, 4.2, and 4.3 (pp. 108, 109, and 110). Over the range of τ_s examined, Fo_s increased and G_s^+ and Bi_s decreased. These changes combined to force more fluid through the system for a longer time at a higher outlet temperature which resulted in a higher percentage of the entering thermal availability being destroyed.

The optimum behavior of the availability distribution ratio, λ, is shown in Figure 4.9. These data show that for all combinations of $T_{f,i,s}/T_\infty$ and V^+, λ increases as τ_s increases. As was the case for the

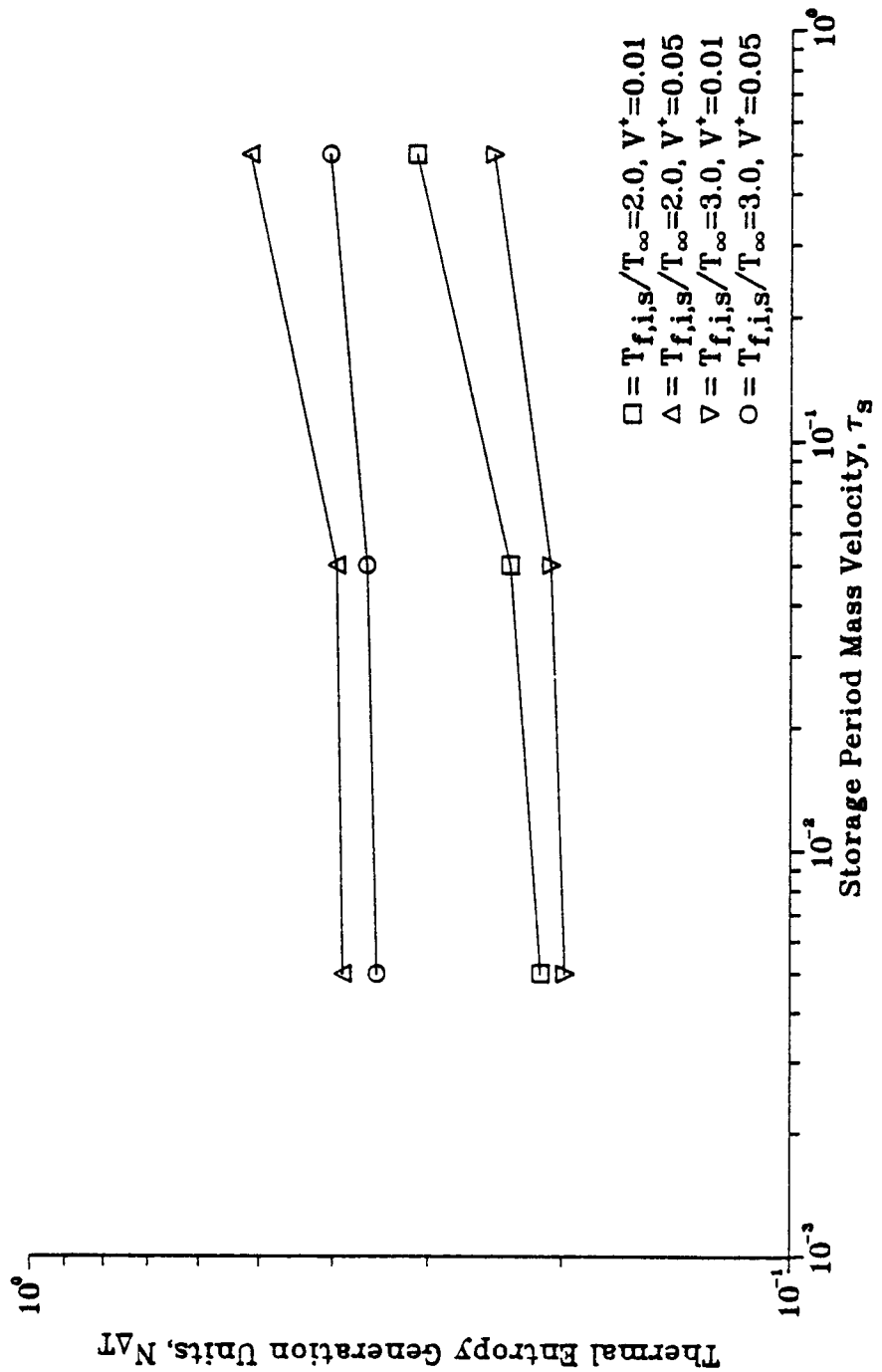


Figure 4.8. Optimum values for the number of thermal entropy units for the unconstrained, counterflow design cases with $T_{m,o,s}/T_\infty$ = 1.1.

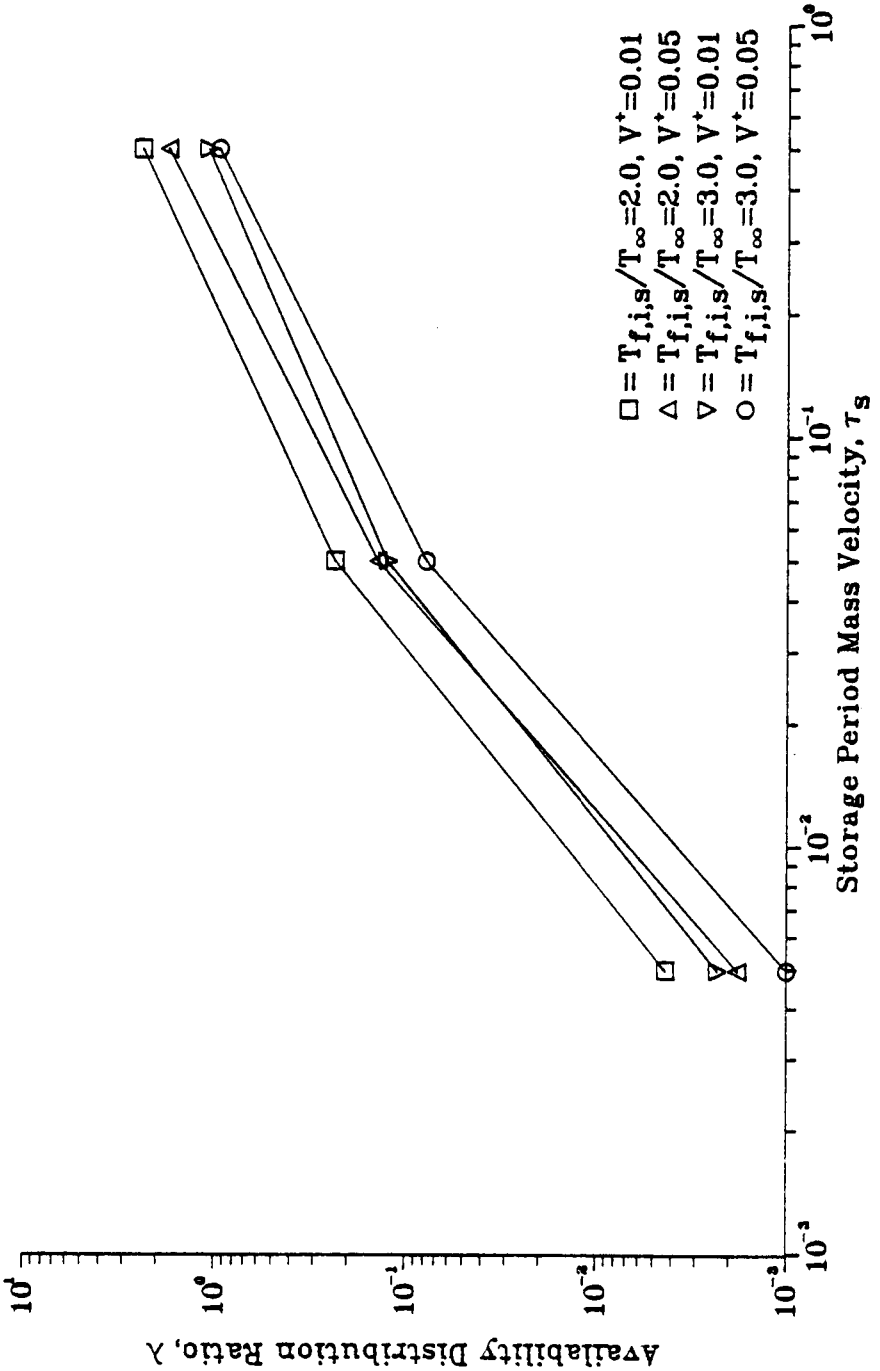


Figure 4.9. Optimum values for the availability distribution ratio for the unconstrained, counterflow design cases with $T_{m,o,s}/T_\infty$ = 1.1.

figure of merit, N_c, τ_s also has the greatest impact of any of the design variables. The reasons for this behavior can best be explained by examining the components of λ. These are the total amounts of pressure and thermal availabilities, $W_{\Delta P}$ and $W_{\Delta T}$, of the fluids that enter during the storage and removal periods. The optimum values of these terms are shown in Figures 4.10 and 4.11. These data show that for low values of τ_s, $W_{\Delta T}$ dominates resulting in low values for λ. As τ_s increases, the optimum value of $W_{\Delta P}$ increases until it is the same order of magnitude as $W_{\Delta T}$. The entering pressure availability shows the expected dependence on V^+ and $T_{f,i,s}/T_\infty$ less for lower values of V^+ and more for higher values of $T_{f,i,s}/T_\infty$. The behavior of the entering thermal availability is consistent with the fact that the optimum storage time increases and the optimum value of G_s^+ decreases for increases in τ_s.

It is the increasing amount of pressure availability that causes the observed behavior of λ. It results from the requirement that the fluid must enter the storage unit at a pressure just great enough to overcome viscous effects. We conclude that the destruction of increasing amounts of pressure availability as τ_s increases causes the observed behavior of the figure of merit, N_c. This dependence is best illustrated by examining the components of the figure of merit for a nominal design case. Typical values for these components are summarized in Table 4.16 for the same medium temperature case that was summarized in Figure 4.4 (pp. 112). This data shows that even though $N_{\Delta P}$ is constant and $N_{\Delta T}$ is always increasing; the increasing value of λ causes the figure of merit to increase as τ_s increases. This results in thermal destruction being the dominant mechanism for low values of τ_s and

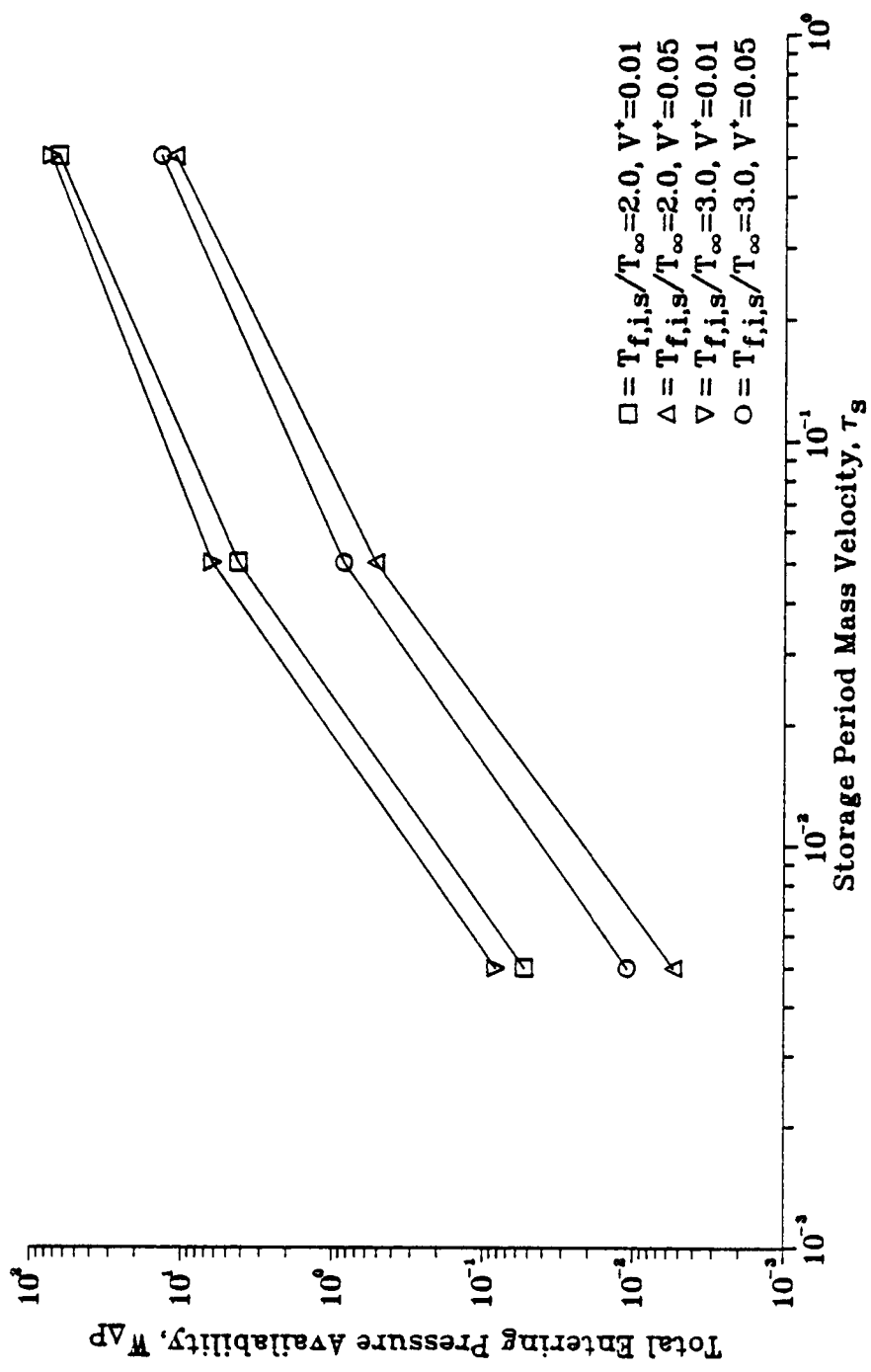


Figure 4.10. Optimum amounts of entering pressure availability for the unconstrained, counterflow design cases with $T_{m,o,s}/T_\infty$ = 1.1.

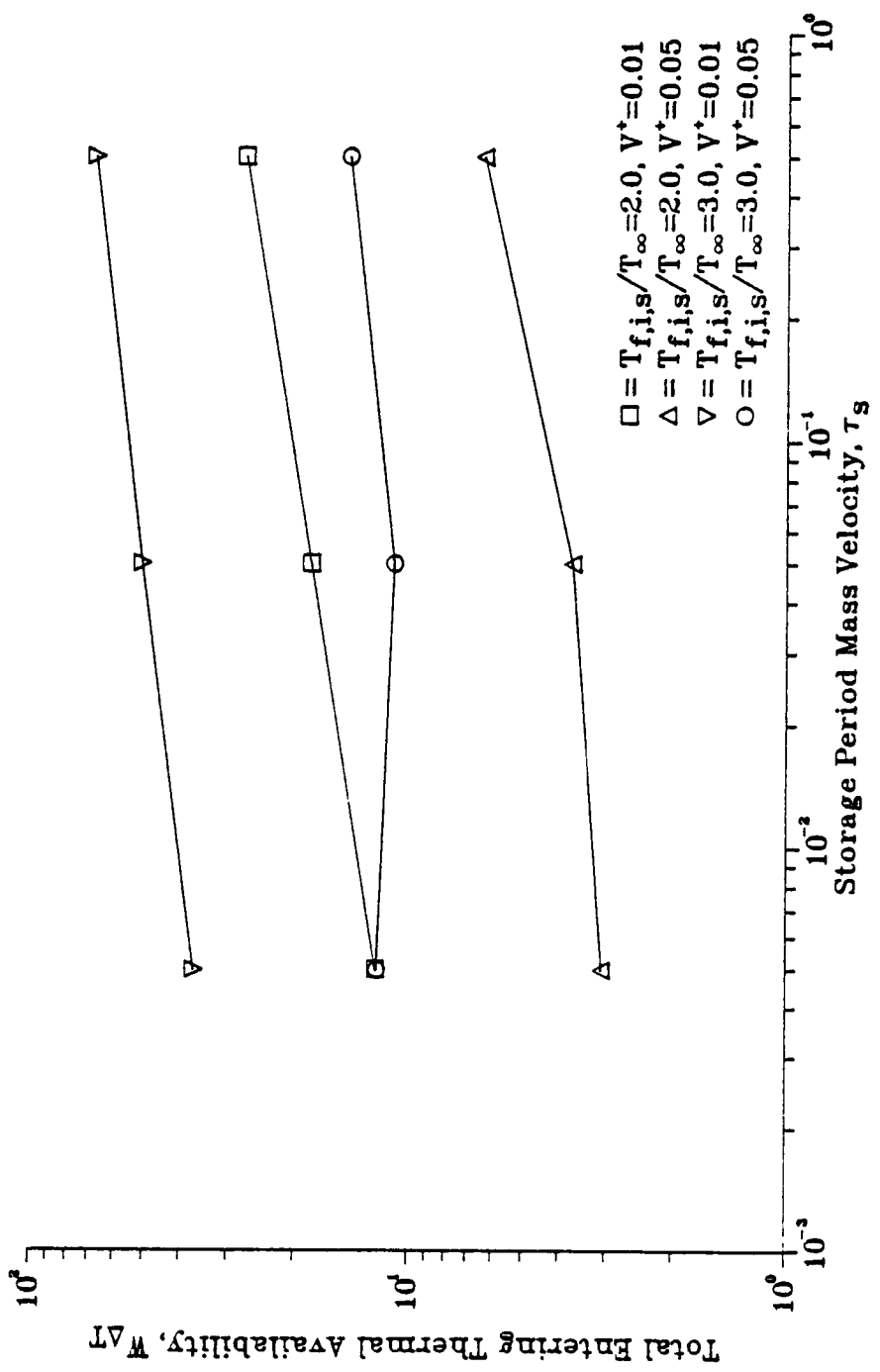


Figure 4.11. Optimum amounts of entering thermal availability for the unconstrained, counterflow design cases with $T_{m,o,s}/T_\infty$ = 1.1.

Table 4.16. Summary of terms in the figure of merit for an optimum, medium temperature design case showing the influence of λ on the behavior of the figure of merit

τ_s	λ	$\frac{\lambda}{1+\lambda}$	$N_{\Delta P}$	$\frac{\lambda}{1+\lambda} N_{\Delta P}$	$\frac{1}{1+\lambda}$	$N_{\Delta T}$	$\frac{1}{1+\lambda} N_{\Delta T}$	N_c
0.005	0.0043	0.0043	1.0	0.0043	0.9957	0.2126	0.2126	0.2169
0.05	0.2340	0.1896	1.0	0.1896	0.8104	0.2335	0.1892	0.3788
0.5	2.3870	0.7048	1.0	0.7048	0.2952	0.3109	0.0918	0.7966

pressure destruction becoming the primary contributor as τ_s approaches its upper limit.

With this understanding of the behavior of the figure of merit, it is now practical to proceed with the analysis of the optimization variables summarized in Figures 4.1, 4.2, and 4.3 (pp. 108, 109, and 110). To begin, we make the following observations:

a. for increasing values of τ_s, the optimum value of G_s^+ and Bi_s decrease and the optimum value of Fo_s increases,

b. changes in τ_s appear to have the most influence on the final value of the optimization variables with V^+ being the next most influential variable, and

c. the rate of decrease of all three variables generally increases as τ_s approaches its upper value.

The continued decrease in the values of G_s^+ and Bi_s for increasing values of τ_s occurs because of the increasing amount of pressure availability being destroyed. As previously explained, decreases in these variables reduce viscous effects and it is therefore reasonable to expect this behavior. The influence of V^+ on the absolute value of these two variables is also consistent with the known physical situation. Increases in V^+ result in a shorter flow channel length and therefore one should expect that smaller decreases in G_s^+ and Bi_s are necessary to achieve a minimum amount of entropy generation. The increase in the rate of change of all three optimization variables can also be attributed to the increasing amount of pressure availability destruction. As the pressure destruction begins to dominate, greater changes in the optimization variables are required to effect reductions in the amount of entropy generation.

The optimum storage unit dimensionless size, NTU, for the counterflow design cases is summarized in Figures 4.12 and shows very clearly that the NTU decreases with increasing τ_s. Except for the value of the NTU, this is the same result that Krane [46] reached for the lumped storage element system. Other optimum size characteristics include:

a. for a given $T_{f,i,s}/T_\infty$ increasing V^+ results in a much smaller sized unit, and

b. for a given value of V^+, an increase in $T_{f,i,s}/T_\infty$ results in a much larger optimum size.

The behavior of the NTU with respect to τ_s is consistent because G_s^+ and Bi_s also decrease with increasing τ_s. Decreases in G_s^+ (for fixed fluid and storage material properties and fixed width of the storage element) correspond to increased mass flows which cause a decrease in the NTU of a unit. Decreases in Bi_s correspond to a decreased heat transfer coefficient which also reduces the value of the NTU. The strong dependence of NTU on V^+ is also consistent with the known physical situation. Decreases in V^+ correspond to a shorter flow channel length which results in a reduced heat transfer surface area and therefore a reduced value of the NTU.

Having summarized optimum second law performance and size characteristics of the storage element, it is now appropriate to make some observations concerning the relationship between the optimum NTU and the corresponding value for N_c. Comparing the results shown in Figures 4.7 (p. 118) and 4.12, it can be seen that reducing τ_s from 0.05 to 0.005 always causes an increase in the optimum NTU of the unit and a decrease in N_c. Furthermore, the size of such a change is a strong function of

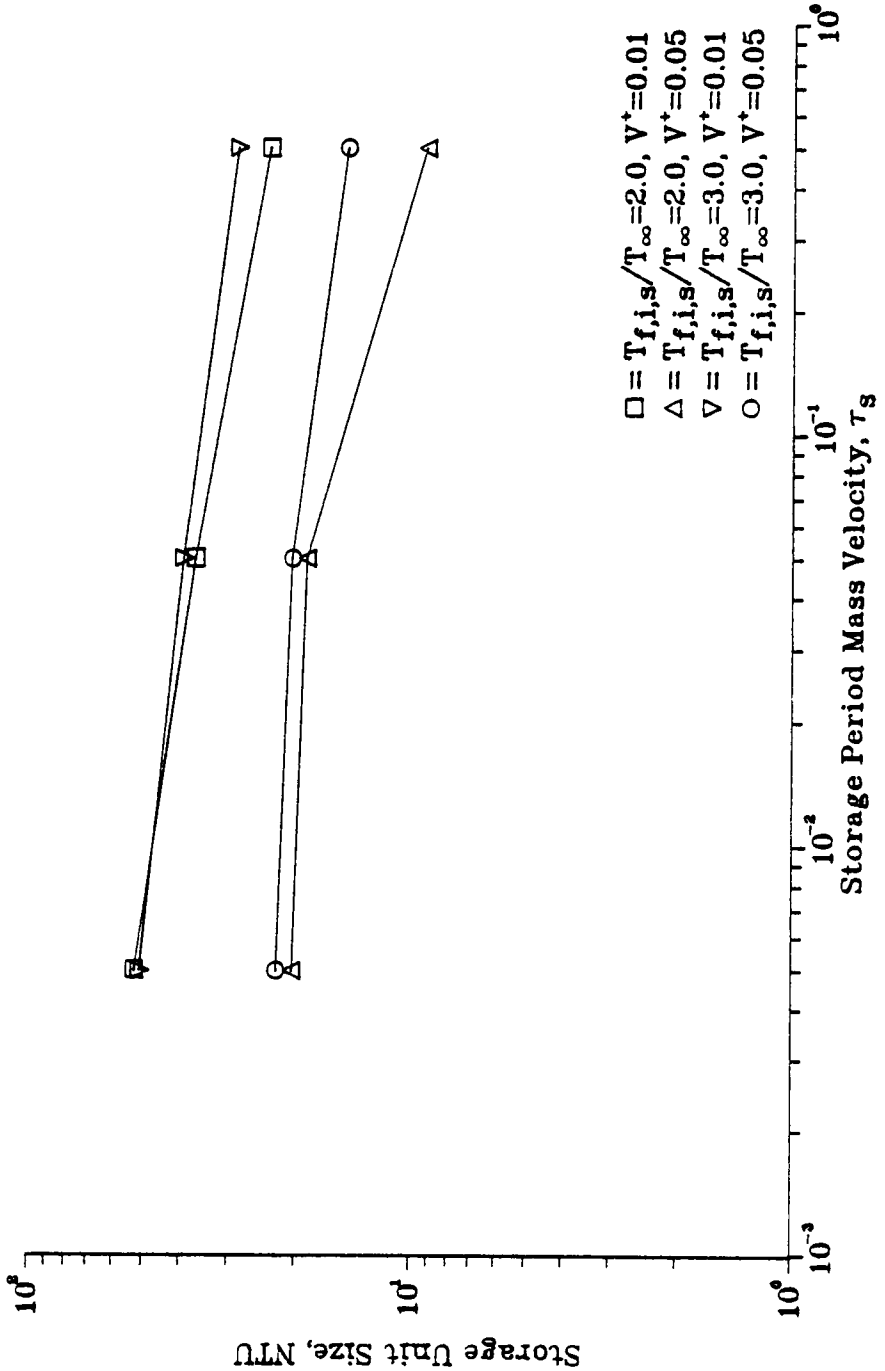


Figure 4.12. Optimum values for the storage system size for the unconstrained, counterflow design cases with $T_{m,o,s}/T_\infty$ = 1.1.

V^+. For the design cases where V^+ was 0.01, there was a corresponding decrease in N_c for a given increase in NTU. The same is not true, however, for the cases where V^+ was 0.05. For the case where $T_{f,i,s}/T_\infty$ was 2.0 and V^+ was 0.01; reducing τ_s the indicated amount caused a 44.% increase in the NTU and a 43.% decrease in N_c. For a $T_{f,i,s}/T_\infty$ of 3.0 and the same V^+; reducing τ_s resulted in a 30.% increase in the NTU and a 32.% decrease in N_c. For the case where V^+ was 0.05 and $T_{f,i,s}/T_\infty$ was 2.0, reducing τ_s the indicated amount increased the NTU by only 9.% but caused N_c to decrease by 17.%. For a $T_{f,i,s}/T_\infty$ of 3.0 and the same V^+; reducing τ_s resulted in a 9.% increase in the NTU but a 14.% decrease in N_c. Thus, we may conclude that for the aspect ratios examined, reducing τ_s can result in moderate gains in performance for relatively small increases in NTU. These results differ from those Krane [46] obtained in that a given increase in NTU for the lumped element system was not matched by a corresponding reduction in the figure of merit.

A somewhat different result was observed when τ_s was increased from 0.05 to 0.5. As before, the relationship between decreases in the optimum NTU and the corresponding reduction in system performance is a strong function of V^+. For the cases where the $T_{f,i,s}/T_\infty$ was 2.0 and V^+ was 0.01; increasing τ_s from 0.05 to 0.5 resulted in a 35.% reduction in NTU but a totally unacceptable 270.% increase in N_c. For the same $T_{f,i,s}/T_\infty$ and a V^+ of 0.05; increasing τ_s the indicated amount resulted in a 51.% decrease in the NTU, but a 75.% increase in N_c.

The first law efficiencies for the optimum counterflow systems are shown in Figure 4.13. This data illustrates a fundamental second law

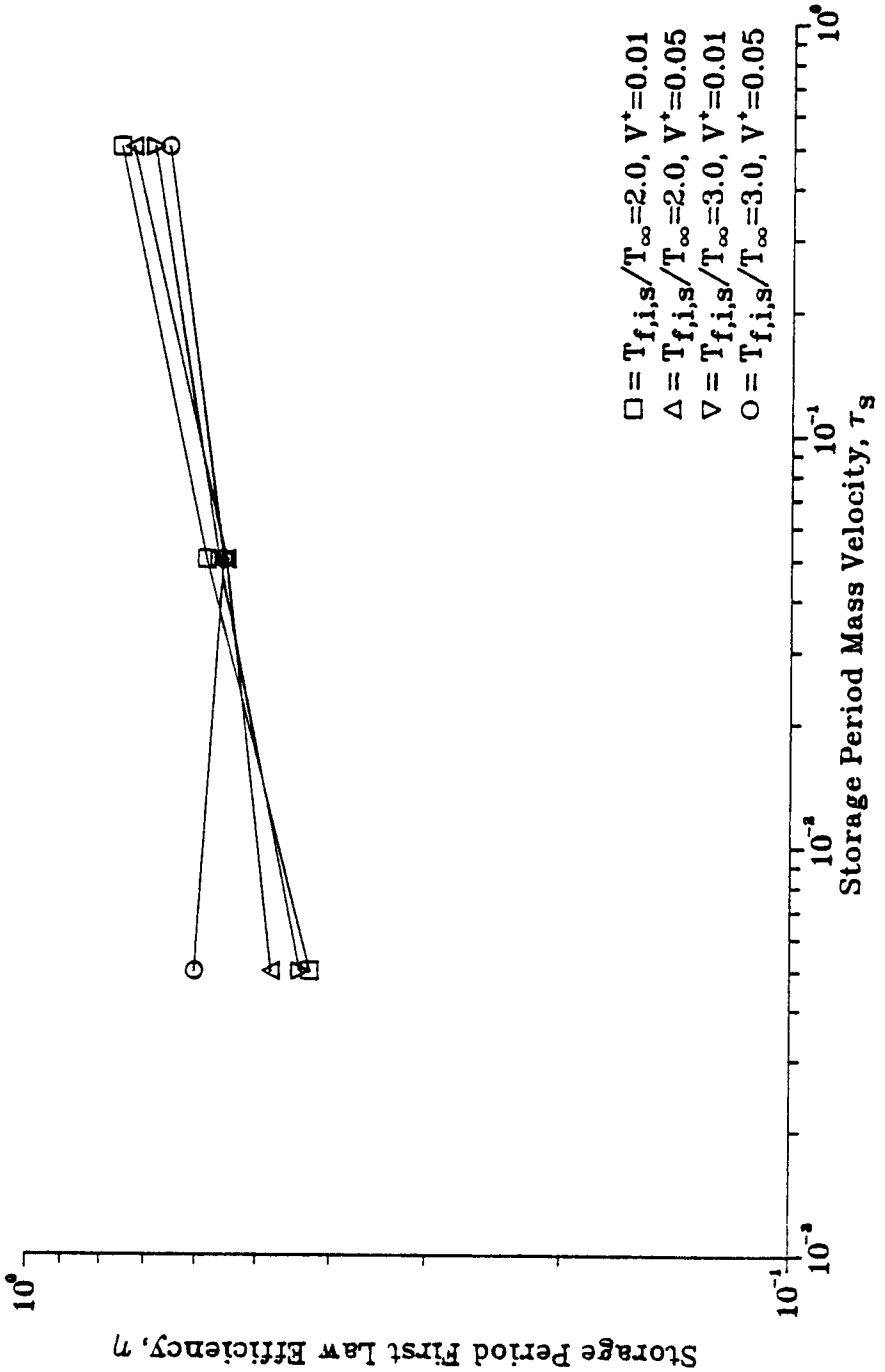


Figure 4.13. First law efficiencies for the optimized, unconstrained, counterflow design cases with $T_{m,o,s}/T_\infty = 1.1$.

considerations; that is these systems have poor first law efficiencies. The storage system with the lowest figure of merit, and therefore the best second law performance, also has the poorest first law efficiency. As the figure of merit increases (indicating a less efficient system), the first law efficiency increases. Similar results were reached by both Bejan [44] and Krane [46]. We note that the first law efficiency increases while the value of Bi_s decreases. Since this term is directly proportional to the average storage material temperature, this behavior would seen contradictory. It is explained, however, by the fact that the optimum storage time increases as Bi_s decreases. We conclude that even though the rate of heat transfer decreases as Bi_s decreases, the total amount of heat transfer increases due to increased storage times.

The distribution of the thermal availability destroyed during the storage period is summarized in Figure 4.14 for the design cases where $T_{f,i,s}/T_\infty$ was 2.0. The results for the cases where it was 3.0 have the same trends and will not be shown here for the sake of brevity. Figure 4.14 shows the fraction of total thermal availability destroyed during the storage period for each of three mechanisms: conduction in the storage material, heat transfer between the fluid and storage material, and heat transfer between the discharged hot fluid and the environment. These data show that the distribution is not a strong function of V^+ and that over the range of τ_s examined, the contribution due to conduction in the storage material dominates until τ_s approaches its upper limit of 0.50. During the this time, the next largest contribution is from heat transfer between the fluid and storage material followed by

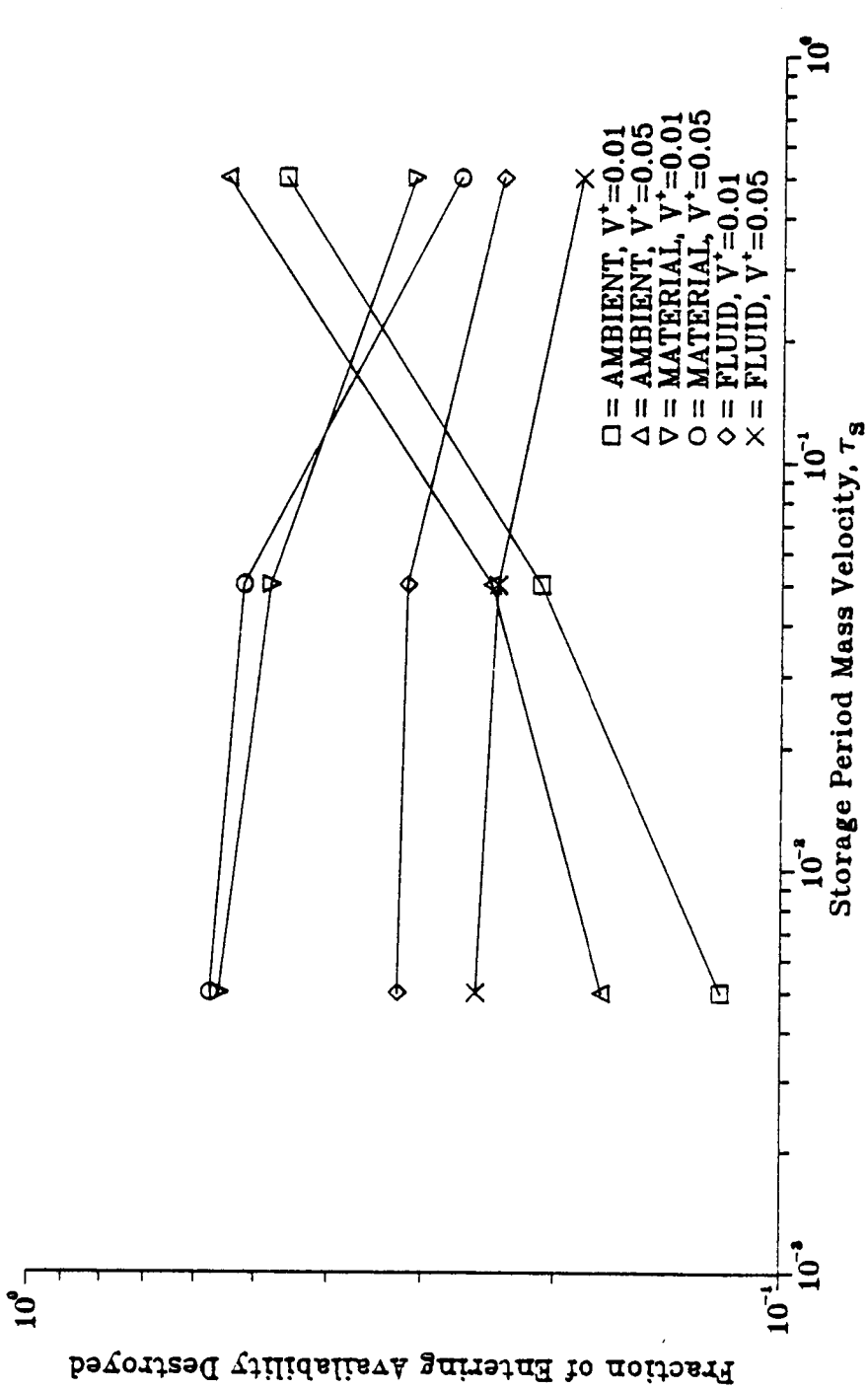


Figure 4.14. Optimum distribution of thermal availability destruction during the storage period for the unconstrained, counterflow, design cases with $T_{m,o,s}/T_\infty = 1.1$ and $T_{f,i,s}/T_\infty = 2.0$.

that due to the discharged hot fluid coming to equilibrium with the environment. As τ_s approaches its upper value of 0.5, the contribution due to heat transfer from exiting hot fluid increases and begins to dominate. As this happens, the contributions from both the conduction in the storage material and heat transfer between the fluid and storage material decrease, with the material conduction fraction always being larger. Again we note that these trends are consistent with the behavior of the optimization variables summarized in Figures 4.1, 4.2, and 4.3 (pp. 108, 109, and 110). Increases in G_s^+ and decreases in Bi_s result in more fluid exiting at a higher temperature. Also, increased values of Fo_s result in a higher percentage of the total availability destruction occurring in the exiting fluid. We conclude that for all but the highest mass velocities, entropy generation within the storage material is a significant contributor to the total entropy generated in a storage-removal cycle.

There is one other significant result concerning the operation of optimum counterflow systems: the distribution of total amounts of entropy generated in the storage and removal periods. An examination of the data in Tables 4.1, 4.3, 4.5, and 4.7 (pp. 89, 91, 93, and 95) shows that for the design cases summarized above, the total amount of entropy generated during the storage period, including that attributable to the exiting fluid, is approximately twice that generated during the removal period. Also, there is consistently less entropy generated in the storage material during the removal period than during the storage period. It is not known if this behavior accurately reflects the physical situation or results from the assumption of a uniform material

temperature at the beginning of the storage period. This disparity however does not hold for entropy generated by heat transfer between the fluid and storage element. As τ_s increases for a given set of design variables, the entropy generated in the fluid during the removal period approaches and in some cases slightly exceeds that of the storage period. The primary result though is the fact that only one third of the total thermal irreversibilities of a cycle occur during the removal period. This raises the concern that as τ_s increases and the influence of the thermal irreversibilities on the figure of merit decreases; entropy generation due to heat transfer during the removal period does not significantly effect the optimization process. This concern will be explored in more detail during the discussion of the performance of the mathematical model.

The optimization results for the design cases where the initial storage material temperature excess, $T_{m,o,s}/T_\infty$ was 1.3 will now be presented. As previously indicated, these results are very similar to those where $T_{m,o,s}/T_\infty$ was 1.1. The qualitative behavior of the optimization variables and other descriptions of system performance were in fact identical. The differences between the cases occurred only in their actual values. The major result of this analysis was that increasing the initial material temperature resulted in slightly lower figures of merit. This behavior is summarized in Figure 4.15 for the same set of design variables utilized for the cases where $T_{m,o,s}/T_\infty$ was 1.1. An examination of the data summarized in Tables 4.1 to 4.8 (pp. 89 through 96) shows the following additional differences for an optimum design with a higher initial material temperature:

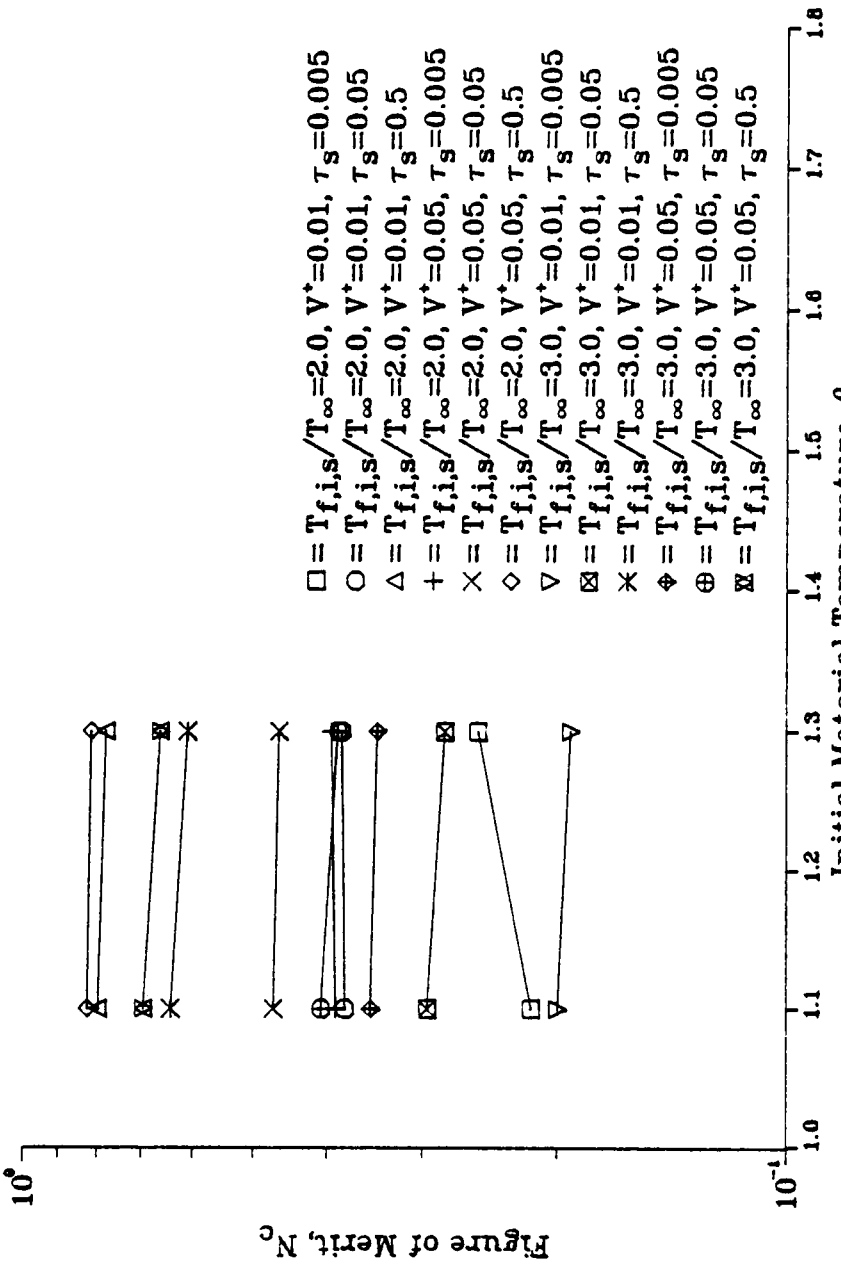


Figure 4.15. Optimum values for the figure of merit for the unconstrained, counterflow design cases with $T_{m,o,s}/T_\infty$ = 1.1 and $T_{m,o,s}/T_\infty$ = 1.3.

a. lower values of Fo_s, higher values of G_s^+, and lower values of Bi_s were generally required for an optimum system,

b. lower total amounts of thermal and pressure availability were destroyed as well as smaller fractions of entering thermal availability,

c. there was less entropy generation due to conduction in the storage material and heat transfer between the fluid and material, and more due to the discharged hot fluid reaching equilibrium with the environment,

d. larger NTUS were required, and

e. first law efficiencies were lower.

We conclude that higher initial material temperatures result in units that are slightly more efficient (i.e., lower values of N_c) but also have large NTUs. These are the same qualitative results that Krane [45] reached for the lumped element system.

Unconstrained Parallel Flow Cases

The parallel flow configuration was optimized with the same set of medium temperature design variables summarized in Figure 4.4 (p. 112). The most general result is that this configuration (with and without a dwell period) resulted in optimum systems with higher figures of merit than the comparable counterflow cases without a dwell period. These results are summarized in Figure 4.16 and show the figure of merit for the two parallel flow designs as well as the comparable counterflow case. These data show that, over the range of τ_s examined, the performance of the parallel flow cases was consistently worse than that for the counterflow base case (i.e., the set of design variables summarized in Figure 4.4). We also note that the figures of merit for both parallel

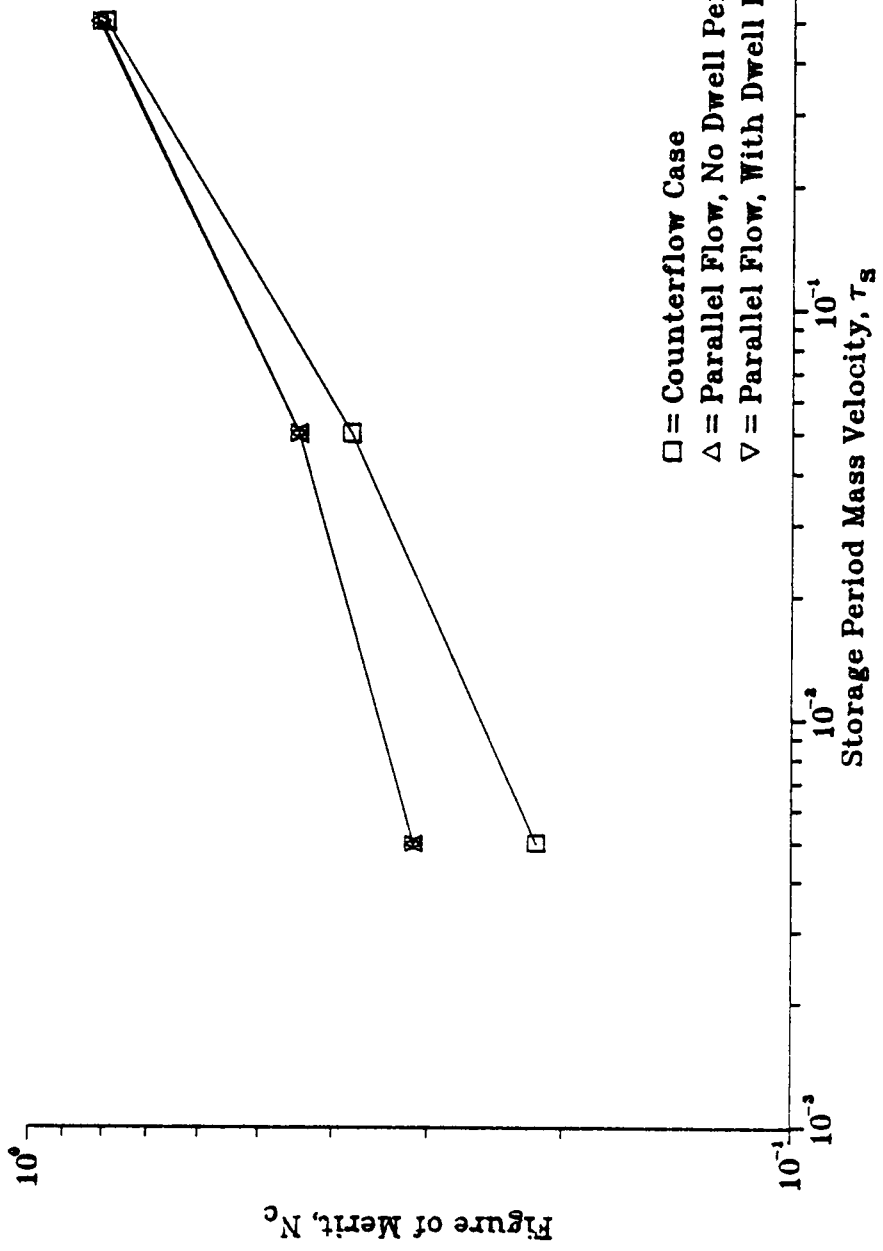


Figure 4.16. Optimum values for the figure of merit for the unconstrained counterflow and unconstrained parallel flow design cases with $T_{m,o,s}/T_\infty = 1.1$.

cases were essentially the same and the difference between them and the counterflow case decreased as τ_s approached its upper value. This behavior is attributed to the increasing amounts of pressure availability destruction. As τ_s increases the influence of the thermal irreversibilities on the value of the figure of merit decreases. It is not unreasonable then to expect the performance of the parallel designs to approach that of the counterflow case in those operating regions where pressure availability destruction dominates.

An examination of the optimization results presented in Tables 4.9 and 4.10 (pp. 97 and 98) shows the following additional optimum operating characteristics of the parallel flow designs:

a. Both designs (i.e., parallel flow configuration with and without a dwell period) generally required longer storage periods and lower values of G_s^+ and Bi_s for an optimum system than the counterflow case.

b. Both designs destroyed higher total amounts of pressure and thermal availability as well as destroying a higher percentage of the entering thermal availability. The design without the dwell period destroyed the largest percentage of entering availability.

c. During the storage period, each of the three entropy generation mechanisms destroyed more availability in the parallel flow designs than in the counterflow case.

d. The first law efficiencies of the parallel flow designs were both higher than the counterflow case, with the design without the dwell period generally having the highest efficiency.

e. Over the range of τ_s examined, both parallel flow designs resulted in a smaller optimum NTU. The design with the smallest size

varied as τ_s increased. For low values, the dwell period design resulted in the smallest NTU. At the maximum value of τ_s the dwell period design had the largest optimum NTU.

f. The dwell period elapsed dimensionless times were on the order of 6500. By comparison, the storage period dimensionless times for all counterflow and parallel cases ranged from 0.5 to about 6.0. The amount of entropy generated by conduction in the storage material during the dwell period averaged 24.% of the amount generated during the storage period and approximately 10.% of the total generated for the entire storage-removal cycle. Depending on the value of τ_s, a dwell period increased the total entropy generated during a cycle from 12.% to 67.% over that for the counterflow case.

We conclude that the parallel flow configuration, with and without a dwell period, results in optimum systems that are less efficient than those of the corresponding counterflow design. This was the same qualitative result that Mathiprakasam and Beeson [45] reached during their simplified second law analysis of thermal energy storage systems.

Constrained Counterflow Cases Without a Dwell Period

The constrained optimizations were defined to assess the sensitivity of the figure of merit, N_c, to two process parameters that are closely related to the economic viability a system design; its size (NTU) and its first law efficiency. Two cases were executed with the same set of medium temperature design variables summarized in Figure 4.4 (p. 112). The principle result obtained was that the second law efficiencies for both cases were poorer than the nominal counterflow case. These results are summarized in Figure 4.17 and show the figure

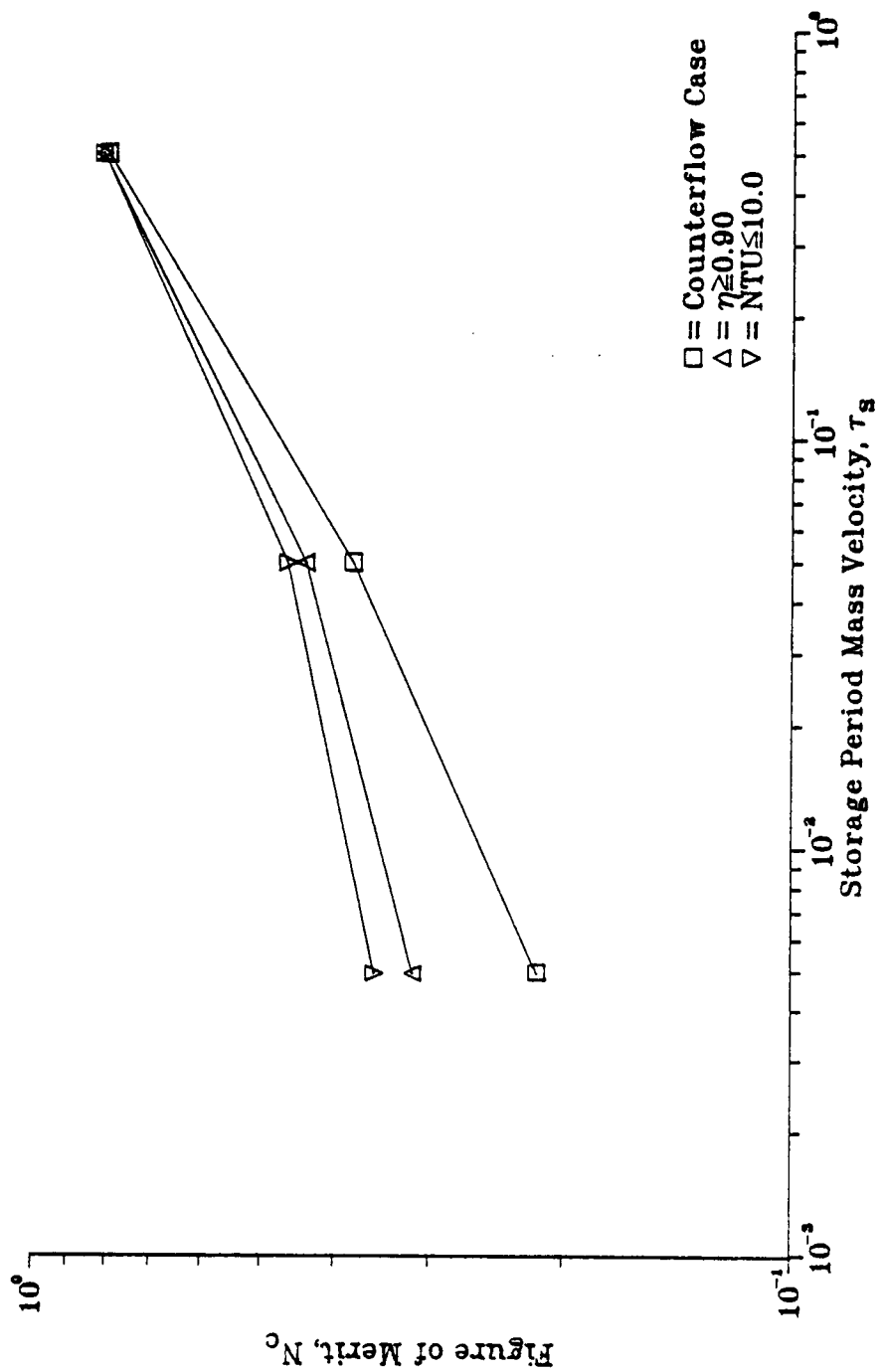


Figure 4.17. Optimum values for the figure of merit for the unconstrained and constrained counterflow design cases.

of merit as a function of τ_s for the two constrained designs as well as for the counterflow case.

Examining the optimization results summarized in Table 4.11 (p. 99) shows the following specific results for the cases where the storage system NTU was constrained to a maximum value of ten:

a. The optimum values of the figure of merit were greater than the counterflow case for all values of τ_s examined. This difference, however, decreased as τ_s approached its maximum value. N_c increased approximately 63.%, 22.%, and 1.5% for values of τ_s of 0.005, 0.05, and 0.5 respectively. Corresponding reductions in the value of NTU were approximately 81.%, 73.%, and 57.%.

b. Compared to the counterflow case, smaller values of G_s^+ and Bi_s and larger values of Fo_s were required for an optimum system. The value of G_s^+ decreased approximately 5.6%, 29.%, and 32.% for values of τ_s of 0.005, 0.05, and 0.5 respectively. Corresponding reductions in Bi_s were 80.%, 61.%, and 38.% respectively. Increases in Fo_s for the corresponding values of τ_s were 48.%, 27.%, and 12.%. Reductions in G_s^+ and Bi_s were expected since these are the two optimization variables that determine the value of the NTU. Their product must decrease if the NTU is to decrease.

c. The first law efficiencies of the constrained systems were consistently higher. Again we note that this behavior is consistent with the longer storage periods.

d. The constrained systems destroyed essentially the same total amount of pressure availability but considerably more total thermal availability than the counterflow base case. For values of τ_s of 0.005,

0.05, and 0.5; increases of 160.%, 230.%, and 174.% respectively were calculated.

We conclude that constraining the dimensionless storage unit size to moderate values results in less efficient units and the degradation of system performance, as measured by the value of N_c, is a strong function of τ_s. This raises the possibility that some units could be operated away from their optimum design point without adversely affecting their second law efficiency. Such a move should be considered carefully though, given the large increases in total thermal irreversibilities that would accompany such off design operation.

The results for the design where the storage period first law efficiency was constrained to a minimum value of 0.90 are summarized in Table 4.12 (p. 100). Specific observations and conclusions are:

a. The optimum values for the figure of merit were larger than the counterflow case for all values of τ_s examined. As was the case when the NTU was constrained, the performance degradation was a strong function of τ_s. N_c increased approximately 46.%, 15.%, and 1.6% as τ_s increased from 0.005 to 0.5. The corresponding reductions in the value of NTU were approximately 1.%, 14.%, and 20.%

b. Smaller values of G_s^+, larger values of Bi_s, and longer storage times were required for an optimum system. The value of G_s^+ decreased approximately 23.%, 4.%, and 24.% as τ_s increased from 0.005 to 0.5. Corresponding increases in the value of Bi_s were 29.%, 10.4%, and 5.6%. Fo_s increased approximately 138.%, 101.%, and 15.% as τ_s increased from 0.005 to 0.5. The behavior of G_s^+ and Bi_s are consistent with the physical system and the type of constraint imposed. Larger

values of Bi_s increase the rate of heat transfer to the storage material. Reductions in the value of G_s^+ increase the temperature drop in the fluid. This would increase the rate of heat transfer to the storage material and consequently reduce the exiting fluid temperature.

c. The constrained systems destroyed more total pressure and thermal availability than the counterflow case and, like previous results, this behavior was a strong function of τ_s. At the three values of τ_s examined, the total thermal availability destruction increased approximately 356.%, 207.%, and 113.%. Increases in total pressure availability destroyed at the same points were 263.%, 48.%, and 23.%.

We conclude that constraining the storage unit first law efficiency results in less efficient units (i.e., larger values of N_c) and that the degree of degradation is a strong function of τ_s. As was the case when size constraints were imposed, this result suggests that the some off-design operation is possible without significantly affecting the second law efficiency of the unit. Again, this option should be considered in conjunction with the increased amounts of total availability destruction that can occur.

Critique of the Mathematical Model

The purpose of this section of the document is to assess the performance of the mathematical model developed for this study. Three specific areas will be addressed:

a. the effects of some of the assumptions utilized in the model,

b. the accuracy of the optimization results, and

c. the performance of the GRG2 optimization routine.

Given the complexity of the problem, the assumption that the storage period begins with a uniform storage material temperature was made for the sake of simplicity. It was eventually proven, however, not to be a good approximation as a substantial temperature gradient existed in the storage material at the end of the removal period. As a consequence, future analyses should include a procedure involving successive iterations using the temperature distributions at the end of the previous removal period as the initial condition for the next storage period. This increased rigor will also permit the identification of the cause for another interesting operating characteristic. It should be recalled that the majority of the counterflow systems optimized destroyed more thermal availability in the material during the storage period than during the removal period. Given that the fluid mass velocities, heat transfer coefficients, and physical geometry were the same for both periods, the most plausible explanation is that there are different time averaged, material-fluid temperature differences for the storage and removal periods. The iterative execution sequence described above would determine if the characteristic is caused by incorrect storage material temperatures during the storage period or is a valid consequence of the lower entering fluid temperature and severe storage material temperature gradient during the removal period.

The accuracy of the results for a given design case were verified by showing that changes in the final value of the optimization variables produced higher values for the figure of merit, N_c. To accomplish this, (n-1) of the n optimization variables were fixed at the value determined by GRG2 during the original optimization. The value of the remaining

optimization variable (i.e., the n^{th} variable) was then varied and the behavior of the figure of merit observed. If it increased for all but the original optimum value, then the original value was shown to be a minimum.

This procedure was executed for six unconstrained, counterflow design cases, which represented a cross section of the design variables utilized for the study. The design variables for each case as well as an indication of how the original optimization was terminated is summarized in Table 4.17. The termination data are presented now but will be discussed later. The results of this verification procedure are summarized in Figures 4.18, 4.19, and 4.20. Figure 4.18 is for the iteration where only G_s^+ was varied, Figure 4.19 where only Bi_s was varied, and Figure 4.20 where only Fo_s was varied. Each figure shows a plot of the figure of merit as function of the particular optimization variable being varied. The original optimum point for each case appears as a large asterisk. Each figure also shows a vertical line which represents the initial value of the variable (i.e., first guess for the optimum value) that was used in the original optimization.

An examination of these results for each optimization variable shows that the value of the figure of merit either increased away from each original optimum value or gradually increased or decreased through the original optimum value. We conclude that GRG2 was successful in locating a minimum value or, at least, a value in a "minimum region" where the figure of merit was changing only slightly. The insensitivity of GRG2 in these "minimum regions" is attributed to two causes; the intense numerical nature of the problem and the step size that GRG2 used to calculate the partial derivatives of the figure of merit.

Table 4.17. Summary of unconstrained, counterflow design cases used to verify the accuracy of the optimization results

Case number	τ_s	$T_{f,i,s}/T_\infty$	V^+	$T_{m,o,s}/T_\infty$	Termination message from GRG2
1	0.50	2.0	0.01	1.1	Kuhn-Tucker criteria met
2	0.50	3.0	0.05	1.3	Could not find a better point
3	0.05	2.0	0.01	1.1	No change in three (3) successive evaluations
4	0.05	3.0	0.05	1.3	Kuhn-Tucker criteria met
5	0.005	3.0	0.05	1.3	Kuhn-Tucker criteria met
6	0.005	2.0	0.01	1.1	No change in three (3) successive evaluations

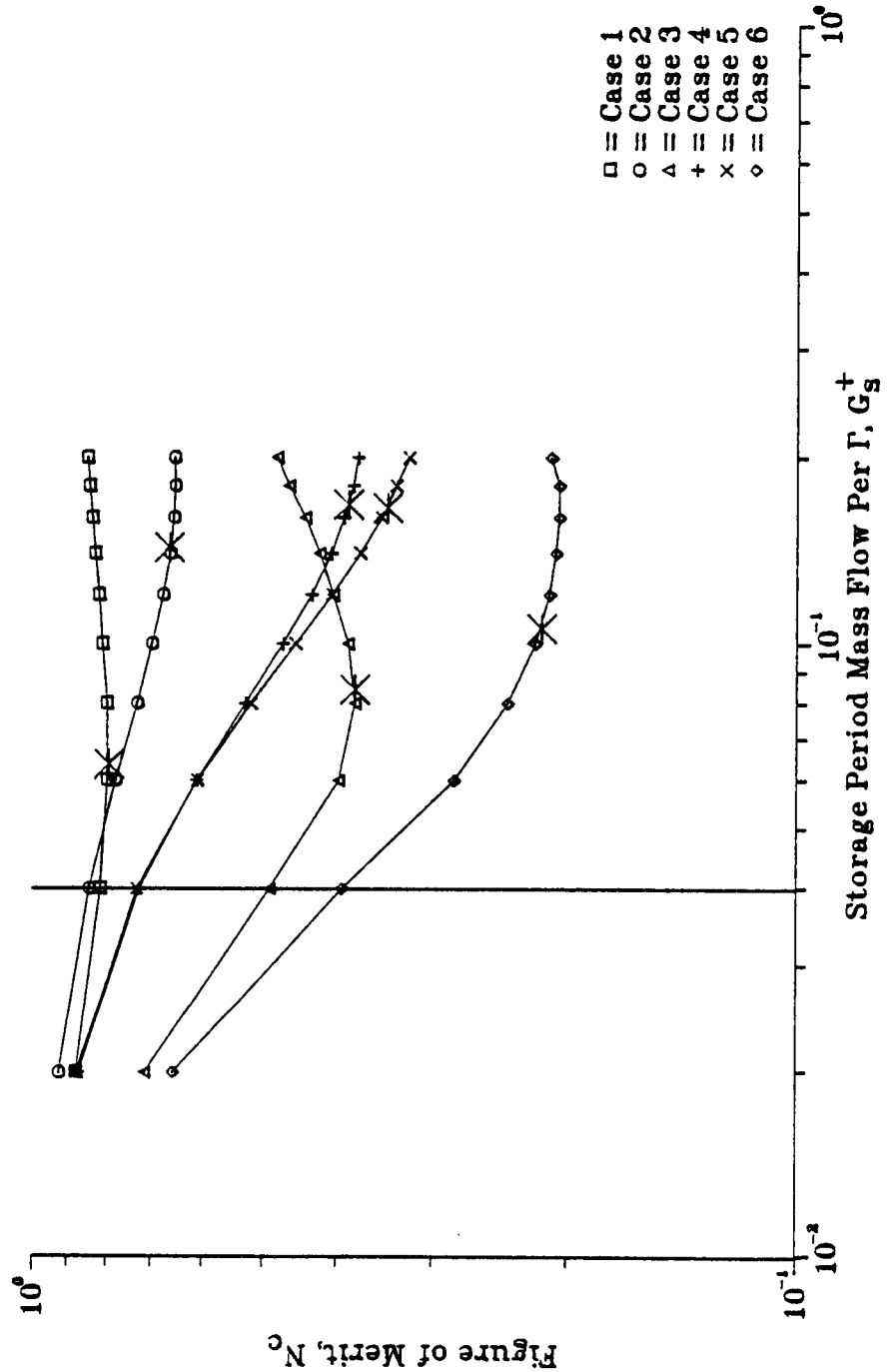


Figure 4.18. Results of the verification procedure for the G_s^+ optimization variable for the counterflow, unconstrained design cases.

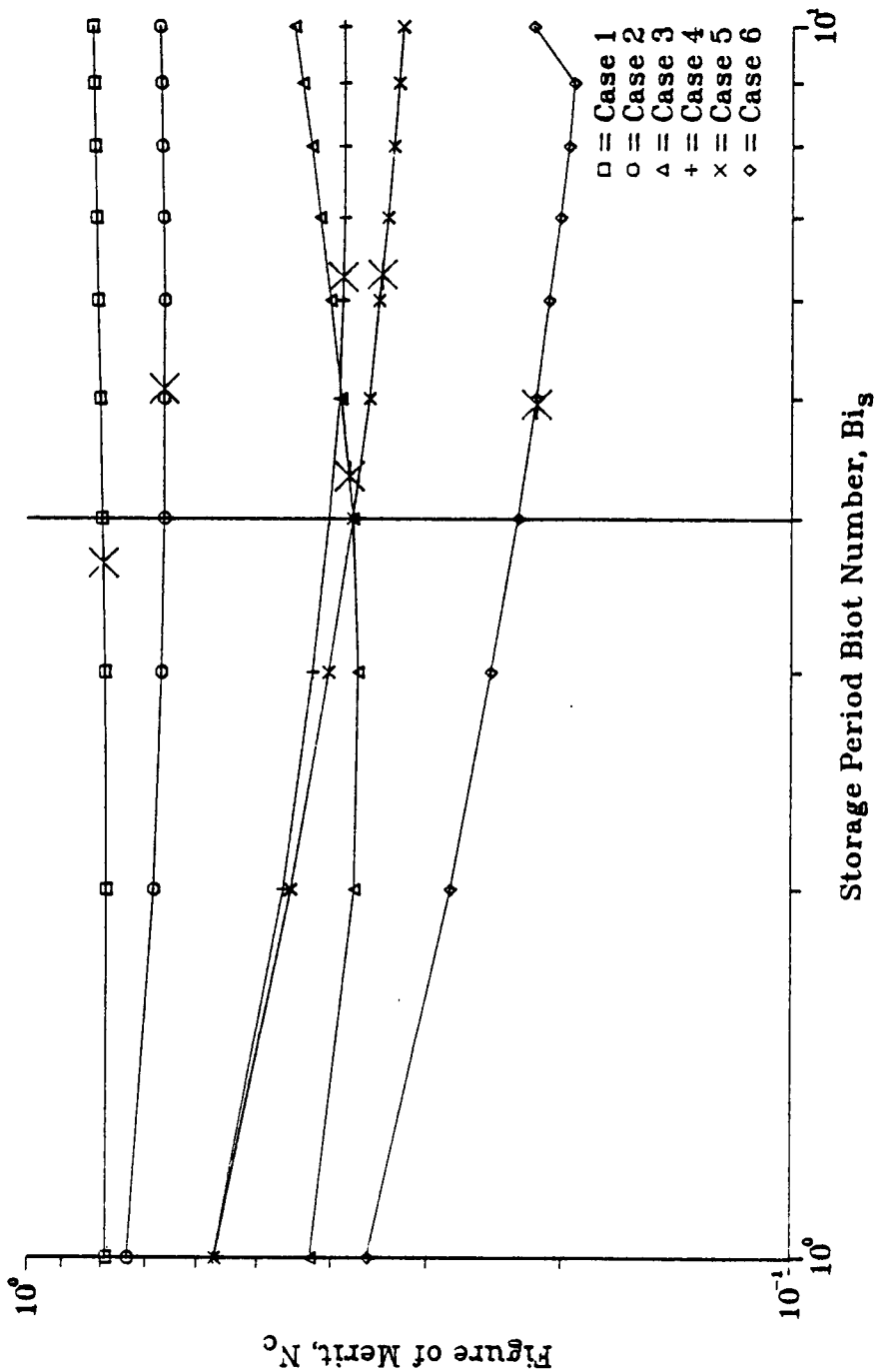


Figure 4.19. Results of the verification procedure for the Bi_s optimization variable for the unconstrained, counterflow design cases.

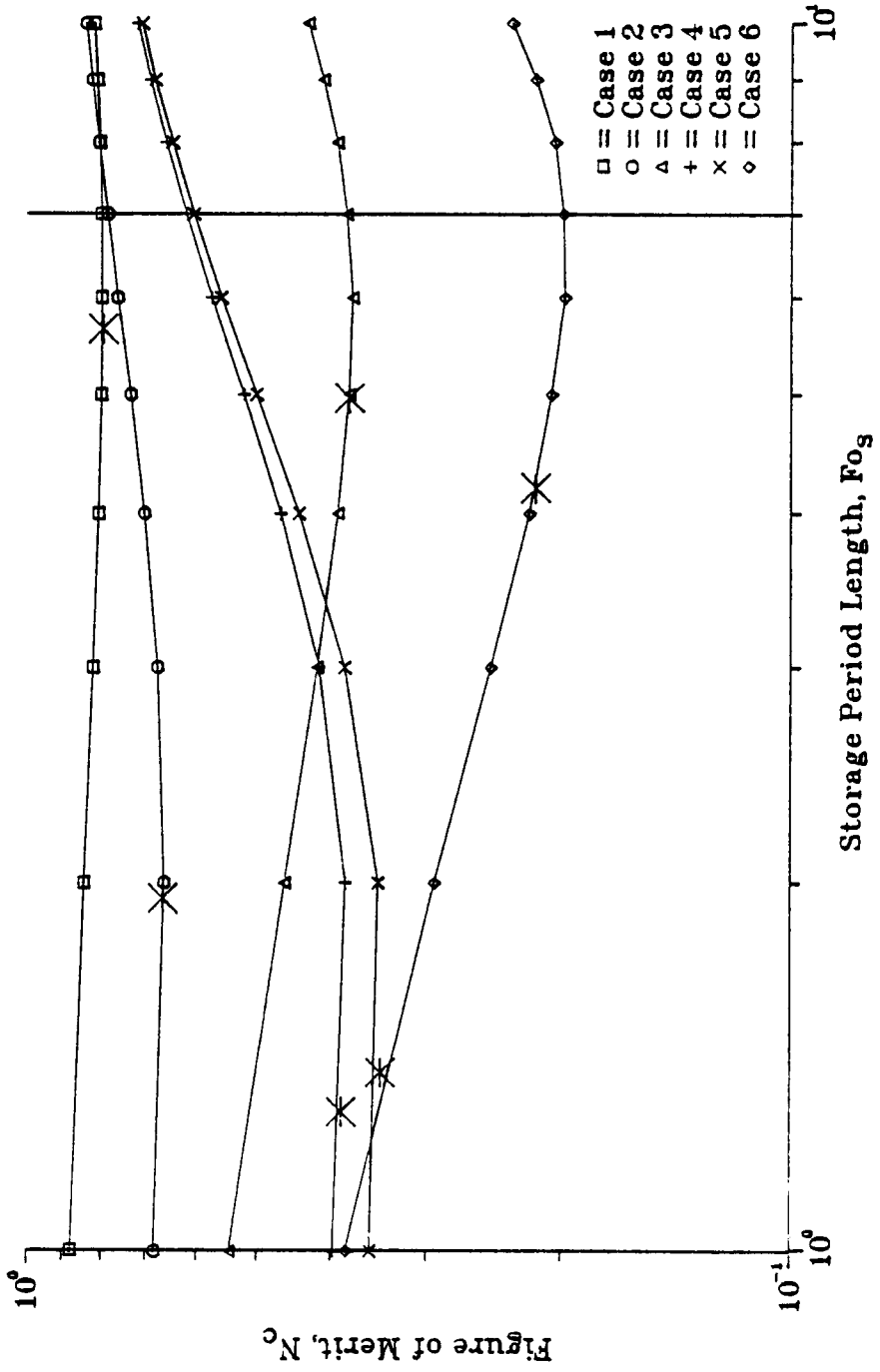


Figure 4.20. Results of the verification procedure for the Fo_s optimization variable for the unconstrained, counterflow design cases.

Calculating a value for the figure of merit requires a large number of individual calculations. For both the storage and removal periods there are a series of 59 transient temperature calculations. Within each time increment there are both one and two-dimensional integrations. At the end of each period there are additional one-dimensional integrations. As previously explained GRG2 was required to calculate objective function partial derivatives with the same routine which calculated a value for the figure of merit, using a fixed increment size. Given these circumstances it is reasonable to expect that "small" step sizes would partially obscure any real changes in the value of the figure of merit because of the errors propagated through the large number of individual calculations that had to be performed.

An example of this type of behavior can be seen in case numbers four and five. GRG2 terminated these runs with its most rigorous status message; that the final point meet the Kuhn-Tucker criteria. Kuhn-Tucker are a set of conditions which indicate that a true local minimum point has been found within the tolerance specified by the user. However, an examination of the results shown in Figures 4.18 through 4.20 indicate that final values of G_s^+ and Fo_s can be changed and further reduce the value of the figure of merit. Since the termination tolerance specified for these runs was 1.0×10^{-4} and reductions in the figure of merit greater than this could have been achieved, we conclude that the increment size used to calculate the partial derivatives was of such a size as to obscure the real change in the figure of merit.

Case two illustrates the effect of beginning an optimization run with improper initial values of the optimization variables. As previously explained, a set of initial values for the optimizations variables was defined during the verification effort and used for all subsequent design cases. As the data in Figures 4.18 through 4.20 shows, using this set for case two resulted in values of the figure of merit in a region of the surface with little sensitivity to Bi_s or Fo_s. As a result, GRG2 could not find a better point after nine complete optimization iterations and terminated. Although a small step size certainly contributed to the inability of GRG2 to determine which direction to proceed, this result is primarily due to poor initial values for the optimization variables.

We conclude that GRG2 is capable of optimizing large, complicated problems but requires considerable preparation to operate properly. Prior to a run it is necessary to specify appropriate initial values for the optimization variables, to define an appropriate incremental length to calculate partial derivatives, and to have correctly scaled the problem. Since each of these requirements can change between problems, and even between cases for the same problem, we also conclude that GRG2 is somewhat problem specific and should be reprepared when significant changes occur in the problem statement.

5. CONCLUSIONS AND RECOMMENDATIONS

Based on the analysis and results presented, the following observations, conclusions, and recommendations can be made about the design and operation of sensible heat thermal energy storage systems that have been optimized to minimize entropy production.

a. The entropy generation attributable to material conduction is a major contributor to the total thermal irreversibilities associated with the operation of sensible heat storage unit. Over the range of variables examined, this contribution accounted for between 26.% and 60.% of the total thermal availability destruction that occurred during a complete storage-removal cycle.

b. The storage material geometry, specifically the storage element aspect ratio, V^+, has a significant impact on the optimum design of these types of systems. The effect of V^+ on the value of N_c is exceeded only by that of the fluid mass velocity, τ_s.

c. The counterflow configuration without a dwell period operates more efficiently than the parallel flow configuration, with or without a dwell period. Dwell periods in general were shown to be impractical because of their extreme length and their negative impact on the figure of merit. Depending on the value of τ_s, a dwell period increased (over the corresponding counterflow design) the total thermal entropy generated from 12.% to 67.%.

d. The thermodynamic efficiencies of these types of storage systems are extremely poor, in that over the range of variables examined in this study, they destroyed from 20.% to 82.% of the entering thermal and pressure availability.

e. The optimum figure of merit is relatively insensitive to changes in the size (NTU) of the storage unit, but this insensitivity is a strong function of τ_s. This agrees with the results of Krane [46,47]. Operation slightly away from an optimum size should be considered carefully, however, because of the large increases in total thermal and pressure availability destruction that can accompany such moves.

These specific results can be generalized to give a generic set of design guidelines for the type of storage unit examined in this study. First, anyone wanting to specify a conceptual design of a storage system that minimizes entropy generation should consider only counterflow units that operate without a dwell period. The following guidelines should then be followed to define a starting point for the design optimization study:

a. Nominal values for τ_s and V^+ on the order of 0.05 and 0.05 respectively should be utilized. These values were shown to produce the most reasonably sized systems.

b. Values of 2.0, 0.15, and 6.0 should be used as the starting values for the optimization variables F_{o_s}, G_s^+, and Bi_s respectively. These values are representative of all the optimum values at or near the nominal value of τ_s defined above and as such are excellent starting points for a design procedure.

The secondary purpose of this study was to demonstrate that it was practical to conduct a sophisticated design optimization study using individual temperature and pressure entropy generation terms. The results presented herein show that such procedures are indeed workable and provide consistent results. There are, however, two comments concerning

the mathematical model and optimization program that are pertinent to future studies:

a. The assumption of a uniform initial material temperature for the start of the storage period was shown to be not representative of the physical situation. Large temperature gradients were found to exist in the storage material at the end of the removal period. The mathematical model and its execution should be modified in future studies to include the effects of these large gradients.

b. The ability of the GRG2 optimization program to find minimum values of the figure of merit was acceptable given its intensely numerical nature but required considerable preparation to use. Future studies should either limit the range of design variables examined or ensure that GRG2 is reprepared when major changes are made in the problem description.

Recommendations for Future Study

The results of this study have also identified areas for future study. These include analyses of heat transfer augmentation devices, the operation of several storage units in series, and a design optimization constrained by economic considerations. These were previously identified as prospective areas for study by Bajan [14] and Krane [46] and their validity has been re-established by this study.

For nominal values of the fluid mass velocity (i. e. $\tau_s \approx 0.05$), a significant fraction of the total entropy generated during a storage-removal cycle occurs as a result of heat transfer through finite temperature differences rather than viscous friction. Relatively simple

design changes however have the potential to significantly reduce the effects of two such mechanisms: convective heat transfer within the flowing fluid and convective heat transfer between the exiting hot fluid and the surroundings.

a. Convective heat transfer between the flowing fluid and the storage material accounted for between 24.% to 36.% of the thermal irreversibilities generated during a complete cycle. Heat transfer augmentation devices have the potential to reduce the fluid-material temperature difference and thus decrease the entropy generation attributable to this mechanism. The effect that these devices might have on the other entropy generation mechanisms is not clear. In any event, their net effect on the optimum design and operation of these types of storage units should be established in some future study.

b. Thermal availability destroyed as a result of the discharged hot fluid reaching equilibrium with the environment accounted for as much as 67.% of the thermal irreversibilities generated during the storage period. This destruction could be greatly reduced by connecting several storage units in series. With this flow arrangement, the availability contained in the exiting hot fluid of the first unit would not be destroyed but would be the availability source for subsequent units. Thus, an investigation to determine the optimum number of units and their operation should be carried out.

As pointed out by Krane [46], the optimum design and performance of a sensible heat storage unit must eventually be defined in economic terms. Given the progress made by this and previous studies [14,46,47]

in defining fundamental, optimum, operating characteristics, it is recommended that future studies concentrate less on the effects of τ_s and define optimum systems for some nominal mass velocity as a function of both economic considerations and the material aspect ratio, V^+. This variable was shown to have a significant impact on the optimum design, and its effect should be defined in greater detail. Futhermore, it is recommended that any economic criterion be treated as constraints on the optimum design rather than as the objective function to be minimized. This has the benefit of allowing a range of constraints, such as different initial capital costs, to be considered. This approach will also provide data to quantify Bejan's definition of an optimal thermal system; namely "the least irreversible system that a designer can afford."

LIST OF REFERENCES

LIST OF REFERENCES

1. Didon, D., Garvin, D., and Snell, J., "A Report on the Relevance of the Second Law of Thermodynamics to Energy Conservation," National Bureau of Standards Technical Note 1115, 1980.

2. Cambel, A. B., Heffernan, G. A., Cutler, D. W., and Ghamarian, A., "Second Law Analysis of Energy Devices and Processes," Proceedings of a Workshop held in Washington, D.C., August 14-14, 1979.

3. Moody, F. J., "Second Law Thinking—Example Applications in Reactor and Containment Technology," Presented at the 22nd National Heat Transfer Conference and Exhibition, Niagara Falls, New York, 1984.

4. Soumerai, H. P., "Second Law Thermodynamic Treatment of Heat Exchangers," Presented at the 22nd National Heat Transfer Conference and Exhibition, Niagara Falls, New York, 1984.

5. Perez-Blanco, H., "Irreversibility in Heat Transfer Equipment," Presented at the 22nd National Heat Transfer Conference and Exhibition, Niagara Falls, New York, 1984.

6. von Spakovsky, M. R. and Evans, R. B., "Detailed Second Law Design of Components in Complex Thermal Systems," Presented at the 22nd National Heat Transfer Conference and Exhibition, Niagara Falls, New York, 1984.

7. Zilberberg, Y. M., "Impact of Heat Exchanger Dynamics of the Second Law Analysis of Thermodynamic Cycles," Presented at the 22nd National Heat Transfer Conference and Exhibition, Niagara Falls, New York, 1984.

8. Sciubba, E., Kelnhofer, J., and della Vida, P. L., "On The Optimization of Cogeneration Plants," Presented at the 22nd National Heat Transfer Conference and Exhibition, Niagara Falls, New York, 1984.

9. Sciubba, E., Kelnhofer, J., and Esmaili, H., "Second Law Analysis of a Combined Gas Turbine-Steam Turbine Cycle Powerplant," Presented at the 22nd National Heat Transfer Conference and Exhibition, Niagara Falls, New York, 1984.

10. Barclay, J. A., "A Comparison of the Efficiency of Gas and Magnetic Refrigerators," Presented at the 22nd National Heat Transfer Conference and Exhibition, Niagara Falls, New York, 1984.

11. Frangopoulos, C. A., "Thermoeconomic Functional Analysis: An Innovative Approach to Optimal Design of Thermal Systems," Presented at the 22nd National Heat Transfer Conference and Exhibition, Niagara Falls, New York, 1984.

12. Frangopoulos, C. A. and Evans, R. B., "Thermoeconomic Isolation and Optimization of Thermal System Components," Presented at the 22nd National Heat Transfer Conference and Exhibition, Niagara Falls, New York, 1984.

13. Hesselman, K., "Optimization of Heat Exchanger Networks," Presented at the 22nd National Heat Transfer Conference and Exhibition, Niagara Falls, New York, 1984.

14. Bejan, A., *Entropy Generation Through Heat and Fluid Flow*, Wiley-Interscience, New York, 1982.

15. Glenn, D. R., *Technical and Economic Feasibility of Thermal Energy Storage*, NTIS-C00-2558-1, 1976.

16. Committee on Advanced Storage Systems, Criteria for Energy Storage R&D, National Academy of Science, Washington, D.C., 1976.

17. Bundy, F. P., Herrick, C. S., and Kosky, P. G., *The Status of Thermal Energy Storage*, Report No. 76CRD041, General Electric Corporation, Schenectady, New York, 1976.

18. Beckman, G. and Gilli, P. V., *Thermal Energy Storage*, Springer-Verlag, New York, 1984.

19. Jensen, J. and Sorensen, B., *Fundamentals of Energy Storage*, John Wiley & Sons, New York, 1984.

20. Meyer, C. F., "Large-Scale Thermal Energy Storage For Cogeneration and Solar Systems," *Proceedings of the Fifth Energy Technology Conference*, Washington, D.C., 1978.

21. Schmidt, F. W. and Willmott, A. J., *Thermal Energy Storage and Regeneration*, McGraw-Hill, New York, 1981.

22. Szego, J., *Transient Behavior of Solid Sensible Heat Thermal Energy Storage Units*, Ph.D. Thesis, Pennsylvania State University, 1978.

23. Schmidt, F. W., Somers, R. R., Szego, J., and Laananen, D. H., "Design Optimization of a Single Fluid, Solid Sensible Heat Storage Unit," *Transaction of the ASME*, 1977.

24. Schmidt, F. W. and Szego, J., "Transient Response of Solid Sensible Heat Thermal Storage Units-Single Fluid," *Journal of Heat Transfer*, 1976.

25. Martin, J. F., Olszewski, M., and Tomlinson, J. J., *Thermal Energy Storage Technical Progress Report April 1983-March 1984*, ORNL/TM-9170, United States Department of Energy, 1984.

26. Segaser, C. S. and Christian, J. E., *Low Temperature Thermal-Energy Storage*, ANL/CES/TE-79-3, United States Department of Energy, 1979.

27. Van Wylen, G. J. and Sonntag, R. E., *Fundamentals of Classical Thermodynamics*, John Wiley and Sons, New York, 1973.

28. Gaggioli, R. A., Yoon, J., Patulski, S. A., Latus, A. J., and Obert, E. F., "Pinpointing the Real Inefficiencies in Power Plants and Energy Systems," *Proceedings of the American Power Conference*, 1975.

29. Bejan, A., "Second Law Analysis in Heat Transfer and Thermal Design," *Advances in Heat Transfer*, Academic Press, 1982.

30. Armor, A. F., "Efficiency Improvement in Fossil-Fired Plants," Presented at the Joint Power Generation Conference, Indianapolis, Indiana, 1983.

31. Gouy, S., "Sur l'energie utilizable," *Journal of Physics*, 1889.

32. Anzelius, A., "Uber Erwarmung Vermittals Durchstromender Median," *Z. Angew Math. Mech.*, 1926.

33. Nusselt, W., "Die Theorie des Windehitzers," *Z. ver. Deut. Ing.*, 1927.

34. Hausen, H., "Uber die Theorie des Warmeaustausches in Regeneratoren," *Z. Angew Math. Mech.*, 1929.

35. Schumann, T. E. W., "Heat Transfer: A Liquid Flowing Through a Porous Prism," *Journal Franklin Institute*, 1929.

36. Larson, F. W., "Rapid Calculations of Temperature in a Regenerative Heat Exchanger Having Arbitrary Initial Solid and Entering Temperatures," *International Journal of Heat Transfer*, 1967.

37. Coppage, J. E., and London, A. L., "The Periodic-Flow Regenerator—A Summary of Design Theory," *Transaction of the ASME*, 1953.

38. Kays, W. M. and London, A. L., *Compact Heat Exchangers*, 2nd Edition, McGraw-Hill, New York, 1964.

39. Willmott, A. J., "Digital Computer Simulation of A Thermal Regenerator," *International Journal of Heat and Mass Transfer*, 1964.

40. Rosen, J. B., "Kinetics of Fixed Bed System for Solid Diffusion into Spherical Particles," *Journal of Chemical Physics*, 1952.

41. Handley, D. and Heggs, P. J., "The Effect of Thermal Conductivity of the Packing on Transient Heat Transfer in a Fixed Bed," *International Journal of Heat and Mass Transfer*, 1969.

42. Jefferson, C. P., "Prediction of Breakthrough Curves in Packed Beds," *American Institute of Chemical Engineers Journal*, 1972.

43. Riaz, M., "Analytical Solutions for Single and Two-Phase Models of Packed-Bed Thermal Storage Systems," *Journal of Heat Transfer, Transaction of the ASME*, 1972.

44. Bejan, A., "Two Thermodynamic Optima in the Design of Sensible Heat Units for Energy Storage," *Journal of Heat Transfer, Transaction of the ASME*, 1978.

45. Mathiprakasam, B. and Beeson, J., "Second Law Analysis of Thermal Energy Storage Devices," *Proceedings of the AIChE Symposium Series*, Seattle, Washington, 1983.

46. Krane, R. J., *A Second Law Analysis of the Optimum Design and Operation of Thermal Energy Storage Systems*, Report No. MAE-SLA-85-1, Department of Mechanical and Aerospace Engineering, University of Tennessee, Knoxville, Tennessee, 1985, (submitted for publication).

47. Krane, R. J., *A Second Law Analysis of a Thermal Energy Storage System With Joulean Heating of the Storage Element*, Report No. MAE-SLA-85-2, Department of Mechanical and Aerospace Engineering, University of Tennessee, Knoxville, Tennessee, 1985, also ASME paper No. 85-WA/HT-19, Presented at the 1985 Winter Annual Meeting of the American Society of Mechanical Engineers, Miami, Florida, Nov. 18-22, 1985.

48. Reklaitis, G. V., Ravindran, A. and Ragsdale, K. M., *Engineering Optimization*, John Wiley and Sons, New York, 1983.

49. Gill, P. E., Murray, W. and Wright, M. H., *Practicle Optimization*, Academic Press, New York, 1981.

50. Lasdon, L. S., Waren, A. D., Jain, A. and Rather, M., "Design and Testing of a Generalized Reduced Gradient Code for Nonlinear Programming," *ACM Transactions on Mathematical Software*, 1978.

51. Lasdon, L. S., Waren, A. D. and Rather, M. W., *GRG2 User's Guide*, Technical Memorandum No. CIS-T8-01, Computer and Information Science Department, Cleveland State University, Cleveland, Ohio, 1978.

52. Ozisik, M. N., *Heat Conduction*, John Wiley and Sons, New York, 1980.

53. Oak Ridge National Laboratory, Martin Marietta Energy Systems, Inc., Oak Ridge, Tennessee.

54. McCormick, J. M. and Salvadori, M. G., *Numerical Methods in FORTRAN*, Prentice-Hall, New Jersey, 1964.

55. *CRC Standard Mathematical Tables*, 20th Edition, CRC Press, Cleveland, Ohio, 1972.

56. Kreith, F., *Principles of Heat Transfer*, Harper and Row, New York, 3rd Edition, 1973.

APPENDIXES

APPENDIX A

ENTROP SUBROUTINE GLOSSARY, PROGRAM LISTING, AND SAMPLE OUTPUT

The following is a glossary of the names and functions of the subroutines in the ENTROP program. They are listed in the same order that they occur and a listing of the program and some typical output is also included. Although mentioned in the body of the report, it should be repeated here that the subroutines DECOMP, DGBFA, DAXPY, DSCAL, IDAMAX, DGBSL, and DDOT were not written by the author but taken from the CORLIB public domain computer library.

GCOMP: This is ENTROP's primary subroutine and the interface to the GRG2 optimization program. It contains the routing to conduct the five most basic calculations. The only calculation it performs itself, besides initializing data arrays, is the figure of merit. This subroutine contains the instructions steps illustrated in Figure 3.1.

B1B2: Calculates the B1 and B2 coefficients of the discretized material conduction equations. These coefficients are defined in Appendix B.

GUTS: Performs the routing and calls to calculate the fluid-material transient temperature response for one time increment. This subroutine contains the iterative sequence illustrated in Figure 3.2.

CONST: Calculates the discretized material conduction equation constant array for each time period.

DECOMP: Decomposes the wall temperature polynomial curve fit coefficient array by a gaussian elimination procedure.

DEFINE: Defines the coefficient array for the discretized material conduction equations and stores this array in DGBFA and DGBSL's working matrix.

DGBFA: Factors the discretized material conduction equation set working matrix using a gaussian elimination procedure.

DAXPY: Performs a vector operation needed by the DGBFA and DGBSL subroutines. It multiplies a constant times a vector, then adds the results to a second vector.

DSCAL: Performs a vector operation needed by DGBFA. It scales a vector by a constant.

IDAMAX: Performs a vector operation needed by DGBFA. It finds the index of an element having the maximum absolute value.

DGBSL: Solves the banded system, A*X=B using the factors supplied by DGBFA.

DDOT: Performs a vector operation needed by DGBSL. It forms the dot product of two vectors.

INTERP: The interpolation routine used to determine material wall temperatures as a part of the fluid temperature solution procedure.

ONEDIM: Performs the one-dimensional integration of discrete data points. This routine is used to integrate rates (i.e., per unit length) of entropy generation along the flow channel during a given time increment and also the rates of material, fluid, and exiting fluid entropy generation at the end of the storage, dwell, and removal periods.

SGEN: Calculates the material, fluid, and existing fluid rates of entropy generation for each of the material and fluid nodes, for each time increment.

SOLVE: Solves the linear system A*X=B. It is used to calculate the coefficients of the wall temperature polynomial curve fit. In this system, A is the curve fit equation set coefficient matrix (that is the summation of the length terms), X is the unknown coefficient matrix, and B is the matrix of known nodal temperatures at the storage materials convective boundary.

SWAP: Initializes the material temperature array at the start of each iteration during the fluid temperature solution procedure. It initializes the material temperature array using the solution from the previous time step. It is also called prior to the removal period and if a two-dimensional material temperature distribution is desired. If a parallel flow arrangement is required, it merely initializes the array. If a counterflow arrangement is required, it "swaps" the horizontal elements of the temperature array.

TBAR: Calculates an average storage material temperature using all the nodal temperatures.

TFLINT: Solves for the fluid temperatures using a fourth-order Runge-Kutta technique. This particular routine determines the wall temperatures using the interpolation technique.

TFLCRV: Solves for the fluid temperatures using a fourth-order Runge-Kutta technique. This routine uses the results of the polynomial curve fit to calculate the wall temperatures.

THCHW: Calculates the coordinate location, that is the (i,j) position, of a material node given that nodes unique number.

TWLCRV: Performs the second-order polynomial curve fit of the wall temperatures. This routine develops the coefficient and constant matrix as a function of the number of nodes in the X direction.

TWODIM: Performs a two-dimensional integration of discrete data points. It integrates the rates (i.e., per unit volume) of entropy generation at each of the nodes during each time increment.

WCHNDE: Determines which particular coefficient array element is being defined in the DEFINE subroutine. It then initializes the appropriate coefficient for that element.

WHCH: Using an (i,j) pair, this routine identifies nodal points by type; such as the (1,1) corner or the Y=0 face.

WHCHT: Determines a unique nodal number for a given (i,j) location.

WRTO1: Writes out a spacially correct material temperature field.

REPORT: Writes the program output. Although written by the author, it is called by GRG2 at the completion of an optimization run.

```
C
C
C
C
      SUBROUTINE GCOMP (G,X)
C
C     PROGRAM AND FILE NAME IS ENTROP.
C
C     PROGRAM TO CALCULATE ENTROPY GENERATION CHARACTERISTICS OF A
C     SENSIBLE HEAT THERMAL ENERGY STORAGE DEVICE.  IT WAS INITIALLY
C     CONSTRUCTED BY M.J. TAYLOR DURING 1985.
C
C     THE FOLLOWING IS A BRIEF SUMMARY OF THE DATA REQUIRED
C     PER RUN.  IN INTERPRETING THIS DATA YOU SHOULD KEEP SEVERAL
C     THINGS IN MIND.  THESE ARE: (A) ALL AMOUNTS ARE DIMENSIONLESS,
C     (B) AN "EXCESS" IS DEFINED AS AN AMOUNT DIVIDED BY EITHER THE
C     AMBIENT TEMPERATURE OR AMBIENT PRESSURE.
C
C             BID (R);     BIOT NUMBER FOR DISCHARGE PERIOD
C             BIS (R);     BIOT NUMBER FOR STORAGE PERIOD
C             CLOSE (R);   TEMPERATURE CONVERGENCE CRITERIA
C             FIPXD (R);   FLUID INLET PRESSURE EXCESS FOR
C                          THE DISCHARGE PERIOD
C             FIPXS (R);   FLUID INLET PRESSURE EXCESS FOR
C                          THE STORAGE PERIOD
C             FITXD (R);   FLUID INLET TEMPERATURE EXCESS FOR
C                          THE DISCHARGE PERIOD
C             FITXS (R);   FLUID INLET TEMPERATURE EXCESS FOR
C                          THE STORAGE PERIOD
C             FNUM (R);    TOTAL ELAPSED STORAGE TIME.
C             GPLSD (R);   G "PLUS" VARIABLE FOR DISCHARGE PERIOD
C             GPLSS (R);   G "PLUS" VARIABLE FOR STORAGE PERIOD
C             IDIST (I);   WHETHER OR NOT A 2-D MATERIAL TEMPERATURE
C                          IS DESIRED FOR THE START OF THE DISCHARGE
C                          PERIOD:
C                          1= UNIFORM TEMPERATURE DESIRED
C                          2= 2-D DISTRIBUTION DESIRED
C             IGEOM (I);   GEOMETRY BEING ANALYZED:
C                          1= FLAT SLAB
C                          2= HOLLOW CYLINDER
C             IWHCH (I);   METHOD TO DETERMINE WALL TEMPERATURES
C                          DURING FLUID TEMPERATURE SOLUTION:
C                          1= CURVE FIT
C                          2= INTERPOLATION
C             ISWAP (I);   WHETHER OR NOT HORIZONTAL MATERIAL
C                          TEMPERATURE FIELD IS SWAPED PRIOR TO
C                          DISCHARGE PERIOD:
C                          1= DO SWAP
C                          2= DON'T SWAP
C             M (I);       NUMBER OF NODES IN THE Z DIRECTION.
C             MITX (R);    INITIAL MATERIAL TEMPERATURE EXCESS
```

```
C               N (I);       NUMBER OF NODES IN THE Y DIRECTION.
C               NTMSS (I);   NUMBER OF INCREMENTS ELAPSED TIMES ARE
C                            BROKEN UP INTO
C               ROVRCP (R); GAS CONSTANT/ SPECIFIC HEAT FOR THE
C                            FLOWING FLUIDS.  ONLY ONE VALUE IS USED
C                            FOR BOTH STORAGE AND DISCHARGE PERIODS.
C               VPLS (R);    1/2 THICKNESS/LENGTH RATIO OF THE STORAGE
C                            MATERIAL.
C
      IMPLICIT REAL*8(A-H,O-Z)
      INTEGER*2 INIT
      REAL*8 IMT,MITX,NDFITS,LRGEST,NDFITD,NSUBS,NDFIPS,NDFIPD,
     *  NTUS,NTUD,MDOTS,MDOTD,MRAT,MATSTR,MATSS,MATDB,MATDE
      DIMENSION ZDIST(10),TFL(10),B(100),TWL(10),AVLM(100),
     *  AVLFL(100),AVLEXT(100),TMINT(100),G(2),X(4),AVMTMP(100),
     *  FLEXS(100),FLDS(10),MATSTR(100),AVLMS(100),AVLFS(100),
     *  AVLES(100),AVGTSS(100),HGHTMP(100),APRSS(100),
     *  AVLMSS(100),FLDSS(10),MATSS(100),MATDB(100),FLDD(100),
     *  TAVG(100),AVLMD(100),AVLFD(100),MATDE(100),TFLDB(10),
     *  TFLDE(10),AVLED(100)
      COMMON/RESULT/M,N,IGEOM,ISWAP,IDIST,IWHCH,KCSS,ISS,KL,
     *  KCDS,IDS,LM,FITXS,FITXD,MITX,
     *  MDOTS,MRAT,VPLS,WPLS,ROVRCP,TKRAT,PR,CLOSE,IMT,FNUM,DFOST,
     *  NDFITS,FIPXS,NDFIPS,BIS,GPLSS,NTUS,REYSTO,TOPT,STOMAT,STOFLD,
     *  STOEXT,STORSM,ETSS,ABSS,DFOSS,AVLSS,ETDS,ABDS,
     *  DFOD,NDFITD,FIPXD,NDFIPD,BID,GPLSD,MDOTD,NTUD,
     *  REYDIS,DISMAT,DISFLD,DISSUM,TP1,TP2,BTM1,BTM2,ALPHA,NSUBS,
     *  FSTCMP,LRGEST,DISEXT
      COMMON/DIM/AVMTMP,FLEXS,FLDS,MATSTR,AVLMS,AVLFS,AVLES,AVGTSS,
     *  HGHTMP,APRSS,AVLMSS,FLDSS,MATSS,MATDB,TAVG,FLDD,AVLMD,
     *  AVLFD,MATDE,TFLDB,TFLDE,AVLED
      COMMON/INITBK/INIT
C
C     READ INPUT DATA THEN INITILIZE SOME GLOBAL CONSTANTS
C     THAT NEVER CHANGE
C
      IF(INIT.EQ.1) READ(5,970) NTMSS,IDIST,M,N,IGEOM,IWHCH,ISWAP
      IF(INIT.EQ.1) READ(5,980) PR,FITXS,FITXD,VPLS,MRAT,MDOTS,
     *  MITX,ROVRCP,CLOSE
      GPLSS=X(1)/1.D+4
      BIS=X(2)/1.D+2
      FNUM=X(3)/1.D+2
      IMT=(MITX-1.D+0)/(FITXS-1.D+0)
      NDFITS=1.D+0
      NDFIPS=1.D+0
      NTUS=GPLSS*BIS/VPLS
      A=PR**.667
      C=NDFITS*(FITXS-1.D+0)+1.D+0
      D=MDOTS**2
      FIPXS=((+1.D+0)+DSQRT(1.D+0+4.D+0*A*NTUS*C*D))/2.D+0
      DBUG=0.D+0
```

```
      DY=1.D+0/(N-1.D+0)
      DZ=1.D+0/(M-1.D+0)
      MN=M*N
      IF(DBUG.GT.0.D+0) WRITE(6,1000)
      IF(DBUG.GT.0.D+0.AND.MN.NE.81) WRITE(6,1010)
      IF(DBUG.GT.0.D+0.AND.MN.NE.81) GO TO 9999
      ML=N
      MU=N
      MM=ML+MU+1
      LDA=2*ML+MU+1
      DO 10 I=1,M
 10   ZDIST(I)=DZ*(I-1)
      DFOST=FNUM/NTMSS
      DO 20 I=1,N
      DO 20 J=1,M
      TWL(J)=0.0D+0
      TFL(J)=1.D+0/J
      N1=I+(J-1)*N
 20   B(N1)=IMT
      TFL(1)=NDFITS
      DO 30 I=1,100
      AVLM(I)=0.0D+0
      AVLFL(I)=0.0D+0
 30   AVLEXT(I)=0.0D+0
C
C     START ACTUAL STORAGE PERIOD
C
      MODE=1
      IF(DBUG.GT.0.D+0) WRITE(6,990) MODE
      CALL B1B2 (IGEOM,DFOST,VPLS,DZ,DY,B1,B2)
      IF(DBUG.GT.0.D+0) CALL WRT01 (TFL,B,M,N,MN)
      JK=1
 100  ICNT=JK
      CALL GUTS(M,N,MN,MU,ML,MM,LDA,BIS,DY,B1,B2,ICNT,
     * IWHCH,TFL,MODE,ZDIST,GPLSS,VPLS,DZ,TWL,B,0.D+0)
      CALL SGEN(VPLS,BIS,FITXS,N,M,MN,TFL,B,DY,DZ,TWL,
     * MODE,0.D+0,AVLM(JK),AVLFL(JK),AVLEXT(JK))
      FLEXS(JK)=TFL(M)
      CALL TBAR(M,N,MN,B,AVMTMP(JK))
C     IF(JK.LE.10) CALL WRT01(TFL,B,M,N,MN)
      AVLMS(JK)=AVLM(JK)
      AVLFS(JK)=AVLFL(JK)
      AVLES(JK)=AVLEXT(JK)
      JK=JK+1
      IF(JK.GT.NTMSS) GO TO 150
      GO TO 100
 150  IF(DBUG.GT.0.D+0) CALL WRT01(TFL,B,M,N,MN)
C
C     DETERMINE AVERAGE MATERIAL TEMPERATURE AND AMOUNT OF
C     ENTROPY GENERATED DURING STORAGE PERIOD
C
```

```
      DO 160 JJ=1,M
160   FLDS(JJ)=TFL(JJ)
      CALL SWAP(M,N,MN,2,B,MATSTR)
      TRGET=DFOST
      CALL TBAR(M,N,MN,B,TOPT)
      CALL ONEDIM(0.D+0,DFOST,AVLM,NTMSS,STOMAT)
      CALL ONEDIM(0.D+0,DFOST,AVLFL,NTMSS,STOFLD)
      CALL ONEDIM(0.D+0,DFOST,AVLEXT,NTMSS,STOEXT)
      STOMAT=STOMAT/VPLS
      STOFLD=(BIS/VPLS)*STOFLD
      STOEXT=STOEXT/GPLSS
      STORSM=STOMAT+STOFLD+STOEXT
      IF(DBUG.GT.0.D+0) WRITE(6,1020) STOMAT,
     * STOFLD,STOEXT,TOPT
C
C     DETERMINE IF A 2-D OR UNIFORM TEMPERATURE IS DESIRED FOR
C     THE START OF THE STORAGE CYCLE AND ACT ACCORDINGLY
C
      IF(IDIST.EQ.2) AVLSS=0.D+0
      IF(IDIST.EQ.2) CALL SWAP(M,N,MN,ISWAP,B,TMINT)
      IF(IDIST.EQ.2) GO TO 550
C
C     AT THIS POINT WE KNOW A UNIFORM TEMPERATURE IS REQUIRED
C     PRIOR TO THE START OF THE DISCHARGE PERIOD.  THE FOLLOWING LOGIC
C     DETERMINES THE APPROXIMATE TIME REQUIRED TO REACH STEADY STATE.
C
      LRGEST=0.D+0
      DO 200 I=1,N
      DO 200 J=1,M
      N1=I+(J-1)*N
      IF (B(N1).GT.LRGEST) NCNT=N1
200   IF (B(N1).GT.LRGEST) LRGEST=B(N1)
      IF(DBUG.GT.0.D+0) WRITE(6,1025) LRGEST,NCNT
      IF(DABS((LRGEST-TOPT)/TOPT).LE.CLOSE) AVLSS=0.D+0
      IF(DABS((LRGEST-TOPT)/TOPT).LE.CLOSE) GO TO 510
      KCSS=0
      ISS=1
      MODE=2
      IF(DBUG.GT.0.D+0) WRITE(6,990) MODE
      ETSS=0.D+0
      DFO=TRGET
      CALL SWAP(M,N,MN,2,B,TMINT)
      IF(DBUG.GT.0.D+0) CALL WRT01 (TFL,B,M,N,MN)
240   CALL B1B2 (IGEOM,DFO,VPLS,DZ,DY,B1,B2)
250   ICNT=ISS
      ETSS=ETSS+DFO
      CALL GUTS(M,N,MN,MU,ML,MM,LDA,0.D+0,DY,B1,B2,ICNT,
     * IWHCH,TFL,MODE,ZDIST,GPLSS,VPLS,DZ,TWL,B,0.D+0)
      ABSS=(B(NCNT)-TOPT)/TOPT
      IF(ABSS.LE.CLOSE) GO TO 300
      ISS=ISS+1
```

```
      IF(ISS.GT.20) GO TO 260
      GO TO 250
 260  KCSS=KCSS+1
      IF(KCSS.GT.100) WRITE(6,1030)ABSS
      IF(KCSS.GT.100) STOP
      DFO=DFO*2.D+0
      ISS=1
      GO TO 240
 300  IF(DBUG.GT.0.D+0) WRITE(6,1050) KCSS,ICNT,ABSS,ETSS
      IF(DBUG.GT.0.D+0) CALL WRT01 (TFL,B,M,N,MN)
C
C     USING THIS APPROXIMATE TIME, DETERMINE ENTROPY GENERATED
C     DURING APPROACH TO STEADY STATE.
C
 350  MODE=3
      IF(DBUG.GT.0.D+0) WRITE(6,990) MODE
      KL=1
      DFOSS=ETSS/NTMSS
      CALL B1B2 (IGEOM,DFOSS,VPLS,DZ,DY,B1,B2)
      CALL SWAP(M,N,MN,2,TMINT,B)
      IF(DBUG.GT.0.D+0) CALL WRT01 (TFL,B,M,N,MN)
 400  ICNT=KL
      IRMN=MOD(ICNT,2)
      CALL GUTS(M,N,MN,MU,ML,MM,LDA,0.D+0,DY,B1,B2,ICNT,IWHCH,
     * TFL,MODE,ZDIST,GPLSS,VPLS,DZ,TWL,B,0.D+0)
      CALL SGEN(VPLS,0.D+0,FITXS,N,M,MN,TFL,B,DY,DZ,TWL,
     * MODE,0.D+0,AVLM(KL),AVLFL(KL),AVLEXT(KL))
      AVLMSS(KL)=AVLM(KL)
      HGHTMP(KL)=B(NCNT)
      CALL TBAR(M,N,MN,B,AVGTSS(KL))
      AB=(B(NCNT)-TOPT)/TOPT
      APRSS(KL)=AB
C     IF(DBUG.GT.0.D+0) WRITE(6,1055) AB
      IF(AB.LE.CLOSE.AND.IRMN.EQ.1) GO TO 500
      KL=KL+1
      IF(KL.EQ.100) WRITE(6,1070)
      IF(KL.EQ.100) STOP
      GO TO 400
 500  CALL ONEDIM(0.D+0,DFOSS,AVLM,KL,AVLSS)
      DO 170 KM=1,M
 170  FLDSS(KM)=TFL(KM)
      CALL SWAP(M,N,MN,2,B,MATSS)
      AVLSS=AVLSS/VPLS
      IF(DBUG.GT.0.D+0) WRITE(6,1065) AVLSS
      IF(DBUG.GT.0.D+0) CALL WRT01 (TFL,B,M,N,MN)
 510  DO 525 I=1,N
      DO 525 J=1,M
      N1=I+(J-1)*N
 525  TMINT(N1)=TOPT
 550  STORSM=STORSM+AVLSS
C
```

```
C       NOW WE WANT TO START THE DISCHARGE PERIOD.  BEGIN BY
C       INITIALIZING SOME VARIABLES.
C
        FIPXM1=FIPXS-1.D+0
        NDFITD=(FITXD-1.D+0)/(FITXS-1.D+0)
        E=(FIPXM1+1.D+0)/FIPXM1
        MDOTD=MDOTS*MRAT
        C=NDFITD*(FITXS-1.D+0)+1.D+0
        GPLSD=GPLSS/MRAT
        BID=BIS*MRAT
        NTUD=GPLSD*BID/VPLS
        FIPXD=1.D+0+DSQRT((A*NTUD*C*MDOTD**2.D+0)/E)
        NDFIPD=(FIPXD-1.D+0)/(FIPXS-1.D+0)
        IF(DBUG.GT.0.D+0) WRITE(6,1072) NDFITD,NDFIPD
        TFL(1)=NDFITD
        TWL(1)=0.D+0
        DO 600 J=2,M
        KK=J-1
        TWL(J)=0.D+0
600     TFL(J)=TFL(KK)+NDFITD/J
        KCDS=0
        IDS=1
        MODE=4
        IF(DBUG.GT.0.D+0) WRITE(6,990) MODE
        ETDS=0.D+0
        DFO=TRGET
        CALL SWAP(M,N,MN,2,TMINT,B)
        IF(DBUG.GT.0.D+0) CALL WRT01 (TFL,B,M,N,MN)
640     CALL B1B2 (IGEOM,DFO,VPLS,DZ,DY,B1,B2)
650     ICNT=IDS
        ETDS=ETDS+DFO
        CALL GUTS(M,N,MN,MU,ML,MM,LDA,BID,DY,B1,B2,ICNT,
     *  IWHCH,TFL,MODE,ZDIST,GPLSD,VPLS,DZ,TWL,B,0.D+0)
        CALL TBAR (M,N,MN,B,AVGT)
        ABDS=(AVGT-IMT)/IMT
        IF(ABDS.LE.CLOSE) GO TO 680
        IDS=IDS+1
        IF(IDS.GT.20) GO TO 660
        GO TO 650
660     KCDS=KCDS+1
        IF(KCDS.GT.100) WRITE(6,1075)ABDS
        IF(KCDS.GT.100) STOP
        DFO=DFO*2.D+0
        IDS=1
        GO TO 640
680     IF(DBUG.GT.0.D+0) WRITE(6,1050) KCDS,ICNT,ABDS,ETDS
        IF(DBUG.GT.0.D+0) CALL WRT01 (TFL,B,M,N,MN)
C
C       USING THIS APPROXIMATE TIME, DETERMINE ENTROPY GENERATED
C       DURING DISCHARGE PERIOD
C
```

```
 700    MODE=5
        IF(DBUG.GT.0.D+0) WRITE(6,990) MODE
        LM=1
        DFOD=ETDS/NTMSS
        CALL B1B2 (IGEOM,DFOD,VPLS,DZ,DY,B1,B2)
        CALL SWAP(M,N,MN,2,TMINT,B)
        IF(DBUG.GT.0.D+0) CALL WRT01 (TFL,B,M,N,MN)
        DO 710 LML=1,M
 710    TFLDB(LML)=TFL(LML)
        CALL SWAP(M,N,MN,2,B,MATDB)
 725    ICNT=LM
        IRMN=MOD(ICNT,2)
        CALL GUTS(M,N,MN,MU,ML,MM,LDA,BID,DY,B1,B2,ICNT,IWHCH,
     *  TFL,MODE,ZDIST,GPLSD,VPLS,DZ,TWL,B,0.D+0)
        CALL SGEN(VPLS,BID,FITXS,N,M,MN,TFL,B,DY,DZ,TWL,
     *  MODE,0.D+0,AVLM(LM),AVLFL(LM),AVLEXT(LM))
        AVLMD(LM)=AVLM(LM)
        AVLFD(LM)=AVLFL(LM)
        AVLED(LM)=AVLEXT(LM)
        FLDD(LM)=TFL(M)
        CALL TBAR(M,N,MN,B,TAVG(LM))
C       IF(DBUG.GT.0.D+0) WRITE(6,1053) TAVG(LM)
        AB=(TAVG(LM)-IMT)/IMT
C       IF(DBUG.GT.0.D+0) WRITE(6,1055) AB
        IF(AB.LE.CLOSE.AND.IRMN.EQ.1) GO TO 750
        LM=LM+1
        IF(LM.EQ.100) WRITE(6,1080)
        IF(LM.EQ.100) STOP
        GO TO 725
 750    IF(DBUG.GT.0.D+0) CALL WRT01(TFL,B,M,N,MN)
        DO 760 LMM=1,M
 760    TFLDE(LMM)=TFL(LMM)
        CALL SWAP(M,N,MN,2,B,MATDE)
C

C       DETERMINE AMOUNT OF ENTROPY GENERATED DURING DISCHARGE PERIOD
C
 800    CALL ONEDIM(0.D+0,DFOD,AVLM,LM,DISMAT)
        CALL ONEDIM(0.D+0,DFOD,AVLFL,LM,DISFLD)
        CALL ONEDIM(0.D+0,DFOD,AVLEXT,LM,DISEXT)
        DISMAT=DISMAT/VPLS
        DISFLD=(BID/VPLS)*DISFLD
        DISEXT=DISEXT/GPLSD
        DISSUM=DISMAT+DISFLD
        IF(DBUG.GT.0.D+0) WRITE(6,1085) SUMMAT,SUMFLD,DISSUM
C
C       DETERMINE FIGURE OF MERIT FOR THIS CYCLE
C
        TP1=(1.D+0/GPLSS)*ROVRCP*DLOG(NDFIPS*(FIPXS-1.D+0)+1.D+0)
     *  *FNUM
        TP2=(1.D+0/GPLSD)*ROVRCP*DLOG(NDFIPD*(FIPXS-1.D+0)+1.D+0)
```

```
     *   *DFOD*LM
         TERM1=NDFITS*(FITXS-1.D+0)
         TERM2=NDFITD*(FITXS-1.D+0)
         BTM1=(1.D+0/GPLSS)*(TERM1-DLOG(TERM1+1.D+0))*FNUM
         BTM2=(1.D+0/GPLSD)*(TERM2-DLOG(TERM2+1.D+0))*DFOD*LM
         TOP=TP1+TP2
         BTM=BTM1+BTM2
         ALPHA=TOP/BTM
         NSUBS=(ALPHA/(ALPHA+1.D+0))+(1.D+0/(ALPHA+1.D+0))*
     *   ((STORSM+DISSUM)/BTM)
         G(1)=NSUBS
C
C        DETERMINE FIRST LAW COMPARISON FOR THIS CYCLE.  ONLY APPLIES
C        TO THE STORAGE PORTION OF THE CYCLE
C
         FSTCMP=(TOPT-IMT)/(NDFITS-IMT)
         IF(DBUG.GT.0.D+0) CALL REPORT
C
C        FORMAT STATEMENTS FOR THIS ROUTINE
C
 970     FORMAT(10X,I2)
 980     FORMAT(11X,D11.6)
 990     FORMAT(//10X,'MODE= ',I2)
 995     FORMAT(5X,'MODE= ',I3,2X,'ICNT= ',I3,2X,'TOPT= ',D16.10)
 1000    FORMAT(//25X,'FROM MAIN')
 1010    FORMAT(5X,'NOT A 9X9 MATRIX.  EXECUTION TERMINATED')
 1020    FORMAT(5X,'STORSM= ',D20.10/5X,'SUMMAT= ',D20.10/
     *   5X,'SUMFLD= ',D20.10/5X,'SUMEXT= ',D20.10/5X,
     *   'TOPT= ',D20.10)
 1025    FORMAT(5X,'LRGEST= ',D20.10/5X,'NCNT= ',I3)
 1030    FORMAT(5X,'UNABLE TO GET PROPER STARTING POINT FOR STEADY
     *   STATE ITERATION.'/5X,'EXECUTION TERMINATING')
 1040    FORMAT(5X,'STEADY STATE ITERATION WILL NOT CLOSE'/5X,
     *   'EXECUTION TERMINATING.')
 1050    FORMAT(5X,'KCOI= ',I5/5X,'ICNT= ',I3/5X,'AB= ',D20.10/
     *   5X,'DFO= ',D20.10)
 1053    FORMAT(5X,'TAVG= ',D20.10)
 1055    FORMAT(5X,'AB= ',D20.10)
 1060    FORMAT(5X,'DIFF= ',D20.10)
 1065    FORMAT(5X,'AVLSS= ',D20.10)
 1070    FORMAT(5X,'SS PRIOR TO START OF DISCHARGE CYCLE NOT
     *   REACHED IN 100 INCRIMENTS.'/5X,'EXECUTION TERMINATING.')
 1072    FORMAT(5X,'NDFITD= ',D20.10/5X,'NDFIPD= ',D20.10)
 1075    FORMAT(5X,'UNABLE TO GET PROPER STARTING POINT FOR
     *DISCHARGE PERIOD.'/5X,'EXECUTION TERMINATING.'/5X,'ABDS= ',
     *   E16.10)
 1080    FORMAT(5X,'RETURN TO INITIAL MATERIAL CONDITIONS NOT
     *   REACHED IN 100 INCRIMENTS.'/5X,'EXECUTION TERMINATING.')
 1085    FORMAT(5X,'SUMMAT= ',D20.10/5X,'SUMFLD= ',D20.10/
     *   5X,'DISSUM= ',D20.10)
 9999    RETURN
```

```
      END
C
C
C
C
C
      SUBROUTINE B1B2(IGEOM,DFO,VPLS,DZ,DY,B1,B2)
C
C     THIS ROUTINE CALCULATES THE B1 AND B2 VARIABLES.
C
      IMPLICIT REAL*8 (A-H,O-Z)
      IF(IGEOM.EQ.2) GO TO 9999
      B1=(DFO*VPLS**2)/(DZ**2)
      B2=DFO/(DY**2)
 9999 RETURN
      END
C
C
C
C
C
      SUBROUTINE GUTS(M,N,MN,MU,ML,MM,LDA,BIOT,DY,B1,B2,ICNT,
     * IWHCH,TFL,MODE,ZDIST,FLWRT,VPLS,DZ,TWL,B,DBUG)
C
C     THIS ROUTINE PERFORMS THE MAJORITY OF THE ROUTING AND
C     CALCULATIONS FOR THE PROGRAM.  IT REALLY IS THE GUTS OF THE
C     PROGRAM.
C
      IMPLICIT REAL*8(A-H,O-Z)
      REAL*8 LSTFLU
      DIMENSION ABD(28,100),IPVT(100),TMINT(100),B(MN),TFL(M),TWL(M),
     * ZDIST(M),BCOF(3),LSTFLU(10)
      IF(DBUG.GT.0.D+0) WRITE(6,990)
      CALL SWAP(M,N,MN,2,B,TMINT)
      IF(ICNT.GT.1) GO TO 140
      CALL DEFINE(M,N,MN,MU,ML,MM,LDA,BIOT,DY,B1,B2,ABD)
      CALL DGBFA(ABD,LDA,MN,ML,MU,IPVT,INFO)
      IF(INFO.GT.0) WRITE(6,1112)
      IF(INFO.GT.0) STOP
C
C     DEFINE CONSTANT ARRAY FOR THIS TIME PERIOD/FLUID TEMPERATURE
C     GUESS
C     AND SOLVE FOR MATERIAL TEMPERATURES.
C
 140  JCOI=0
 150  IF(DBUG.GT.0.D+0) WRITE(6,1000) ICNT,JCOI
      DO 400 IJK=1,M
 400  LSTFLU(IJK)=TFL(IJK)
      CALL CONST(DBUG,N,M,MN,TMINT,B,BIOT,B2,DY,TFL)
      CALL DGBSL(ABD,LDA,MN,ML,MU,IPVT,B,0)
      IF(DBUG.GT.0.D+0) WRITE(6,1005)
```

```
      IF(DBUG.GT.5.D+0) CALL WRT01(TFL,B,M,N,MN)
      IF(MODE.EQ.2.OR.MODE.EQ.3) GO TO 9999
C               SOLVE FOR FLUID TEMPERATURES
      DO 200 JK=1,M
      N1=N+(JK-1)*N
 200  TWL(JK)=B(N1)
      IF(IWHCH.EQ.2) CALL TFLINT(DBUG,FLWRT,BIOT,VPLS,TWL,
     *  ZDIST,M,DZ,TFL)
      IF(IWHCH.EQ.1) CALL TWLCRV(DBUG,ZDIST,TWL,M,BCOF)
      IF(IWHCH.EQ.1) CALL TFLCRV(DBUG,FLWRT,BIOT,VPLS,BCOF,
     *  ZDIST,M,DZ,TFL)
C               SEE IF FLUID TEMPERATURES HAVE CONVERGED.
      SUM=0.0D+0
      DO 300 JK=2,M
 300  SUM=SUM+DABS(TFL(JK)-LSTFLU(JK))
      QUOT=SUM/(M-1)
      IF(DBUG.GT.0.D+0) WRITE(6,1010) QUOT
      IF(QUOT.LE.5.D-4) GO TO 9999
      JCOI=JCOI+1
      IF(JCOI.GT.45) WRITE(6,2223)
      IF(JCOI.GT.45) WRITE(6,2224) MODE,ICNT,QUOT
      IF(JCOI.GT.45) STOP
      GO TO 150
C
C     FORMAT STATEMENTS FOR THIS ROUTINE
C
 990  FORMAT(//25X,'FROM GUTS')
 1000 FORMAT(/5X,'ICNT= ',I2,1X,'JCOI= ',I2)
 1005 FORMAT(//5X,'TEMPERATURE SOLUTION FOR THIS ITERATION')
 1010 FORMAT(/5X,'QUOT= ',D20.10)
 1112 FORMAT(5X,'SINGULAR MATRIX IN MATERIAL TEMPERATURE SOLUTION
    *ROUTINE.'/5X,'EXECUTION TERMINATED.')
 2223 FORMAT(5X,'FLUID TEMPERATURE ITERATION WILL NOT CLOSE.'/
    *5X,'EXECUTION TERMINATED.')
 2224 FORMAT(5X,'MODE= ',I3/5X,'ICNT= ',I3/5X,
    *  'AVG DIFFERENCE BETWEEN ITERATIONS= ',D20.10)
 9999 RETURN
      END
C
C
C
C
C
      SUBROUTINE CONST(DBUG,N,M,MN,TMINT,B,BIOT,B2,DY,TFL)
C
C     THIS ROUTINE DETERMINES THE CONSTANT ARRAY FOR EACH TIME STEP
C
      IMPLICIT REAL*8(A-H,O-Z)
      DIMENSION TFL(M),B(MN),TMINT(MN)
      IF(DBUG.GT.0.D+0) WRITE(6,1000) ICNT
      DO 100 I=1,N
```

```
      C1=0.D+0
      IF(I.EQ.N) C1=1.D+0
      DO 100 J=1,M
      N1=I+(J-1)*N
  100 B(N1)=-(TMINT(N1)+C1*(2.D+0*BIOT*B2*DY*TFL(J)))
      IF(DBUG.GT.0.D+0) CALL WRT01(TFL,B,M,N,MN)
C
C     FORMAT STATEMENTS FOR THIS ROUTINE
C
 1000 FORMAT(//25X,'FROM CONST, ICNT= ',I3)
 9999 RETURN
      END
C
C
C
C
C
      SUBROUTINE DECOMP(NDIM,N,A,COND,IPVT,WORK)
C
C     THIS ROUTINE DECOMPOSES A DOUBLE PRECISION MATRIX BY
C     GAUSSIAN ELIMINATION AND ESTIMATES THE CONDITION OF THE
C     MATRIX
C
      INTEGER NDIM,N
      DOUBLE PRECISION A(NDIM,N),COND,WORK(N)
      INTEGER IPVT(N)
      DOUBLE PRECISION EK, T, ANORM, YNORM, ZNORM
      INTEGER NM1, I, J, K, KP1, KB, KM1, M
      DOUBLE PRECISION DABS, DSIGN
C
      IPVT(N) = 1
      IF (N .EQ. 1) GO TO 80
      NM1 = N - 1
C
C     COMPUTE 1-NORM OF A
C
      ANORM = 0.0D0
      DO 10 J = 1, N
         T = 0.0D0
         DO 5 I = 1, N
            T = T + DABS(A(I,J))
    5    CONTINUE
         IF (T .GT. ANORM) ANORM = T
   10 CONTINUE
C
C     GAUSSIAN ELIMINATION WITH PARTIAL PIVOTING
C
      DO 35 K = 1,NM1
         KP1= K+1
C
C        FIND PIVOT
```

```
C
      M = K
      DO 15 I = KP1,N
         IF (DABS(A(I,K)) .GT. DABS(A(M,K))) M = I
15    CONTINUE
      IPVT(K) = M
      IF (M .NE. K) IPVT(N) = -IPVT(N)
      T = A(M,K)
      A(M,K) = A(K,K)
      A(K,K) = T
C
C     SKIP STEP IF PIVOT IS ZERO
C
      IF (T .EQ. 0.0D0) GO TO 35
C
C     COMPUTE MULTIPLIERS
C
      DO 20 I = KP1,N
          A(I,K) = -A(I,K)/T
20    CONTINUE
C
C     INTERCHANGE AND ELIMINATE BY COLUMNS
C
      DO 30 J = KP1,N
          T = A(M,J)
          A(M,J) = A(K,J)
          A(K,J) = T
          IF (T .EQ. 0.0D0) GO TO 30
          DO 25 I = KP1,N
             A(I,J) = A(I,J) + A(I,K)*T
25        CONTINUE
30    CONTINUE
35 CONTINUE
C
C     SOLVE (A-TRANSPOSE)*Y = E
C
      DO 50 K = 1, N
         T = 0.0D0
         IF (K .EQ. 1) GO TO 45
         KM1 = K-1
         DO 40 I = 1, KM1
            T = T + A(I,K)*WORK(I)
40       CONTINUE
45       EK = 1.0D0
         IF (T .LT. 0.0D0) EK = -1.0D0
         IF (A(K,K) .EQ. 0.0D0) GO TO 90
         WORK(K) = -(EK + T)/A(K,K)
50 CONTINUE
      DO 60 KB = 1, NM1
         K = N - KB
         T = 0.0D0
```

```
            KP1 = K+1
            DO 55 I = KP1, N
               T = T + A(I,K)*WORK(K)
      55    CONTINUE
            WORK(K) = T
            M = IPVT(K)
            IF (M .EQ. K) GO TO 60
            T = WORK(M)
            WORK(M) = WORK(K)
            WORK(K) = T
      60 CONTINUE
C
         YNORM = 0.0D0
         DO 65 I = 1, N
            YNORM = YNORM + DABS(WORK(I))
      65 CONTINUE
C
C        SOLVE A*Z = Y
C
         CALL SOLVE(NDIM, N, A, WORK, IPVT)
C
         ZNORM = 0.0D0
         DO 70 I = 1, N
            ZNORM = ZNORM + DABS(WORK(I))
      70 CONTINUE
C
C        ESTIMATE CONDITION
C
         COND = ANORM*ZNORM/YNORM
         IF (COND .LT. 1.0D0) COND = 1.0D0
         RETURN
C
C        1-BY-1
C
      80 COND = 1.0D0
         IF (A(1,1) .NE. 0.0D0) RETURN
C
C        EXACT SINGULARITY
C
      90 COND = 1.0D+32
         RETURN
         END
C
C
C
C
C
           SUBROUTINE DEFINE(M,N,MN,MU,ML,MM,LDA,BIOT,DY,B1,B2,ABD)
C
C          THIS ROUTINE DEFINES THE COEFFICIENT ARRAY.  IT STORES THE ARRAY
C          IN BANDED FORM.  REFERENCE IS ORNL CORLIB DGBFA/DGBSL PROGRAM.
```

```
C
        IMPLICIT REAL*8(A-H,O-Z)
        DIMENSION ABD(LDA,MN)
        DO 20 J=1,MN
        JJ=J
        I1=MAXO(1,J-MU)
        I2=MINO(MN,J+ML)
        DO 20 I=I1,I2
        II=I
        K=I-J+MM
        CALL WCHNDE(II,JJ,M,N,BIOT,DY,B1,B2,COEF)
20      ABD(K,J)=COEF
9999    RETURN
        END
C
C
C
C
C
      SUBROUTINE DGBFA(ABD,LDA,N,ML,MU,IPVT,INFO)
C
C     DGBFA FACTORS A DOUBLE PRECISION BAND MATRIX BY ELIMINATION
C
      INTEGER LDA,N,ML,MU,IPVT(1),INFO
      DOUBLE PRECISION ABD(LDA,1)
      DOUBLE PRECISION T
      INTEGER I,IDAMAX,IO,J,JU,JZ,JO,J1,K,KP1,L,LM,M,MM,NM1
      M = ML + MU + 1
      INFO = 0
C
C     ZERO INITIAL FILL-IN COLUMNS
C
      JO = MU + 2
      J1 = MINO(N,M) - 1
      IF (J1 .LT. JO) GO TO 30
      DO 20 JZ = JO, J1
      IO = M + 1 - JZ
      DO 10 I = IO, ML
      ABD(I,JZ) = 0.0DO
   10 CONTINUE
   20 CONTINUE
   30 CONTINUE
      JZ = J1
      JU = 0
C
C     GAUSSIAN ELIMINATION WITH PARTIAL PIVOTING
C
      NM1 = N - 1
      IF (NM1 .LT. 1) GO TO 130
      DO 120 K = 1, NM1
      KP1 = K + 1
```

```
C
C         ZERO NEXT FILL-IN COLUMN
C
          JZ = JZ + 1
          IF (JZ .GT. N) GO TO 50
          IF (ML .LT. 1) GO TO 50
          DO 40 I = 1, ML
             ABD(I,JZ) = 0.0D0
      40     CONTINUE
      50  CONTINUE
C
C         FIND L = PIVOT INDEX
C
          LM = MINO(ML,N-K)
          L = IDAMAX(LM+1,ABD(M,K),1) + M - 1
          IPVT(K) = L + K - M
C
C         ZERO PIVOT IMPLIES THIS COLUMN ALREADY TRIANGULARIZED
C
          IF (ABD(L,K) .EQ. 0.0D0) GO TO 100
C
C            INTERCHANGE IF NECESSARY
C
             IF (L .EQ. M) GO TO 60
                T = ABD(L,K)
                ABD(L,K) = ABD(M,K)
                ABD(M,K) = T
     60       CONTINUE
C
C            COMPUTE MULTIPLIERS
C
             T = -1.0D0/ABD(M,K)
             CALL DSCAL(LM,T,ABD(M+1,K),1)
C
C            ROW ELIMINATION WITH COLUMN INDEXING
C
             JU = MINO(MAXO(JU,MU+IPVT(K)),N)
             MM = M
             IF (JU .LT. KP1) GO TO 90
             DO 80 J = KP1, JU
                L = L - 1
                MM = MM - 1
                T = ABD(L,J)
                IF (L .EQ. MM) GO TO 70
                   ABD(L,J) = ABD(MM,J)
                   ABD(MM,J) = T
     70           CONTINUE
                CALL DAXPY(LM,T,ABD(M+1,K),1,ABD(MM+1,J),1)
     80       CONTINUE
     90       CONTINUE
          GO TO 110
```

```
  100  CONTINUE
          INFO = K
  110 CONTINUE
  120 CONTINUE
  130 CONTINUE
      IPVT(N) = N
      IF (ABD(M,N) .EQ. 0.0D0) INFO = N
      RETURN
      END
C
C
C
C
C
      SUBROUTINE DAXPY(N,DA,DX,INCX,DY,INCY)
C
C     CONSTANT TIMES A VECTOR PLUS A VECTOR.
C     USES UNROLLED LOOPS FOR INCREMENTS EQUAL TO ONE.
C     JACK DONGARRA, LINPACK, 3/11/78.
C
      DOUBLE PRECISION DX(1),DY(1),DA
      INTEGER I,INCX,INCY,IXIY,M,MP1,N
C
      IF(N.LE.0)RETURN
      IF (DA .EQ. 0.0D0) RETURN
      IF(INCX.EQ.1.AND.INCY.EQ.1)GO TO 20
C
C        CODE FOR UNEQUAL INCREMENTS OR EQUAL INCREMENTS
C          NOT EQUAL TO 1
C
      IX = 1
      IY = 1
      IF(INCX.LT.0)IX = (-N+1)*INCX + 1
      IF(INCY.LT.0)IY = (-N+1)*INCY + 1
      DO 10 I = 1,N
        DY(IY) = DY(IY) + DA*DX(IX)
        IX = IX + INCX
        IY = IY + INCY
   10 CONTINUE
      RETURN
C
C        CODE FOR BOTH INCREMENTS EQUAL TO 1
C
C
C        CLEAN-UP LOOP
C
   20 M = MOD(N,4)
      IF( M .EQ. 0 ) GO TO 40
      DO 30 I = 1,M
        DY(I) = DY(I) + DA*DX(I)
   30 CONTINUE
```

```
      IF( N .LT. 4 ) RETURN
   40 MP1 = M + 1
      DO 50 I = MP1,N,4
        DY(I) = DY(I) + DA*DX(I)
        DY(I + 1) = DY(I + 1) + DA*DX(I + 1)
        DY(I + 2) = DY(I + 2) + DA*DX(I + 2)
        DY(I + 3) = DY(I + 3) + DA*DX(I + 3)
   50 CONTINUE
      RETURN
      END
C
C
C
C
C
      SUBROUTINE  DSCAL(N,DA,DX,INCX)
C
C     SCALES A VECTOR BY A CONSTANT.
C     USES UNROLLED LOOPS FOR INCREMENT EQUAL TO ONE.
C     JACK DONGARRA, LINPACK, 3/11/78.
C
      DOUBLE PRECISION DA,DX(1)
      INTEGER I,INCX,M,MP1,N,NINCX
C
      IF(N.LE.0)RETURN
      IF(INCX.EQ.1)GO TO 20
C
C        CODE FOR INCREMENT NOT EQUAL TO 1
C
      NINCX = N*INCX
      DO 10 I = 1,NINCX,INCX
        DX(I) = DA*DX(I)
   10 CONTINUE
      RETURN
C
C        CODE FOR INCREMENT EQUAL TO 1
C
C
C        CLEAN-UP LOOP
C
   20 M = MOD(N,5)
      IF( M .EQ. 0 ) GO TO 40
      DO 30 I = 1,M
        DX(I) = DA*DX(I)
   30 CONTINUE
      IF( N .LT. 5 ) RETURN
   40 MP1 = M + 1
      DO 50 I = MP1,N,5
        DX(I) = DA*DX(I)
        DX(I + 1) = DA*DX(I + 1)
        DX(I + 2) = DA*DX(I + 2)
```

```
        DX(I + 3) = DA*DX(I + 3)
        DX(I + 4) = DA*DX(I + 4)
   50 CONTINUE
      RETURN
      END
C
C
C
C
C
      INTEGER FUNCTION IDAMAX(N,DX,INCX)
C
C     FINDS THE INDEX OF ELEMENT HAVING MAX. ABSOLUTE VALUE.
C     JACK DONGARRA, LINPACK, 3/11/78.
C
      DOUBLE PRECISION DX(1),DMAX
      INTEGER I,INCX,IX,N
C
      IDAMAX = 0
      IF( N .LT. 1 ) RETURN
      IDAMAX = 1
      IF(N.EQ.1)RETURN
      IF(INCX.EQ.1)GO TO 20
C
C        CODE FOR INCREMENT NOT EQUAL TO 1
C
      IX = 1
      DMAX = DABS(DX(1))
      IX = IX + INCX
      DO 10 I = 2,N
         IF(DABS(DX(IX)).LE.DMAX) GO TO 5
         IDAMAX = I
         DMAX = DABS(DX(IX))
    5    IX = IX + INCX
   10 CONTINUE
      RETURN
C
C        CODE FOR INCREMENT EQUAL TO 1
C
   20 DMAX = DABS(DX(1))
      DO 30 I = 2,N
         IF(DABS(DX(I)).LE.DMAX) GO TO 30
         IDAMAX = I
         DMAX = DABS(DX(I))
   30 CONTINUE
      RETURN
      END
C
C
C
C
```

```
C
      SUBROUTINE DGBSL(ABD,LDA,N,ML,MU,IPVT,B,JOB)
C
C     THIS ROUTINE SOLVES THE DOUBLE PRECISION BAND SYSTEM
C               A*X=B OR TRANS(A)*X=B
C
      INTEGER LDA,N,ML,MU,IPVT(1),JOB
      DOUBLE PRECISION ABD(LDA,1),B(1)
      DOUBLE PRECISION DDOT,T
      INTEGER K,KB,L,LA,LB,LM,M,NM1
C
      M = MU + ML + 1
      NM1 = N - 1
      IF (JOB .NE. 0) GO TO 50
C
C        JOB = 0 , SOLVE  A * X = B
C        FIRST SOLVE L*Y = B
C
         IF (ML .EQ. 0) GO TO 30
         IF (NM1 .LT. 1) GO TO 30
            DO 20 K = 1, NM1
               LM = MIN0(ML,N-K)
               L = IPVT(K)
               T = B(L)
               IF (L .EQ. K) GO TO 10
                  B(L) = B(K)
                  B(K) = T
   10          CONTINUE
               CALL DAXPY(LM,T,ABD(M+1,K),1,B(K+1),1)
   20       CONTINUE
   30    CONTINUE
C
C        NOW SOLVE  U*X = Y
C
         DO 40 KB = 1, N
            K = N + 1 - KB
            B(K) = B(K)/ABD(M,K)
            LM = MIN0(K,M) - 1
            LA = M - LM
            LB = K - LM
            T = -B(K)
            CALL DAXPY(LM,T,ABD(LA,K),1,B(LB),1)
   40    CONTINUE
      GO TO 100
   50 CONTINUE
C
C        JOB = NONZERO, SOLVE  TRANS(A) * X = B
C        FIRST SOLVE  TRANS(U)*Y = B
C
         DO 60 K = 1, N
            LM = MIN0(K,M) - 1
```

```
            LA = M - LM
            LB = K - LM
            T = DDOT(LM,ABD(LA,K),1,B(LB),1)
            B(K) = (B(K) - T)/ABD(M,K)
   60     CONTINUE
C
C        NOW SOLVE TRANS(L)*X = Y
C
         IF (ML .EQ. 0) GO TO 90
         IF (NM1 .LT. 1) GO TO 90
            DO 80 KB = 1, NM1
               K = N - KB
               LM = MINO(ML,N-K)
               B(K) = B(K) + DDOT(LM,ABD(M+1,K),1,B(K+1),1)
               L = IPVT(K)
               IF (L .EQ. K) GO TO 70
                  T = B(L)
                  B(L) = B(K)
                  B(K) = T
   70          CONTINUE
   80       CONTINUE
   90    CONTINUE
  100 CONTINUE
      RETURN
      END
C
C
C
C
C
      DOUBLE PRECISION FUNCTION DDOT(N,DX,INCX,DY,INCY)
C
C     FORMS THE DOT PRODUCT OF TWO VECTORS.
C     USES UNROLLED LOOPS FOR INCREMENTS EQUAL TO ONE.
C     JACK DONGARRA, LINPACK, 3/11/78.
C
      DOUBLE PRECISION DX(1),DY(1),DTEMP
      INTEGER I,INCX,INCY,IX,IY,M,MP1,N
C
      DDOT = 0.0D0
      DTEMP = 0.0D0
      IF(N.LE.0)RETURN
      IF(INCX.EQ.1.AND.INCY.EQ.1)GO TO 20
C
C        CODE FOR UNEQUAL INCREMENTS OR EQUAL INCREMENTS
C          NOT EQUAL TO 1
C
      IX = 1
      IY = 1
      IF(INCX.LT.0)IX = (-N+1)*INCX + 1
      IF(INCY.LT.0)IY = (-N+1)*INCY + 1
```

```
      DO 10 I = 1,N
        DTEMP = DTEMP + DX(IX)*DY(IY)
        IX = IX + INCX
        IY = IY + INCY
   10 CONTINUE
      DDOT = DTEMP
      RETURN
C
C        CODE FOR BOTH INCREMENTS EQUAL TO 1
C
C
C        CLEAN-UP LOOP
C
   20 M = MOD(N,5)
      IF( M .EQ. 0 ) GO TO 40
      DO 30 I = 1,M
        DTEMP = DTEMP + DX(I)*DY(I)
   30 CONTINUE
      IF( N .LT. 5 ) GO TO 60
   40 MP1 = M + 1
      DO 50 I = MP1,N,5
        DTEMP = DTEMP + DX(I)*DY(I) + DX(I + 1)*DY(I + 1) +
     *   DX(I + 2)*DY(I + 2) + DX(I + 3)*DY(I + 3) + DX(I + 4)*DY(I + 4)
   50 CONTINUE
   60 DDOT = DTEMP
      RETURN
      END
C
C
C
C
C
        SUBROUTINE INTERP(N,X1,H,Y,M,XO,YVALUE)
C
C       THIS ROUTINE INTERPRETS VALUES OF THE WALL TEMPERATURE.
C       IT IS CALLED DURING THE SOLUTION FOR FLUID TEMPERATURES
C
        IMPLICIT REAL*8 (A-H,O-Z)
        DIMENSION Y(N),Z(10)
        M2=(M+1)/2
        K=(XO/H)+1
        IF(K-M2) 10,10,11
 10     L=K
        GO TO 12
 11     IF(N-K-M2) 21,21,20
 20     L=M2
        GO TO 12
 21     L=M+1-N+K
 12     M1=M+1
        DO 22 I=1,M1
        I1=I+K-L
```

```
 22     Z(I)=Y(I1)
        AK=K
        AL=L
        P=(XO-X1-(AK-AL)*H)/H
        DO 24 J=1,M
        AJ=J
        MJ=M+1-J
        DO 24 I=1,MJ
        AI=I
 24     Z(I)=((AI-P+AJ-1.D+0)*Z(I)+(P-AI+1.D+0)*
     *  Z(I+1))/AJ
        YVALUE=Z(1)
 9999   RETURN
        END
C
C
C
C
C
        SUBROUTINE ONEDIM(DBUG,H,Y,M,SUM)
C
C       THIS ROUTINE PERFORMS A 1-D NUMERICAL INTEGRATION OF DATA.  IT
C       IS BASED ON SIMPSONS RULE AND REQUIRES AN ODD NUMBER OF
C       DATA SETS.  REFERENCE IS MCCORMICK AND SALVADORI, PP.165
C
        IMPLICIT REAL*8(A-H,O-Z)
        DIMENSION Y(M)
        IF(DBUG.GT.0.D+0) WRITE(6,990)
        NUM=(M-1)/2
        N1=1
        SUM=0.D+0
        DO 100 I=1,NUM
        N2=N1+1
        N3=N2+1
        SUM=SUM+(H/3.D+0)*(Y(N1)+4.D+0*Y(N2)+Y(N3))
 100    N1=N3
        IF(DBUG.GT.0.D+0) WRITE(6,1000) SUM
C
C       FORMAT STATEMENTS FOR THIS ROUTINE
C
 990    FORMAT(//25X,'FROM ONEDIM')
 1000   FORMAT(5X,'1-D SUM= ',D20.10)
 9999   RETURN
        END
C
C
C
C
C
        SUBROUTINE SGEN(VPLS,BIOT,FITXS,N,M,MN,TFL,B,DY,DZ,
     *  TWL,MODE,DBUG,SUMMAT,SUMFLD,EXTFLD)
```

```
C
C       THIS ROUTINE CALCULATES THE ENTROPY GENERATION TERMS FOR THE
C       CURRENT TIME PERIOD.
C
        IMPLICIT REAL*8(A-H,O-Z)
        DIMENSION TFL(M),B(MN),TWL(M),SGNMT(100),SGNF(10)
        IF(DBUG.GT.0.D+0) WRITE(6,1000)
        TRM1=FITXS-1.D+0
        TRM12=TRM1**2
C
C       DETERMINE RATE OF ENTROPY GENERATION AT EACH POINT IN THE
C       STORAGE MATERIAL AND INTEGRATE TO GET A TOTAL FOR THIS TIME
C       PERIOD.
C
        DO 100 I=1,N
        DO 100 J=1,M
        II=I
        JJ=J
        N1=I+(J-1)*N
        N2=I+(J-2)*N
        N3=I+J*N
        N4=(I-1)+(J-1)*N
        N5=(I+1)+(J-1)*N
C
C       DETERMINE WHICH TYPE OF NODE THIS IS AND BRANCH TO GRADIENT
C       CALCULATION.  NON ZERO GRADIENTS THAT ARE NOT A BOUNDARY
C       CONDITION ARE CALCULATED USING A CENTRAL DIFFERENCE SCHEME.
C
        CALL WHCH(II,JJ,M,N,1WHCH)
        IF(IWHCH.LE.4) VOLFRC=.25D+0
        IF(IWHCH.GT.4.AND.IWHCH.LT.9) VOLFRC=.5D+0
        IF(IWHCH.EQ.9) VOLFRC=1.D+0
        GO TO (1,2,3,4,5,6,7,8,9), IWHCH
C               FOR 1,1 CORNER NODE
 1      GRDZ=0.D+0
        GRDY=0.D+0
        GO TO 95
C               FOR N,1 CORNER NODE
 2      GRDZ=0.D+0
        GRDY=BIOT*(TFL(J)-B(N1))
        GO TO 95
C               FOR N,M CORNER NODE
 3      GRDZ=0.D+0
        GRDY=BIOT*(TFL(J)-B(N1))
        GO TO 95
C               FOR 1,M CORNER NODE
 4      GRDZ=0.D+0
        GRDY=0.D+0
        GO TO 95
C               FOR Y=0 INSULATED FACE.  GRADIENT BASED ON CENTRAL
C               DIFFERENCE SCHEME.
```

```
 5      GRDZ=(B(N3)-B(N2))/(DZ*2.D+0)
        GRDY=0.D+0
        GO TO 95
C               FOR Z=0 INSULATED FACE
 6      GRDZ=0.D+0
        GRDY=(B(N5)-B(N4))/(DY*2.D+0)
        GO TO 95
C               FOR Y=1 CONVECTIVE FACE
 7      GRDZ=(B(N3)-B(N2))/(DZ*2.D+0)
        GRDY=BIOT*(TFL(J)-B(N1))
        GO TO 95
C               FOR Z=1 INSULATED FACE
 8      GRDZ=0.D+0
        GRDY=(B(N5)-B(N4))/(DY*2.D+0)
        GO TO 95
C               FOR INTERIOR NODES.
 9      GRDZ=(B(N3)-B(N2))/(DZ*2.D+0)
        GRDY=(B(N5)-B(N4))/(DY*2.D+0)
 95     TOP=(VPLS**2)*(GRDZ**2)+GRDY**2
        BTM=(B(N1)*TRM1+1.D+0)**2
 100    SGNMT(N1)=(TRM12*TOP/BTM)*VOLFRC
C
C       INTEGRATE OVER MATERIAL VOLUME TO GET A TOTAL FOR THIS TIME
C       PERIOD.  AN ODD NUMBER OF DATA POINTS ARE REQUIRED
C
        CALL TWODIM(DBUG,SGNMT,DZ,DY,M,N,MN,SUMMAT)
        IF(MODE.EQ.3) GO TO 9999
C
C       DETERMINE RATE OF ENTROPY GENERATION AT EACH POINT IN THE FLUID
C       AND INTEGRATE TO GET A TOTAL FOR THIS TIME PERIOD.
C
        DO 200 KK=1,M
        DSTFRC=1.D+0
        IF(KK.EQ.1.OR.KK.EQ.M) DSTFRC=.5D+0
        TOP=TRM1*(TFL(KK)-TWL(KK))
        BTM=TFL(KK)*TRM1+1.D+0
 200    SGNF(KK)=((TOP/BTM)**2)*DSTFRC
        IF(DBUG.GT.0.D+0) CALL WRTO1(SGNF,SGNMT,M,N,MN)
C
C       INTEGRATE OVER CHANNEL LENGTH TO GET A TOTAL FOR THIS TIME
C       PERIOD.  AN ODD NUMBER OF POINTS ARE REQUIRED.
C
        CALL ONEDIM(DBUG,DZ,SGNF,M,SUMFLD)
C
C       DETERMINE AVAILABILITY OF EXITING FLUID FOR THIS TIME PERIOD.
C
        FRST=TRM1*TFL(M)
        SCND=DLOG(TFL(M)*TRM1+1.D+0)
        EXTFLD=FRST-SCND
        IF(DBUG.GT.0.D+0) WRITE(6,1010) EXTFLD
C
```

```
C       FORMAT STATEMENTS FOR THIS ROUTINE
C
 1000   FORMAT(//25X,'FROM SGEN')
 1010   FORMAT(5X,'EXTFLD= ',D20.10)
 9999   RETURN
        END
C
C
C
C
C
      SUBROUTINE SOLVE(NDIM, N, A, B, IPVT)
C
C     THIS ROUTINE SOLVES THE LINEAR SYSTEM A*X=B.
C     DO NOT USE IF DECOMP HAS DETECTED A SINGULARITY
C
      INTEGER NDIM, N, IPVT(N)
      DOUBLE PRECISION A(NDIM,N),B(N)
      INTEGER KB, KM1, NM1, KP1, I, K, M
      DOUBLE PRECISION T
C
C     FORWARD ELIMINATION
Cw
      IF (N .EQ. 1) GO TO 50
      NM1 = N-1
      DO 20 K = 1, NM1
         KP1 = K+1
         M = IPVT(K)
         T = B(M)
         B(M) = B(K)
         B(K) = T
         DO 10 I = KP1, N
             B(I) = B(I) + A(I,K)*T
   10    CONTINUE
   20 CONTINUE
C
C     BACK SUBSTITUTION
C
      DO 40 KB = 1,NM1
         KM1 = N-KB
         K = KM1+1
         B(K) = B(K)/A(K,K)
         T = -B(K)
         DO 30 I = 1, KM1
             B(I) = B(I) + A(I,K)*T
   30    CONTINUE
   40 CONTINUE
   50 B(1) = B(1)/A(1,1)
      RETURN
      END
C
```

```
C
C
C
C
      SUBROUTINE SWAP(M,N,MN,ISWAP,B,TMINT)
C
C     THIS ROUTINE IS CALLED AT THE START OF EACH TIME INCREMENT,
C     DURING THE FLUID TEMPERATURE ITERATION.  IT INITIALIZES THE
C     MATERIAL TEMPERATURE ARRAY TO THE SOLUTION FROM THE PREVIOUS
C     TIME STEP.
C
C     IT IS ALSO CALLED PRIOR TO THE START OF THE DISCHARGE PORTION
C     OF THE CYCLE IF A 2-D TEMPERATURE DISTRIBUTION IS REQUIRED.  IF
C     A COUNTERFLOW CONFIGURATION IS DESIRED, IT "SWAPS" THE
C     HORIZONTAL TEMPERATURE FIELD AS IT INITIALIZES THE MATERIAL
C     TEMPERATURE ARRAY.
C     IF A PARALLEL CONFIGURATION IS DESIRED, IT JUST REINTIALIZES THE
C     MATERIAL TEMPERATURE ARRAY.
C
C                     ISWAP=1: SWAP HORIZONTAL TEMPERATURE FIELD
C                     ISWAP=2: DON'T SWAP TEMPERATURE FIELD
C
      IMPLICIT REAL*8(A-H,O-Z)
      DIMENSION B(MN),TMINT(MN)
      DO 100 I=1,N
      DO 100 J=1,M
      N1=I+(J-1)*N
      JJ=M-(J-1)
      N2=I+(JJ-1)*N
      IF(ISWAP.EQ.1) TMINT(N1)=B(N2)
  100 IF(ISWAP.EQ.2) TMINT(N1)=B(N1)
 9999 RETURN
      END
C
C
C
C
C
      SUBROUTINE TBAR(M,N,MN,B,TAVG)
C
C     THIS ROUTINE DETERMINES AN AVERAGE MATERIAL TEMPERATURE.
C
      IMPLICIT REAL*8(A-H,O-Z)
      REAL*8 IMT
      DIMENSION B(MN)
      SUM=0.D+0
      NVOLS=(M-1)*(N-1)
      DO 100 I=1,N
      DO 100 J=1,M
      II=I
      JJ=J
```

```
      CALL WHCH(II,JJ,M,N,IWHCH)
      IF(IWHCH.LE.4) VOLFRC=.25D+0
      IF(IWHCH.GT.4.AND.IWHCH.LT.9) VOLFRC=.5D+0
      IF(IWHCH.EQ.9) VOLFRC=1.D+0
      N1=I+(J-1)*N
  100 SUM=SUM+B(N1)*VOLFRC
      TAVG=SUM/NVOLS
 9999 RETURN
      END
C
C
C
      SUBROUTINE TFLINT(DBUG,GPLS,BIOT,VPLS,TWL,DIST,M,DZ,TFL)
C
C     THIS ROUTINE SOLVES FOR THE FLUID TEMPERATURES USING A 4TH ORDER
C     RUNGE-KUTTA TECHNIQUE. REFERENCE IS MCCORMICK AND SALVADORI,PP
C     245.
C
      IMPLICIT REAL*8(A-H,O-Z)
      DIMENSION TWL(M),DIST(M),TFL(M)
C             DEFINE FUNCTION OF INTEREST
      F(Z,Y)=(GPLS*BIOT/VPLS)*(Z-Y)
C     F(X,Y)=.5D+0*(1.D+0+X)*Y*Y
      IF(DBUG.GT.0.D+0) WRITE(6,1000)
      KK=1
      H=DZ/5.D+0
      X=DIST(1)
      Y=TFL(1)
      DO 200 I=2,M
    1 ARG=X
      CALL INTERP(M,DIST(1),DZ,TWL,KK,ARG,Z)
      DEL1=F(Z,Y)
      ARG=X+.5D+0*H
      CALL INTERP(M,DIST(1),DZ,TWL,KK,ARG,Z)
      DEL2=F(Z,Y+.5D+0*H*DEL1)
      DEL3=F(Z,Y+.5D+0*H*DEL2)
      ARG=X+H
      CALL INTERP(M,DIST(1),DZ,TWL,KK,ARG,Z)
      DEL4=F(Z,Y+H*DEL3)
      Y=Y+H*(DEL1+2.D+0*DEL2+2.D+0*DEL3+DEL4)/6.D+0
      X=X+H
      DIF=(X-DIST(I))/DIST(I)
      IF(DABS(DIF).LE.1.D-3) GO TO 3
      GO TO 1
    3 TFL(I)=Y
      IF(DBUG.GT.0.D+0) WRITE(6,1010) I,X,TFL(I)
  200 CONTINUE
C
C     FORMAT STATEMENTS FOR THIS ROUTINE
C
 1000 FORMAT(//25X,'FROM TFLINT')
```

```
 1010   FORMAT(5X,'I= ',I2/5X,'X= ',D20.15/5X,'TFL= ',D20.15)
 9999   RETURN
        END
C
C
C
C
C
        SUBROUTINE TFLCRV(DBUG,GPLS,BIOT,VPLS,B,DIST,M,DZ,TFL)
C
C       THIS ROUTINE SOLVES FOR THE FLUID TEMPERATURES USING A 4TH ORDER
C       RUNGE-KUTTA TECHNIQUE. REFERENCE IS MCCORMICK AND SALVADORI,PP
C       245.
C       INTERMEDIATE FUNCTIONAL VALUES GENERATED BY CURVE FIT
C
        IMPLICIT REAL*8(A-H,O-Z)
        DIMENSION B(3),DIST(M),TFL(M)
C               DEFINE FUNCTION OF INTEREST
        F(X,Y)=(GPLS*BIOT/VPLS)*((B(1)+B(2)*X+B(3)*X**2)-Y)
C       F(X,Y)=.5D+0*(1.D+0+X)*Y*Y
        IF(DBUG.GT.0.D+0) WRITE(6,1000)
        H=DZ/5.D+0
        X=DIST(1)
        Y=TFL(1)
        DO 200 I=2,M
 1      DEL1=F(X,Y)
        DEL2=F(X+.5D+0*H,Y+.5D+0*H*DEL1)
        DEL3=F(X+.5D+0*H,Y+.5D+0*H*DEL2)
        DEL4=F(X+H,Y+H*DEL3)
        Y=Y+H*(DEL1+2.D+0*DEL2+2.D+0*DEL3+DEL4)/6.D+0
        X=X+H
        DIF=(X-DIST(I))/DIST(I)
        IF(DABS(DIF).LE.1.D-3) GO TO 3
        GO TO 1
 3      TFL(I)=Y
        IF(DBUG.GT.0.D+0) WRITE(6,1010) I,X,TFL(I)
 200    CONTINUE
C
C       FORMAT STATEMENTS FOR THIS ROUTINE
C
 1000   FORMAT(//25X,'FROM TFLCRV')
 1010   FORMAT(5X,'I= ',I2/5X,'X= ',D20.15/5X,'TFL= ',D20.15)
 9999   RETURN
        END
C
C
C
C
C
        SUBROUTINE THCHW(NTH,N,I,J)
C
```

```
C       THIS ROUTINE DETERMINES A MATRIX LOCATION FOR A GIVEN UNIQUE
C       NUMBER.
C
        IMPLICIT REAL*8(A-H,O-Z)
        IWHL=NTH/N
        IRMN=NTH-IWHL*N
        IF(IRMN.EQ.0) J=IWHL
        IF(IRMN.EQ.0) I=N
        IF(IRMN.GT.0) J=IWHL+1
        IF(IRMN.GT.0) I=IRMN
 9999   RETURN
        END
C
C
C
C
C
        SUBROUTINE TWLCRV(DBUG,X,Y,M,B)
C
C       THIS ROUTINE DOES A 3RD ORDER POLYNOMIAL CURVE FIT OF THE
C       STORAGE MATERIAL WALL TEMPERATURES.  IT WILL BE USED IN THE
C       ROUTINE TO SOLVE FOR FLUID TEMPERATURES.
C
        IMPLICIT REAL*8(A-H,O-Z)
        DIMENSION X(M),Y(M),B(3),COF(3,3),IPVT(3),WORK(3)
        IF(DBUG.GT.0.D+0) WRITE(6,1000)
        IFLG=0
        DO 10 I=1,3
        B(I)=0.D+0
        DO 10 J=1,3
 10     COF(I,J)=0.D+0
        COF(1,1)=M
        DO 20 K=1,M
        B(1)=B(1)+Y(K)
        B(2)=B(2)+X(K)*Y(K)
        B(3)=B(3)+(X(K)**2)*Y(K)
        COF(1,2)=COF(1,2)+X(K)
        COF(1,3)=COF(1,3)+X(K)**2
        COF(2,3)=COF(2,3)+X(K)**3
 20     COF(3,3)=COF(3,3)+X(K)**4
        DO 30 I=2,3
        DO 30 J=1,2
        II=I-1
        JJ=J+1
 30     COF(I,J)=COF(II,JJ)
C
C       SOLVE THIS SET OF EQUATIONS.  REALIZE THE FOLLOWING:
C               IN THE DECOMP SUBROUTINE, COF GOES OUT
C               AS THE COEFFICIENT MATRIX AND RETURNS AS
C               THE TRIANGULARIZED MATRIX.
C
```

```
C               IN THE SOLVE SUBROUTINE, B GOES OUT AS THE
C               CONSTANT MATRIX AND RETURNS AS THE SOLUTION
C               MATRIX.
C
        CALL DECOMP(3,3,COF,COND,IPVT,WORK)
        IF(COND.EQ.1.D+32) IFLG=100
        IF(IFLG.GT.0) WRITE(6,1111)
        IF(IFLG.GT.0) STOP
        CALL SOLVE(3,3,COF,B,IPVT)
C
C       DEBUGGING INFORMATION
C
        IF(DBUG.EQ.0.D+0) GO TO 9999
        WRITE(6,1010) (I,B(I),I=1,3)
        DO 777 I=1,M
        CRV=B(1)+B(2)*X(I)+B(3)*X(I)**2.D+0
 777    WRITE(6,888) X(I),Y(I),CRV
C
C       FORMAT STATEMENTS FOR THIS ROUTINE
C
 888    FORMAT(1X,'X= 'D10.5,2X,'TWL= ',D10.5,2X,'CRV= ',D10.5)
 1000   FORMAT(//25X,'FROM TWLCRV')
 1010   FORMAT(5X,'B(',I1,')= ',D20.10)
 1111   FORMAT(/5X,'SINGULAR MATRIX IN FLUID TEMPERATURE CURVE FITTIN
     *G ROUTINE.'/5X,'EXECUTION TERMINATED.'//)
 9999   RETURN
        END
C
C
C
C
C
        SUBROUTINE TWODIM(DBUG,TSOL,DZ,DY,M,N,MN,SUM)
C
C       THIS ROUTINE PERFORMS A 2-D NUMERICAL INTEGRATION OF DATA.  IT
C       IS BASED ON SIMPSONS RULE AND REQUIRES AN ODD NUMBER OF DATA
C       SETS.
C       REFERENCE IS SALVADORI AND MCCORMICK, PP 316
C
        IMPLICIT REAL*8(A-H,O-Z)
        DIMENSION NJ(3),NI(3),F(9),TSOL(MN)
        IF(DBUG.GT.0.D+0) WRITE(6,1000)
        KKL=(M-1)/2
        JJL=(N-1)/2
        SUM=0.D+0
        NJ(1)=1
        NJ(2)=NJ(1)+1
        NJ(3)=NJ(2)+1
C               FOR EACH Z STRIP
        DO 100 KK=1,KKL
        NI(1)=1
```

```
      NI(2)=NI(1)+1
      NI(3)=NI(2)+1
      DO 200 MM=1,3
      CALL WHCHT(NI(1),NJ(MM),N,NTH)
 200  F(MM)=TSOL(NTH)
C               FOR EACH Y BLOCK IN A Z STRIP
      DO 80 JJ=1,JJL
      DO 300 MM=1,3
      ICNT=MM+3
      CALL WHCHT(NI(2),NJ(MM),N,NTH)
 300  F(ICNT)=TSOL(NTH)
      DO 400 MM=1,3
      ICNT=MM+6
      CALL WHCHT(NI(3),NJ(MM),N,NTH)
 400  F(ICNT)=TSOL(NTH)
      SUM=SUM+(DZ*DY/9.D+0)*(F(1)+F(3)+F(7)+F(9)+4.D+0*(
     * F(2)+F(4)+F(6)+F(8))+16.D+0*F(5))
      F(1)=F(7)
      F(2)=F(8)
      F(3)=F(9)
      NI(2)=NI(3)+1
 80   NI(3)=NI(2)+1
      NJ(1)=NJ(3)
      NJ(2)=NJ(1)+1
 100  NJ(3)=NJ(2)+1
      IF(DBUG.GT.0.D+0) WRITE(6,1010) SUM
C
C     FORMAT STATEMENTS FOR THIS ROUTINE
C
 1000 FORMAT(//25X,'FROM TWODIM')
 1010 FORMAT(5X,'2-D SUM= ',D20.10)
 9999 RETURN
      END
C
C
C
C
C
      SUBROUTINE WCHNDE(ICAP,JCAP,M,N,BIOT,DY,B1,B2,COEF)
C
C     THIS ROUTINE DETERMINES WHICH NODE WITHIN THE STORAGE MATERIAL
C     IS CURRENTLY BEING DEFINED IN THE "DEFINE" ROUTINE.  IT THEN
C     DEFINES THE NEIGHBOR NODES AND INITIALIZES THE COEFFICIENT
C     DEPENDING ON THE VARIABLE JCAP.
C
      IMPLICIT REAL*8(A-H,O-Z)
      COEF=0.D+0
      TAIL=(1.D+0+(BIOT*DY))
      X=2.D+0*B1
      Y=2.D+0*B2
C
```

```
C       DETERMINE THE LOCATION WITHIN THE STORAGE MATERIAL NODAL
C       NETWORK AND INSURE THAT IT IS ACCURATE.
C
        CALL THCHW(ICAP,N,I,J)
        N1=I+(J-1)*N
        IF(N1.NE.ICAP) WRITE(6,1111)
        IF(N1.NE.ICAP) STOP
C
C       DETERMINE NEIGHBOR NODES AND TYPE OF NODE (I,J) IS, THEN
C       BRANCH.
C
        N2=I+(J-2)*N
        N3=I+J*N
        N4=(I-1)+(J-1)*N
        N5=(I+1)+(J-1)*N
        CALL WHCH(I,J,M,N,IWHCH)
        GO TO (1,2,3,4,5,6,7,8,9), IWHCH
C               FOR 1,1 CORNER NODE
 1      IF(JCAP.EQ.N3) COEF=X
        IF(JCAP.EQ.N5) COEF=Y
        IF(JCAP.EQ.N1) COEF=-(1.D+0+2.D+0*(B1+B2))
        GO TO 9999
C               FOR N,1 CORNER NODE
 2      IF(JCAP.EQ.N3) COEF=X
        IF(JCAP.EQ.N4) COEF=Y
        IF(JCAP.EQ.N1)COEF=-(1.D+0+X+Y*TAIL)
        GO TO 9999
C               FOR N,M CORNER NODE
 3      IF(JCAP.EQ.N2) COEF=X
        IF(JCAP.EQ.N4) COEF=Y
        IF(JCAP.EQ.N1) COEF=-(1.D+0+X+Y*TAIL)
        GO TO 9999
C               FOR 1,M CORNER NODE
 4      IF(JCAP.EQ.N2) COEF=X
        IF(JCAP.EQ.N5) COEF=Y
        IF(JCAP.EQ.N1) COEF=-(1.D+0+X+Y)
        GO TO 9999
C
C       FOR Y=0 INSULATED FACE
C
 5      IF(JCAP.EQ.N2) COEF=B1
        IF(JCAP.EQ.N3) COEF=B1
        IF(JCAP.EQ.N5) COEF=Y
        IF(JCAP.EQ.N1) COEF=-(1.D+0+X+Y)
        GO TO 9999
C
C       FOR Z=0 FACE
C
 6      IF(JCAP.EQ.N3) COEF=X
        IF(JCAP.EQ.N4) COEF=B2
        IF(JCAP.EQ.N5) COEF=B2
```

```
      IF(JCAP.EQ.N1) COEF=-(1.D+0+X+Y)
      GO TO 9999
C             FOR Y=1 CONVECTIVE FACE
 7    IF(JCAP.EQ.N2) COEF=B1
      IF(JCAP.EQ.N3) COEF=B1
      IF(JCAP.EQ.N4) COEF=Y
      IF(JCAP.EQ.N1) COEF=-(1.D+0+X+Y*TAIL)
      GO TO 9999
C             FOR Z=1 INSULATED FACE
 8    IF(JCAP.EQ.N2) COEF=X
      IF(JCAP.EQ.N4) COEF=B2
      IF(JCAP.EQ.N5) COEF=B2
      IF(JCAP.EQ.N1) COEF=-(1.D+0+X+Y)
      GO TO 9999
C             FOR INTERIOR NODES
 9    IF(JCAP.EQ.N2) COEF=B1
      IF(JCAP.EQ.N3) COEF=B1
      IF(JCAP.EQ.N4) COEF=B2
      IF(JCAP.EQ.N5) COEF=B2
      IF(JCAP.EQ.N1) COEF=-(1.D+0+X+Y)
C
C     FORMAT STATEMENTS FOR THIS ROUTINE
C
 1111 FORMAT(5X,'WCHNDE ROUTINE IS NOT RETURNING CORRECT NODAL
     * LOCATION.'/5X,'EXECUTION TERMINATED.')
 9999 RETURN
      END
C
C
C
C
C
      SUBROUTINE WHCH(I,J,M,N,IWHCH)
C
C     THIS ROUTINE IDENTIFIES NODAL POINTS BY TYPE.
C
      IMPLICIT REAL*8(A-H,O-Z)
      IF(I.EQ.1.AND.J.EQ.1) IWHCH=1
      IF(I.EQ.N.AND.J.EQ.1) IWHCH=2
      IF(I.EQ.N.AND.J.EQ.M) IWHCH=3
      IF(I.EQ.1.AND.J.EQ.M) IWHCH=4
      IF(I.EQ.1.AND.J.GT.1.AND.J.LT.M) IWHCH=5
      IF(I.GT.1.AND.I.LT.N.AND.J.EQ.1) IWHCH=6
      IF(I.EQ.N.AND.J.GT.1.AND.J.LT.M) IWHCH=7
      IF(I.GT.1.AND.I.LT.N.AND.J.EQ.M) IWHCH=8
      IF(I.GT.1.AND.I.LT.N.AND.J.GT.1.AND.J.LT.M) IWHCH=9
 9999 RETURN
      END
C
C
C
```

```
C
C
      SUBROUTINE WHCHT(I,J,N,NTH)
C
C     THIS ROUTINE DETERMINES A UNIQUE NUMBER FOR A GIVEN LOCATION IN
C     A MATRIX OF N ROWS.
C
      NTH=I+(J-1)*N
 9999 RETURN
      END
C
C
C
C
C
      SUBROUTINE WRT01 (TFL,B,M,N,MN)
C
C     THIS ROUTINE WRITE OUT SPATIALLY CORRECT TEMPERATURE
C     FIELDS
C
      IMPLICIT REAL*8 (A-H,O-Z)
      DIMENSION TFL(M),B(MN),NTH(9)
      WRITE(6,990)
      WRITE(6,1000) (TFL(I),I=1,M)
      WRITE(6,1010)
      DO 100 I=1,N
      II=N-(I-1)
      DO 200 J=1,M
 200  NTH(J)=II+(J-1)*N
 100  WRITE(6,1000) (B(NTH(J)),J=1,M)
      WRITE(6,990)
C
C     FORMAT STATEMENTS FOR THIS ROUTINE
C
 990  FORMAT(' ')
 1000 FORMAT(3X,9(D13.6,1X))
 1010 FORMAT(' ')
 9999 RETURN
      END
C
C
C
C
C
      SUBROUTINE REPORT (G,X,MM,NN,CON,VAR,XO)
C
C     THIS ROUTINE WRITES OUT THE RESULTS OF THE FINAL OPTIMIZATION
C     RUN.
C
      IMPLICIT REAL*8 (A-H,O-Z)
      INTEGER*2 INIT
```

```
      REAL*8 MITX,MDOTS,MRAT,IMT,NDFITS,NDFIPS,NTUS,NDFITD,NDFIPD,
     *  MDOTD,NTUD,NSUBS,MATSTR,MATSS,MATDB,MATDE,LRGEST
      DIMENSION X(NN),G(MM),CON(MM),VAR(NN),XO(NN),CONFG(2),
     *  FLWDIR(2),ENDDST(2),TFLSLV(2),AVMTMP(100),FLEXS(100),FLDS(10),
     *  MATSTR(100),AVLMS(100),AVLFS(100),AVLES(100),AVGTSS(100),
     *  HGHTMP(100),APRSS(100),AVLMSS(100),FLDSS(10),MATSS(100),
     *  MATDB(100),FLDD(100),TAVG(100),AVLMD(100),AVLFD(100),MATDE(100),
     *  TFLDB(10),TFLDE(10),AVLED(100)

      COMMON/RESULT/M,N,IGEOM,ISWAP,IDIST,IWHCH,KCSS,ISS,KL,
     *  KCDS,IDS,LM,FITXS,FITXD,MITX,
     *  MDOTS,MRAT,VPLS,WPLS,ROVRCP,TKRAT,PR,CLOSE,IMT,FNUM,DFOST,
     *  NDFITS,FIPXS,NDFIPS,BIS,GPLSS,NTUS,REYSTO,TOPT,STOMAT,STOFLD,
     *  STOEXT,STORSM,ETSS,ABSS,DFOSS,AVLSS,ETDS,ABDS,
     *  DFOD,NDFITD,FIPXD,NDFIPD,BID,GPLSD,MDOTD,NTUD,
     *  REYDIS,DISMAT,DISFLD,DISSUM,TP1,TP2,BTM1,BTM2,ALPHA,NSUBS,
     *  FSTCMP,LRGEST,DISEXT
      COMMON/INITBK/INIT
      COMMON/DIM/AVMTMP,FLEXS,FLDS,MATSTR,AVLMS,AVLFS,AVLES,AVGTSS,
     *  HGHTMP,APRSS,AVLMSS,FLDSS,MATSS,MATDB,TAVG,FLDD,AVLMD,
     *  AVLFD,MATDE,TFLDB,TFLDE,AVLED
      DATA CONFG/'FLAT','CYLN'/
      DATA FLWDIR/'CNTR','PARL'/
      DATA ENDDST/'UNFM',' 2-D'/
      DATA TFLSLV/'CRFT','INTR'/
C
C     START WRITE SUMMARY, BEGIN BY CALLING GRG2 WITH THE OPTIMUM
C     VARIABLES IN ORDER TO GET A GOOD PRINTOUT.
C
      IF(INIT.EQ.1) RETURN
      IF(INIT.EQ.0) CALL GCOMP(G,X)
C             GRG2 SUMMARY
      WRITE(6,500)
      WRITE(6,510) CON(1),G(1)
      WRITE(6,510) CON(2),G(2)
      WRITE(6,520) VAR(1),X(1),XO(1),VAR(2),X(2),XO(2)
      WRITE(6,520) VAR(3),X(3),XO(3)
C             INPUT SUMMARY
      WRITE(6,1000)
      WRITE(6,1010)
      WRITE(6,1020) M,N,CONFG(IGEOM),FLWDIR(ISWAP),ENDDST(IDIST),
     *  TFLSLV(IWHCH)
      WRITE(6,1030) FITXS,FITXD,MITX,MDOTS,MRAT
      WRITE(6,1040) VPLS,WPLS,ROVRCP,TKRAT,PR
      WRITE(6,1050) CLOSE
C             MODE 1 (STORAGE) SUMMARY
      WRITE(6,2000)
      WRITE(6,2010) IMT,FNUM,DFOST,NDFITS,FIPXS
      WRITE(6,2020) NDFIPS,BIS,GPLSS,NTUS,REYSTO
      WRITE(6,2030) TOPT,STOMAT,STOFLD,STOEXT,STORSM
      PCTM=STOMAT/STORSM
```

```
      PCTF=STOFLD/STORSM
      PCTX=STOEXT/STORSM
      WRITE(6,2035) PCTM,PCTF,PCTX
      WRITE(6,2040)
      DO 100 I=1,59
      AVLMS(I)=AVLMS(I)/VPLS
      AVLFS(I)=AVLFS(I)*(BIS/VPLS)
      AVLES(I)=AVLES(I)/GPLSS
      TOTAL=AVLMS(I)+AVLFS(I)+AVLES(I)
100   WRITE(6,2050) I,AVLMS(I),AVLFS(I),AVLES(I),TOTAL,
     * AVMTMP(I),FLEXS(I)
      WRITE(6,2060)
      CALL WRT01(FLDS,MATSTR,M,N,MN)
C             MODE 2 SUMMARY
      IF(IDIST.EQ.2) WRITE(6,2070)
      IF(IDIST.EQ.2) GO TO 300
      WRITE(6,3000)
      WRITE(6,3010) ETSS,ABSS,KCSS,ISS
C             MODE 3 SUMMARY
      WRITE(6,4000)
      PCTSS=AVLSS/STORSM
      WRITE(6,4010) DFOSS,KL,AVLSS,PCTSS,LRGEST
      WRITE(6,4020)
      DO 200 J=1,KL
      AVLMSS(J)=AVLMSS(J)/VPLS
200   WRITE(6,4030) J,AVLMSS(J),AVGTSS(J),HGHTMP(J),APRSS(J)
      WRITE(6,4040)
      CALL WRT01(FLDSS,MATSS,M,N,MN)
C             MODE 4 SUMMARY
300   WRITE(6,5000)
      WRITE(6,5010) ETDS,ABDS,KCDS,IDS
C             MODE 5 (DISCHARGE) SUMMARY
      WRITE(6,6000)
      WRITE(6,6010) DFOD,NDFITD,FIPXD,NDFIPD,LM
      WRITE(6,6020) BID,GPLSD,MDOTD,NTUD,REYDIS
      WRITE(6,6030) DISMAT,DISFLD,DISEXT,DISSUM
      PCTM=DISMAT/DISSUM
      PCTF=DISFLD/DISSUM
      WRITE(6,6035) PCTM,PCTF
      WRITE(6,6040)
      CALL WRT01(TFLDB,MATDB,M,N,MN)
      WRITE(6,2040)
      DO 400 K=1,LM
      AVLMD(K)=AVLMD(K)/VPLS
      AVLFD(K)=AVLFD(K)*(BID/VPLS)
      AVLED(K)=AVLED(K)/GPLSD
      TOTAL=AVLMD(K)+AVLFD(K)
400   WRITE(6,6050) K,AVLMD(K),AVLFD(K),AVLED(K),TOTAL,TAVG(K),
     * FLDD(K)
      WRITE(6,6060)
      CALL WRT01(TFLDE,MATDE,M,N,MN)
```

```
C               FIGURE OF MERIT SUMMARY
      WRITE(6,7000)
      WRITE(6,7010) TP1,TP2,BTM1,BTM2,ALPHA,NSUBS,FSTCMP
C
C     FORMAT STATEMENTS FOR THIS ROUTINE
C
  500 FORMAT(48X,'GRG2 CONTROLLED VARIABLES'/48X,
     * '---- ---------- ---------'/)
  510 FORMAT(3X,A8,'= ',D16.10)
  520 FORMAT(3X,A8,'= ',D16.10,3X,'(IV= ',D16.10,')',5X,
     * A8,'= ',D16.10,3X,'(IV= ',D16.10,')')
 1000 FORMAT(///43X,'ENTROP PROGRAM GENERATED VARIABLES'/43X,
     * '------ ------- --------- ---------'/)
 1010 FORMAT(3X,'INPUT DATA SUMMARY'/3X,'----- ---- -------')
 1020 FORMAT(3X,'M= ',I3,5X,'N= ',I3,5X,'GEOMETRY= ',A4,5X,
     * 'FLW DIR= ',A4,5X,'MAT TMP @ DIS 1= ',A4,5X,
     * 'TFL SOLV TYPE= ',A4)
 1030 FORMAT(3X,'FITXS=  ',D16.10,2X,'FITXD=  ',D16.10,2X,'MITX=   ',
     * D16.10,2X,'MDOTS=  ',D16.10,2X,'MRAT=   ',D16.10)
 1040 FORMAT(3X,'VPLS=   ',D16.10,2X,'WPLS=   ',D16.10,2X,'ROVRCP= ',
     * D16.10,2X,'TKRAT=  ',D16.10,2X,'PR=     ',D16.10)
 1050 FORMAT(3X,'CLOSE=  ',D16.10/)
 2000 FORMAT(3X,'MODE 1 (STORAGE) SUMMARY'/3X,
     * '---- - --------- -------')
 2010 FORMAT(3X,'IMT=    ',D16.10,2X,'FNUM=   ',D16.10,2X,'DFOST=  ',
     * D16.10,2X,'NDFITS= ',D16.10,2X,'FIPXS=  ',D16.10)
 2020 FORMAT(3X,'NDFIPS= ',D16.10,2X,'BIS=    ',D16.10,2X,'GPLSS=  ',
     * D16.10,2X,'NTUS=   ',D16.10,2X,'REYSTO= ',D16.10)
 2030 FORMAT(3X,'TOPT=   ',D16.10,2X,'STOMAT= ',D16.10,2X,'STOFLD= ',
     * D16.10,2X,'STOEXT= ',D16.10,2X,'STORSM= ',D16.10)
 2035 FORMAT(3X,'PCTM=   ',D16.10,2X,'PCTF=   ',D16.10,2X,
     * 'PCTX=   ',D16.10/)
 2040 FORMAT(88X,'AVG',12X,'EXITING'/3X,'TIME',25X,
     * 'ENTROPY GENERATION TERMS',29X,'MATERIAL',11X,
     * 'FLUID'/3X,'STEP',6X,'MATERIAL',11X,'FLUID',12X,
     * 'EXT FLD',12X,'TOTAL',10X,'TEMPERATURE',7X,
     * 'TEMPERATURE'/3X,'----',2X,'----------------',2X,
     * '----------------',2X,'----------------',2X,
     * '----------------',2X,'----------------',2X,
     * '----------------'/)
 2050 FORMAT(3X,I3,6(2X,D16.10))
 2060 FORMAT(/3X,'MATERIAL AND FLUID TEMPERATURE DISTRIBUTION',1X,
     * 'AT END OF STORAGE PERIOD ARE:')
 2070 FORMAT(/3X,'MODES 2&3 NOT REQUIRED FOR THIS RUN'/
     * 3X,'----- --- --- -------- --- ---- ---'/)
 3000 FORMAT(3X,'MODE 2 SUMMARY'/3X,'---- - -------')
 3010 FORMAT(3X,'ETSS=   ',D16.10,2X,'ABSS=   ',D16.10,2X,'KCSS=   ',
     * I3,'/100',2X,'ISS=    ',I3,'/20'/)
 4000 FORMAT(3X,'MODE 3 SUMMARY'/3X,'---- - -------')
 4010 FORMAT(3X,'DFOSS=  ',D16.10,2X,'KL=    ',I3,2X,'AVLSS=  ',
     * D16.10,2X,'PCTSS = ',D16.10,2X,'LRGEST= ',D16.10/)
```

```
4020   FORMAT(13X,'ENTROPY',11X,'AVERAGE'/3X,'TIME',5X,
    *  'GENERATED',10X,'MATERIAL',10X,'HIGHEST'/3X,'STEP',
    *  6X,'MATERIAL',9X,'TEMPERATURE',7X,'TEMPERATURE',7X,
    *  'DIFFERENCE'/3X,'----',2X,'----------------',2X,
    *  '----------------',2X,'----------------',2X,
    *  '----------------'/)
4030   FORMAT(3X,I3,4(2X,D16.10))
4040   FORMAT(/3X,'MATERIAL AND FLUID TEMPERATURE DISTRIBUTION',1X,
    * 'AT END OF STEADY STATE PERIOD.')
5000   FORMAT(3X,'MODE 4 SUMMARY'/3X,'---- - -------')
5010   FORMAT(3X,'ETDS=    ',D16.10,2X,'ABDS=    ',D16.10,2X,'KCDS=    ',
    *  I3,'/100',2X,'IDS=     ',I3,'/20'/)
6000   FORMAT(3X,'MODE 5 (DISCHARGE) SUMMARY'/3X,
    *  '---- - ---------- -------')
6010   FORMAT(3X,'DFOD=    ',D16.10,2X,'NDFITD= ',D16.10,2X,'FIPXD=  ',
    *  D16.10,2X,'NDFIPD= ',D16.10,2X,'LM= ',I3)
6020   FORMAT(3X,'BID=     ',D16.10,2X,'GPLSD=  ',D16.10,2X,'MDOTD=  ',
    *  D16.10,2X,'NTUD=    ',D16.10,2X,'REYDIS= ',D16.10)
6030   FORMAT(3X,'DISMAT= ',D16.10,2X,'DISFLD= ',D16.10,2X,'DISEXT= ',
    *  D16.10,2X,'DISSUM= ',D16.10)
6035   FORMAT(3X,'PCTM=    ',D16.10,2X,'PCTF=    ',D16.10/)
6040   FORMAT(/3X,'MATERIAL AND FLUID TEMPERATURE DISTRIBUTION',1X,
    * 'PRIOR TO START OF DISCHARGE PERIOD.')
6050   FORMAT(3X,I3,2X,D16.10,2X,D16.10,2X,D16.10,2X,D16.10,2X,
    *  D16.10,2X,D16.10)
6060   FORMAT(/3X,'MATERIAL AND FLUID TEMPERATURE DISTRIBUTION',1X,
    * 'AT END OF DISCHARGE PERIOD.')
7000   FORMAT(3X,'FIGURE OF MERIT SUMMARY'/3X,
    *  '------ -- ----- -------')
7010   FORMAT(3X,'PRS AVL, STORAGE= ',D16.10,5X,'PRS AVL, DISCHARGE= ',
    *  D16.10/3X,'TMP AVL, STORAGE= ',D16.10,5X,'TMP AVL, DISCHARGE= ',
    *  D16.10/3X,'ALPHA= ',D16.10,3X,'NSUBS= ',D16.10,3X,
    *  '1ST LAW COMP= ',D16.10///)
9999   RETURN
       END
```

NSUBS = 0.34387319240+00
GPLSS = 0.16650759040+04 (IV= 0.40000000000+031) BIS = 0.63039772580+03 (IV= 0.40000000000+031)
FNUM = 0.13983675230+03 (IV= 0.70000000000+031)

ENTROP PROGRAM GENERATED VARIABLES

INPUT DATA SUMMARY

M= 9 N= 9 GEOMETRY= FLAT FLW DIR= CNTR MAT TMP @ DIS 1= 2-D TFL SOLV TYPE= INTR
FITXS= 0.30000000000+01 FITXD= 0.10000000000+01 MITX= 0.13000000000+01 MDOTS= 0.50000000000-02 MRAT= 0.10000000000+01
WPLS= 0.50000000000-01 WPLS= 0.0 MDVRCP= 0.28430000000+00 TKRAT= 0.0 PR= 0.71000000000+00
CLOSE= 0.10000000000-02

MODE 1 (STORAGE) SUMMARY

IMI= 0.15000000000+00 FNUM= 0.13983675230+01 DFOST= 0.23701144470-01 NDFITS= 0.10000000000+01 FIPXS= 0.10312513710+01
NDFIPS= 0.10000000000+01 BIS= 0.63039772580+01 GPLSS= 0.16650759040+03 NTUS= 0.20993231260+02 KEYSTO= 0.0
TCPT= 0.50334482250+00 STUMAT= 0.84357357350+00 STOFLD= 0.34069504550+00 STOEXT= 0.52259679920+00 STCRS%= 0.17068654180+01
PCTM= 0.49422383540+00 PCTF= 0.19960275830+00 PCTX= 0.30617340630+00

TIME STEP	ENTROPY GENERATION TERMS MATERIAL	FLUID	EXT FLD	TOTAL	AVG MATERIAL TEMPERATURE	EXITING FLUID TEMPERATURE
1	0.54854381160+00	0.72445392710+00	0.22634293050+00	0.14993406700+01	0.15773614630+00	0.15011280840+00
2	0.76452281660+00	0.61995216870+00	0.22658908850+00	0.16110640740+01	0.16495312030+00	0.15320154230+00
3	0.88294653120+00	0.55000517230+00	0.22705714880+00	0.16600088520+01	0.17194261320+00	0.15037015580+00
4	0.95349166890+00	0.49985177540+00	0.22782017320+00	0.16811636180+01	0.17881662090+00	0.15064471550+00
5	0.99495909190+00	0.46192961490+00	0.22889522140+00	0.16857839280+01	0.18560795300+00	0.15103089970+00
6	0.10161790990+01	0.43194563670+00	0.23028298420+00	0.16784077200+01	0.19233496310+00	0.15152830050+00
7	0.10224574720+01	0.40741339940+00	0.23197764590+00	0.16618485170+01	0.19900897780+00	0.15213403580+00
8	0.10156971640+01	0.38728707460+00	0.23381486480+00	0.16367991040+01	0.20560061840+00	0.15278858200+00
9	0.10019336620+01	0.36979412690+00	0.23595704150+00	0.16076848300+01	0.21215351380+00	0.15354910880+00
10	0.98283194330+00	0.35444974510+00	0.23838560020+00	0.15756672890+01	0.21867123290+00	0.15440783810+00
11	0.96003065890+00	0.34083032430+00	0.24108936010+00	0.15419503430+01	0.22515606430+00	0.15535960550+00
12	0.93467940640+00	0.32860828490+00	0.24405994820+00	0.15075476400+01	0.23160958460+00	0.15643019870+00
13	0.90842355010+00	0.31753398420+00	0.24729070610+00	0.14732482400+01	0.23803291730+00	0.15752597530+00
14	0.88144479310+00	0.30741579870+00	0.25077639390+00	0.14396369860+01	0.24442688040+00	0.15873376300+00
15	0.85451120160+00	0.29810486630+00	0.25451307020+00	0.14071291280+01	0.25079208010+00	0.16002081920+00
16	0.82802369580+00	0.28948399690+00	0.25849799750+00	0.13760056900+01	0.25712897280+00	0.16138479790+00
17	0.80225541020+00	0.28145982850+00	0.26272954010+00	0.13464447790+01	0.26343790690+00	0.16282371330+00
18	0.77738350750+00	0.27395696430+00	0.26720705120+00	0.13185475230+01	0.26971915100+00	0.16433589770+00
19	0.75351417660+00	0.26691379920+00	0.27193075470+00	0.12923587300+01	0.27597291390+00	0.16591995890+00
20	0.73070190350+00	0.26027938110+00	0.27690162600+00	0.12678829110+01	0.28219935710+00	0.16757473630+00
21	0.70896411850+00	0.25401107300+00	0.28212127680+00	0.12450966680+01	0.28839860500+00	0.16929926010+00
22	0.68829220700+00	0.24807279070+00	0.28759184650+00	0.12239568440+01	0.29457075020+00	0.17109271260+00
23	0.66865970710+00	0.24243366490+00	0.29331590320+00	0.12044092750+01	0.30071585920+00	0.17295439390+00
24	0.65002836140+00	0.23706701860+00	0.29929635320+00	0.11863917330+01	0.30683397470+00	0.17488369210+00
25	0.63235254360+00	0.23194957930+00	0.30553636160+00	0.11698384850+01	0.31292511870+00	0.17688005650+00
26	0.61558246560+00	0.22706086860+00	0.31203928260+00	0.11546826170+01	0.31898929420+00	0.17894297660+00
27	0.59966647310+00	0.22238272590+00	0.31880859820+00	0.11408577970+01	0.32502648650+00	0.18107196330+00
28	0.58455266530+00	0.21789893330+00	0.32584786600+00	0.11282996650+01	0.33103666520+00	0.18326653430+00
29	0.57019001430+00	0.21359491920+00	0.33316067500+00	0.11169456090+01	0.33701978470+00	0.18552620250+00

30	0.5565291174D+00	0.2094575210D+00	0.3407506067D+00	0.1106737245D+01	0.3429757857D+00	0.1878504667D+00
31	0.5435226810D+00	0.2054747937D+00	0.3486212032D+00	0.1097618678D+01	0.3489045960D+00	0.1902388050D+00
32	0.5311258107D+00	0.2016358544D+00	0.3567759403D+00	0.1089537605D+01	0.3548061316D+00	0.1926906693D+00
33	0.5192961608D+00	0.1979307552D+00	0.3652182035D+00	0.1082445119D+01	0.3606802977D+00	0.1952054821D+00
34	0.5079939861D+00	0.1943503766D+00	0.3739512694D+00	0.1076295632D+01	0.3665269896D+00	0.1977826341D+00
35	0.4971821236D+00	0.1908863398D+00	0.3829702886D+00	0.1071046752D+01	0.3723460933D+00	0.2004214830D+00
36	0.4868259283D+00	0.1875309311D+00	0.3923022717D+00	0.1066659131D+01	0.3781374867D+00	0.2031213531D+00
37	0.4768931770D+00	0.1842770383D+00	0.4019260776D+00	0.1063096293D+01	0.3839010403D+00	0.2058815354D+00
38	0.4673539539D+00	0.1811180956D+00	0.4118524033D+00	0.1060324453D+01	0.3896366179D+00	0.2087012881D+00
39	0.4581805254D+00	0.1780480356D+00	0.4220837746D+00	0.1058312336D+01	0.3953440776D+00	0.2115798378D+00
40	0.4493472056D+00	0.1750612473D+00	0.4326225389D+00	0.1057030996D+01	0.4010232721D+00	0.2145163805D+00
41	0.4408302459D+00	0.1721525393D+00	0.4434708586D+00	0.1056453644D+01	0.4066740500D+00	0.2175100832D+00
42	0.4326076669D+00	0.1693171060D+00	0.4546307049D+00	0.1056555478D+01	0.4122962559D+00	0.2205600854D+00
43	0.4246591749D+00	0.1665504987D+00	0.4661038536D+00	0.1057313527D+01	0.4178897314D+00	0.2236655033D+00
44	0.4169660231D+00	0.1638485986D+00	0.4778918800D+00	0.1058706502D+01	0.4234543154D+00	0.2268254170D+00
45	0.4095109042D+00	0.1612075923D+00	0.4899961555D+00	0.1060714652D+01	0.4289898452D+00	0.2300389018D+00
46	0.4022778449D+00	0.1586239501D+00	0.5024178442D+00	0.1063319639D+01	0.4344961563D+00	0.2333049996D+00
47	0.3952521076D+00	0.1560944056D+00	0.5151579007D+00	0.1066504414D+01	0.4399730835D+00	0.2366227360D+00
48	0.3884200985D+00	0.1536159371D+00	0.5282170669D+00	0.1070253102D+01	0.4454204612D+00	0.2399911180D+00
49	0.3817692814D+00	0.1511857505D+00	0.5415958712D+00	0.1074550903D+01	0.4508381239D+00	0.2434091365D+00
50	0.3752881001D+00	0.1488012636D+00	0.5552946263D+00	0.1079383990D+01	0.4562259063D+00	0.2468757667D+00
51	0.3689659036D+00	0.1464600914D+00	0.5693134289D+00	0.1084739423D+01	0.4615836444D+00	0.2503899703D+00
52	0.3627928763D+00	0.1441600321D+00	0.5836521586D+00	0.1090605067D+01	0.4669111752D+00	0.2539506961D+00
53	0.3567599806D+00	0.1418990550D+00	0.5983104782D+00	0.1096969514D+01	0.4722083373D+00	0.2575568819D+00
54	0.3508588930D+00	0.1396752885D+00	0.6132878336D+00	0.1103822015D+01	0.4774749715D+00	0.2612074551D+00
55	0.3450819528D+00	0.1374870088D+00	0.6285845460D+00	0.1111152416D+01	0.4827109207D+00	0.2649013345D+00
56	0.3394221124D+00	0.1353326299D+00	0.6441963560D+00	0.1118951098D+01	0.4879160305D+00	0.2686374306D+00
57	0.3338728907D+00	0.1332106938D+00	0.6601253388D+00	0.1127208923D+01	0.4930901491D+00	0.2724146476D+00
58	0.3284283309D+00	0.1311198616D+00	0.6763689921D+00	0.1135917185D+01	0.4982331282D+00	0.2762318837D+00
59	0.3230829610D+00	0.1290589049D+00	0.6929256950D+00	0.1145067561D+01	0.5033448225D+00	0.2800880323D+00

MATERIAL AND FLUID TEMPERATURE DISTRIBUTION AT END OF STORAGE PERIOD ARE:

0.1000000+01	0.919222D+00	0.8156130+00	0.7009790+00	0.588562D+00	0.4871960+00	0.401374D+00	0.3323000+00	0.2800880+00
0.975824D+00	0.8855710+00	0.773598D+00	0.6565710+00	0.5464030+00	0.4501000+00	0.3705760+00	0.3079210+00	0.2621370+00
0.957271D+00	0.8601220+00	0.742199D+00	0.6236900+00	0.5154360+00	0.4230470+00	0.3486220+00	0.2903680+00	0.2492590+00
0.940167D+00	0.8371560+00	0.7143190+00	0.5948370+00	0.4885320+00	0.3997500+00	0.3292020+00	0.2754860+00	0.2383660+00
0.924928D+00	0.8170510+00	0.6902410+00	0.5701710+00	0.4657290+00	0.3801540+00	0.3132820+00	0.2631370+00	0.2293470+00
0.911923D+00	0.8001340+00	0.6702080+00	0.5498200+00	0.4470690+00	0.3642050+00	0.3004010+00	0.2532020+00	0.2221030+00
0.901467D+00	0.7866820+00	0.6544190+00	0.5338880+00	0.4325090+00	0.3518550+00	0.2904750+00	0.2455810+00	0.2165540+00
0.893813D+00	0.7769140+00	0.6430300+00	0.5224530+00	0.4221190+00	0.3430640+00	0.2834360+00	0.2401940+00	0.2126370+00
0.889145D+00	0.7709890+00	0.6361520+00	0.5155700+00	0.4158830+00	0.3378020+00	0.2792320+00	0.2369850+00	0.2103050+00
0.8875770+00	0.7690040+00	0.6338520+00	0.5132720+00	0.4138040+00	0.3360500+00	0.2778340+00	0.2359190+00	0.2095390+00

MODES 263 NOT REQUIRED FOR THIS RUN

MODE 4 SUMMARY

ETDS= 0.2370114447D+01 ABDS= -.8501736786D-02 KCDS= 2/100 IDS= 10/20

MODE 5 (DISCHARGE) SUMMARY

DFDD=	0.4017143130D-01	NDFITD=	0.0	FIPXD=	0.1000722479D+01	NDFIPD=	0.5773502692D+00	LM=	59
BID=	0.6303977258D+01	GPLSD=	0.1665075904D+00	MDOTD=	0.5000000000D-02	NTUD=	0.2099320126D+02	REYDIS=	0.0
DISMAT=	0.5628768536D+00	DISFLD=	0.3295192649D+00	DISEXT=	0.4628891289D+01	DISSUM=	0.8923961185D+00		
PCTM=	0.6307477609D+00	PCTF=	0.3692522391D+00						

MATERIAL AND FLUID TEMPERATURE DISTRIBUTION PRIOR TO START OF DISCHARGE PERIOD.

0.0	0.882867D-02	0.2460690-01	0.4884810-01	0.8197330-01	0.1241790+00	0.1755860+00	0.2356780+00	0.298415D+00
0.2621370+00	0.3079210+00	0.3705760+00	0.4501000+00	0.5464030+00	0.6565710+00	0.7735980+00	0.8855710+00	0.9758240+00
0.2492590+00	0.2903680+00	0.3482620+00	0.4230470+00	0.5154360+00	0.6236900+00	0.7421990+00	0.8601220+00	0.9572710+00
0.2383660+00	0.2754860+00	0.3292020+00	0.3997500+00	0.4885320+00	0.5948370+00	0.7143190+00	0.8371560+00	0.9401670+00
0.2293470+00	0.2631370+00	0.3132820+00	0.3801540+00	0.4657290+00	0.5701710+00	0.6902410+00	0.8173510+00	0.9249280+00
0.2221030+00	0.2532020+00	0.3004010+00	0.3642050+00	0.4470490+00	0.5498200+00	0.6702080+00	0.8001340+00	0.9119230+00
0.2165540+00	0.2455810+00	0.2904750+00	0.3518550+00	0.4325090+00	0.5338880+00	0.6544190+00	0.7866820+00	0.9014670+00
0.2126370+00	0.2401940+00	0.2834360+00	0.3430640+00	0.4221190+00	0.5224530+00	0.6430300+00	0.7769140+00	0.8938130+00
0.2103050+00	0.2369850+00	0.2792320+00	0.3378020+00	0.4158830+00	0.5155700+00	0.6361520+00	0.7709890+00	0.8891450+00
0.2095300+00	0.2359190+00	0.2778340+00	0.3360500+00	0.4138040+00	0.5132720+00	0.6338520+00	0.7690040+00	0.8875770+00

TIME STEP	ENTROPY GENERATION TERMS MATERIAL	FLUID	EXT FLD	TOTAL	AVG MATERIAL TEMPERATURE	EXITING FLUID TEMPERATURE
1	0.1492637049D+00	0.3661799143D+00	0.4326412025D+01	0.5154436193D+00	0.4924265639D+00	0.8608003036D+00
2	0.1734127990D+00	0.2999559834D+00	0.4020801241D+01	0.4733687824D+00	0.4823948254D+00	0.8202195945D+00
3	0.2142583915D+00	0.2713913028D+00	0.3810326343D+01	0.4856496942D+00	0.4728240531D+00	0.7918261334D+00
4	0.2541164324D+00	0.2533047316D+00	0.3645297394D+01	0.5074211640D+00	0.4635543389D+00	0.7692855080D+00
5	0.2873119611D+00	0.2401340162D+00	0.3508691982D+01	0.5274597730D+00	0.4545329210D+00	0.7504287670D+00
6	0.3113703505D+00	0.2299266103D+00	0.3393662202D+01	0.5412969608D+00	0.4457691096D+00	0.7344022847D+00
7	0.3285276995D+00	0.2214257358D+00	0.3290722301D+01	0.5499534353D+00	0.4371872699D+00	0.7199392364D+00
8	0.3395976692D+00	0.2141145058D+00	0.3197120855D+01	0.5537121750D+00	0.4287722169D+00	0.7066841469D+00
9	0.3458343865D+00	0.2076540838D+00	0.3110575479D+01	0.5534884703D+00	0.4205128489D+00	0.6943599210D+00
10	0.3484249632D+00	0.2018213704D+00	0.3029406295D+01	0.5502463335D+00	0.4124007870D+00	0.6826707946D+00
11	0.3483521649D+00	0.1964658479D+00	0.2952399870D+01	0.5448180129D+00	0.4044295615D+00	0.6715254254D+00
12	0.3449201823D+00	0.1916507570D+00	0.2881469850D+01	0.5365709393D+00	0.3966456872D+00	0.6611892302D+00
13	0.3409947115D+00	0.1870511995D+00	0.2811846624D+01	0.5280459109D+00	0.3889905096D+00	0.6509753498D+00
14	0.3364792471D+00	0.1826699479D+00	0.2743948853D+01	0.5191491950D+00	0.3814605163D+00	0.6409470993D+00
15	0.3315127853D+00	0.1784826652D+00	0.2677689486D+01	0.5099954504D+00	0.3740531481D+00	0.6310940992D+00
16	0.3262423957D+00	0.1744654546D+00	0.2612924896D+01	0.5007078502D+00	0.3667662008D+00	0.6213972151D+00
17	0.3207849820D+00	0.1705983111D+00	0.2549529265D+01	0.4913832930D+00	0.3595976826D+00	0.6118395054D+00
18	0.3152263262D+00	0.1668648764D+00	0.2487403716D+01	0.4820912026D+00	0.3525457542D+00	0.6024376873D+00
19	0.3096271521D+00	0.1632517085D+00	0.2426472970D+01	0.4728788606D+00	0.3456086935D+00	0.5930917471D+00
20	0.3040294639D+00	0.1597476226D+00	0.2366680180D+01	0.4637770865D+00	0.3387848700D+00	0.5838842606D+00
21	0.2984617261D+00	0.1563431807D+00	0.2307982327D+01	0.4548049068D+00	0.3320727268D+00	0.5747797624D+00
22	0.2929427811D+00	0.1530303110D+00	0.2250346568D+01	0.4459730921D+00	0.3254707669D+00	0.5657742458D+00
23	0.2874871060D+00	0.1498020285D+00	0.2193747476D+01	0.4372867391D+00	0.3189775425D+00	0.5568647774D+00
24	0.2820948927D+00	0.1466522282D+00	0.2138164991D+01	0.4287471209D+00	0.3125916472D+00	0.5480492119D+00
25	0.2767774635D+00	0.1435755310D+00	0.2083582925D+01	0.4203529945D+00	0.3063117093D+00	0.5393259796D+00
26	0.2715343516D+00	0.1405671673D+00	0.2029987861D+01	0.4121015189D+00	0.3001363871D+00	0.5306939316D+00
27	0.2663660047D+00	0.1376228873D+00	0.1977368363D+01	0.4039888920D+00	0.2940643649D+00	0.5221522258D+00
28	0.2612719001D+00	0.1347388909D+00	0.1925714389D+01	0.3960107911D+00	0.2880943496D+00	0.5137002434D+00
29	0.2562508999D+00	0.1319117719D+00	0.1875016878D+01	0.3881626718D+00	0.2822250684D+00	0.5053375287D+00
30	0.2513014982D+00	0.1291384721D+00	0.1825267432D+01	0.3804399702D+00	0.2764552662D+00	0.4970637433D+00
31	0.2464219913D+00	0.1264162436D+00	0.1776458104D+01	0.3728382349D+00	0.2707837041D+00	0.4888786342D+00
32	0.2416105948D+00	0.1237426171D+00	0.1728581225D+01	0.3653532119D+00	0.2652091580D+00	0.4807820090D+00
33	0.2368655217D+00	0.1211153740D+00	0.1681629286D+01	0.3579808956D+00	0.2597304169D+00	0.4727737179D+00
34	0.2321850345D+00	0.1185325225D+00	0.1635594852D+01	0.3507175570D+00	0.2543462822D+00	0.4648536408D+00
35	0.2275674789D+00	0.1159922768D+00	0.1590470495D+01	0.3435597556D+00	0.2490555664D+00	0.4570216765D+00
36	0.2230113041D+00	0.1134930376D+00	0.1546248743D+01	0.3365043418D+00	0.2438570927D+00	0.4492777355D+00
37	0.2185150742D+00	0.1110333757D+00	0.1502922048D+01	0.3295484500D+00	0.2387496938D+00	0.4416217341D+00
38	0.2140774733D+00	0.1086120160D+00	0.1460482757D+01	0.3226894893D+00	0.2337322118D+00	0.4340535896D+00
39	0.2096973060D+00	0.1062278235D+00	0.1418923089D+01	0.3159251295D+00	0.2288034974D+00	0.4265732171D+00

40	0.20537349570+00	0.10387979080+00	0.13782351270+01	0.30925328650+00	0.22396240940+00	0.41918052600+00
41	0.20110508000+00	0.10156702560+00	0.13384108000+01	0.30267210560+00	0.21920781450+00	0.41187541850+00
42	0.19689120540+00	0.99288740360-01	0.12994418790+01	0.29617994580+00	0.21453858680+00	0.40465778700+00
43	0.19273112140+00	0.97044241670-01	0.12613199710+01	0.28977536300+00	0.20995360770+00	0.39752751270+00
44	0.18862417280+00	0.94832921350-01	0.12240365160+01	0.28345709420+00	0.20545176550+00	0.39048446460+00
45	0.18456979400+00	0.92654247620-01	0.11875827820+01	0.27722404160+00	0.20103195530+00	0.38352849810+00
46	0.18056750100+00	0.90507757220-01	0.11519498710+01	0.27107525820+00	0.19669307880+00	0.37665945390+00
47	0.17521397880+00	0.88560305310-01	0.11196467030+01	0.26377428410+00	0.19248361100+00	0.37036998220+00
48	0.17066712360+00	0.86573175210-01	0.10870018240+01	0.25724029880+00	0.18835200960+00	0.36395101220+00
49	0.16649187550+00	0.84588672040-01	0.10547008490+01	0.25108054750+00	0.18429593110+00	0.35753451190+00
50	0.16253385460+00	0.82619781280-01	0.10229456870+01	0.24515363590+00	0.18031416900+00	0.35116033060+00
51	0.15872413210+00	0.80671860630-01	0.99181457930+00	0.23939599270+00	0.17640572780+00	0.34484467650+00
52	0.15502619240+00	0.78747647190-01	0.96134346160+00	0.23377383960+00	0.17256965000+00	0.33859593780+00
53	0.15141837470+00	0.76848739600-01	0.93154974090+00	0.22826711430+00	0.16880498140+00	0.33241890500+00
54	0.14788690420+00	0.74976147760-01	0.90244109320+00	0.22286305200+00	0.16511076420+00	0.32631658330+00
55	0.14442265580+00	0.73130538310-01	0.87401941500+00	0.21755319420+00	0.16148603780+00	0.32029090230+00
56	0.14101944460+00	0.71312361300-01	0.84628288620+00	0.21233180590+00	0.15792983990+00	0.31434310220+00
57	0.13767302810+00	0.69521923100-01	0.81922717490+00	0.20719495120+00	0.15444120840+00	0.30847395370+00
58	0.13438048240+00	0.67759431710-01	0.79284619740+00	0.20213991410+00	0.15101918300+00	0.30268389880+00
59	0.13113979110+00	0.66025026200-01	0.76713262370+00	0.19716481730+00	0.14766280630+00	0.29697314420+00

MATERIAL AND FLUID TEMPERATURE DISTRIBUTION AT END OF DISCHARGE PERIOD.

0.0	0.8608800-02	0.2416340-01	0.4820450-01	0.8115790-01	0.1232090+00	0.1744660+00	0.2343990+00	0.2969730+00
0.2038050-02	0.1242880-01	0.3100580-01	0.5837270-01	0.9475290-01	0.1402890+00	0.1950640+00	0.2582110+00	0.3208330+00
0.3598710-02	0.1530050-01	0.3608190-01	0.6584840-01	0.1046820+00	0.1527010+00	0.2099780+00	0.2753920+00	0.3379480+00
0.5032500-02	0.1789620-01	0.4062270-01	0.7249110-01	0.1134610+00	0.1636380+00	0.2230860+00	0.2904580+00	0.3529530+00
0.6306310-02	0.2017170-01	0.4456910-01	0.7823180-01	0.1210180+00	0.1730240+00	0.2343110+00	0.3033320+00	0.3657750+00
0.7390830-02	0.2208850-01	0.4786990-01	0.8301130-01	0.1272880+00	0.1807930+00	0.2435850+00	0.3139530+00	0.3763520+00
0.8261190-02	0.2361410-01	0.5048230-01	0.8678030-01	0.1322190+00	0.1868920+00	0.2508560+00	0.3222670+00	0.3846320+00
0.8897470-02	0.2472250-01	0.5237280-01	0.8950030-01	0.1357710+00	0.1912780+00	0.2560790+00	0.3282350+00	0.3905740+00
0.9285140-02	0.2539520-01	0.5351690-01	0.9114340-01	0.1379140+00	0.1939220+00	0.2592250+00	0.3318280+00	0.3941520+00
0.9415360-02	0.2562070-01	0.5389990-01	0.9169300-01	0.1386300+00	0.1948050+00	0.2602760+00	0.3330270+00	0.3953460+00

FIGURE OF MERIT SUMMARY

PRS AVL, STORAGE= 0.29d5923596D-02 PRS AVL, DISCHARGE= 0.29226768850-02
TMP AVL, STORAGE= 0.75700531040+01 TMP AVL, DISCHARGE= 0.0
ALPHA= 0.78052298970-03 NSUBS= 0.34387319240+00 1ST LAW COMP= 0.41565979120+00

```
SECOND LAW OPTIMIZATION OF A SENSIBLE HEAT STORAGE DEVICE

NUMBER OF VARIABLES IS      3

NUMBER OF ROWS IS      1

CEILING ON HESSIAN IS      3

CEILING ON BINDING CONSTRAINTS IS      1

ACTUAL LENGTH OF Z ARRAY IS      79
BOU
 R     1    1 1.0000000D+02 9.0000000D+03
 R     2    2 1.0000000D+02 1.0000000D+04
 R     3    3 5.0000000D+01 1.0000000D+03
END
INI
TOG
  4.00000000D+02  4.00000000D+02  7.00000000D+02
END
VAR
GPLSS          1
BIS            2
FNUM           3
END
ROWS
 G    1
END
FUN
NSUBS          1
END
PRI
IPR      4
PN4     -1
END
LIM
NST      3
END
EPS
EPT       0.1000000D-03
END
MET
FUC
END
GO

EPNEWT =  1.0000D-04  EPINIT =  1.0000D-04  EPSTOP =  1.0000D-04  EPPIV =  1.0000D-03  PHIEPS = 0.0

NSTEP =     3  ITLIM =    10  LIMSER =      10000

IPR =     4  PN4 =    -1  PN5 =     0  PN6 =     0  PER =     0  DUMP =     0

TANGENT VECTORS WILL BE USED FOR INITIAL ESTIMATES OF BASIC VARIABLES

THE FINITE DIFFERENCE PARSH USING CENTRAL DIFFERENCES WILL BE USED

OBJECTIVE FUNCTION WILL BE MINIMIZED.
```

```
GRAD ARRAY IS

FOR GI  II
 -2.33462E-04 -4.25184E-05  1.03375E-04
INBV IS    1   2   3
IUB IS     0   0   0
REDUCED GRADIENT IS
 -2.33461746D-04 -4.25184408D-05  1.03374579D-04

ITERATION  OBJECTIVE    NO.BINDING  NO.SUPER-     NUMBER      NORM RED.     HESSIAN    HESSIAN              DEGENERATE
  NUMBER     FUNCTION   CONSTRAINTS   BASICS     INFEASIBLE   GRADIENT    CONDITION   UPDATE     STEPSIZE     STEP
     0      9.2081250-01       0           3           0       2.335D-04   1.0000+00     F        0.0
G IS
  1 9.2081249D-01
X IS
  1 4.0000000D+02       2 4.0000000D+02       3 7.0000000D+02
CHOLESKY FACTOR OF HESSIAN RESET TO I.
DIRECTION VECTOR IS
  2.334620-04  4.25184D-05 -1.03375D-04
       A              B              C                    FA             FB             FC                    D
0.2741350+07 0.5482700+07 0.6287810+07              0.6394667D+00 0.3444596D+00 0.3821637D+00             0.5347576D+07
              QUADRATIC INTERPOLATION

ITERATION  OBJECTIVE    NO.BINDING  NO.SUPER-     NUMBER      NORM RED.     HESSIAN    HESSIAN              DEGENERATE
  NUMBER     FUNCTION   CONSTRAINTS   BASICS     INFEASIBLE   GRADIENT    CONDITION   UPDATE     STEPSIZE     STEP
     1      3.4416030-01       0           3           0       2.335D-04   1.0000+00     F        5.3480+06
G IS
  1 3.4416026D-01
X IS
  1 1.6484544D+03       2 6.2737059D+02       3 1.4719658D+02
INBV IS    1   2   3
IUB IS     0   0   0
REDUCED GRADIENT IS
 -1.012821740-04 -6.935586080-05  8.846733540-05
DIRECTION VECTOR IS
  1.502250+03  2.735920+02 -6.651810+02
       A              B              C                    FA             FB             FC                    D
0.0            0.1106440-01 0.2212880-01              0.3441603D+00 0.3438732D+00 0.3442954D+00             0.1001023D-01
              QUADRATIC INTERPOLATION

ITERATION  OBJECTIVE    NO.BINDING  NO.SUPER-     NUMBER      NORM RED.     HESSIAN    HESSIAN              DEGENERATE
  NUMBER     FUNCTION   CONSTRAINTS   BASICS     INFEASIBLE   GRADIENT    CONDITION   UPDATE     STEPSIZE     STEP
     2      3.4387320-01       0           3           0       1.013D-04   1.607D+06     T        1.1060-02
G IS
  1 3.4387319D-01
X IS
  1 1.6650759D+03       2 6.3039773D+02       3 1.3983675D+02
INBV IS    1   2   3
IUB IS     0   0   0
REDUCED GRADIENT IS
 -9.371305350-05 -8.655538840-05  3.651154110-05

TERMINATION CRITERION MET.  KUHN-TUCKER CONDITIONS SATISFIED TO WITHIN  1.000000-04 AT CURRENT POINT
```

OUTPUT OF INITIAL VALUES

SECOND LAW OPTIMIZATION OF A SENSIBLE HEAT STORAGE DEVICE

SECTION 1 -- CONSTRAINTS

NO.	CONSTRAINT NAME	STATUS	TYPE	INITIAL VALUE	LOWER LIMIT	UPPER LIMIT
1	NSUBS		OBJ	9.20812490-01		

SECTION 2 -- VARIABLES

NO.	VARIABLE NAME	STATUS	INITIAL VALUE	LOWER LIMIT	UPPER LIMIT
1	SPLSS		4.00000300+02	1.00000000+02	9.00000000+03
2	DIS		4.00000000+02	1.00000000+02	1.00000000+04
3	FNUM		7.00000000+02	5.00000000+01	1.00000000+03

FINAL RESULTS

SECOND LAW OPTIMIZATION OF A SENSIBLE HEAT STORAGE DEVICE

SECTION 1 -- CONSTRAINTS

NO.	NAME	INITIAL VALUE	FINAL VALUE	STATUS	DISTANCE FROM NEAREST BOUND	LAGRANGE MULTIPLIER
1	NSUBS	9.20812D-01	3.43873D-01	OBJ		

SECTION 2 -- VARIABLES

NO.	NAME	INITIAL VALUE	FINAL VALUE	STATUS	DISTANCE FROM NEAREST BOUND	REDUCED GRADIENT
1	DPLSS	4.000000D+02	1.66508D+03	SUPBASIC	1.565D+03:L	-9.37131D-05
2	DIS	4.000000D+02	6.30398D+02	SUPBASIC	5.304D+02:L	-8.65554D-05
3	FNUM	7.000000D+02	1.39837D+02	SUPBASIC	8.984D+01:L	3.65115D-05

SECOND LAW OPTIMIZATION OF A SENSIBLE HEAT STORAGE DEVICE

RUN STATISTICS

NUMBER OF ONE-DIMENSIONAL SEARCHES = 2

NEWTON CALLS = 0 NEWTON ITERATIONS = 0 AVERAGE = 0.0

FUNCTION CALLS = 13 GRADIENT CALLS = 3 ACTUAL FUNCTION CALLS (INC. FOR GRADIENT) = 31

NUMBER OF TIMES BASIC VARIABLE VIOLATED A BOUND = 0

NUMBER OF TIMES NEWTON FAILED TO CONVERGE = 0

TIMES STEPSIZE CUT BACK DUE TO NEWTON FAILURE = 0

APPENDIX B

DEVELOPMENT OF DISCRETIZED TRANSIENT CONDUCTION EQUATIONS FOR THE STORAGE ELEMENT

This appendix explains the steps that were taken to enable ENTROP to define the individual terms of the discretized material conduction equation coefficient matrix at run time and as a function of the number of material nodes.

First, it is necessary to define a consistent coordinate system and nodal numbering sequence. The one developed for this study is illustrated in Figure B.1. It has the standard "i" and "j" axis designation and a numbering system that gives each node a unique number. Figure B.1 shows a 4x7 network but the mathematical relationships developed are valid for any size system. If we define the number of nodes in the X direction as m and the number of nodes in the Y direction as n, the following characteristics of the nodal system shown in Figure B.1 can be noted:

a. the node number for any given (i,j) node can be uniquely defined as [i+(j-1)*n],

b. the node directly above any given (i,j) node can be defined as (i+1,j) and has a unique number given by [(i+1)+(j-1)*n],

c. the node directly below it can be defined as (i-1,j) and has a unique number given by [(i-1)+(j-1)*n],

d. the one to its right can be defined as (i,j+1) and has a unique number given by [i+j*n], and

e. the one to its left can be defined as (i,j-1) and has a unique number given by [i+(j-2)*n].

The coefficient matrix that results from this nodal network has certain characteristics that are also of interest. The first of these

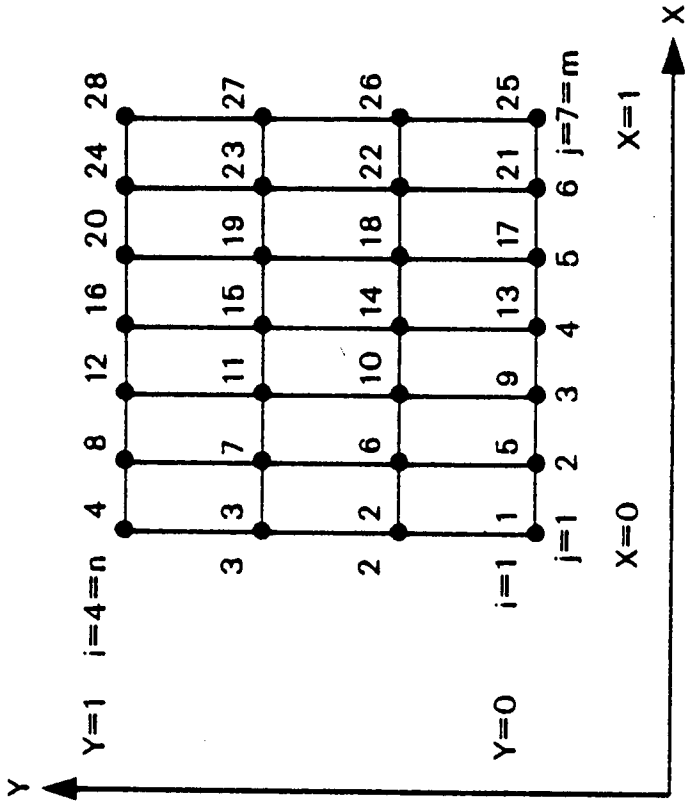


Figure B.1. Illustration of the coordinate system and nodal numbering sequence used in the discretization of the material conduction equation.

is that the matrix is square with an order equal to nxm. Therefore the sample 4x7 arrangement shown in Figure B.1 would result in a 28x28 coefficient matrix. In addition, each row of the matrix would represent a particular material node and the entries in that row would represent either the particular node or one of its neighbors. This matrix would also have a unique physical appearance. The non-zero coefficients would be arranged in a band centered around the main diagonal. These traits are illustrated in Figure B.2 and the "x's" represent the non-zero coefficients. This figure shows a very important characteristic of this type of coefficient matrix; that is the upper and lower band widths are equal to the number of material nodes in the "i" direction.

To understand the requirement that we must be able to define each individual term in the coefficient matrix, it is necessary to examine the instruction string provided with subroutines DGBFA and DGBSL to load their working matrix. It is:

```
M = ML + MU
DO 20 I = 1,N
I1 = MAXO (1,I - MU)
I2 = MINO (N,I + ML)
DO 20 J = I1,I2
K = J - I + M
20 ABD (K,I) = A(J,I)
```

where:

ML = Band width below the main diagonal

MU = Band width above the main diagonal

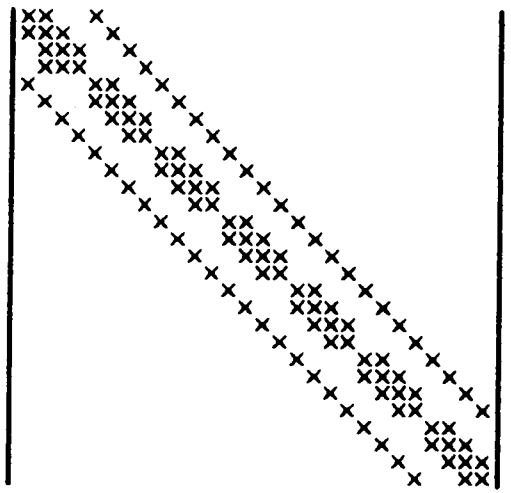


Figure B.2. Illustration of the form of a typical coefficient matrix for discretized flat slab conduction equations.

N = Size of the original, large, sparse coefficient matrix, A, and is equal to nxm

ABD = DGBFA's working matrix

The purpose of this instruction string is quite simple. Using the total number of nodes plus the upper and lower band width of the original sparse matrix, it skips over the zero entries and "reads" only the non-zero entries of each row. The "I" counter on the outer loop causes it to look at each row of the original matrix and represents the unique number of a particular material node. The "J" counter on the inner loop represents the unique numbers of the neighbor nodes, that is the neighbors of the node represented by "I". Therefore once the instruction string has defined a particular element, (i.e., an "I" and "J") it "reads" the value of that element from the original sparse, coefficient matrix into DGBFA's working matrix. The operation of this instruction string can best be illustrated by calculating the "I", "I1", and "I2" counters for a few iterations and then comparing them to the example coefficient matrix in Figure B.2. The results of these few iterations, using the nodal network in Figure B.1, are shown in Table B.1.

The problem that results is that both the original sparse, coefficient matrix and the working matrix have to be defined. This is undesirable because even moderate sized nodal systems require large amounts of computer memory. To solve this problem it was necessary to incorporate the ability to calculate a coefficient array element given any "I", "J" pair. The steps taken to develop this capability are described below.

Table B.1. Partial summary of the operation of the original instruction string to read the banded matrix

Outer loop counter	Inner loop counter	
	I1	I2
1	1	5
2	1	6
3	1	7
4	1	8
5	1	9
6	2	10
7	3	11
8	4	12
.	.	.
.	.	.
23	19	27
24	20	28
25	21	28
26	22	28
27	23	28
28	24	28

The key to providing this capability is to have a discretized conduction equation with a uniform physical construction that is applicable to every type of node. The most general form of a discretized, fully implicit, transient conduction equation for any particular (i,j) node in the system shown in Figure B.1 is:

$$-\left(\theta_{i,j}^{n} + C1\right) = C2\theta_{i,j-1}^{n+1} + C3\theta_{i,j+1}^{n+1} + C4\theta_{i-1,j}^{n+1} + C5\theta_{i+1,j}^{n+1} - C6\theta_{i,j}^{n+1} \tag{B.1}$$

As can be seen, equation (B.1) contains a total of six terms, each with a leading coefficient or associated constant. The six terms are:

a. the temperature of the (i,j) node for the next time period,

b. the current temperature of the (i,j) node, and

c. the current temperatures of the four neighbor nodes.

The value of a leading coefficient or associated constant is a function of the physical location of the particular (i,j) node within the system, its neighbor nodes, and the boundary conditions. For the system under study, there are nine different types of nodes. They are:

a. the interior nodes,

b. the corner node located at i=1 and j=1,

c. the nodes on the X=0 face but not at a corner;

that is j=n, i>2, and i<n,

d. the corner node located at i=n and j=1,

e. the nodes on the Y=1 face but not at a corner;

that is i=n, j>2, and j<m,

f. the corner node located at i=n and j=m,

g. the nodes on the X=1 face but not at a corner;

that is j=m, i>2, and i<n,

h. the corner node located at i=1 and j=m, and

i. the nodes on the Y=0 face but not at a corner;

that is i=1, j>2, and j<m.

The leading coefficients and constants for each of the six terms in the most general equation form and for each of the nine nodes were computed and are summarized in Table B.2. The actual algebra is quite straightforward but very long and involved and will not be repeated here for the sake of brevity. The reader is invited to read reference [52] for details.

With this information, it is now a fairly simple operation to define any given coefficient array element and this procedure is summarized as follows:

a. Given the value of the "I" counter and therefore the unique number of a node; determine it's (i,j) location.

b. Based on the (i,j) location; determine which one of the nine types of nodes is represented.

c. Using the value of the "J" counter; determine which neighbor node is represented.

d. Finally, with the particular type of node and neighbor identified, pick the appropriate coefficient from Table B.2.

This coefficient is then loaded directly into DGBFA's working array in the location desired by DGBFA.

Table B.2. Summary of coefficients and associated constants for discretized, non-dimensionalized material conduction equations

Nodal location	C1		C2	C3	C4	C5	C6	
	During dwell period	With convective boundary					During dwell period	With convective boundary
(1,1) corner	0	0	0	$2B1^a$	0	$2B2^b$	$-[1 + 2B1 + 2B2]$	$-[1 + 2B1 + 2B2]$
X=0 face	0	0	0	2B1	B2	B2	$-[1 + 2B1 + 2B2]$	$-[1 + 2B1 + 2B2]$
(n,1) corner	0	$2B2Bi\Delta Y\theta_f^{n+1}$	0	2B1	2B2	0	$-[1 + 2B1 + 2B2]$	$-[1 + 2B1 + 2B2 (1 + Bi\Delta Y)]$
Y=1 face	0	$2B2Bi\Delta Y\theta_f^{n+1}$	B1	B1	2B2	0	$-[1 + 2B1 + 2B2]$	$-[1 + 2B1 + 2B2 (1 + Bi\Delta Y)]$
(n,m) corner	0	$2B2Bi\Delta Y\theta_f^{n+1}$	2B1	0	2B2	0	$-[1 + 2B1 + 2B2]$	$-[1 + 2B1 + 2B2 (1 + Bi\Delta Y)]$
X=1 face	0	0	2B1	0	B2	B2	$-[1 + 2B1 + 2B2]$	$-[1 + 2B1 + 2B2]$
(1,m) corner	0	0	2B1	0	0	2B2	$-[1 + 2B1 + 2B2]$	$-[1 + 2B1 + 2B2]$
Y=0 face	0	0	B1	B1	0	2B2	$-[1 + 2B1 + 2B2]$	$-[1 + 2B1 + 2B2]$
Interior	0	0	B1	B1	B2	B2	$-[1 + 2B1 + 2B2]$	$-[1 + 2B1 + 2B2]$

$$a_{B1} = \frac{\Delta Fo V^{+2}}{\Delta X^2}$$

$$b_{B2} = \frac{\Delta Fo}{\Delta Y^2}$$

APPENDIX C

DESCRIPTION OF MODIFICATIONS TO PERMIT INTEGRATION OF DISCRETE VALUES

The following information summarizes the modifications that were made to the Simpson's One-Third Rule algorithm to permit integration of discrete data points instead of continuous functions. One- and two-dimensional numerical integrations were required at several locations within ENTROP, and it was decided that it would be more accurate to use the discrete points rather than a curve fit of the discrete points.

For a one-dimensional integration, the reader will recall that the traditional procedure has the following preliminary steps:

a. define a continuous function, F, and the limits of integration, A to B,

b. define the number of divisions, D, that the continuous function is to be divided into,

c. using the limits of integration and the number of divisions, calculate the length, H, of each division using the relationship (B-A)/D, and finally

d. divide the number of divisions by two to determine the number of "groups of three evaluations" in the interval from A to B.

The actual integration of the continuous function is accomplished using this information and the following instructional string:

```
      X1=A
      NUM=DIV/2.0
      SUM=0.0
      DO 100 I=1,NUM
      SUM=SUM+H/3.*[F(X1)+4.*F(X1+H)+F(X1+2.*H)]
100   X1=X1+2.*H
```

The numerical integration proceeds as the value of the X1 variable is incremented and continues until all the "groups of three evaluations" have been processed.

To modify this string to use discrete values, we first do the following:

a. define some number of discrete nodes in the interval from A to B as M, and specify an odd number of nodes,

b. define a single dimensioned array, Y, that contains the values at each node,

c. realize that the interval between nodes, dX, is the same as the length interval, H, used in the traditional technique, and

d. realize that for these definitions, the number of "groups of three nodes" is equal to (M-1)/2.

An illustration of this physical system is shown in Figure C.1 and shows the original interval from A to B discretized with seven nodes. Using these definitions we can rewrite the traditional instructional string as follows:

```
      NUM = (M-1)/2.0
      N1=1
      SUM=0.0
      DO 100 I=1,NUM
      N2=N1+1
      N3=N2+1
      SUM=SUM+[(dX)/3.]*[Y(N1)+4.*Y(N2)+Y(N3)]
100   N1=N3
```

This modified sequence then steps through the discrete points in the same order (i.e., the same "groups of three nodes") as the traditional procedure. The N1, N2, and N3 counters, which are redefined for each increment of the do-loop, specify the points being processed. The numerical integration is complete when the last "group of three" has

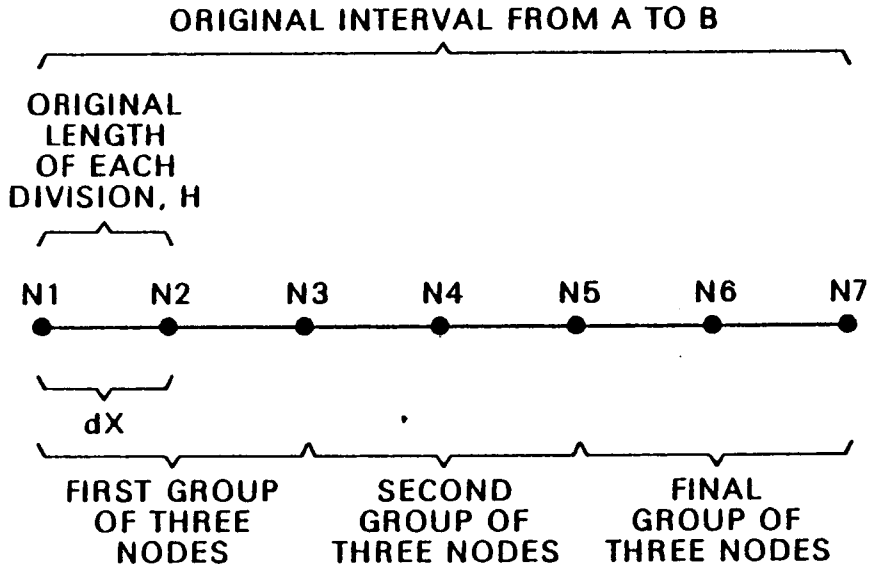


Figure C.1. Illustration of the physical system used to permit the one-dimensional integration of discrete values.

been processed. This modified string was programmed and installed in the ENTROP program as the subroutine ONEDIM.

A two-dimensional integration using the traditional one-third rule proceeds in a similar manner. The only difference is that for each "group of three evaluations" in the X direction, it must also evaluate all the "groups of three evaluations" in the Y direction. The primary difficulty in implementing such a procedure is defining a method to keep track of which node numbers are being processed at any given time. In a one-dimensional system, the node numbers proceeded in order; that is N1, N2, N3, then N3, N4, and N5 until the last "group of three" has been processed. In a two-dimensional system, the node numbers in a given direction are not sequential. This is due to the numbering sequence used to identify nodes. The reader can review this sequence by referring to Figure B.1 (p. 217). Before discussing the specific modifications that were made, it is necessary to briefy summarize the traditional two-dimensional integration procedure.

The two-dimensional, one-third rule algorithm requires the same types of information as its one-dimensional counterpart. It must have limits of integration and interval lengths for both the X and Y direction. The running total, that is the result of the integration, is also similar except that it sums nine values instead of three and has the following form:

```
SUM=SUM+(HX*HY/9.)*(F1+F3+F7+F9+4.*(F2+F4+F6+F8)+16.*F5.)    (C.1)
```

The nine "F's" in equation (C.1) represent values of the continuous function at specific X and Y coordinate points. To define these function values, assume that the integration process has just begun. The current X and Y values would be the respective lower limits of integration. Designating these initial values as X1 and Y1 and defining HX and HY as the X and Y interval lengths, we define the following qualitative relationships for the nine function values:

```
F1=F(X1,Y1), F2=F(X2,Y1), F3=F(X3,Y1)
F4=F(X1,Y2), F5=F(X2,Y2), F6=F(X3,Y2)                    (C.2)
F7=F(X1,Y3), F8=F(X2,Y3), F9=F(X3,Y3),
```

where:

```
X2=X1+HX, X3=X1+2.*HX, Y2=Y1+HY, Y3=Y1=2.*HY.            (C.3)
```

These geometric relationships are illustrated for a hypothetical problem in Figure C.2. As in the one-dimensional case, the numerical integration proceeds by summing the function evaluations for given initial values of X1 and Y1 then incrementing their value until all the "groups of three evaluations" have been processed. The only difference is that for <u>each</u> X "group of three evaluations", <u>all</u> the Y "evaluations" have to be performed before moving on to the next X "group of three evaluations."

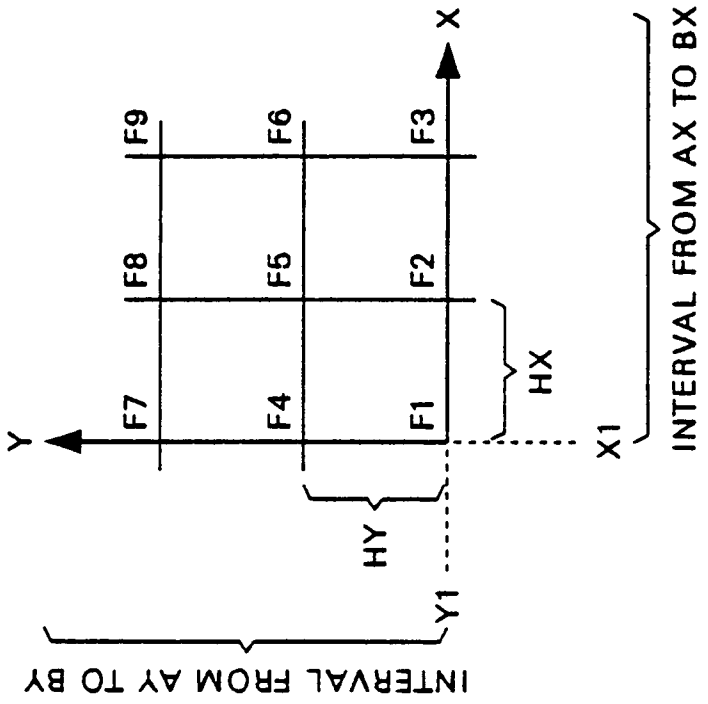


Figure C.2. Illustration of the physical system used by Simpson's one third rule for two-dimensional integration.

To modify these relationships to accommodate discrete points, it only necessary to realize two facts. These are:

a. that the X and Y coordinate positions, that is the X1, X2, . ., XM and the Y1, Y2, . ., YN values, also represent the (i,j) coordinates of the material nodes, and

b. the (X,Y) coordinates can therefore be used to define a unique node number using the relationship developed in Appendix B.

With this information, a straightforward computing scheme can be defined to permit the integration of discrete values. This scheme can be best explained using the logic diagram in Figure C.3. This diagram was prepared by:

a. assuming an odd number of material nodes in the X and Y direction,

b. using the same coordinate system and nodal numbering sequence as shown in Figure B.1 (p. 217), and

c. assuming that the function values to be integrated are contained in a single subscripted array, T(B); where B represents a unique nodal number.

The steps outlined in Figure C.3 were programmed and installed in the ENTROP program as the subroutine TWODIM.

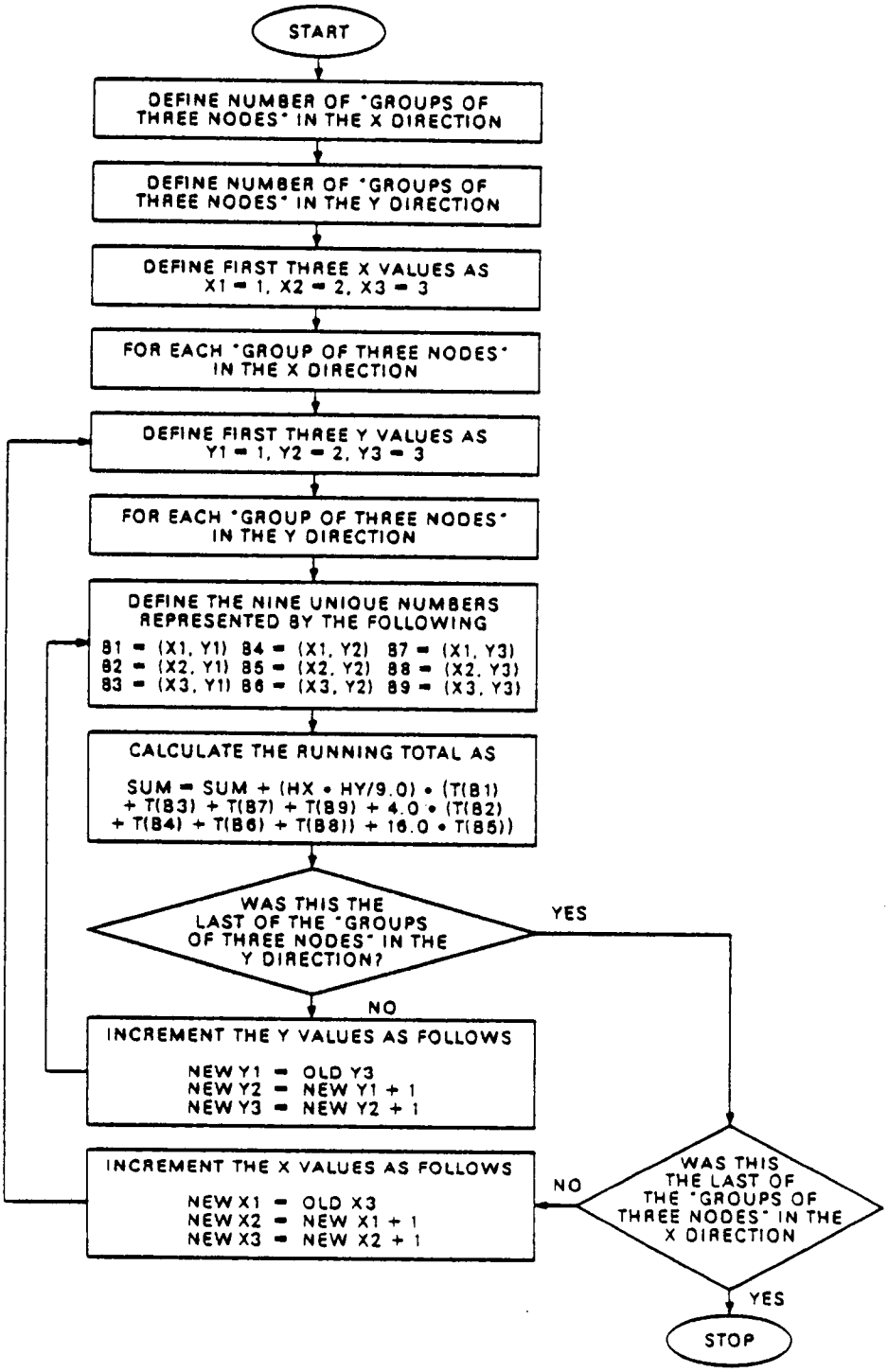


Figure C.3. Schematic representation of the calculating sequence used to perform two-dimensional integration of discrete values.

APPENDIX D

VERIFICATION OF TWO CRITICAL CALCULATIONS PERFORMED BY THE ENTROP COMPUTER PROGRAM

This appendix summarizes the steps that were taken to verify two critical calculations of the ENTROP computer program: the storage material transient temperature distributions and the figure of merit, N_c. To verify that ENTROP was correctly calculating storage material transient temperatures, a comparison was made with a simplified storage system example problem contained in Schmidt and Willmott's [21] text. The ability of the ENTROP computer program to accurately calculate a value for the figure of merit was verified by having it duplicate a design case that had also been evaluated by the computer program Krane used for his lumped storage element study [46].

The accuracy of the storage material two-dimensional transient temperatures as calculated by ENTROP could not be verified directly because similar temperature data was not available with which to make a comparison. Even though Szego [22] published results based on such calculations, actual storage material temperature distributions were not included. Consequently, a comparison had to be made using a one-dimensional storage system example problem from reference [21]. This particular problem was chosen, in part, because it utilized an analytical solution for the storage material transient temperature distribution that had been non-dimensionalized with many of the same variables utilized in this study. This problem described the situation where the fluid was assumed to have an infinite heat capacity (i.e., constant temperature along the flow channel) and the temperature gradients within the storage material were not negligible. The one-dimensional material temperature distribution for these conditions can be written as:

$$\theta_m = 1.0 - \sum_{j=1}^{\infty} 2 \frac{\sin M_j}{(\sin M_j \cos M_j + M_j)} \exp\left[-(M_j^2) F_o\right] \cos (M_j Y) \qquad (D.1a)$$

where:

$$\theta_m = \frac{T_{m,o} - T_\infty}{T_{f,i} - T_\infty} \qquad (D.1b)$$

and

$$M_j \tan M_j = Bi \ . \qquad (D.1c)$$

It should be noted that equation (D.1) utilizes a dimensionless temperature different from the one used in this study. This is mentioned here because it somewhat complicated the verification procedure.

Comparing ENTROP's two-dimensional temperature distribution against a one-dimensional distribution was possible only because a small value for the storage material aspect ratio, V^+ could be specified. This is the ratio of the half-thickness of a section of storage material to its length and small values minimize the effects of longitudinal conduction. Therefore, once a two-dimensional distribution for a storage unit with a small value of V^+ had been calculated, it was reasonable to interpret it as a group of individual one-dimensional distributions. Each of these groups could then be compared to the one-dimensional distribution calculated by equation (D.1).

A computer program was written to solve equation (D.1) and together with ENTROP was used to conduct the verification procedure. This sequence proceeded as follows:

a. Values for Bi_s and Fo_s were defined and storage material temperatures at 25 equally spaced points, corresponding to an elapsed time equal to Fo_s, were calculated using equation (D.1).

b. Using the same Bi_s and Fo_s defined above, dividing Fo_s into 99 equal increments, defining values for $T_{f,i,s}/T_\infty$ and $T_{m,o,s}/T_\infty$ defining a value for V^+ as well as the ratio of G_s^+ to V^+, and specifying a specific material-fluid nodal arrangement, ENTROP was made to solve the one-dimensional fluid and two-dimensional storage material temperature distributions for these conditions. This resulted in nine dimensionless fluid temperatures in the longitudinal direction and 25 dimensionless material temperatures through the thickness of the storage material for each of the nine fluid temperatures.

c. One of the nine dimensionless fluid temperature calculated by ENTROP was then converted to its appropriate dimensional value. This value, a dimensional ambient temperature, the dimensional fluid temperature used to define $T_{f,i,s}/T_\infty$, and the dimensional initial material temperature used to define $T_{m,o,s}/T_\infty$ were used to convert the 25 material temperatures calculated by equation (D.1) to their appropriate dimensional value. These dimensional temperatures were in turn non-dimensionalized with the scheme utilized in this study and then compared to the corresponding dimensionless material temperatures calculated by ENTROP.

Step c was actually performed on two of the nine fluid temperatures and the results of these comparisons are summarized in Table D.1. These data show that the agreement between ENTROP and equation (D.1) was on the order of 2.%. Given that approximate two-dimensional temperature distributions were being compared to exact one-dimensional distributions, the agreement was considered excellent and it was concluded that ENTROP was correctly calculating transient material temperature distributions.

It was equally difficult to verify the operation of the ENTROP program for a complete storage-removal cycle. Although individual parts of the program had been verified separately, no data were available to insure that the figure of merit, N_c, was being calculated correctly. Accordingly, it was decided to define a specific set of design parameters and then have both ENTROP and the computer program Krane used for his lumped element study [46] calculate values for lambda, λ, and the figure of merit, N_c. This required a considerable effort that consisted of the following major steps:

a. A hypothetical storage system was defined using air as the flowing fluid and feolite as the storage material. This design utilized feolite and air physical properties, arbitrary values for the storage material half-thickness and length, and a unit width into the paper. The physical design and operating parameters of this system were specified to approximate a lumped element. This was accomplished by specifying small values of Bi_s to approximate a storage material with a very large thermal conductivity, and small values of G_s^+ to minimize the temperature drop in the flowing fluid.

Table D.1 Comparison of storage material temperatures calculated by ENTROP with those calculated by Equation D.1

Dimensionless Y distance	For the dimensionless fluid temperature calculated by ENTROP having a value of			
	0.9982		0.9891	
	ENTROP	Eqn. D.1	ENTROP	Eqn. D.1
0.0000	0.2346	0.2394	0.2321	0.2373
0.0417	0.2346	0.2395	0.2322	0.2373
0.0833	0.2348	0.2397	0.2324	0.2375
0.1250	0.2352	0.2400	0.2327	0.2378
0.1667	0.2356	0.2405	0.2331	0.2383
0.2083	0.2362	0.2410	0.2337	0.2388
0.2500	0.2369	0.2417	0.2344	0.2395
0.2917	0.2377	0.2426	0.2352	0.2404
0.3333	0.2387	0.2435	0.2362	0.2413
0.3750	0.2398	0.2446	0.2373	0.2424
0.4167	0.2410	0.2458	0.2385	0.2436
0.4583	0.2423	0.2471	0.2400	0.2449
0.5000	0.2438	0.2486	0.2412	0.2463
0.5417	0.2454	0.2502	0.2428	0.2479
0.5833	0.2471	0.2519	0.2445	0.2496
0.6250	0.2489	0.2537	0.2463	0.2514
0.6667	0.2509	0.2557	0.2483	0.2534
0.7083	0.2530	0.2578	0.2504	0.2554
0.7500	0.2552	0.2600	0.2526	0.2576
0.7917	0.2576	0.2623	0.2549	0.2599
0.8333	0.2601	0.2648	0.2574	0.2624
0.8750	0.2626	0.2674	0.2600	0.2649
0.9167	0.2654	0.2701	0.2626	0.2676
0.9583	0.2682	0.2729	0.2655	0.2704
1.0000	0.2712	0.2758	0.2684	0.2733

b. Using this hypothetical design, two equivalent sets of dimensionless design variables were defined: one for ENTROP and one for Krane's model.

Both models were run and the values of λ and N_c compared. ENTROP calculated a value for λ of 0.7419×10^{-7} and a value for N_c of 0.9653. Krane's model calculated values of 0.1920×10^{-5} and 0.9980 for λ and N_c respectively. Given that it was not possible to completely simulate a lumped element, the agreement was considered good and it was concluded that ENTROP was correctly calculating values for λ and N_c.

VITA

Michael Taylor was born on June 1, 1947 in Orlando, Florida and lived in coastal central Florida until 1965 when he enlisted in the United States Marine Corps. He served in the Marine Corps from December, 1965 until December, 1969. Shortly after his discharge from the military, Michael enrolled at the University of South Carolina where he attended classes from February, 1972 to December, 1974 and earned a Bachelor of Science in Mechanical Engineering. He enrolled in The University of Tennessee in March of 1981 and began work on a Masters of Science Degree in Mechanical Engineering.

Since graduating from the University of South Carolina, Michael has worked at Martin Marietta Energy Systems in Oak Ridge, Tennessee. He has been responsible for all aspects of the K-25 Gaseous Diffusion Plant Thermal Systems including, construction and operation of computer models for both component and systems analysis, severe accident analysis, optimization of a retrofit waste heat recovery design, and field testing of both prototype and existing heat transfer equipment. His current assignment is with the Engineering Technology Division of the Oak Ridge National Laboratory where he is responsible for economic and technical analyses of both fossil-fueled and nuclear powered generating plants.